North Carolina
Climate Science Report

North Carolina
Climate Science Report

Authors

Kenneth E. Kunkel	D. Reide Corbett	L. Baker Perry
David R. Easterling	Kathie D. Dello	Walter A. Robinson
Andrew Ballinger	Jenny Dissen	Laura E. Stevens
Solomon Bililign	Gary M. Lackmann	Brooke C. Stewart
Sarah M. Champion	Richard A. Luettich Jr.	Adam J. Terando

March 2020

NCICS

Climate Science Advisory Panel

Kenneth E. Kunkel | David R. Easterling | Ana P. Barros | Solomon Bililign | D. Reide Corbett

Kathie D. Dello | Gary M. Lackmann | Wenhong Li | Yuh-lang Lin | Richard A. Luettich Jr.

Douglas K. Miller | L. Baker Perry | Walter A. Robinson | Adam J. Terando

Foreword

The North Carolina Climate Science Report is a scientific assessment of historical climate trends and potential future climate change in North Carolina under increased greenhouse gas concentrations. It supports Governor Cooper's Executive Order 80 (EO80), "North Carolina's Commitment to Address Climate Change and Transition to a Clean Energy Economy," by providing an independent peer-reviewed scientific contribution to the EO80.

The report was prepared independently by North Carolina-based climate experts informed by (i) the scientific consensus on climate change represented in the Fourth United States National Climate Assessment and the Fifth Assessment Report of the Intergovernmental Panel on Climate Change, (ii) the latest research published in credible scientific journals, and (iii) information in the North Carolina State Climate Summary.

An advisory panel ("Climate Science Advisory Panel") was formed to provide oversight and review of the report. This panel consisted of North Carolina university and federal research scientists with national and international reputations in their specialty areas of climate science.

The report underwent several rounds of review and revision, including an anonymous peer review organized by NOAA's National Centers for Environmental Information (NCEI). The report is available via: ncics.org/nccsr.

North Carolina Climate Science Report

Authors and Report Development Team

Authors

Kenneth E. Kunkel, North Carolina Institute for Climate Studies, North Carolina State University
David R. Easterling, NOAA National Centers for Environmental Information
Andrew Ballinger, The University of Edinburgh
Solomon Bililign, North Carolina A&T State University
Sarah M. Champion, North Carolina Institute for Climate Studies, North Carolina State University
D. Reide Corbett, Integrated Coastal Programs, East Carolina University
Kathie D. Dello, State Climate Office, North Carolina State University
Jenny Dissen, North Carolina Institute for Climate Studies, North Carolina State University
Gary M. Lackmann, Dept of Marine, Earth and Atmospheric Sciences, North Carolina State University
Richard A. Luettich Jr., Institute of Marine Science, University of North Carolina-Chapel Hill
L. Baker Perry, Appalachian State University
Walter A. Robinson, Dept of Marine, Earth and Atmospheric Sciences, North Carolina State University
Laura E. Stevens, North Carolina Institute for Climate Studies, North Carolina State University
Brooke C. Stewart, North Carolina Institute for Climate Studies, North Carolina State University
Adam J. Terando, U.S. Geological Survey, Southeast Climate Adaptation Science Center

Recommended Citation

Kunkel, K.E., D.R. Easterling, A. Ballinger, S. Bililign, S.M. Champion, D.R. Corbett, K.D. Dello, J. Dissen, G.M. Lackmann, R.A. Luettich, Jr., L.B. Perry, W.A. Robinson, L.E. Stevens, B.C. Stewart, and A.J. Terando, 2020: *North Carolina Climate Science Report*. North Carolina Institute for Climate Studies, 233 pp. https://ncics.org/nccsr

Climate Science Advisory Panel

Kenneth E. Kunkel, North Carolina Institute for Climate Studies, North Carolina State University
David R. Easterling, NOAA National Centers for Environmental Information
Ana P. Barros, Duke University
Solomon Bililign, North Carolina A&T State University
D. Reide Corbett, Integrated Coastal Programs, East Carolina University
Kathie D. Dello, State Climate Office, North Carolina State University
Gary M. Lackmann, Dept of Marine, Earth and Atmospheric Sciences, North Carolina State University
Wenhong Li, Duke University
Yuh-lang Lin, North Carolina A&T State University
Richard A. Luettich Jr., Institute of Marine Science, University of North Carolina-Chapel Hill
Douglas K. Miller, University of North Carolina-Asheville
L. Baker Perry, Appalachian State University
Walter A. Robinson, Dept of Marine, Earth and Atmospheric Sciences, North Carolina State University
Adam J. Terando, U.S. Geological Survey, Southeast Climate Adaptation Science Center

Technical Contributors

James Biard, North Carolina Institute for Climate Studies, North Carolina State University
Kelley Depolt, State Climate Office, North Carolina State University
Ashley Hiatt, State Climate Office, North Carolina State University
Tami Houston, External Review Coordinator, NOAA National Centers for Environmental Information
Katharine Johnson, North Carolina Institute for Climate Studies, North Carolina State University
James Kossin, NOAA National Centers for Environmental Information
Ronnie Leeper, North Carolina Institute for Climate Studies, North Carolina State University
Liqiang Sun, North Carolina Institute for Climate Studies, North Carolina State University
William Sweet, NOAA

Report Management Team

Kenneth E. Kunkel, North Carolina Institute for Climate Studies, North Carolina State University
David R. Easterling, NOAA National Centers for Environmental Information
Otis Brown, North Carolina Institute for Climate Studies, North Carolina State University
Sarah M. Champion, North Carolina Institute for Climate Studies, North Carolina State University
Jenny Dissen, North Carolina Institute for Climate Studies, North Carolina State University
Brooke C. Stewart, North Carolina Institute for Climate Studies, North Carolina State University

Production Team

Jessicca Griffin, Lead Graphics Artist, North Carolina Institute for Climate Studies, North Carolina State University
Thomas Maycock, Lead Technical Editor, North Carolina Institute for Climate Studies, North Carolina State University
Andrea McCarrick, Lead Copy Editor, North Carolina Institute for Climate Studies, North Carolina State University
Brooke C. Stewart, Lead Science Writer, North Carolina Institute for Climate Studies, North Carolina State University
Ciara Lemery, U.S. Global Change Research Program/ICF
S. Elizabeth Love-Brotak, NOAA National Centers for Environmental Information
Tiffany Means, North Carolina Institute for Climate Studies, North Carolina State University
Deborah J. Misch, Innovative Consulting & Management Services, LLC

External Reviewers

Ryan Boyles, U.S. Geological Survey, Southeast Climate Adaptation Science Center
Gregory Carbone, University of South Carolina
John Nielson-Gammon, Texas A&M University
Beth Hall, Purdue University
Pam Knox, University of Georgia
David Robinson, Rutgers University

Report Findings

These findings present key conclusions of this report about observed and projected changes in the climate of the state of North Carolina.

Quantitative projections for temperature, precipitation, and sea level rise are provided for two future scenarios: a higher scenario (RCP8.5), in which greenhouse gas emissions continue to increase through the end of this century, and a lower scenario (RCP4.5), in which emissions increase at a slower rate, peak around the middle of this century, and then begin to decrease. Future increases in temperature are dependent on greenhouse gas emissions, with higher emissions resulting in greater warming. Qualitative projections are based on expert judgment and assessment of the relevant scientific literature and draw on multiple lines of scientific evidence as well as model simulations.

Global average temperature has increased about 1.8°F since 1895. Scientists have ***very high confidence*** that this warming is largely due to human activities that have significantly increased atmospheric concentrations of carbon dioxide (CO_2) and other greenhouse gases. It is ***virtually certain*** that global warming will continue, assuming greenhouse gas concentrations continue to increase. By the end of this century (2080–2099), global average temperature is projected to increase by about 4°–8°F compared to the recent climate (1996–2015) under the higher scenario (RCP8.5) and by about 1°–4°F under the lower scenario (RCP4.5).

Global average sea level has increased by about 7–8 inches since 1900, with almost half of this increase occurring since 1993. It is ***virtually certain*** that global sea level will continue to rise due to expansion of ocean water from warming and melting of ice on land, such as the Greenland and Antarctic ice sheets.

Observed and Projected Changes for North Carolina

Except where noted, statements about future changes refer to projections through the end of this century.

- Our scientific understanding of the climate system strongly supports the conclusion that large changes in North Carolina's climate, much larger than at any time in the state's history, are ***very likely*** by the end of this century under both the lower and higher scenarios.

Temperature

- North Carolina annual average temperature has increased by about 1.0°F since 1895, somewhat less than the global average. The most recent 10 years (2009–2018), however, represent the warmest 10-year period on record in North Carolina, averaging about 0.6°F warmer than the warmest decade in the 20th century (1930–1939). Recently released data indicate that 2019 was the warmest year on record for North Carolina.

- Although regional changes in temperature can vary from global changes, it is ***very likely*** that North Carolina temperatures will also increase substantially in all seasons. Annual average temperature increases relative to the recent climate (1996–2015) for North Carolina are projected to be on the order of 2°–5°F under a higher scenario (RCP8.5) and 2°–4°F under a lower scenario (RCP4.5) by the middle of this century. By the end of this century, annual average temperature increases relative to the recent climate (1996–2015) for North Carolina are projected to be on the order of 6°–10°F under a higher scenario (RCP8.5) and 2°–6°F under a lower scenario (RCP4.5).

- North Carolina has not experienced an increase in the number of hot (daytime maximum temperatures above 90°F) and very hot (daytime maximum temperatures above 90°F) summer days since 1900. However, it has seen an increase in the number of warm (nighttime minimum temperatures above 70°F) and very warm nights (nighttime minimum temperatures above 75°F).

- It is ***very likely*** that the number of warm and very warm nights will increase.

- It is ***very likely*** that summer heat index values will increase because of increases in absolute humidity.

- It is ***likely*** that the number of hot and very hot days will increase.

- It is ***likely*** that the number of cold days (daytime maximum temperatures below 32°F) will decrease.

Precipitation

- There is no long-term trend in annual total precipitation averaged across the state. However, there is an upward trend in the number of heavy rainfall events (3 inches or more in a day), with the last four years (2015–2018) having seen the greatest number of events since 1900.

- It is ***likely*** that annual total precipitation for North Carolina will increase.

- It is ***very likely*** that extreme precipitation frequency and intensity in North Carolina will increase due to increases in atmospheric water vapor content.

Sea Level

- Sea level along the northeastern coast of North Carolina has risen about twice as fast as along the southeastern coast, averaging 1.8 inches per decade since 1978 at Duck, NC, and 0.9 inches per decade since 1935 at Wilmington, NC.

- It is ***virtually certain*** that sea level along the North Carolina coast will continue to rise due to expansion of ocean water from warming and melting of ice on land, such as the Greenland and Antarctic ice sheets. Under a higher scenario (RCP8.5), storm-driven

water levels that have a 1% chance of occurring each year in the beginning of the 21st century may have as much as a 30%–100% chance of occurring each year in the latter part of the century. High tide flooding, defined as water levels of 1.6–2.1 feet (0.5–0.65 meters) above Mean Higher High Water, is projected to become a nearly daily occurrence by 2100 under both the lower and higher scenarios.

Hurricanes

- The intensity of the strongest hurricanes is *likely* to increase with warming, and this could result in stronger hurricanes impacting North Carolina. Confidence in this result is *high* for global hurricane changes but lower for individual regions such as North Carolina.

- Heavy precipitation accompanying hurricanes that pass near or over North Carolina is *very likely* to increase, which would in turn increase the potential for freshwater flooding in the state.

- There is *low confidence* concerning future changes in the number of landfalling hurricanes in North Carolina.

Storms

- It is *likely* that the frequency of severe thunderstorms in North Carolina will increase.

- It is *likely* that total snowfall and the number of heavy snowstorms in North Carolina will decrease due to increasing winter temperatures.

- There is *low confidence* concerning future changes in the number of winter coastal storms.

- There is *low confidence* concerning future changes in the number of ice storms in North Carolina.

Floods, Droughts, and Wildfire

- It is *virtually certain* that rising sea level and increasing intensity of coastal storms, especially hurricanes, will lead to an increase in storm surge flooding in coastal North Carolina.

- It is *likely* that increases in extreme precipitation will lead to increases in inland flooding in North Carolina.

- It is *likely* that future severe droughts in North Carolina will be more intense due to higher temperatures leading to increased evaporation. As a result, it is *likely* that the frequency of climate conditions conducive to wildfires in North Carolina will increase.

Other Compound Events

- It is *likely* that future urban growth will increase the magnitude of the urban heat island effect, with stronger warming in North Carolina urban centers.

- There is *low confidence* concerning future changes in conditions favorable for near-surface ozone formation in North Carolina because of counteracting influences from increases in both temperature and water vapor.

Engineering Design Standards

- It is *very likely* that some current climate design standards for North Carolina buildings and other infrastructure will change by the middle of the 21st century. This includes increases in design values for precipitation, temperature, and humidity. Several professional societies, however, are actively working on methods to incorporate climate change into national standards, and updated standards appropriate for use in a changing climate may be available in the near future.

Guide to the Report

Guide to the Content of the Climate Science Report

Below is a brief overview of the contents of this report:

Report Findings
Overarching findings of this report

Guide to the Report
Important background information, an explanation of the confidence and likelihood language used in the report, and a list of additional resources

Introduction
Motivations and development process

Executive Summary
A more detailed discussion of the key conclusions and report findings

Chapter 1: Components of Physical Climate Change
An introduction to the physical science of climate change and observed projected changes at the global, national, and regional scales

Chapter 2: Statewide Changes in Temperature, Precipitation, and Storms
Observed and projected changes in statewide averages for various aspects of North Carolina's climate, including temperature and precipitation averages and extremes, droughts, hurricanes, winter storms, other severe weather events, and several other important metrics, including changes in the growing (freeze free) season, heating and cooling demand, and snowmaking conditions for the ski industry

Chapter 3: Regional Changes in Temperature, Precipitation, and Storms
As in Chapter 2, but for each of the three regions used in this report (see "Three Regions Used in This Report" below for details). Note: Some information common to all three regions is replicated in each regional section in order to provide a comprehensive picture of trends for that region.

Chapter 4: Sea Level Rise and Coastal Water Levels
Observed and projected changes in sea level and related coastal impacts, including how changes vary along the North Carolina coast

Chapter 5: Compound Events
Observed and projected changes involving multiple aspects of the climate system or interactions between climate and other human or natural systems, including inland flooding, wildfire, forest ecosystem changes, urban heat island effects, and air pollution

Chapter 6: Engineering Design Standards
  Assessment of changes in key temperature and precipitation metrics relevant for building and infrastructure design standards

Appendix A: Datasets and Scenarios
  Details on the observational datasets used in this report and the scenarios that form the basis of projected changes

Appendix B: Supplemental Graphics
  Additional figures showing observed and projected changes in statewide and regional temperature extremes, including hot days, warm nights, and maximum and minimum temperature

Appendix C: Acronyms and Abbreviations
  Explanations of acronyms and abbreviations used in the report

Three Regions Used in This Report

In order to provide local and regional stakeholders with relevant information, this report presents information on observed and projected climate trends for both the state as a whole and for three distinct regions in North Carolina: the Western Mountains, the Piedmont, and the Coastal Plain (Figure 1). The boundaries for the three regions were chosen based on the U.S. climate divisions defined by NOAA's National Centers for Environmental Information (NCEI 2020).

Chapter 3 provides most of the region-specific information in this report, but other sections of the report also provide regional perspectives where applicable.
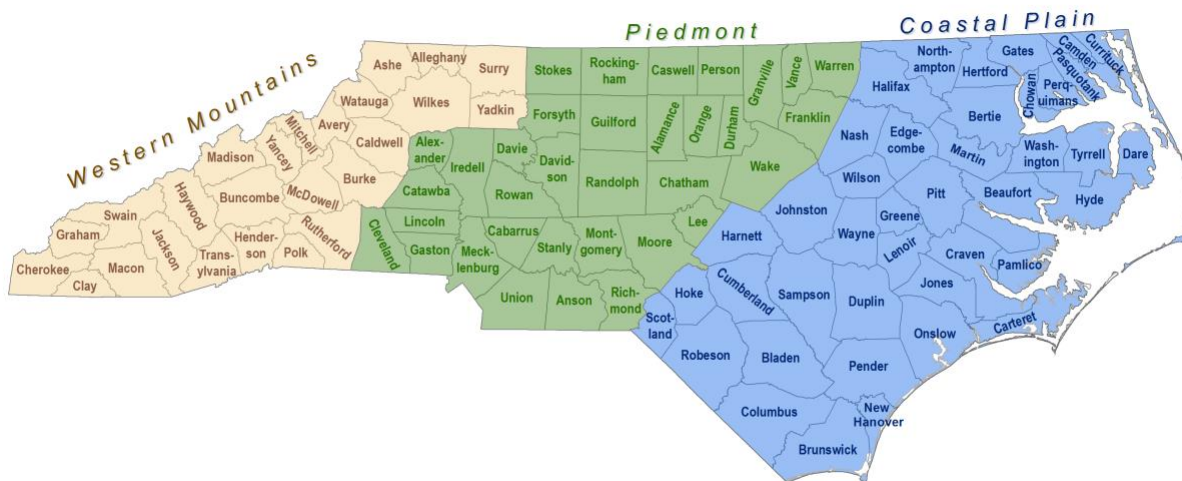

Figure 1. This map of North Carolina shows the counties that compose the three regions used in this report: Western Mountains, Piedmont, and Coastal Plain. Source: NCICS.

Sources Used in This Report

The findings in this report are based on analyses using well-established and carefully evaluated observational and modeling datasets, national and international climate assessments (see "Additional Resources" below), and an assessment of the latest peer-reviewed scientific literature, complemented by other sources where appropriate. All of these sources were determined to meet the standards of the federal Information Quality Act (NOAA 2014).

Observed Changes

The descriptions of historical climate conditions in this report are based primarily on analyses of two observational datasets: NOAA's National Centers for Environmental Information (NCEI) Climate Divisional Dataset (nClimDiv) and NOAA NCEI's Global Historical Climatology Network-Daily (GHCN-D). Monthly data from nClimDiv were used for seasonal and annual temperature and precipitation analyses for the period 1895–2018. Figures illustrating daily extreme metrics of temperature and precipitation are based on GHCN-D, with data analyzed for the period 1900–2018. Each of these analyses is presented as a bar graph with data averaged over 5-year periods, overlaid with annual time series. See Appendix A for additional details on these datasets.

Projected Changes

Climate model projections in this report are shown for two hypothetical climate futures: a higher scenario (Representative Concentration Pathway 8.5, or RCP8.5), in which greenhouse gas emissions continue to increase through the end of the century, and a lower scenario (RCP4.5), in which emissions increase at a slower rate, peak around the middle of the century, and then begin to decrease. See Appendix A for more information on the RCP scenarios.

Global- and national-scale projections of future climate are based on results from the climate models in the Coupled Model Intercomparison Project Phase 5 (CMIP5; Taylor et al 2012). State- and regional-scale projections use data from the Localized Constructed Analogs (LOCA) statistically downscaled dataset, which is derived from CMIP5. The LOCA dataset (Pierce et al. 2014) makes it possible to provide projections at finer spatial scales than are available in CMIP5.

The CMIP5 and LOCA projections include historical simulations based on observed greenhouse gas concentrations (and other factors that influence the climate) and future simulations based on the projected greenhouse gas concentrations in the RCP scenarios.

Maps of mean (average) projected changes in temperature and precipitation across North Carolina are shown for two mid-century time periods: 2021–2040 (under RCP8.5) and 2041–2060 (under RCP4.5 and RCP8.5). These changes are relative to the 1996–2015 average. Projections for 2021–2040 are given only for RCP8.5 because there is very little difference between RCP8.5 and RCP4.5 until later in the century. The average projected changes are a result of averaging all the climate simulations obtained from the CMIP5 archive for this report. Additionally, each individual simulation was given a weight based on the climate model's ability

to reproduce the observed climate and the model's similarity with other climate models—this follows the methodology used in the U.S. Fourth National Climate Assessment. For more information, see Sanderson and Wehner (2017).

Temperature and precipitation mean (average) time series figures include LOCA simulations for the historical period of 1970–2005 and projections for 2006–2100 under both scenarios. An envelope of model simulations is shown, indicating the 10% to 90% confidence intervals from the set of climate models. Since the maps show average values, the 10% to 90% confidence intervals on the time series can be used with the corresponding maps to give the reader a sense of the possible range of values on the maps. In other words, since the maps are an average of a set of model simulations, the actual value at a given location may be somewhat higher or lower than the average. These time series figures also include observations for 1970–2013 derived from the Livneh observational dataset. More information on LOCA, CMIP5, and the Livneh dataset can be found in Appendix A.

Assessments of Confidence and Likelihood

Where applicable, this report uses specific terms to convey information about the degree of scientific confidence and certainty associated with important findings, observations, and projections. The terms used are the same as those used in the Intergovernmental Panel on Climate Change Fifth Assessment Report (Mastrandrea et al. 2010, 2011) and fall into two categories: confidence and likelihood.

The confidence terms used are *very high*, *high*, *medium*, *low*, and *very low* and reflect the overall confidence of the author team in the accuracy or validity of the associated statements, based on their expert assessment of the relevant evidence. Higher confidence levels generally indicate an abundance of evidence in the scientific literature and a good agreement across that evidence base. Lower confidence levels imply a more limited quantity of evidence, more disagreement in the literature, or both.

The likelihood terms, shown in the table below, reflect a probabilistic assessment of the uncertainty associated with a statement, including statements regarding observed changes or events as well as projected future changes. These likelihood assessments may be based on statistical analyses, modeling results, or expert judgments.

Likelihood Term	Probability of Outcome
Virtually certain	99–100%
Very likely	90–100%
Likely	66–100%
About as likely as not	33–66%
Unlikely	0–33%
Very unlikely	0–10%
Exceptionally unlikely	0–1%

Figure 2 provides an overview of the process used to arrive at assessments of confidence and, where applicable, likelihood.
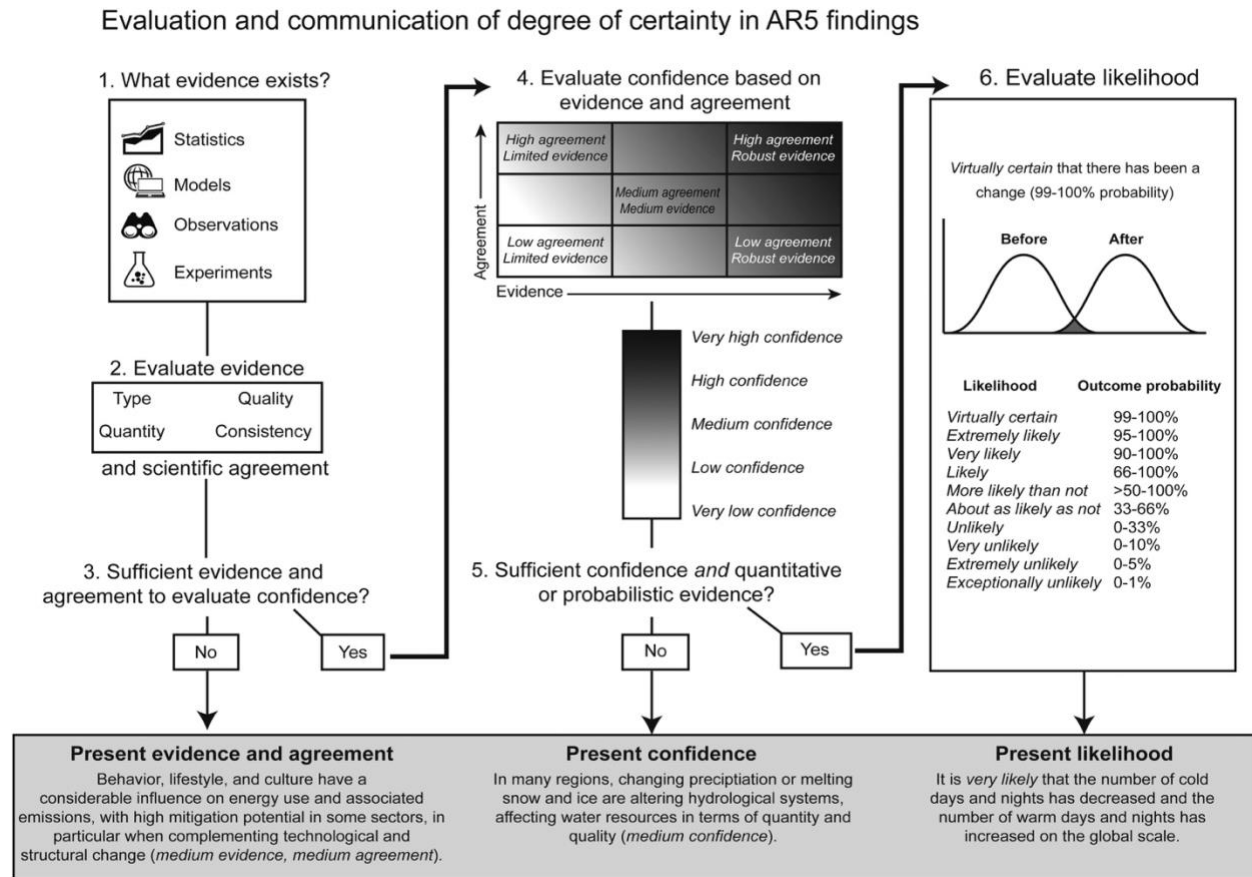
Figure 2. This figure illustrates the process used in Intergovernmental Panel on Climate Change assessment reports to determine i) whether to assign a confidence level to a given finding, ii) whether or not a likelihood can be assigned, and iii) if so, what that likelihood should be. This report uses a very similar approach. Source: Mach et al. 2017 [Creative Commons CC BY NC ND].

Peer Review Process

The Climate Science Advisory Panel members provided input and review of the report outline and intermediate drafts of the report. The report was then subject to a final, formal two-phase review process. First, the Climate Science Advisory Panel members were given a final opportunity to provide individual comments on the report material, and seven members provided comments. Second, a set of twelve climate scientists from around the United States with extensive climate research experience were identified as potential anonymous reviewers. A Federal employee of the National Centers for Environmental Information who was not involved with the report was tasked with contacting each of the twelve potential reviewers to solicit their help in reviewing the report. This process established a layer between the report authors and the

reviewers to ensure anonymity of the reviewers if they so desired. Of the twelve potential reviewers, five provided anonymous review comments, and one additional reviewer provided a signed review. This resulted in just under four hundred review comments that have been addressed. The comments and responses will be made publicly available.

Additional Resources

The resources listed below served as valuable inputs for this report and are all recommended as reliable sources for additional information on climate change, including technical details on the science of climate change as well as discussions of impacts and options for responding to climate change at global, national, state, and local scales.

The Fourth National Climate Assessment, Volumes I and II
The legally mandated National Climate Assessment (NCA) serves as the official federal government assessment of climate change in the United States, including observed and projected trends, impacts, adaptation, and mitigation. The Fourth NCA consists of two volumes, released in 2017 and 2018, respectively:

- Volume I: Climate Science Special Report
  https://science2017.globalchange.gov/

- Volume II: Impacts, Risk, and Adaptation in the United States
  https://nca2018.globalchange.gov/

State Climate Office of North Carolina
The State Climate Office provides a wide range of tools, information, and other resources related to climate and weather in North Carolina.

- http://climate.ncsu.edu/

NOAA State Climate Summaries—North Carolina
NOAA's state climate summaries, produced by scientists from NCICS, NOAA NCEI, and other experts from around the country, provide an overview of observed and projected climate trends and analyses of key climate-related events for all 50 states and Puerto Rico and the U.S. Virgin Islands. The North Carolina summary, available at the link below, has been updated to include data through 2018.

- https://statesummaries.ncics.org/chapter/nc/

NOAA National Centers for Environmental Information (NCEI) "Climate at a Glance"
NCEI's Climate at a Glance site provides interactive tools for viewing maps, time series charts, and tables of observed data and trends at global, national, regional, state, climate division, and county scales and for selected cities in the United States.

- https://www.ncdc.noaa.gov/cag/

Intergovernmental Panel on Climate Change (IPCC)

The IPCC provides periodic global-scale assessment reports consisting of contributions from three working groups. Working Groups I, II, and III focus on the physical scientific basis; mitigating climate change; and impacts, adaptation, and vulnerability, respectively. The contributions to the Fifth Assessment Report were published in 2013 and 2014. The Sixth Assessment Report cycle is currently underway, with three special reports released already—one on global warming of 1.5°C, one on climate change and land, and one on the ocean and cryosphere in a changing climate.

- https://www.ipcc.ch/

References

Mach, K.J., M.D. Mastrandrea, J. Freeman, and C.B. Field, 2017: Unleashing expert judgment in assessment. *Global Environmental Change,* **44**, 1–4. http://dx.doi.org/10.1016/j.gloenvcha.2017.02.005

Mastrandrea, M.D., C.B. Field, T.F. Stocker, O. Edenhofer, K.L. Ebi, D.J. Frame, H. Held, E. Kriegler, K.J. Mach, P.R. Matschoss, G.-K. Plattner, G.W. Yohe, and F.W. Zwiers, 2010: Guidance Note for Lead Authors of the IPCC Fifth Assessment Report on Consistent Treatment of Uncertainties. Intergovernmental Panel on Climate Change (IPCC), 7 pp. https://wg1.ipcc.ch/AR6/documents/AR5_Uncertainty_Guidance_Note.pdf

Mastrandrea, M.D., K.J. Mach, G.-K. Plattner, O. Edenhofer, T.F. Stocker, C.B. Field, K.L. Ebi, and P.R. Matschoss, 2011: The IPCC AR5 guidance note on consistent treatment of uncertainties: a common approach across the working groups. *Climatic Change,* **108** (4), 675. http://dx.doi.org/10.1007/s10584-011-0178-6

NCEI, 2020: U.S. Climate Divisions. NOAA National Centers for Environmental Information, accessed February 4, 2020. https://www.ncdc.noaa.gov/monitoring-references/maps/us-climate-divisions.php?section=grdd

NOAA, 2014: National Oceanic and Atmospheric Administration Information Quality Guidelines. http://www.cio.noaa.gov/services_programs/IQ_Guidelines_103014.html

Pierce, D.W., D.R. Cayan, and B.L. Thrasher, 2014: Statistical downscaling using Localized Constructed Analogs (LOCA). *Journal of Hydrometeorology,* **15** (6), 2558-2585. http://dx.doi.org/10.1175/jhm-d-14-0082.1

Sanderson, B.M. and M.F. Wehner, 2017: Appendix B: Model weighting strategy. *Climate Science Special Report: Fourth National Climate Assessment, Volume I*. Wuebbles, D.J., D.W. Fahey, K.A. Hibbard, D.J. Dokken, B.C. Stewart, and T.K. Maycock, Eds. U.S. Global Change Research Program, Washington, DC, USA, 436–442. http://dx.doi.org/10.7930/J06T0JS3

Taylor, K.E., R.J. Stouffer, and G.A. Meehl, 2012: An Overview of CMIP5 and the Experiment Design. *Bulletin of the American Meteorological Society,* **93** (4), 485–498. http://dx.doi.org/10.1175/BAMS-D-11-00094.1

Introduction

Background/Context

On October 29, 2018, North Carolina Governor Roy Cooper issued Executive Order No. 80, which outlines North Carolina's commitment to addressing climate change and transition to a clean energy economy. In Section 9 of the Executive Order, Governor Cooper directed North Carolina's cabinet agencies to "integrate climate adaptation and resiliency planning into their policies, programs and operations (i) to support communities and sectors of the economy that are vulnerable to the effects of climate change and (ii) to enhance the agencies' ability to protect human life and health, property, natural and built infrastructure, cultural resources and other public and private assets of value to North Carolinians. DEQ [the Department of Environmental Quality], with the support of cabinet agencies and informed by stakeholder engagement, shall prepare a North Carolina Climate Risk and Resiliency Plan [the March 2020 NC Risk Assessment and Resilience Plan (RARP)] … to submit to the Governor by March 1, 2020" (North Carolina Office of the Governor 2019).

The order also states that the North Carolina Climate Change Interagency Council "shall support communities that are interested in assessing risks and vulnerabilities to natural and built infrastructure and in developing community-level adaptation and resilience plans" (North Carolina Office of the Governor 2019).

Cabinet Agency Roles

Department of Environmental Quality, with Support of Other Agencies
- March 2020 NC Risk Assessment and Resilience Plan—provide a scientific assessment of current and projected climate impacts on North Carolina and prioritize effective resiliency strategies.

All Cabinet Agencies—Assess and Address Climate Change
- Evaluate the impacts of climate change on agency programs and operations
- Integrate climate change mitigation and adaptation practices into agency programs and operations
- Support communities and sectors vulnerable to climate change impacts

This report, the North Carolina Climate Science Report (NCCSR), represents one component of the March 2020 NC Risk Assessment and Resilience Plan and provides the science basis to assess current and projected climate impacts on North Carolina. The broad objectives for the NCCSR were to:

- Represent the best and most comprehensive synthesis of climate science information for North Carolina across its regions (the Western Mountains, the Piedmont, and the Coastal Plain)

- Provide and describe data on variability, change, and projections for select climate and meteorological variables of relevance to the various cabinet agencies across the regions

- Serve as input to, and integrate with, the vulnerability and risk assessment activities, and other aspects of the March 2020 NC Risk Assessment and Resilience Plan

- Support the State, local governments, and planners in understanding the information in the report to enable decision-making, policy-making, and identifying innovative opportunities for economic and societal growth

The Process

Starting in early 2019, North Carolina State University's North Carolina Institute for Climate Studies (NCICS) worked closely with DEQ and other cabinet agencies to determine the approach and plan for providing a scientific assessment of current and projected climate impacts on North Carolina. DEQ and the other agencies provided information related to climate hazards and stressors, based upon available historical and current reports, assessments, and the state of knowledge to develop a user-driven perspective on the climate science report.

A Climate Science Advisory Panel (CSAP) was established to provide scientific oversight of contents of the report. The Panel consisted of climate scientists from North Carolina research universities and federal centers (see front matter for the list of members).

The input, needs, and requirements provided by the cabinet designees were reviewed and validated together by DEQ, cabinet designee members, NCICS, and the CSAP through a series of workshops, webinars, conference calls, and discussions. This iterative engagement process with key stakeholder input informed the development of the NCCSR.

The author team comprises NCICS scientists and some members of the CSAP. Additional review of the report contents was provided by nationally known climate science experts.

Technical, editorial, documentation and scientific support for the report was provided by the U.S. National Climate Assessment Technical Support Unit (TSU), hosted at the National Oceanic and Atmospheric Administration's (NOAA) National Centers for Environmental Information in Asheville, NC. The TSU is staffed mainly by NC State personnel who are supported by NOAA through the Cooperative Institute for Climate and Satellites–North Carolina under Cooperative Agreement NA14NES432003. Any use of trade, firm, or product names is for descriptive purposes only and does not imply endorsement by the U.S. Government.

References

North Carolina Office of the Governor, 2019: Executive Order 80. North Carolina's Commitment to Address Climate Change and Transition to a Clean Energy Economy. Raleigh, NC. 4 pp. https://files.nc.gov/ncdeq/climate-change/EO80--NC-s-Commitment-to-Address-Climate-Change---Transition-to-a-Clean-Energy-Economy.pdf

Executive Summary

Our scientific understanding of the climate system strongly supports the conclusion that North Carolina's climate has changed in recent decades and the expectation that large changes—much larger than at any time in the state's history—will occur if current trends in greenhouse gas concentrations continue. Even under a scenario where emissions peak around 2050 and decline thereafter, North Carolina will experience substantial changes in climate. The projected changes with the highest level of scientific confidence include increases in temperature, increases in summer absolute humidity, increases in sea level, and increases in extreme precipitation. It is also *likely* that there will be increases in the intensity of the strongest hurricanes.

A full appreciation for past and future changes in North Carolina's climate requires a global perspective. Earth's climate has warmed substantially since the late 19th century, with most of that warming occurring in the last 50 years. This warming trend is clear from global temperature records and many other indicators, including rising global sea levels and rapid decreases in arctic sea ice cover. Scientists have ***very high confidence*** that this warming is largely due to human activities that have significantly increased atmospheric concentrations of carbon dioxide (CO_2) and other greenhouse gases. Extensive research has examined other potential causes of this warming, and the increase in greenhouse gas concentrations is the only plausible cause that is consistent with the observed data and the physics that govern the climate system.

Observed Changes

In North Carolina, annual average temperature has increased about 1°F since 1895, compared to the global average increase of about 1.8°F during that period. Annual average temperatures have been consistently above normal since the 1990s, with the most recent 10 years (2009–2018) representing the warmest 10-year period on record—about 0.6°F warmer than the warmest decade of the 1900s (1930–1939). Data for 2019, which were released during the review of this report, indicate that 2019 was the warmest year on record for North Carolina.

Most other temperature indicators also show warming. Average temperatures have increased in all four seasons. There has been an increase in the number of very warm nights. The length of the growing season has increased and is now about 1.5 weeks longer than the long-term average. There is an upward trend in the number of cooling degree days (a temperature indicator related to air conditioning demand) and a downward trend in the number of heating degree days (an indicator of heating demand)—both changes are consistent with a warming climate. However, a few indicators that would be expected to change with warmer conditions have not. For example, the number of very hot days has not increased, and there is no overall trend in the number of cold days and cold nights.

There is no long-term trend in annual total precipitation averaged across the state; however, 2018 was the wettest year on record, in part due to the torrential rainfall from Hurricane Florence. There has been an upward trend in the number of heavy rainfall events (days with more than 3

inches of rain), indicating that a larger portion of the annual total precipitation is occurring in heavy events. Temperature and precipitation trends in the three regions of the state (Coastal Plain, Piedmont, and Western Mountains) are generally similar to statewide trends.

Most observing stations outside of the mountains have experienced a downward trend in snowfall. In the Western Mountains, there is no century-long trend in snowfall, although stations in the southern mountains have seen decreasing trends over the last 50 years. Conditions favorable for snow-cover maintenance and snowmaking in the Western Mountains have been highly variable since 1981, but recent years have seen below average percentages of time when conditions are favorable.

Global average sea level has increased by about 7–8 inches since 1900, with almost half of this increase occurring since 1993—a rate of about 1.2 inches per decade. Sea level along the northeastern coast of North Carolina is rising about twice as fast as along the southeastern coast, averaging 1.8 inches per decade since 1978 at Duck, NC, and 0.9 inches per decade at Wilmington, NC, mainly due to different rates of land subsidence.

Projected Changes

The projections of North Carolina climate conditions presented in this report are based on the *virtual certainty* that greenhouse gas concentrations, particularly CO_2, will continue to rise. It may take decades for non-carbon-based sources of energy to replace most of the production based on fossil fuels. The basic principles of physics dictate that increases in greenhouse gas concentrations will have a warming effect, with *virtual certainty*, due to the increase in atmospheric absorption of infrared energy.

Quantitative projections for temperature, precipitation, and sea level rise are provided for two future scenarios: a higher scenario (RCP8.5), in which greenhouse gas emissions continue to increase through the end of this century, and a lower scenario (RCP4.5), in which emissions increase at a slower rate, peak around the middle of this century, and then begin to decrease. RCP8.5 and RCP4.5 are Representative Concentration Pathways—scenarios used in climate model simulations to examine how Earth's climate would respond to differing levels of greenhouse gas concentrations. The numbers 8.5 and 4.5 refer to the magnitude of the energy imbalance in the climate system (in units of watts per square meter) that would result in the year 2100 from the increases in greenhouse gas concentrations specified by the respective scenarios. By comparison, the increase in concentrations since the initiation of the Industrial Revolution has resulted in an imbalance of approximately 2.3 watts per square meter.

A very low scenario (RCP2.6) is also used occasionally in this report, but this scenario is very unlikely because there has been no slowdown in the annual growth rate of CO_2. Qualitative projections are based on expert judgment and assessment of the relevant scientific literature and draw on multiple lines of scientific evidence as well as model simulations. Except where noted, statements below about future changes refer to projections through the end of this century.

By the end of this century (2080–2099), global average temperature is projected to increase by about 4°–8°F compared to the current climate (1996–2015) under the higher scenario (RCP8.5) and by about 1°–4°F under the lower scenario (RCP4.5). The warming is projected to be greater in the middle and high latitudes and less at tropical latitudes.

Regional changes in temperature can differ from global changes, at least temporarily, as shown by the historical lower rate of warming in North Carolina compared to the global average. Seasonal and annual average temperatures, however, have been rising in North Carolina in recent decades, and it is *very likely* that North Carolina temperatures will continue to increase substantially in all seasons.

- By the middle of this century, annual average temperature increases relative to the current climate (1996–2015) for North Carolina are projected to be on the order of 2°–5°F under the higher scenario (RCP8.5) and 2°–4°F under the lower scenario (RCP4.5).

- By the end of this century, annual average temperature increases relative to the current climate (1996–2015) for North Carolina are projected to be on the order of 6°–10°F under the higher scenario (RCP8.5) and 2°–6°F under the lower scenario (RCP4.5).

Temperature extremes are also projected to change:

- It is *very likely* that the number of very warm nights will increase, continuing recent trends.

- It is *likely* that the number of very hot days will increase, although the level of confidence is lower than for very warm nights because of the lack of recent trends.

- It is *likely* that the number of cold days and very cold nights will decrease, but again the level of confidence is lower than for very warm nights because of the lack of recent trends.

Several additional climate features directly tied to temperature are also projected to change, with a high level of certainty:

- It is *very likely* that extreme precipitation frequency and intensity will increase because global ocean surface temperatures will continue to increase gradually. In turn, near-surface air temperature and absolute humidity will increase over the oceans because maximum water vapor content is strongly related to temperature, increasing by about 3.5% per °F.

- It is *virtually certain* that global sea level will continue to rise due to both the expansion of ocean water from warming and from the melting of ice on land, including the Greenland and Antarctic ice sheets. It is *virtually certain* that sea level along the North Carolina coast will also continue to rise. Under the higher scenario (RCP8.5), storm-driven water levels having a 1% chance of occurring each year in the beginning of the 21st century may have as much as a 30%–100% chance of occurring each year in the

latter part of the century. High tide flooding is projected to become nearly a daily occurrence by 2100 under both the lower and higher scenarios.

- It is *very likely* that summer heat index values will increase because of increases in absolute humidity.

- It is *likely* that the probability of snowfall and snow cover will decrease nearly everywhere in North Carolina because of warmer temperatures.

For climate variables where the temperature dependence is more complex, projected changes are less certain:

- Inland flooding depends not only on extreme precipitation but also on characteristics of the land surface, including land use, land cover, and soil moisture conditions. It also depends on whether deliberate adaptive measures are implemented proactively. It is *likely* that the frequency and severity of inland flooding will increase because of increases in the frequency and intensity of extreme precipitation. This lower level of certainty compared to projections for changes in extreme precipitation stems from the additional factors that determine flooding.

- It is *likely* that annual total precipitation in the state will increase, but there is less certainty for annual total precipitation than for projected increases in extreme precipitation, because total precipitation is a function of both atmospheric water vapor and the frequency and intensity of weather systems that cause precipitation. Future changes in the intensity and frequency of such weather systems are more uncertain.

Hurricanes have some of the most important impacts on the state, often catastrophic (storm surge, wind, and flooding damage) but sometimes beneficial (rainfall recharging soil moisture and groundwater aquifers). An understanding of future changes in hurricanes has been the subject of extensive research by climate scientists. While that understanding continues to evolve, a recent assessment of the science leads to the conclusion that the intensity of the strongest hurricanes is *likely* to increase with warming, and this could result in stronger hurricanes impacting North Carolina. Confidence in this result is *high* for tropical cyclone changes on a global scale but lower on a regional level, such as North Carolina.

It is *virtually certain* that rising sea level and increasing intensity of coastal storms, especially hurricanes, will lead to increases in storm surge flooding in coastal North Carolina. There is *low confidence* concerning future changes in the total number of hurricanes. The total number of hurricanes depends on a variety of meteorological factors, such as vertical wind shear (changes in wind speed or direction with height in the atmosphere), and not just ocean surface temperatures, and there is considerable uncertainty about changes in these other factors. Heavy precipitation accompanying hurricanes is *very likely* to increase, increasing the potential for freshwater floods.

Severe thunderstorms (hail, tornadoes, and strong winds) are a regular occurrence in North Carolina, particularly in the spring. Severe thunderstorms require two primary atmospheric conditions: an unstable atmosphere and high vertical wind shear. It is *very likely* that vertical instability will increase, but it is also *likely* that vertical wind shear will decrease. These may counteract one another. Recent research suggests that the increases in atmospheric instability will dominate. While this remains an active area of research, it is *likely* that there will be increases in the frequency of severe thunderstorms.

Other important weather systems include snowstorms, winter coastal storms, and ice storms. There is considerable uncertainty about future changes in the number and severity of extratropical cyclones—the weather phenomenon that causes each of these winter storm types. In the case of snow, temperature is an important factor, and it is *likely* that total snowfall and the number of heavy snowstorms will decrease because of increasing temperatures. There is *low confidence* concerning future changes in the number of ice storms and winter coastal storms.

Drought can have major impacts on the state, including agricultural production and wildfires. It is *likely* that major droughts will become more severe because of higher temperatures that will increase evaporation rates. As a result, it is *likely* that the climate conditions conducive to wildfires in North Carolina will increase in the future.

The major urban areas of the state have expanded substantially over the past few decades, and this trend shows no signs of abating. The urban heat island effect results from the conversion of vegetated surfaces (such as forests and farmland) to urban and suburban landscapes with substantial percentages of impervious, non-vegetated surfaces, reducing the amount of natural cooling from evapotranspiration (the combination of evaporation of water from the surface and transpiration of water vapor from vegetation) and increasing the amount of heat retained in darker, paved surfaces as compared to natural land cover. It is *likely* that future warming in urban areas will be enhanced by future growth of those areas.

Near-surface ozone is a major component of air pollution, and harmful levels of near-surface ozone result from a combination of climate conditions and human-caused emissions of compounds necessary for the formation of ozone, including nitrogen oxides, carbon monoxide, and volatile organic compounds (referred to as ozone precursor compounds). Near-surface ozone concentrations tend to increase with temperature. However, changes in other climate conditions, such as increased precipitation, can counteract the temperature effect. Overall, it is uncertain what the net effect will be. Thus, there is *low confidence* concerning future changes in the conditions favorable for near-surface ozone concentrations.

Climate design values, which provide information on the average and extreme climate conditions experienced in a given location, are important for planning and designing many types of infrastructure. Many climate design values are projected to change because of warming. Because of the high level of confidence in increased temperature and extreme precipitation, it is *very likely* that some current climate design standards for building and other infrastructure will change by the middle of this century. This includes increases in design values for precipitation,

temperature, and humidity. In fact, current design values are based on historical data and do not incorporate recent trends; thus, some standards may already be out of date. Several professional societies, however, are actively working on methods to incorporate climate change into national standards, and updated standards appropriate for use in a changing climate may be available in the near future.

1. Components of Physical Climate Change

1.1. Introduction

Earth's climate is changing faster now than at any point in modern history, and the impacts of these changes are being felt around the world, across the Nation, and locally in North Carolina. Our understanding of the causes of past and present climate change and our confidence in projections of future changes depend on our ability to understand and model Earth's climate system. That understanding is challenged by the complexity and interconnectedness of the components of the climate system: atmosphere, land, ocean, and cryosphere (the frozen water part of the Earth system; USGCRP 2017, USGCRP 2018).

Despite the complexity of the climate system, the drivers of climate change—both natural and human-caused—are well understood. Observational evidence does not support any credible natural explanations for the amount of warming seen across the globe since the middle of the last century. Instead, it consistently points to human activities, especially emissions of greenhouse gases, as the dominant cause of the rapidly changing climate (USGCRP 2017, USGCRP 2018). This observational evidence is consistent with our understanding of the physics of the climate system (see Section 1.4).

1.2. Physical Drivers of Climate Change

1.2.1. Energy Balance and the Greenhouse Effect

Earth's global climate is governed by the balance between incoming and outgoing energy. Earth gains energy from the sun (in the form of incoming shortwave radiation), and some of that energy is reflected back to outer space by clouds, by tiny particles in the atmosphere (known as aerosols), and by reflective land surfaces such as ice and snow. The remainder of the incoming energy is absorbed by Earth's surface and atmosphere and is then re-emitted (lost to outer space) in the form of infrared, or longwave, radiation. These flows of energy—sunlight in and infrared out—are in approximate balance.

Greenhouse gases in the atmosphere—including water vapor, carbon dioxide (CO_2), nitrous oxide, methane, ozone, and others—absorb infrared radiation coming from Earth's surface and emit some of that energy to space and some back towards the surface. In so doing, they act like a blanket, trapping energy near the surface and making surface temperatures significantly higher than they would be were these gases absent. This warming is known as the greenhouse effect, and without it, Earth would be almost 60°F colder.

Global average temperature remains stable when the outgoing flow of energy balances with the incoming flow of energy. However, human activities have changed this "radiative balance" of the planet, primarily by adding greenhouse gases and aerosol particles to the atmosphere and through changes in the way land is used. Changes in the planet's radiative balance (or climate

forcings) result in changes in various aspects of the climate, such as temperature and precipitation (Fahey et al. 2017).

1.2.2. Climate Feedbacks and Sensitivity

Climate feedbacks are processes that either amplify or diminish the effects of climate forcings. A process that increases total warming in response to an initial warming is called a positive feedback, and one that decreases warming in response to an initial warming is a negative feedback (NASA n.d.). One of the most powerful positive feedbacks is the water vapor feedback. As air temperature increases—for example, in response to increasing CO_2 concentrations—evaporation increases and so does the maximum amount of water vapor that can be held in the atmosphere. Since water vapor is a strong greenhouse gas, greater amounts of water vapor in the atmosphere will lead to more warming. Thus, water vapor functions as a positive feedback: the initial warming from the CO_2 increase causes an increase in water vapor, which causes an increase in temperature, which leads to additional increases in water vapor, and so on.

The term climate sensitivity refers to the amount by which a given aspect of the climate system (such as temperature) changes in response to a given climate forcing (such as increases in greenhouse gas concentrations). This sensitivity is determined by the net effect of positive and negative feedbacks in the climate system. Climate sensitivity is commonly defined as the amount of warming that would eventually occur as a result of an instantaneous doubling of CO_2 from preindustrial levels (e.g., from 270 parts per millions to 540 parts per million) once the climate reaches equilibrium with the new CO_2 levels (an estimate referred to as "equilibrium climate sensitivity"). There is uncertainty in the exact value of the equilibrium climate sensitivity owing to the interconnected nature of the ocean–atmosphere–land system; however, it is generally thought to be in the range of about 2.5°F to 8°F (IPCC 2013).

1.2.3. Natural Climate Forcings

Global climate change results from climate forcings (also called radiative forcings), which are factors that change the planet's energy balance. These forcings are both natural and human produced. The only significant natural climate forcings in the industrial era are changes in the sun's irradiance (or brightness) and volcanic eruptions (Fahey et al. 2017).

The brightness of the sun changes due to cycles and fluctuations in its internal dynamics. For example, the number of sunspots visible on the solar surface varies in a cyclical way, with the length of the cycle averaging around 11 years. Since the advent of satellites in the 1960s, solar brightness has been measured with high accuracy and precision. The sun's output varies by only a small amount, with just a 0.2% difference between the brightest (solar maximum) and least bright (solar minimum) points in the sunspot cycle. Scientists are confident that the effects of these changes are small compared to the effects of the increase in greenhouse gas concentrations since the pre-industrial era (Fahey et al. 2017).

Over thousands of years, the seasonal and regional distribution of solar heating varies due to fluctuations in Earth's orbit and the tilt of its axis of rotation. Such variations are primarily responsible for the cooling and warming of the planet in ice-age cycles. However, changes in Earth's movement occur over these geologic timescales and are too slow to hold relevance for climate change on historical timescales or as projected into the next few centuries.

Another natural forcing comes from volcanic eruptions. The timing of eruptions is determined by tectonic processes deep within the Earth and appears to be random, with several major eruptions typically occurring within each century. Volcanic eruptions affect the climate primarily by injecting sulfur dioxide into the stratosphere—the stable layer of the atmosphere above clouds and rain. In the stratosphere, the sulfur dioxide gas is chemically converted to tiny droplets of sulfuric acid. These form a haze layer that can remain in the stratosphere for a few years, scattering sunlight that otherwise would reach Earth's surface and thus cooling the climate. The most recent eruption with a strong cooling impact was Mount Pinatubo, in the Philippines. Its 1991 eruption is estimated to have cooled Earth's surface (in the global average) by up to 0.5°F for a period of around two years (Parker et al. 1996).

1.2.4. Anthropogenic Climate Forcings

Human-generated (anthropogenic) climate forcings include the emission of greenhouse gases and aerosols and the reworking of Earth's surface in ways that change the amount of energy received from the sun that is reflected from Earth's surface back to space. All available scientific evidence points to greenhouse gases emitted by human activity as the source of most of the recent global warming. Among these, CO_2 is most important, but methane, nitrous oxide, and some other chemicals are also significant. When fossil fuels (coal, oil, and natural gas) are burned, carbon that was stored within Earth by natural processes that occurred over hundreds of millions of years is released to the atmosphere in the form of CO_2. Thus, by extracting and consuming these fossil fuels, the release of this carbon is accelerated by a factor of roughly a million. Carbon dioxide is also released by some changes in land use, such as the irreversible destruction of certain types of forests, as well as land clearing and agricultural practices that release the carbon stored in the organic components of soils. It is worth noting that growing and consuming food does not, in and of itself, release CO_2 to the atmosphere, since there is a balance between the carbon removed from the atmosphere during photosynthesis, when crops are grown, and the carbon released by plant and animal respiration and by the decay of organic matter. Land-use change also alters the Earth's albedo (reflectivity)—the global effects of these changes are small relative to other forcings, but they can have an impact on the climate, particularly on a local or regional basis.

Continuing increases in atmospheric CO_2 concentrations are expected to be the principal cause of future warming. CO_2 levels have already increased from about 284 parts per million (ppm) in 1850 to 411 ppm in 2019 (Tans and Keeling 2020), and are currently growing at about 0.6% per year. If this growth rate continues, the concentration of CO_2 would double to 800 ppm by 2130. Concentrations of other significant greenhouse gases are also increasing due to human activities.

Methane is released by livestock, by flooded rice paddies, and, to a largely unknown extent, inadvertently in the production of natural gas. Nitrous oxide is released during industrial and agricultural activities, fossil fuel and solid waste burning, and wastewater treatment. Other manufactured greenhouse gases that serve as fire suppressants and refrigerants also end up in the atmosphere from a variety of industrial processes.

The overall climate influence of a given greenhouse gas depends on its atmospheric concentration, its effectiveness in absorbing infrared radiation, and its lifetime in the atmosphere, as well as the time span of climate change being considered. Because CO_2 is removed from the atmosphere both geochemically and biologically, it has an ill-defined atmospheric lifetime, although some fraction of human-produced CO_2 will remain in the atmosphere for centuries. Methane is much more effective at absorbing infrared radiation than CO_2, but it is destroyed chemically in the atmosphere on a timescale of just over a decade, while nitrous oxide, which is also more effective at trapping heat than CO_2, remains in the atmosphere for more than a century. As a result, the effects of any efforts to reduce emissions of greenhouse gases will have differing near-term and long-term impacts on warming, depending on which greenhouse gases are targeted.

The tiny aerosol particles produced by certain human activities can have either a cooling or a warming effect, depending on their makeup. The most common of these substances, especially in the past, are sulfuric acid aerosols, produced in much the same way as a volcanic aerosol, except that the sulfur dioxide is released by the combustion of sulfur-containing fossil fuels, especially coal. Even a thin layer of these particles in the atmosphere reflects a significant amount of sunlight back to space, and therefore they are believed to have had a substantial cooling effect on the climate since the dawn of the Industrial Revolution. Soot particles, on the other hand, which are also released in combustion (e.g., in diesel engines), absorb solar radiation and therefore warm the climate. Most particles released into the lower atmosphere are, however, rapidly removed by rain, so they have no long-term effect once they are no longer being generated.

In the last century, the Clean Air Act and its amendments greatly reduced sulfate emissions from coal burning in the United States, and similar regulation had a like effect in Europe. At the same time, sulfate emissions have increased in other areas, such as China, leading to mixed effects on global and regional temperatures. Two factors render past estimates of aerosol radiative forcing highly uncertain. First, we have no direct measurements of the concentrations of these particles prior to the last few decades. Second, an important way in which some types of particles cool the climate is by making clouds reflect more sunlight. This is called the aerosol indirect effect, and its magnitude is neither well understood nor well measured. If the past cooling effect of particles was large, it implies that there is a strong "hidden" warming that will be manifested when the release of particles is further reduced by efforts to mitigate unhealthy air pollution.

Approximate values for the relative importance of these different forcings are provided by the Intergovernmental Panel on Climate Change (IPCC). In its 5th Assessment Report (IPCC 2013), the Panel finds that since the beginning of the industrial revolution, circa 1750, CO_2 accounts for

well over half of the positive human-induced climate forcing and that the cooling effect of particles has offset approximately a third of the net positive forcing (see Figures 8.15 and 8.17 in Myrhe et al. 2013). These estimates, especially for aerosols, are accompanied by large uncertainties. On a global level, other forcings, such as changes in land cover that alter Earth's reflection of solar radiation, are small.

1.3. Observed Changes

1.3.1. Global Climate Variability

The global climate undergoes intrinsic, or unforced, variations that appear as bumps or wiggles in any time-series depiction of the observed global temperature record (see Figure 1.1). Some of these can be attributed to well-characterized phenomena, such as the slight global warming associated with El Niño events (see below), but most are best described as "noise." The exchange of heat between the atmosphere and the ocean is driven by weather and so is highly variable in space and time. In a given year, if more heat flows from the ocean to the atmosphere, a slight global warming results; if less heat flows from the ocean to the atmosphere, a slight global cooling results. For example, in an El Niño event, there is a net flow of heat from the ocean into the atmosphere; as a result, the global temperature typically increases in El Niño years.

The most publicized fluctuation of this sort is the so-called global warming hiatus at the turn of this century (1998–2013). The appearance that warming had slowed or stopped can be attributed to the fact that following the record high global temperature of 1998, which was associated with a very strong El Niño event, it was not until 2013 that global temperatures were consistently above the 1998 record. Because there is noise in the system, however, even in a persistently warming climate, we should not expect to see record warmth in every new year. "Hiatuses" are an inevitable consequence of intrinsic noise in the climate system (e.g., Easterling and Wehner 2009).

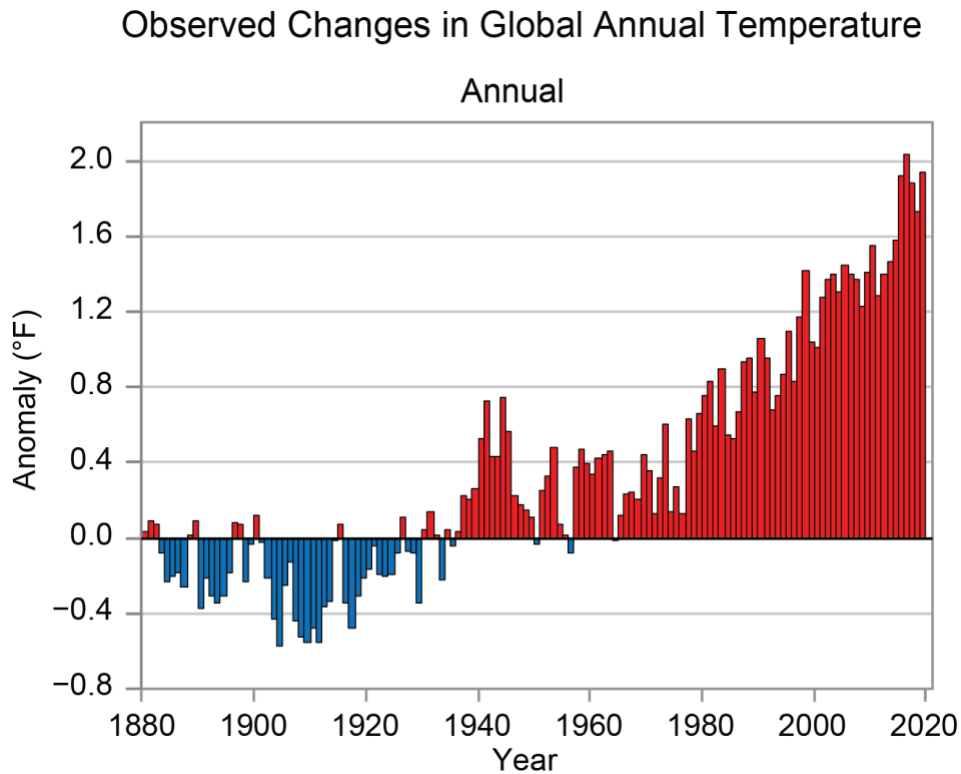## Observed Changes in Global Annual Temperature

Annual

Figure 1.1. The graph shows the global annual average surface (land and ocean) temperature for 1880–2019, shown as differences from the 1901–1960 average. Temperatures vary from year to year throughout the record, but with a warming trend from around 1900 through the 1940s, relatively stable temperatures through the mid-1970s, and then a strong warming trend since the late 1970s. Temperatures have been more than 1.6°F above the long-term average in each of the last five years. Source: adapted from NCEI 2019.

1.3.2. Regional Climate Variability

Global average climate conditions are not what people experience from day to day. For most decision-makers, stakeholders, and individuals, information on regional and local climate averages and variability are more salient than global-scale information. But climate records at smaller scales—cities, states, or regions—are inherently noisier than records averaged across the globe, because natural variability in the climate system has more noticeable effects at these smaller scales. This makes it difficult or, in some cases, impossible to confidently attribute past variations in local climates to either natural or external causes.

From year to year, many local or regional variations are truly random, resulting from the occurrence or absence of one or two weather systems of a given type. At the same time, there are organized structures of variability that act over years or even decades and arise from the internal dynamics of the climate system. Known patterns of natural variability include the North Atlantic Oscillation (NAO), the Atlantic Multidecadal Oscillation (AMO), the Pacific Decadal Oscillation (PDO), and the El Niño–Southern Oscillation (ENSO), among others.

For North Carolina, ENSO is the most significant known mechanism of year-to-year natural variability. During an El Niño event, ocean temperatures warm in a belt straddling the equator, stretching from the International Date Line to the west coast of South America. This ocean warming releases great amounts of energy into the atmosphere, raising (as noted above) the global temperature and affecting weather patterns over much of the world. El Niños are associated with droughts and wildfire in Australia and Indonesia and with flooding rains in California. In North Carolina, El Niño winters tend to be cooler and wetter than normal. In addition, the North Atlantic Oscillation—an atmospheric pressure pattern with centers near Iceland and the Azores—also has a major impact on winter in North Carolina. The NAO varies such that when air pressure is low over Iceland, it is high over the Azores (NAO positive) and vice versa (NAO negative). Recent research by the State Climate Office of North Carolina suggests that North Carolina has milder winters during a positive NAO, while a negative NAO results in an increased potential for wintry weather (State Climate Office of North Carolina n.d.).

1.3.3. Regional Climate Change

Regional variations also occur across decades. Figure 1.2 shows annual average temperature changes for the United States. With the exception of the southeastern United States, all areas show warming, including Alaska, Hawai‘i, and Puerto Rico (not shown on map). Warming is as large as 3°F in some areas of the western United States and Alaska. The southeastern United States and extending into Oklahoma is one of the few areas that shows slight net cooling over the 20th and into the 21st century. The reasons for this have been the subject of much research, and hypothesized causes include both human and natural influences (Vose et al. 2017, Meehl et al. 2012, Walsh et al. 2014, Pan et al. 2004, Partridge et al. 2018). A closer examination of temperature data reveals further detail about the observed cooling. The Southeast region experienced high annual average temperatures in the 1920s and 1930s, followed by cooler temperatures until the 1970s. Since then, annual average temperatures have increased to levels above the 1930s, and the decade of the 2010s through 2018 has been warmer than any previous decade, both for average daily maximum and average daily minimum temperature. Seasonal warming has varied. The decade of the 2010s through 2018 is the warmest for average daily minimum temperature in all seasons and for average daily maximum temperature in winter and spring but not in summer and fall. Thus, based on the current warming trend in the Southeast, the small areas of cooling seen in Figure 1.2 are projected to disappear in the next 10–30 years.

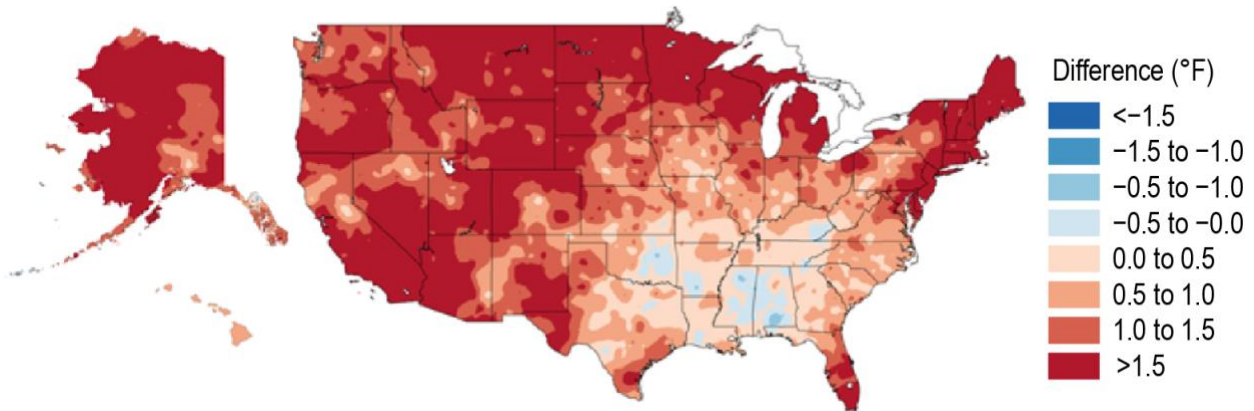## Observed Changes in U.S. Annual Temperature

Figure 1.2. The map shows observed changes in annual average temperature (°F). Changes are the difference between the average for present day (1986–2016) and the average for the first half of the last century (1901–1960) for the contiguous United States (1925–1960 for Alaska and Hawai'i). With the exception of portions of the southeastern United States, all areas show warming. Source: Vose et al. 2017.

1.3.4. Observed Changes in Climate

Surface temperature (land and ocean) in Earth's climate has increased by about 1.8°F (1°C) since the start of the 20th century, and surface temperature continues to increase (Figure 1.1). Although there is a distinct long-term trend, global temperatures do not increase smoothly. There is year-to-year natural variability—due to natural factors such as volcanic eruptions or the El Niño–Southern Oscillation—superimposed on the long-term trend. However, 18 of the 19 warmest years on record have occurred since 2001. Only 1998 was among the 19 warmest prior to 2001, and as noted above, that was mainly due to a powerful El Niño event that typically leads to warm global temperatures.

Spatially, the greatest warming has occurred at the higher latitudes, with some areas of higher-latitude Canada, Alaska, and parts of eastern Russia warming over 3.6°F (2°C), more than twice the change in the global average. However, not all parts of the globe have warmed over this period. In addition to the small net cooling of the southeastern United States discussed above, sea surface temperatures southeast of Greenland also show slight cooling since the start of the 20th century.

Annual average precipitation across global land areas exhibits a slight rise over the past century. However, a statistically significant trend cannot be detected due to a lack of data coverage early in the record (Figure 1.3). Inter-annual and inter-decadal variability is clearly found in all precipitation evaluations, owing to factors such as the North Atlantic Oscillation and El Niño–Southern Oscillation. Unlike surface temperature, which is expected to increase everywhere, annual average precipitation is not expected to increase or decrease in a consistent manner across

31

the globe. Some studies have identified a climate change pattern of wet areas getting wetter and dry areas getting drier (e.g., Greve et al. 2014, Skliris et al. 2016). This pattern is expected with a poleward expansion of the general large-scale tropical circulation (known as the Hadley cell) that should lead to more drying in the subtropics and a poleward shift of storm tracks that should lead to increases in annual average precipitation in wet regions. While this high/low rainfall behavior appears to be valid over ocean areas, changes over land are more complicated (Figure 1.3).
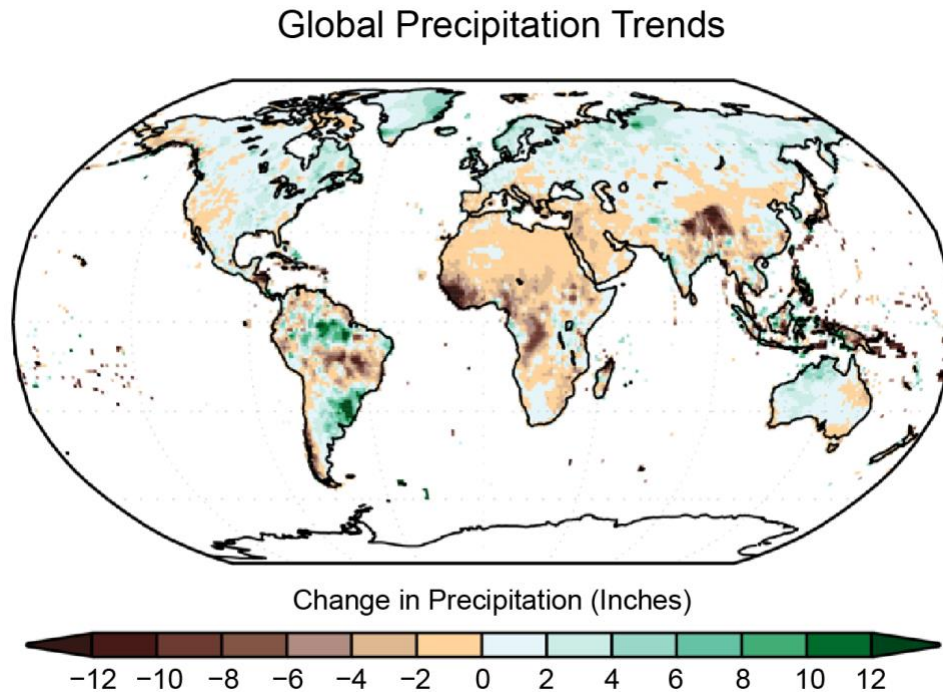

Figure 1.3. The map shows changes in annual average precipitation (in inches) over land for the period 1986–2015 relative to 1901–1960. The data are from land-based stations with long-term records, so precipitation changes over the ocean and Antarctica cannot be evaluated. The trends are not considered to be statistically significant because a lack of data coverage early in the record increases the uncertainty of any trend. The relatively coarse resolution (0.5° × 0.5°) of these maps does not capture the finer details associated with mountains, coastlines, and other small-scale effects. Source: Wuebbles et al. 2017.

Warming of the atmosphere has led to changes in other parts of the climate system. In particular, warming leads to increases in atmospheric water vapor. Increasing temperature results in a greater saturation vapor pressure of about 3.5% per degree Fahrenheit of warming. Global observations of near-surface atmospheric water vapor show that it has increased, consistent with the observed warming of the climate (Seneviratne et al. 2012).

As atmospheric water vapor has increased, observations of extreme precipitation in many parts of the world have also increased (Seneviratne et al. 2012). In the United States, a clear signal of increases in heavy precipitation events has emerged (Easterling et al. 2017). Figure 1.4 shows

regional changes in different measures of heavy precipitation for two different time periods, 1901–2016 and 1958–2016. Averaged across the United States, all measures show an increase over their respective time period (not shown). Regionally, the largest increases have occurred in the northeastern and midwestern United States. However, other regions show much smaller increases, and for the 48-hour accumulation definitions, the southwestern United States shows a small decline, and Hawai'i and Puerto Rico both show declines for the time periods for which there are enough data to analyze.
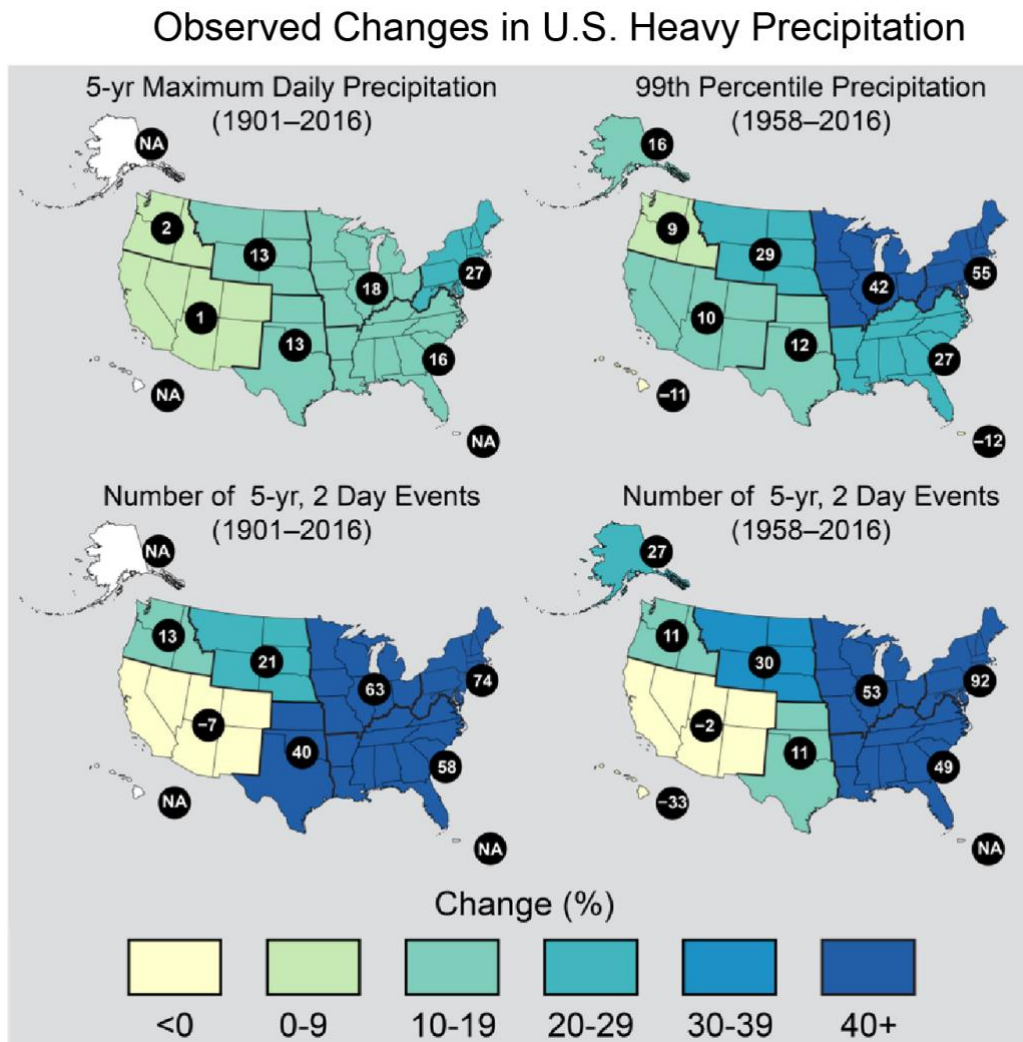

Figure 1.4. These maps show regional changes in several metrics of extreme precipitation. The upper left map shows the percent change in maximum daily precipitation in consecutive 5-year blocks (e.g., the largest amount for each 5-year block rather than the annual maximum values), calculated over 1901–2016. The upper right map shows the percent change in the amount of precipitation falling on days with precipitation totals exceeding the 99th percentile of all non-zero precipitation days, calculated over 1958–2016. The two bottom maps show the percent change in the number of 2-day events with a precipitation total that exceeds the amount

expected to occur once every 5 years; the bottom left is calculated over 1901–2016, and the lower right is calculated over 1958–2016. Source: Easterling et al. 2017.

1.3.5. Other Indicators of a Changing Climate

There are many different types of physical observations, or indicators, that can be used to track how climate is changing. These indicators include changes in temperature and precipitation, as well as observations of arctic sea ice, snow cover, alpine glaciers, growing season length, drought, wildfires, lake levels, and heavy precipitation. Some of these indicators, especially those derived from air temperature and precipitation observations, have nearly continuous data that extend back to the 1800s at a few locations in the United States (e.g., the Blue Hill Meteorological Observatory in Milton, MA; Conover 1990) and the 1600s in Europe (the Central England Temperature Record; Parker, et al. 1992). These long-term datasets document century-scale changes in climate. Satellite-based indicators, on the other hand, extend back only to the late 1970s but provide a comprehensive record of the changes in Earth's surface and atmosphere over the past four decades.

Taken individually, each indicator simply shows changes that are occurring in one aspect of the climate system. Taken as a whole, however, in the context of scientific understanding of the climate system, the cumulative changes documented by each of these indicators paint a compelling and consistent picture of a warming world. For example, arctic sea ice has declined since the late 1970s, most glaciers have retreated, the frost-free season has lengthened, heavy precipitation events have increased in the United States and elsewhere in the world, and sea level has risen. Each of these indicators, and many more, are changing in ways that are consistent with a warming climate (see Figure 1.2 in Jay et al. 2018).

1.4. Detection and Attribution

Detection and attribution studies are used to determine whether a human influence on certain observed changes in climate can be distinguished from natural variability. These studies are performed through the systematic comparison of climate models and observations using various statistical methods, and they can be performed on a variety of scales from global to regional. Detection and attribution studies can help determine whether model simulations of historical climate conditions are consistent with observed climate trends. Results from these studies can help inform decision-making on climate policy and adaptation (Knutson et al. 2017).

Detection and attribution studies of several types can be used to examine the cause of changes in long-term climate trends (such as changes in average temperature or precipitation), changes in extremes (such as extreme heat or heavy precipitation), specific weather or climate events, and climate-related impacts. These studies can also be used to estimate the climate sensitivity by using observations to constrain climate models. Paleoclimate data (derived by analyzing natural sources including tree rings, ice cores, and corals) can provide a much longer-term record against which recent observations can be compared (Knutson et al. 2017).

Figure 1.5 shows a comparison of observed global annual average temperatures (calculated as annual differences from the 1901–1960 average) with historical simulations from climate models. The spread of different individual model simulations (the blue and orange shading) arises both from differences in how the different models respond to the various climate forcing agents (natural and anthropogenic) and from internal (unforced) climate variability. Observed annual temperatures after about 1960 are shown to be inconsistent with models that include only natural forcings (blue shading) but are consistent with the model simulations that include both human and natural forcing (orange shading). This implies that the observed global warming is attributable in large part to anthropogenic forcing. Furthermore, these studies—as well as the consistency of observed changes in other variables such as increases in sea level, atmospheric water vapor, and heavy precipitation events and decreases in arctic sea ice cover—led the Intergovernmental Panel on Climate Change to state in their 5th Assessment Report of 2013, "It is *extremely likely* that more than half of the observed increase in global average surface temperature from 1951 to 2010 was caused by the anthropogenic increase in greenhouse gas concentrations and other anthropogenic forcings together" (IPCC 2013). More recently, the IPCC report on global warming of 1.5°C concluded that amount of human-induced warming matches the observed warming to within ±20% (the *likely* range; IPCC 2018).
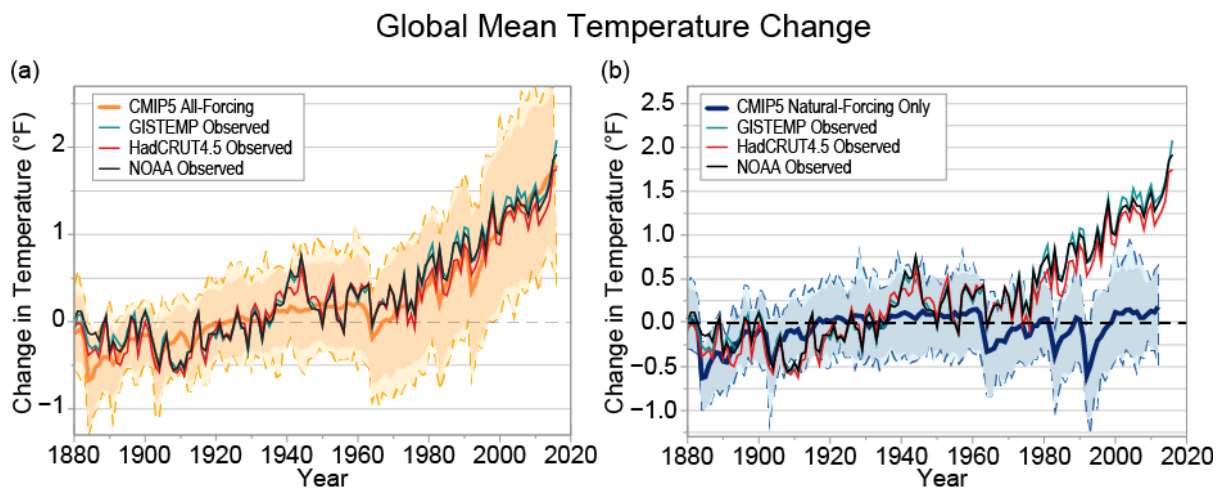

Figure 1.5. The figure compares observed global surface air temperature, computed as differences from the 1901–1960 average, to global climate model historical experiments from the Coupled Model Intercomparison Project 5 (CMIP5) for the 1880–2016 period using (a) human forcings (greenhouse gas increases and land-use and aerosol changes) and natural forcings (solar variations and volcanic eruptions) and (b) only natural forcings. In (a), the thick orange line shows the average from 36 CIMP5 models, while the orange shading and outer dashed lines depict the ±2 standard-deviation and absolute ranges, respectively, of annual differences across all the model simulations. In (b), the blue line and shading depict the same information, but for results from 18 CMIP5 models using only natural forcings. Because the modeling of natural forcings alone, shown by the blue line, exhibits no net change in

temperature from 1800–2016, it is clear that the observed warming is not explained by natural variability alone. Source: Knutson et al. 2017.

Another area of attribution deals with individual extreme events, such as droughts or hurricanes. When an extreme weather event occurs, people often ask whether the event was caused by climate change. A more appropriate framing for the question is whether climate change has altered the odds of occurrence of an extreme event. Extreme event attribution studies to date have generally been concerned with answering the latter question. The European heat wave of 2003 and Australia's extreme temperatures and heat indices of 2013 (e.g., Arblaster et al. 2014, King et al. 2014, Knutson et al. 2013, Lewis and Karoly 2014, Perkins et al. 2014) are examples of extreme weather or climate events where relatively strong evidence for a human contribution to the event has been found. In a new twist on event attribution, and highly relevant to North Carolina, recent research into Hurricane Florence in a forecasting sense predicted in advance that the storm would be slightly more intense, have increased rainfall, and would be a larger storm than what would have occurred without anthropogenic forcing (Reed et al. 2020). Post-storm analysis showed that, indeed, all three changes did occur and could be attributed to climate change, although none of the three were as large as predicted.

1.5. Climate Models

Climate models are the main tool scientists use to examine how the climate will change in response to future changes in greenhouse gases, land use, and other forcing factors. They are also useful for examining how much impact humans have already had on the climate. Climate models, which are similar to the computer models used to forecast weather, are complex computer programs based on equations that represent fundamental laws of nature and the many processes that affect Earth's climate system. These models represent the atmosphere, land, and ocean system as an aggregate of adjacent small boxes. The equations are solved for each box to represent the global weather patterns. By stepping forward sequentially in time, the climate models capture the evolving short-term (e.g., daily) patterns of atmospheric pressures, winds, temperatures, and precipitation. Over longer time frames (e.g., weeks to months), these models simulate wind patterns, high- and low-pressure systems, ocean currents, ice and snowpack accumulation and melting, soil moisture, extreme weather occurrences, and other environmental characteristics that make up the climate system.

Some important processes, including cloud formation and atmospheric mixing, are represented by approximate relationships, either because the processes are too complex to model given current technologies or they operate at scales that are too small scale to represent directly. These approximations lead to uncertainties in model simulations of climate. In addition to uncertainties due to model formulation, there are uncertainties related to how greenhouse gases, land use, and other forcing factors will change in the future.

1.6. Climate Projections and Scenarios

Human production of greenhouse gases has already increased the natural greenhouse effect, resulting in a planet that is in a state of energy imbalance, in which infrared radiation escaping to space does not match the incoming flux of solar radiation. This extra energy goes primarily to warming Earth's oceans. How much climate change occurs over the next few decades will mainly depend on the amount of greenhouse gases that are emitted to the atmosphere; how much is absorbed by the biosphere, oceans, and other sinks; and the sensitivity of the climate to those emissions (Hawkins and Sutton, 2009).

Since the Earth's climate system takes time to fully respond to changes in greenhouse gas concentrations, even if greenhouse gas levels stabilized today, it is ***virtually certain*** that the climate will continue to warm. Further, it is ***virtually certain*** that other changes in the climate system, such as sea level rise, will continue (Allen et al. 2018). In short, the climate system has inertia, and this would need to be accounted for in order to avoid certain climate thresholds. Much as a ship must reverse its engines long before it strikes a dock, emissions must be reduced long before climate thresholds are reached.

Continued warming is ***virtually certain*** if greenhouse gas concentrations continue to increase from human activities, including fossil fuel combustion and large-scale deforestation (Figure 1.6; Hayhoe et al. 2018). With additional emissions, the projected changes in global average temperature for the end of this century (2080–2099) relative to 1996–2015 are 3.6°–8.2°F under a higher scenario (RCP8.5) and 1.1°–4.1°F under a lower scenario (RCP4.5) (see the Guide to the Report for more information on these scenarios; following Hayhoe et al. 2017). If society were to reduce net emissions to near zero over the next decade to two, the climate would still warm but by smaller amounts. Further, given the very long times needed for the oceans to absorb excess heat, emissions of greenhouse gases through the rest of this century will have a lasting legacy of warming that will persist for more than 10,000 years (Friedlingstein et al. 2011).

Virtually all model simulations show the greatest warming occurring at the highest latitudes in both hemispheres. As discussed above, with the expected warming of the climate, an increase in atmospheric water vapor is also expected. However, model projections of heavy precipitation remain problematic because heavy rainstorms are too small in spatial extent to be captured by current climate models (Hayhoe et al. 2017); models universally show large increases in heavy precipitation events in both low- and high-emissions simulations for the 21st century.
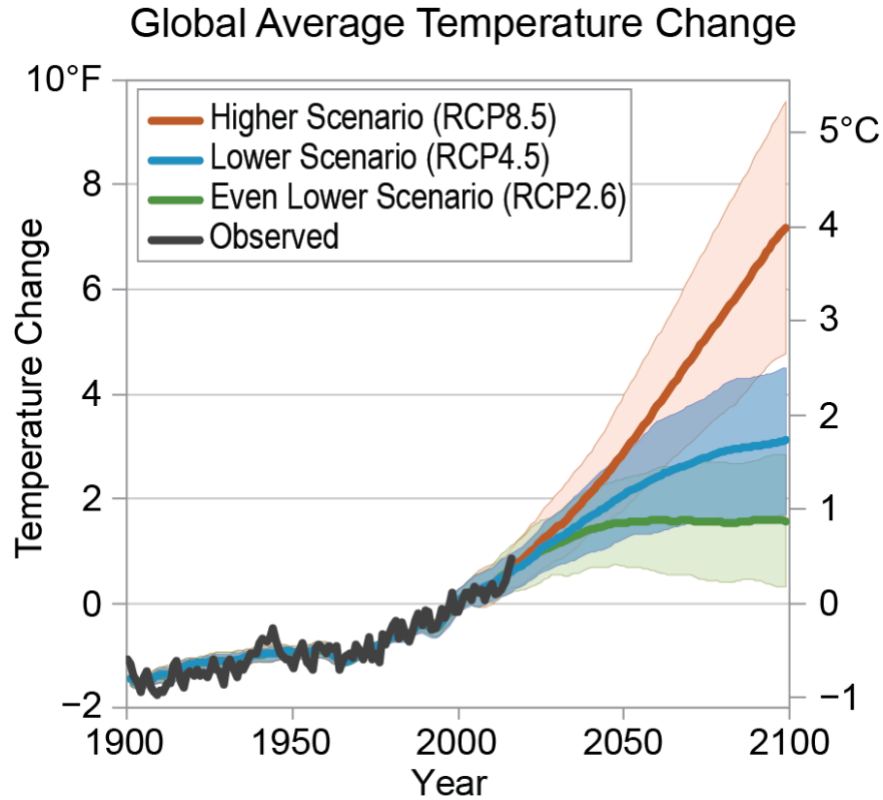
Global Average Temperature Change

Figure 1.6. The figure shows observed and multimodel simulations of globally averaged surface temperature change relative to the 1986–2015 average. Observations (heavy black line) are shown for the 1901–2016 period. Model simulations for the historical period (1900–2005) are based on observed changes in greenhouse gases, aerosols, and land-use change, and projections (2006–2100) are based on three Representation Concentration Pathway scenarios (see Guide to the Report). The burnt-orange, blue, and green lines for the model simulations show the averages from multiple climate models, and the shaded ranges show the 5% to 95% confidence intervals for the respective simulations. Source: adapted from Hayhoe et al. 2018.

1.7 References

Allen, M.R., O.P. Dube, W. Solecki, F. Aragón-Durand, W. Cramer, S. Humphreys, M. Kainuma, J. Kala, N. Mahowald, Y. Mulugetta, R. Perez, M. Wairiu, and K. Zickfeld, 2018: Framing and Context. *Global Warming of 1.5°C. An IPCC Special Report on the impacts of global warming of 1.5°C above pre-industrial levels and related global greenhouse gas emission pathways, in the context of strengthening the global response to the threat of climate change, sustainable development, and efforts to eradicate poverty*. Masson-Delmotte, V., P. Zhai, H.-O. Pörtner, D. Roberts, J. Skea, P.R. Shukla, A. Pirani, W. Moufouma-Okia, C. Péan, R. Pidcock, S. Connors, J.B.R. Matthews, Y. Chen, X. Zhou, M.I. Gomis, E. Lonnoy, T. Maycock, M. Tignor, and T. Waterfield, Eds. World Meteorological Organization, in press. https://www.ipcc.ch/sr15/

Arblaster, J.M., E.-P. Lim, H.H. Hendon, B.C. Trewin, M.C. Wheeler, G. Liu, and K. Braganza, 2014: Understanding Australia's hottest September on record [in "Explaining Extreme Events of 2013 from a Climate Perspective"]. *Bulletin of the American Meteorological Society,* **95 (9)**, S37–S41. http://dx.doi.org/10.1175/1520-0477-95.9.S1.1

Conover, J.H., 1990: *The Blue Hill Meteorological Observatory: The First 100 Years, 1885–1985*. American Meteorological Society, Boston, MA, 514 pp.

Easterling, D.R. and M.F. Wehner, 2009: Is the climate warming or cooling? *Geophysical Research Letters,* **36** (8). http://dx.doi.org/10.1029/2009GL037810

Easterling, D.R., K.E. Kunkel, J.R. Arnold, T. Knutson, A.N. LeGrande, L.R. Leung, R.S. Vose, D.E. Waliser, and M.F. Wehner, 2017: Precipitation change in the United States. *Climate Science Special Report: Fourth National Climate Assessment, Volume I*. Wuebbles, D.J., D.W. Fahey, K.A. Hibbard, D.J. Dokken, B.C. Stewart, and T.K. Maycock, Eds. U.S. Global Change Research Program, Washington, DC, USA, 207–230. http://dx.doi.org/10.7930/J0H993CC

Fahey, D.W., S. Doherty, K.A. Hibbard, A. Romanou, and P.C. Taylor, 2017: Physical drivers of climate change. *Climate Science Special Report: Fourth National Climate Assessment, Volume I*. Wuebbles, D.J., D.W. Fahey, K.A. Hibbard, D.J. Dokken, B.C. Stewart, and T.K. Maycock, Eds. U.S. Global Change Research Program, Washington, DC, USA, 73–113. http://dx.doi.org/10.7930/J0513WCR

Friedlingstein, P., S. Solomon, G.K. Plattner, R. Knutti, P. Ciais, and M.R. Raupach, 2011: Long-term climate implications of twenty-first century options for carbon dioxide emission mitigation. *Nature Climate Change,* **1**, 457–461. http://dx.doi.org/10.1038/nclimate1302

Greve, P., B. Orlowsky, B. Mueller, J. Sheffield, M. Reichstein, and S.I. Seneviratne, 2014: Global assessment of trends in wetting and drying over land. *Nature Geoscience,* **7** (10), 716–721. http://dx.doi.org/10.1038/ngeo2247

Hawkins, E. and R. Sutton, 2009: The potential to narrow uncertainty in regional climate predictions. *Bulletin of the American Meteorological Society,* **90** (8), 1095–1107. http://dx.doi.org/10.1175/2009BAMS2607.1

Hayhoe, K., J. Edmonds, R.E. Kopp, A.N. LeGrande, B.M. Sanderson, M.F. Wehner, and D.J. Wuebbles, 2017: Climate models, scenarios, and projections. *Climate Science Special Report: Fourth National Climate Assessment, Volume I*. Wuebbles, D.J., D.W. Fahey, K.A. Hibbard, D.J. Dokken, B.C. Stewart, and T.K. Maycock, Eds. U.S. Global Change Research Program, Washington, DC, USA, 133–160. http://dx.doi.org/10.7930/J0WH2N54

Hayhoe, K., D.J. Wuebbles, D.R. Easterling, D.W. Fahey, S. Doherty, J. Kossin, W. Sweet, R. Vose, and M. Wehner, 2018: Our Changing Climate. *Impacts, Risks, and Adaptation in the United States: Fourth National Climate*

Assessment, Volume II. Reidmiller, D.R., C.W. Avery, D. Easterling, K. Kunkel, K.L.M. Lewis, T.K. Maycock, and B.C. Stewart, Eds. U.S. Global Change Research Program, Washington, DC, USA, 72–144. http://dx.doi.org/10.7930/NCA4.2018.CH2

IPCC, 2013: *Climate Change 2013: The Physical Science Basis. Contribution of Working Group I to the Fifth Assessment Report of the Intergovernmental Panel on Climate Change*. Stocker, T.F., D. Qin, G.-K. Plattner, M. Tignor, S.K. Allen, J. Boschung, A. Nauels, Y. Xia, V. Bex, and P.M. Midgley, Eds. Cambridge University Press, Cambridge, UK and New York, NY, 1535 pp. http://www.climatechange2013.org/report/

IPCC, 2018: Summary for Policymakers. *Global Warming of 1.5°C. An IPCC special report on the impacts of global warming of 1.5°C above pre-industrial levels and related global greenhouse gas emission pathways, in the context of strengthening the global response to the threat of climate change, sustainable development, and efforts to eradicate poverty*. Masson-Delmotte, V., P. Zhai, H.-O. Pörtner, D. Roberts, J. Skea, P.R. Shukla, A. Pirani, W. Moufouma-Okia, C. Péan, R. Pidcock, S. Connors, J.B.R. Matthews, Y. Chen, X. Zhou, M.I. Gomis, E. Lonnoy, T. Maycock, M. Tignor, and T. Waterfield, Eds. World Meteorological Organization, Geneva, Switzerland, 32. https://www.ipcc.ch/sr15/chapter/spm/

Jay, A., D.R. Reidmiller, C.W. Avery, D. Barrie, B.J. DeAngelo, A. Dave, M. Dzaugis, M. Kolian, K.L.M. Lewis, K. Reeves, T. West, and D. Winner, 2018: Overview. *Impacts, Risks, and Adaptation in the United States: Fourth National Climate Assessment, Volume II*. Reidmiller, D.R., C.W. Avery, D. Easterling, K. Kunkel, K.L.M. Lewis, T.K. Maycock, and B.C. Stewart, Eds. U.S. Global Change Research Program, Washington, DC, USA, 33–71. http://dx.doi.org/10.7930/NCA4.2018.CH1

King, A.D., D.J. Karoly, M.G. Donat, and L.V. Alexander, 2014: Climate change turns Australia's 2013 big dry into a year of record-breaking heat [in "Explaining Extreme Events of 2013 from a Climate Perspective"]. *Bulletin of the American Meteorological Society,* **95 (9)**, S41–S45. http://dx.doi.org/10.1175/1520-0477-95.9.S1.1

Knutson, T., J.P. Kossin, C. Mears, J. Perlwitz, and M.F. Wehner, 2017: Detection and attribution of climate change. *Climate Science Special Report: Fourth National Climate Assessment, Volume I*. Wuebbles, D.J., D.W. Fahey, K.A. Hibbard, D.J. Dokken, B.C. Stewart, and T.K. Maycock, Eds. U.S. Global Change Research Program, Washington, DC, USA, 114–132. http://dx.doi.org/10.7930/J01834ND

Knutson, T.R., F. Zeng, and A.T. Wittenberg, 2013: Multimodel assessment of regional surface temperature trends: CMIP3 and CMIP5 twentieth-century simulations. *Journal of Climate,* **26** (22), 8709–8743. http://dx.doi.org/10.1175/JCLI-D-12-00567.1

Lewis, S. and D.J. Karoly, 2014: The role of anthropogenic forcing in the record 2013 Australia-wide annual and spring temperatures [in "Explaining Extreme Events of 2013 from a Climate Perspective"]. *Bulletin of the American Meteorological Society,* **95 (9)**, S31–S33. http://dx.doi.org/10.1175/1520-0477-95.9.S1.1

Meehl, G.A., J.M. Arblaster, and G. Branstator, 2012: Mechanisms contributing to the warming hole and the consequent US east–west differential of heat extremes. *Journal of Climate,* **25** (2012), 6394–6408. http://dx.doi.org/10.1175/JCLI-D-11-00655.1

Myhre, G., D. Shindell, F.-M. Bréon, W. Collins, J. Fuglestvedt, J. Huang, D. Koch, J.-F. Lamarque, D. Lee, B. Mendoza, T. Nakajima, A. Robock, G. Stephens, T. Takemura, and H. Zhang, 2013: Anthropogenic and natural radiative forcing. *Climate Change 2013: The Physical Science Basis. Contribution of Working Group I to the Fifth Assessment Report of the Intergovernmental Panel on Climate Change*. Stocker, T.F., D. Qin, G.-K. Plattner, M. Tignor, S.K. Allen, J. Boschung, A. Nauels, Y. Xia, V. Bex, and P.M. Midgley, Eds. Cambridge University Press, Cambridge, United Kingdom and New York, NY, USA, 659–740. http://www.climatechange2013.org/images/report/WG1AR5_Chapter08_FINAL.pdf

NASA, n.d.: Earth System Science: The Study of Earth as an Integrated System. National Aeronautics and Space Administration, accessed November 20, 2019. https://climate.nasa.gov/nasa_science/science/

NCEI, 2019: Climate at a Glance. Global Time Series: Global Land and Ocean Temperature Anomalies, 1880–2018 [web tool]. NOAA National Centers for Environmental Information (NCEI), Asheville, NC, accessed November 19, 2019. https://www.ncdc.noaa.gov/cag/global/time-series/globe/land_ocean/ytd/12/1880-2018

Pan, Z., R.W. Arritt, E.S. Takle, W.J. Gutowski, Jr., C.J. Anderson, and M. Segal, 2004: Altered hydrologic feedback in a warming climate introduces a "warming hole". *Geophysical Research Letters,* **31** (17), L17109. http://dx.doi.org/10.1029/2004GL020528

Parker, D.E., T.P. Legg, and C.K. Folland, 1992: A new daily central England temperature series, 1772–1991. *International Journal of Climatology,* **12** (4), 317–342. http://dx.doi.org/10.1002/joc.3370120402

Parker, D.E., H. Wilson, P.D. Jones, J.R. Christy, and C.K. Folland, 1996: The impact of Mount Pinatubo on world-wide temperatures *International Journal of Climatology,* **16** (5), 487–497. http://dx.doi.org/10.1002/(SICI)1097-0088(199605)16:5<487::AID-JOC39>3.0.CO;2-J

Partridge, T.F., J.M. Winter, E.C. Osterberg, D.W. Hyndman, A.D. Kendall, and F.J. Magilligan, 2018: Spatially Distinct Seasonal Patterns and Forcings of the U.S. Warming Hole. *Geophysical Research Letters,* **45** (4), 2055–2063. http://dx.doi.org/10.1002/2017GL076463

Perkins, S.E., S.C. Lewis, A.D. King, and L.V. Alexander, 2014: Increased simulated risk of the hot Australian summer of 2012/13 due to anthropogenic activity as measured by heat wave frequency and intensity [in "Explaining Extreme Events of 2013 from a Climate Perspective"]. *Bulletin of the American Meteorological Society,* **95 (9)**, S34–S37. http://dx.doi.org/10.1175/1520-0477-95.9.S1.1

Reed, K.A., A.M. Stansfield, M.F. Wehner, and C.M. Zarzycki, 2020: Forecasted attribution of the human influence on Hurricane Florence. *Science Advances,* **6** (1), eaaw9253. http://dx.doi.org/10.1126/sciadv.aaw9253

Seneviratne, S.I., N. Nicholls, D. Easterling, C.M. Goodess, S. Kanae, J. Kossin, Y. Luo, J. Marengo, K. McInnes, M. Rahimi, M. Reichstein, A. Sorteberg, C. Vera, and X. Zhang, 2012: Changes in climate extremes and their impacts on the natural physical environment. *Managing the Risks of Extreme Events and Disasters to Advance Climate Change Adaptation. A Special Report of Working Groups I and II of the Intergovernmental Panel on Climate Change (IPCC).* Field, C.B., V. Barros, T.F. Stocker, Q. Dahe, D.J. Dokken, K.L. Ebi, M.D. Mastrandrea, K.J. Mach, G.-K. Plattner, S.K. Allen, M. Tignor, and P.M. Midgley, Eds. Cambridge University Press, Cambridge, UK, and New York, NY, USA, 109–230. https://www.ipcc.ch/report/managing-the-risks-of-extreme-events-and-disasters-to-advance-climate-change-adaptation/

Skliris, N., J.D. Zika, G. Nurser, S.A. Josey, and R. Marsh, 2016: Global water cycle amplifying at less than the Clausius-Clapeyron rate. *Scientific Reports,* **6** (1), 38752. http://dx.doi.org/10.1038/srep38752

State Climate Office of North Carolina, n.d.: Global Patterns: Arctic and North Atlantic Oscillations, accessed February 11, 2020. https://climate.ncsu.edu/climate/patterns/nao

Tans, P. and R. Keeling, 2020: Trends in Atmospheric Carbon Dioxide. NOAA Earth System Research Laboratory. https://www.esrl.noaa.gov/gmd/ccgg/trends/data.html

USGCRP, 2017: Scenarios for the National Climate Assessment: LOCA Viewer [web tool]. U.S. Global Change Research Program, Washington, DC. https://scenarios.globalchange.gov/loca-viewer/

USGCRP, 2018: *Impacts, Risks, and Adaptation in the United States: Fourth National Climate Assessment, Volume II*. Reidmiller, D.R., C.W. Avery, D.R. Easterling, K.E. Kunkel, K.L.M. Lewis, T.K. Maycock, and B.C. Stewart, Eds. U.S. Global Change Research Program, Washington, DC, USA, 1515 pp. http://dx.doi.org/10.7930/NCA4.2018

Vose, R.S., D.R. Easterling, K.E. Kunkel, A.N. LeGrande, and M.F. Wehner, 2017: Temperature changes in the United States. *Climate Science Special Report: Fourth National Climate Assessment, Volume I*. Wuebbles, D.J., D.W. Fahey, K.A. Hibbard, D.J. Dokken, B.C. Stewart, and T.K. Maycock, Eds. U.S. Global Change Research Program, Washington, DC, USA, 185–206. http://dx.doi.org/10.7930/J0N29V45

Walsh, J., D. Wuebbles, K. Hayhoe, J. Kossin, K. Kunkel, G. Stephens, P. Thorne, R. Vose, M. Wehner, J. Willis, D. Anderson, S. Doney, R. Feely, P. Hennon, V. Kharin, T. Knutson, F. Landerer, T. Lenton, J. Kennedy, and R. Somerville, 2014: Ch. 2: Our changing climate. *Climate Change Impacts in the United States: The Third National Climate Assessment*. Melillo, J.M., T.C. Richmond, and G.W. Yohe, Eds. U.S. Global Change Research Program, Washington, DC, 19–67. http://dx.doi.org/10.7930/J0KW5CXT

Wuebbles, D.J., D.R. Easterling, K. Hayhoe, T. Knutson, R.E. Kopp, J.P. Kossin, K.E. Kunkel, A.N. LeGrande, C. Mears, W.V. Sweet, P.C. Taylor, R.S. Vose, and M.F. Wehner, 2017: Our globally changing climate. *Climate Science Special Report: Fourth National Climate Assessment, Volume I*. Wuebbles, D.J., D.W. Fahey, K.A. Hibbard, D.J. Dokken, B.C. Stewart, and T.K. Maycock, Eds. U.S. Global Change Research Program, Washington, DC, USA, 35–72. http://dx.doi.org/10.7930/J08S4N35

2. Statewide Changes in Temperature, Precipitation, and Storms

2.1 Introduction

North Carolina has a humid climate with very warm summers and moderately cold winters. The climate exhibits substantial regional variation due to the state's diverse topography, which includes the Appalachian Mountains in the west, the Piedmont Plateau in the central region, and the Coastal Plain to the east. Elevations across the state range from sea level along the Atlantic coast to over 6,000 feet at the peak of Mt. Mitchell, the highest point east of the Mississippi River. In summer, the state's elevation and proximity to the ocean keep temperatures relatively cooler in the mountains and along the coast compared to inland. In winter, temperatures are somewhat moderated by the Appalachian Mountains, which partially block cold air coming from the Midwest (Frankson et al. 2017, 2019 update).

There are no distinct wet and dry seasons in North Carolina. However, summer precipitation is normally the greatest and most variable, owing to shower and thunderstorm activity, and fall is generally the driest season. The mountains show large spatial variability in rainfall due to orographic (mountain) effects on precipitation. For example, Lake Toxaway and Asheville are the wettest and driest places in the state, respectively, in terms of average annual precipitation, and they are separated by only about 40 miles (State Climate Office of North Carolina n.d.). Lake Toxaway is close to where the mountains rise up from the Piedmont, so it gets a lot of upslope rainfall, which is where moist air rises up the slope and cools, causing the moisture to condense into clouds and rain. Asheville is east of the Smokies and in a rain shadow, meaning much of the rainfall is blocked by the high mountains to the west.

See Appendix A for details on the datasets and scenarios used in this chapter.

2.2 Temperature Changes in North Carolina

2.2.1 Averages

North Carolina's annual average temperature has increased by about 1°F since 1895, which is less than temperature increases in northern and western portions of the United States. North Carolina is part of a larger region of the southeastern United States that has exhibited less overall warming in surface temperatures than the rest of the United States over the 20th century. During the 40-year period of the 1920s through 1950s, a majority (25) of the years were warmer than the long-term average, followed by a cool period in the 1960s and 1970s, when only 3 years were above average. Since that time, temperatures have steadily increased, with average temperatures being consistently above normal since the 1990s (Figure 2.1) and with 20 out of the last 29 years being above the long-term (1895–2018) average. Summer average temperatures have been the warmest on record over the last 14 years (Figure 2.2), including the first (2010), second (2011),

and third (2016) warmest summers. Winter average temperatures have been warmer than normal over the last 14 years (Figure 2.2), but not record breaking, with two earlier historical 14-year periods (1989–2002 and 1921–1934) being equally warm.

Climate models suggest the current warming trend will continue and project significant increases by the middle and end of the century. Projected values are shown for two climate futures: a higher scenario (RCP8.5), in which greenhouse gas emissions continue to increase, and a lower scenario (RCP4.5), in which emissions increase at a slower rate (Figure 2.3). By 2050, models project that the annual average temperature in North Carolina will increase by 2°–4°F under a lower scenario and by 2°–5°F under a higher scenario, compared to the average temperature for 1996-2015. By the 2100, the average temperature is projected to increase by 2°–6°F under a lower scenario and by 6°–10°F under a higher scenario, compared to the average temperature for 1996–2015. Figure 2.3 also shows the observed average temperature value for the period 1970–2013 (this average is based on a different observational dataset than the one shown in Figure 2.1 in order to provide the most consistent comparison with model simulations—see Appendix A for details).

The observed temperatures have tended to be on the lower end of the range of historical model simulations (Frankson et al. 2017; 2019 update), which suggests that the lower end of the projected values is a more likely outcome for the future. However, since the causes of the lesser warming observed in the Southeast are not yet fully understood and recent years have exhibited substantial warming, the higher end of the projected values should not be discounted as a possibility.

Observed Annual Average Temperature
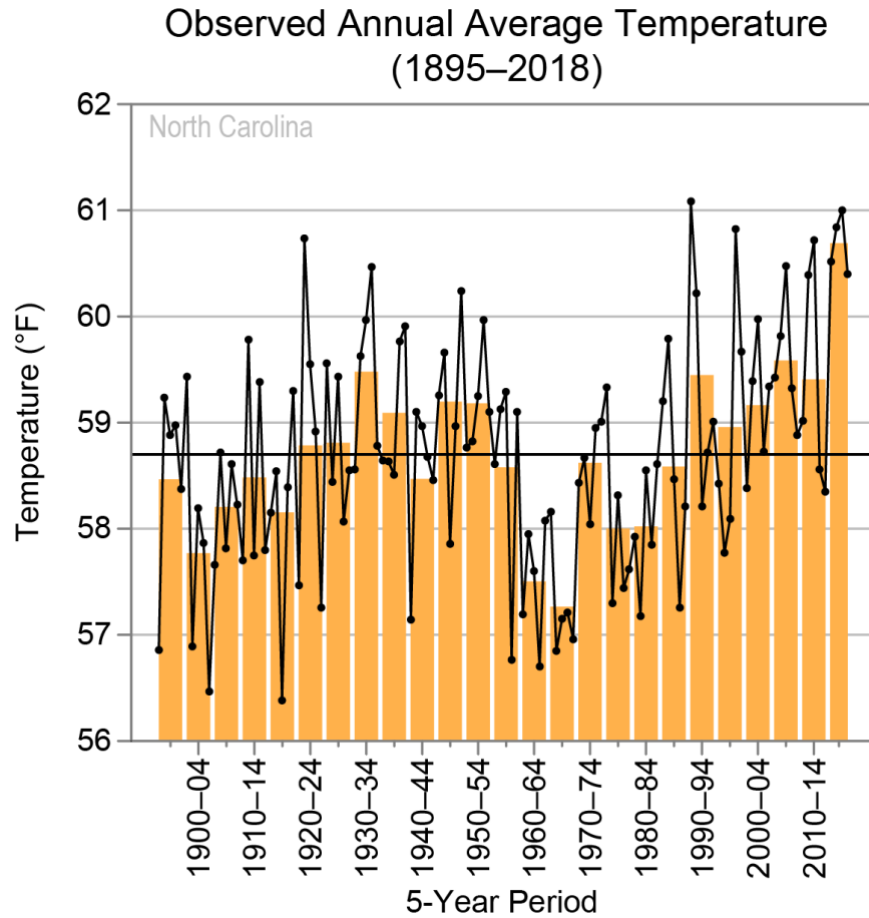## (1895–2018)

Figure 2.1. The bar graph shows the observed annual average temperature for North Carolina for 1895–2018, as averaged over 5-year periods, with the last bar representing a 4-year period (2015–2018). Dots show annual values. The horizontal black line shows the long-term average of 58.7°F for 1895–2018. Source: Frankson et al. 2017, 2019 update.
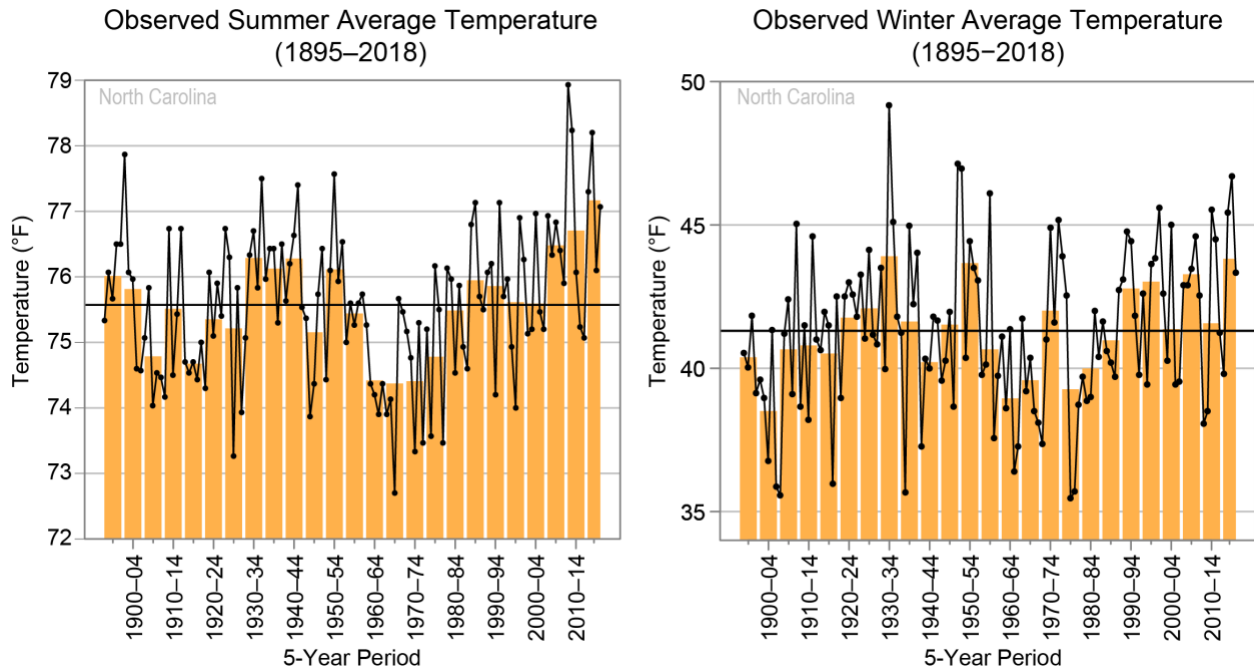
Figure 2.2. The bar graphs show the observed summer and winter average temperatures for North Carolina for 1895–2018, as averaged over 5-year periods, with the last bar representing a 4-year period (2015–2018). Dots show annual values. The horizontal black lines show the long-term summer average of 75.6°F and winter average of 41.3°F for 1895–2018. The 1930s and 1950s were some of the warmest periods in North Carolina's history, while the 1960s–70s was a cool period for the state. The summer multiyear averages over the last 14 years (2005–2018) have been the warmest on record. The winter multiyear average of 2005–2018 ties for the warmest on record with 1921–1934 and 1989–2002. Source: Frankson et al. 2017, 2019 update.

Observed and Projected
Annual Average Temperature (1970–2100)
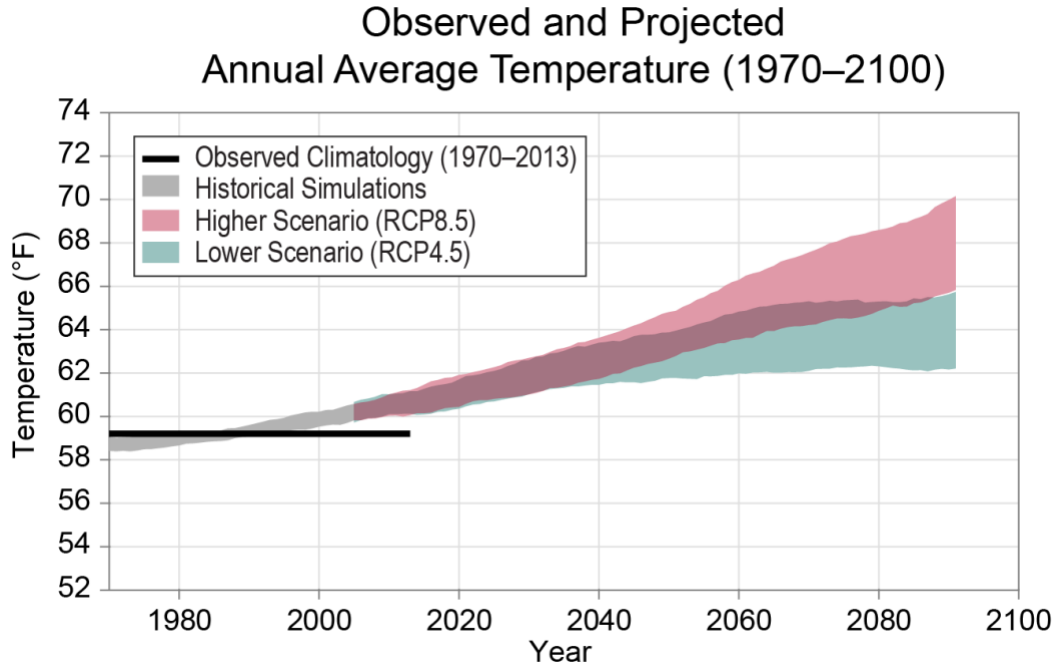
Figure 2.3. These time series show the simulated historical and projected annual average temperature for North Carolina from the LOCA data and the observed climatological value averaged for the period 1970–2013 (black line). Historical simulations (gray shading) are shown for 1970–2005. Projected changes for 2006–2100 are shown for a higher scenario (RCP8.5; red shading) and a lower scenario (RCP4.5; green shading). The shaded ranges indicate the 10% to 90% confidence intervals of 20-year running averages from the set of climate models. Sources: NCICS and The University of Edinburgh.

2.2.2 Extremes

The frequency of very hot days (maximum temperature of 95°F or higher; Figure 2.4) was highest in the 1930s through early 1950s. This was followed by a period of very low occurrences in the 1960s and early 1970s. Since the late 1970s, the number has fluctuated around the long-term (1900–2018) average of 10 days per year with no trend. By contrast, the number of very warm nights (minimum temperature of 75°F or higher) has been well above average since 2005, with 2010 setting a record with a statewide average of 14 (Figure 2.5). The number of very warm nights during 2008–2017 is higher than during any other consecutive 10-year period.

Observed Annual Number of Very Hot Days
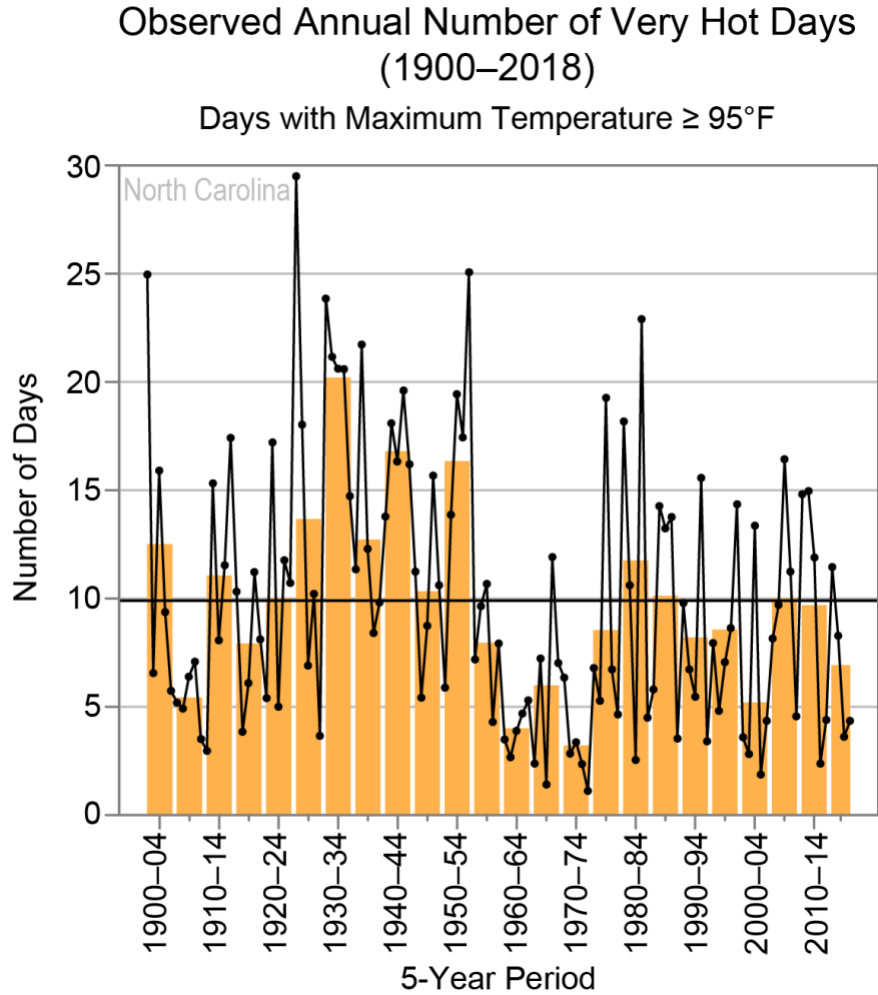## (1900–2018)

Days with Maximum Temperature ≥ 95°F
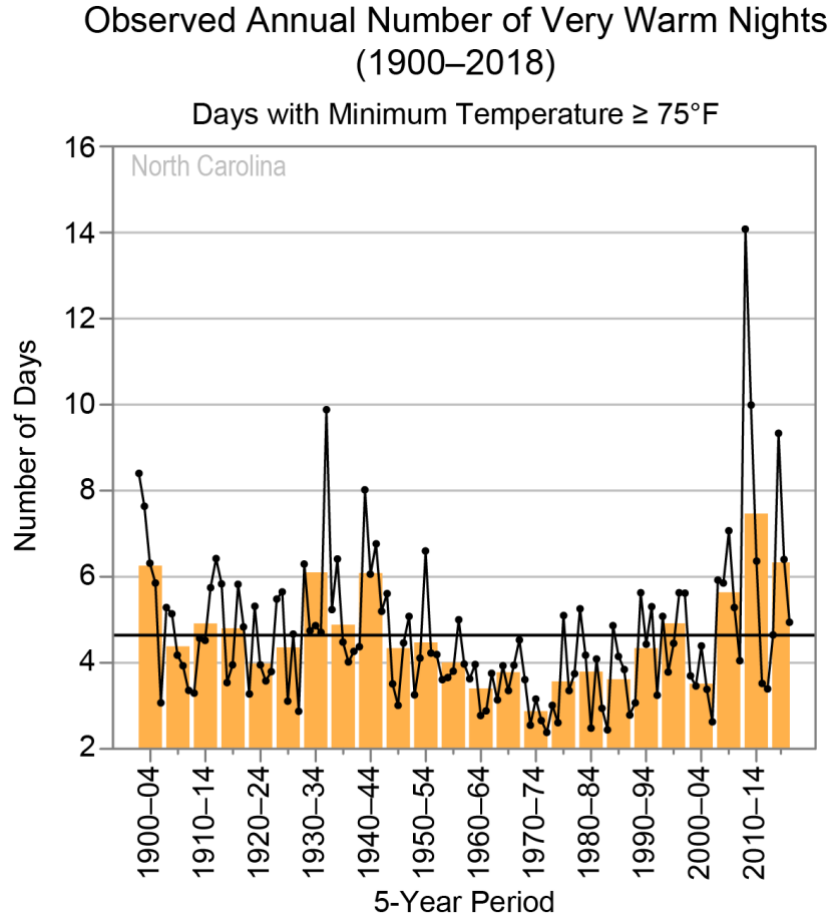

Figure 2.4. The bar graph shows the observed annual number of very hot days (maximum temperature of 95°F or higher) for North Carolina for 1900–2018, as averaged over 5-year periods, with the last bar representing a 4-year period (2015–2018). Dots show annual values. The horizontal black line shows the long-term average of 9.9 very hot days per year for 1900–2018. North Carolina has not experienced an increase in the frequency of very hot days. Source: Frankson et al. 2017, 2019 update.

Observed Annual Number of Very Warm Nights
(1900–2018)

Days with Minimum Temperature ≥ 75°F

Figure 2.5. The bar graph shows the observed annual number of very warm nights (minimum temperature of 75°F or higher) for North Carolina for 1900–2018, as averaged over 5-year periods, with the last bar representing a 4-year period (2015–2018). Dots show annual values. The horizontal black line shows the long-term average of 4.6 very warm nights per year for 1900–2018. The second half of the 20th century was a cool period for North Carolina, with the frequency of very warm nights well below the long-term average. The 5-year period of 2010–2014 saw the largest number of very warm nights in the historical record, almost double the long-term average. Source: Frankson et al. 2017, 2019 update.

Extreme temperatures above these thresholds are far more common in the Piedmont and Coastal Plain than in the Western Mountains. However, climate models project increases across most of the state, including the Mountains, by 2041–2060 (Figure 2.6 and Figure 2.7).

For 2021–2040, climate models project little to no change in the number of very hot days or very warm nights in the Mountains. However, across much of the Piedmont and Coastal Plain, the number of very hot days is projected to increase by 10 to 20 days per year as compared to the 1996–2015 average (Figure 2.6a). The number of very warm nights is projected to increase by 3 to 15 per year across much of the Piedmont and Coastal Plain, with some areas projected to increase by 18 or more per year over the 1996–2015 average (Figure 2.7a).

By 2041–2060, projected increases are notably larger for both very hot days and very warm nights under both the higher (RCP8.5) and lower (RCP4.5) scenarios. Under the lower scenario, the number of very hot days is projected to increase across most of the state, with increases in the Mountains of up to 15 days per year in the westernmost tip of the state. Increases in the Piedmont are generally between 15 and 25 days per year, with some isolated regions exceeding an increase of 25 days per year (Figure 2.6b). There is little to no expected change in the number of very warm nights in the Mountains for this time period, but increases across the rest of North Carolina are between 6 and 25 per year, with the largest increases in the southern and eastern areas of the state (Figure 2.7b).

Under the higher scenario (for the period 2041–2060), the general pattern of changes is the same, but the magnitude of those changes is notably larger. The number of very hot days is projected to increase by 10 to 15 days per year in many areas of the Mountains and by 20 days or more in the westernmost tip of the state. And increases of 25 days or more are expected across the majority of the Piedmont and Coastal Plain (Figure 2.6c). There is little to no change projected in the number of very warm nights in the Mountains, but increases of 18 to 35 per year are expected across the majority of the Piedmont and Coastal Plain (Figure 2.7c).

The projections for increases in the number of very warm nights are consistent with recent observations. Because of this consistency, it is **very likely** that the model-projected increases in the number of very warm nights will occur. However, the projected increase in the number of very hot days is not consistent with the lack of an observed trend. Since the causes of the lack of an increase in the number of very hot days is not yet fully understood, our level of confidence is less. However, summers have become warmer, and that warming is projected to continue. Thus, it is **likely** that the number of very hot days will eventually increase.

Projected Changes in Annual Number of Very Hot Days
Days with Maximum Temperature ≥ 95°F

(a) Higher Scenario (RCP8.5), 2021–2040

(b) Lower Scenario (RCP4.5), 2041–2060

(c) Higher Scenario (RCP8.5), 2041–2060

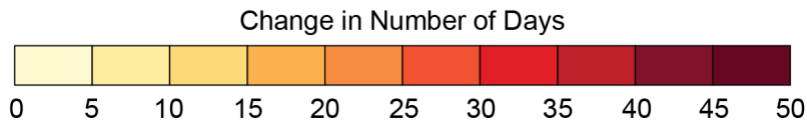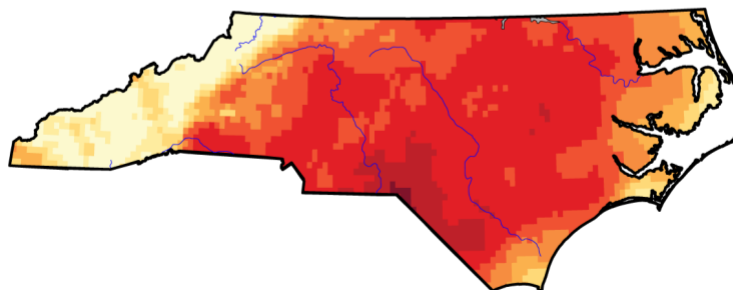Change in Number of Days
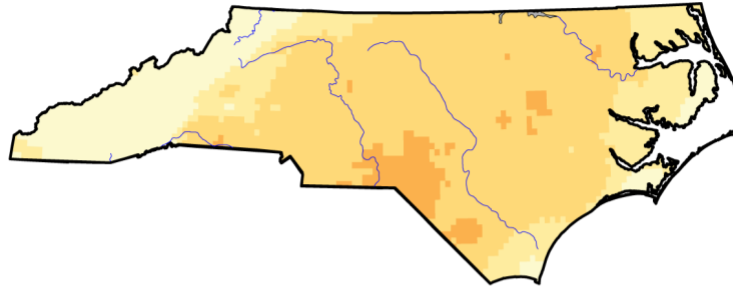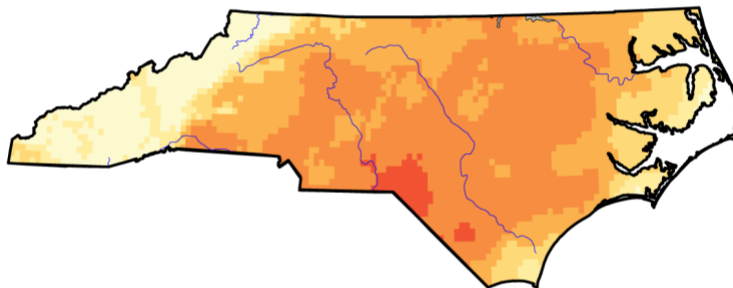
0   5   10   15   20   25   30   35   40   45   50

Figure 2.6. The maps show projected changes in the annual number of very hot days (maximum temperature of 95°F or higher) for North Carolina for two mid-century time periods and two climate futures. All projected values are shown as changes compared to the 1996–2015 average. Panel (a) shows projected changes for 2021–2040 under a higher scenario (RCP8.5). Panel (b) depicts projected changes for 2041–2060 under a lower scenario (RCP4.5), and panel (c) shows projected changes under the higher scenario for the same time period. Sources: NCICS and The University of Edinburgh.

Projected Changes in Annual Number of Very Warm Nights

Days with Minimum Temperature ≥ 75°F

(a)   Higher Scenario (RCP8.5), 2021–2040

(b)   Lower Scenario (RCP4.5), 2041–2060

(c)   Higher Scenario (RCP8.5), 2041–2060

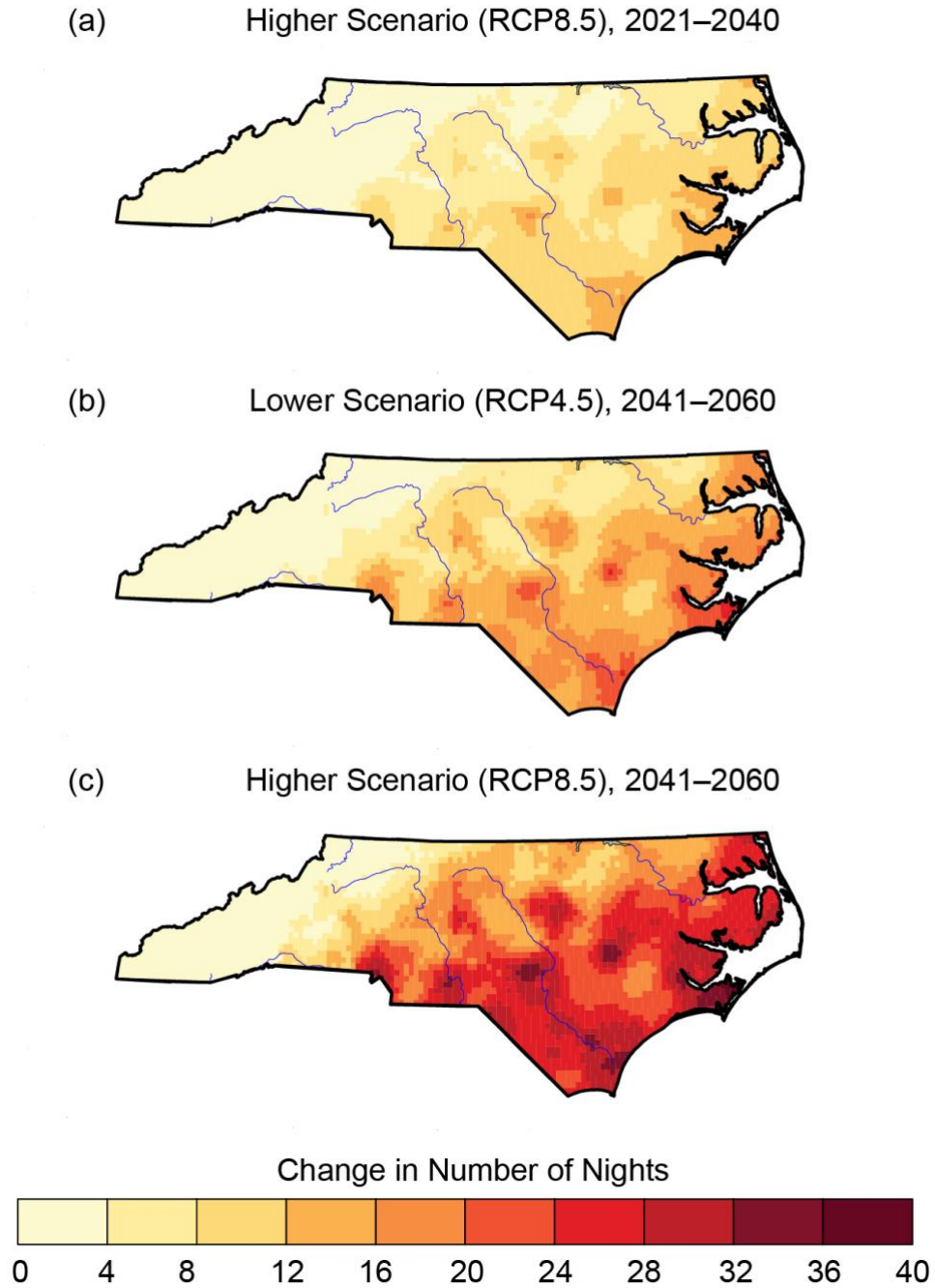Change in Number of Nights

0   4   8   12   16   20   24   28   32   36   40

Figure 2.7. The maps show projected changes in the annual number of very warm nights (minimum temperature of 75°F or higher) for North Carolina for two mid-century time periods and two climate futures. All projected values are shown as changes compared to the 1996–2015 average. Panel (a) shows projected changes for 2021–2040 under a higher scenario

(RCP8.5). Panel (b) depicts projected changes for 2041–2060 under a lower scenario (RCP4.5), and panel (c) shows projected changes under the higher scenario for the same time period. Sources: NCICS and The University of Edinburgh.

Though there is no long-term trend in the number of cold days (maximum temperature of 32°F or lower), the annual number of such days has been above average for the last five years (Figure 2.8). The number of cold nights (minimum temperature of 32°F or lower) has been generally near average since the 1990s (Figure 2.9). The number of cold days and cold nights was generally below average during the 1920s through the 1950s, a period of generally above average winter temperatures (Figure 2.2). Interestingly, the recent period of above average winter temperatures has not been accompanied by a similarly below average number of cold days and nights. The lack of trends in the number of cold days and cold nights in recent years was caused in part by occurrences of a winter weather pattern popularly known as the polar vortex— an area of upper-level low pressure that is nearly always present over the North and South Poles. Occasionally, the arctic vortex is displaced southward over eastern North America and becomes nearly stationary, bringing unusually cold weather to the eastern United States. While the sporadic southward displacement of the vortex is a natural feature of the winter climate, some recent years have featured unusually persistent patterns, resulting in episodes of extended cold and stormy weather in the eastern United States, notably in the winters of 2009–10, 2010–11, 2013–14, and 2014–15. A number of research studies have found empirical evidence of a link between cold winter episodes and the fact that the Arctic region is warming more rapidly than lower latitudes (a phenomenon referred to as arctic amplification). The current scientific consensus is that observed winter temperature trends, including the lack of recent warming in the eastern United States, cannot be explained without including the potential effects of Arctic warming (Cohen et al. 2020). By contrast, the number of very cold nights (minimum temperature of 0°F or lower) has been below average throughout the 2000s, with the exception of 2014 and 2015, when the polar vortex dominated weather patterns in the eastern United States (Figure 2.10).
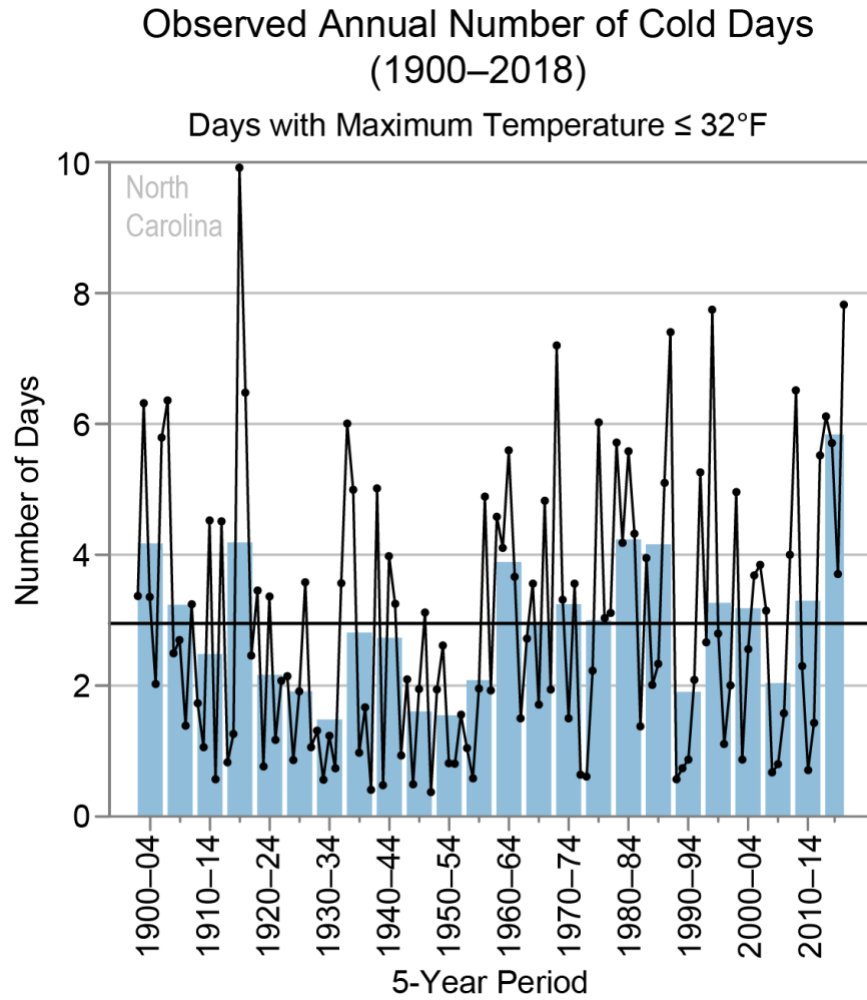
Observed Annual Number of Cold Days
(1900–2018)

Days with Maximum Temperature ≤ 32°F

Figure 2.8. The bar graph shows the observed annual number of cold days (maximum temperature of 32°F or lower) for North Carolina for 1900–2018, as averaged over 5-year periods, with the last bar representing a 4-year period (2015–2018). Dots show annual values. The horizontal black line shows the long-term average of 3 cold days per year for 1900–2018. Source: Frankson et al. 2017, 2019 update.
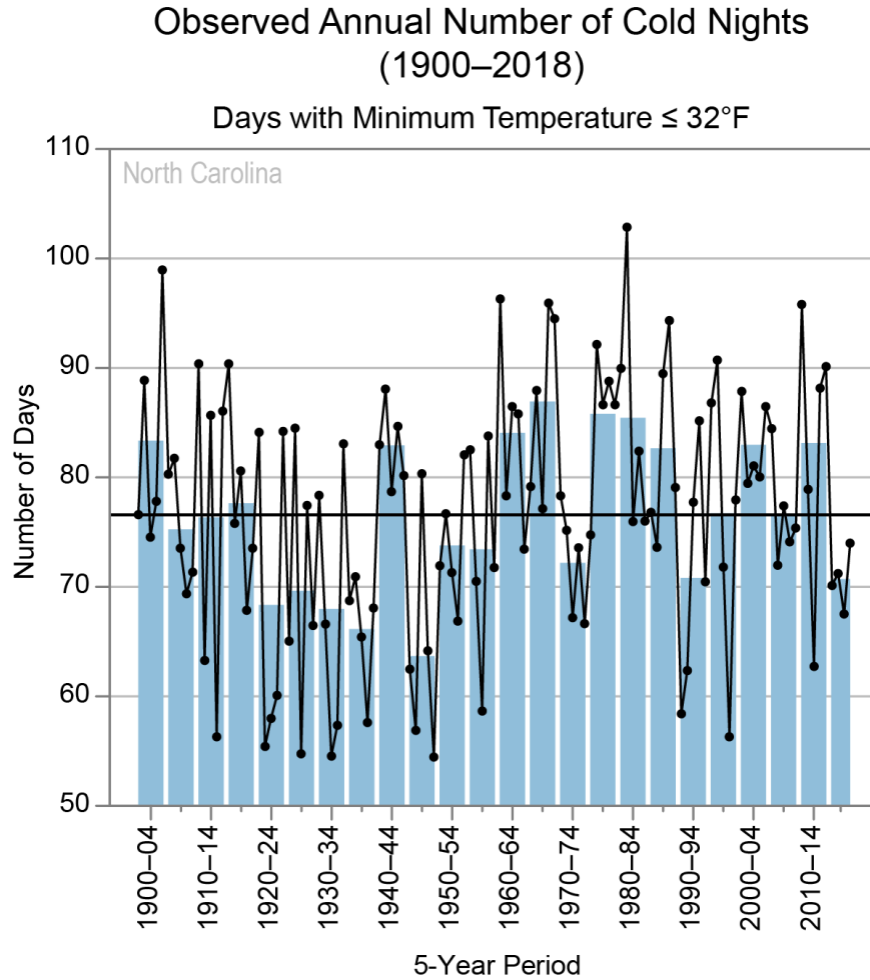
Observed Annual Number of Cold Nights
(1900–2018)

Figure 2.9. The bar graph shows the observed annual number of cold nights (minimum temperature of 32°F or lower) in North Carolina for 1900–2018, as averaged over 5-year periods, with the last bar representing a 4-year period (2015–2018). Dots show annual values. The horizontal black line shows the long-term average of 77 cold nights per year for 1900–2018. Source: NCICS.
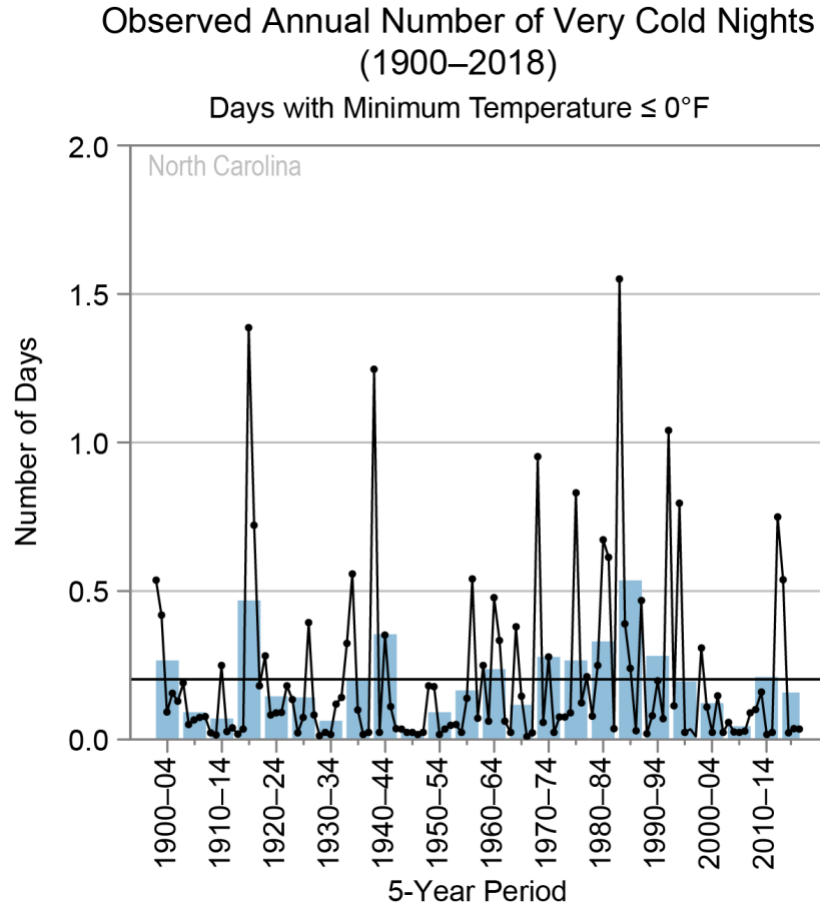
Observed Annual Number of Very Cold Nights (1900–2018)

Days with Minimum Temperature ≤ 0°F

Figure 2.10. The bar graph shows the observed annual number of very cold nights (minimum temperature of 0°F or lower) for North Carolina for 1900–2018, as averaged over 5-year periods, with the last bar representing a 4-year period (2015–2018). Dots show annual values. The horizontal black line shows the long-term average of 0.2 very cold nights per year for 1900–2018. Source: Frankson et al. 2017, 2019 update.

Cold days are rare in the Piedmont and Coastal Plain regions, as are very cold nights. The projected changes expected in the occurrence of such cold days and nights in these regions is very small simply because current climatological values are very small. However, in the Western Mountains, where the annual average number of such days and nights is higher, climate models project decreases in the occurrence of both cold days and very cold nights. The magnitude of decreases varies across the Mountains region, with larger decreases seen at higher elevations. By 2021–2040, projected decreases are small, with the number of cold days dropping by about 1 to 3 days per year (Figure 2.11a) and the frequency of very cold nights dropping by about 1 to 2 per year (Figure 2.12a). By 2041–2060, the number of cold days is projected to decrease by 3 to 7 days per year in the Mountains (under the higher scenario), and decreases of 2 to 3 days per year are expected in the Piedmont region along the northern border of the state (Figure 2.11c). By 2041–2060, the number of very cold nights is projected to decrease by 1 to 4 per year in the Mountains under the higher scenario (Figure 2.12c)

The number of cold nights (minimum temperature of 32°F or lower), which are more common in all regions, is projected to decrease significantly across the entire state (Figure 2.13). By 2021–2040, decreases of 6 to 12 cold nights per year are projected across all three regions of North Carolina, with the Coastal Plain seeing the smallest changes. By 2041–2060, decreases of 12 cold nights or more per year are projected across the majority of the state under the lower scenario, and decreases of 18 or more are expected under the higher scenario.

The projections for decreases in the number of very cold nights are consistent with observations over the last three decades. Because of this consistency, it is *very likely* that decreases in the number of very cold nights will occur. For cold days, however, the projected decrease is not consistent with the lack of an observed trend. As noted above, one reason for the lack of an observed trend is the recent occurrences of an unusually persistent southward-displaced polar vortex over eastern North America. It has been hypothesized that Arctic warming may be responsible for these recent polar vortex excursions, but there is no scientific consensus that continued Arctic warming will lead to an increase in the number or persistence of southward-displaced polar vortex occurrences over eastern North America. In any case, winters have become warmer overall, and that warming is projected to continue. Thus, it is *likely* that the number of cold days will eventually decrease.

Projected Changes in Annual Number of Cold Days
Days with Maximum Temperature ≤ 32°F

(a) Higher Scenario (RCP8.5), 2021–2040

(b) Lower Scenario (RCP4.5), 2041–2060

(c) Higher Scenario (RCP8.5), 2041–2060
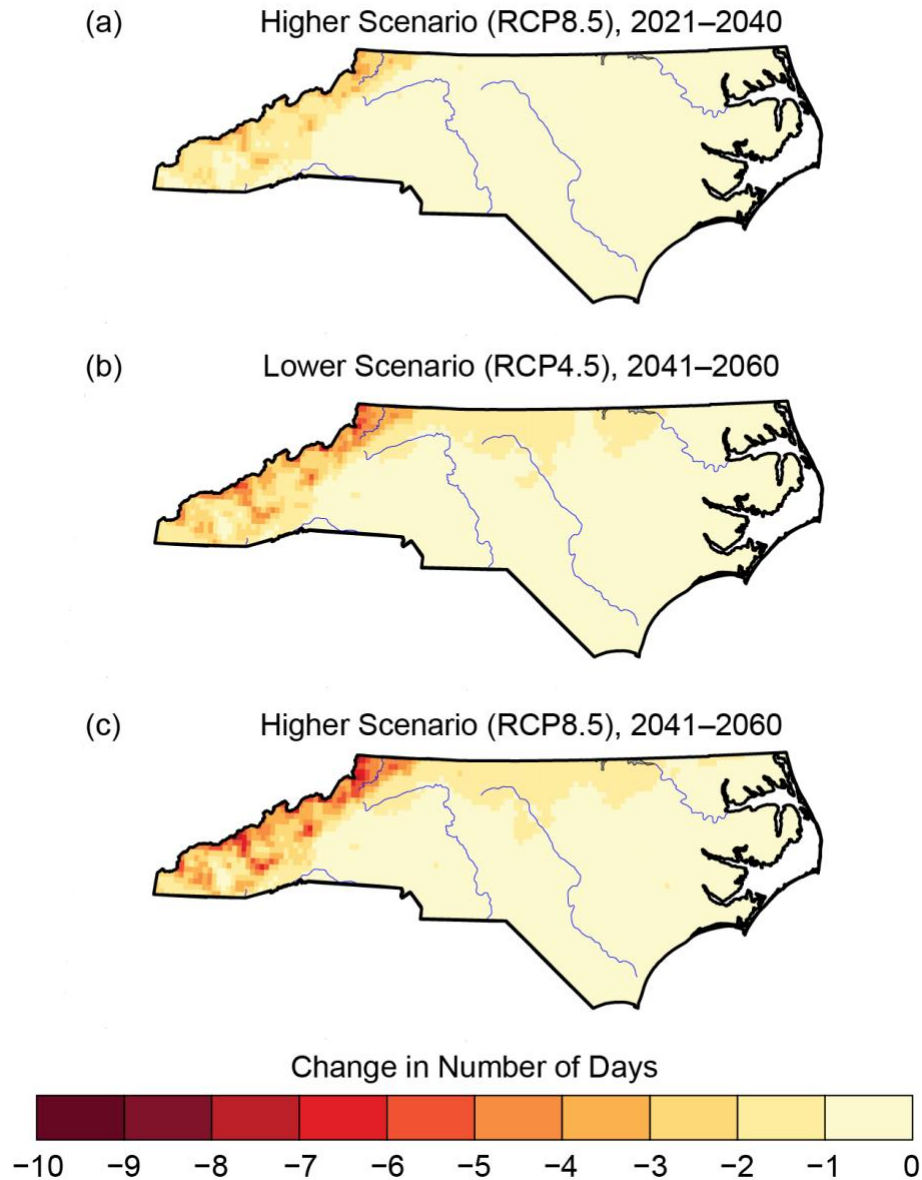
Change in Number of Days

−10 −9 −8 −7 −6 −5 −4 −3 −2 −1 0

Figure 2.11. The maps show projected changes in the annual number of cold days (maximum temperature of 32°F or lower) for North Carolina for two mid-century time periods and two climate futures. All projected values are shown as changes compared to the 1996–2015 average. Panel (a) shows projected changes for 2021–2040 under a higher scenario (RCP8.5). Panel (b) depicts projected changes for 2041–2060 under a lower scenario (RCP4.5), and panel (c) shows projected changes under the higher scenario for the same time period. Darker shades of red indicate decreases in the number of cold days. Sources: NCICS and The University of Edinburgh.

Projected Changes in Annual Number of Very Cold Nights
Days with Minimum Temperature ≤ 0°F
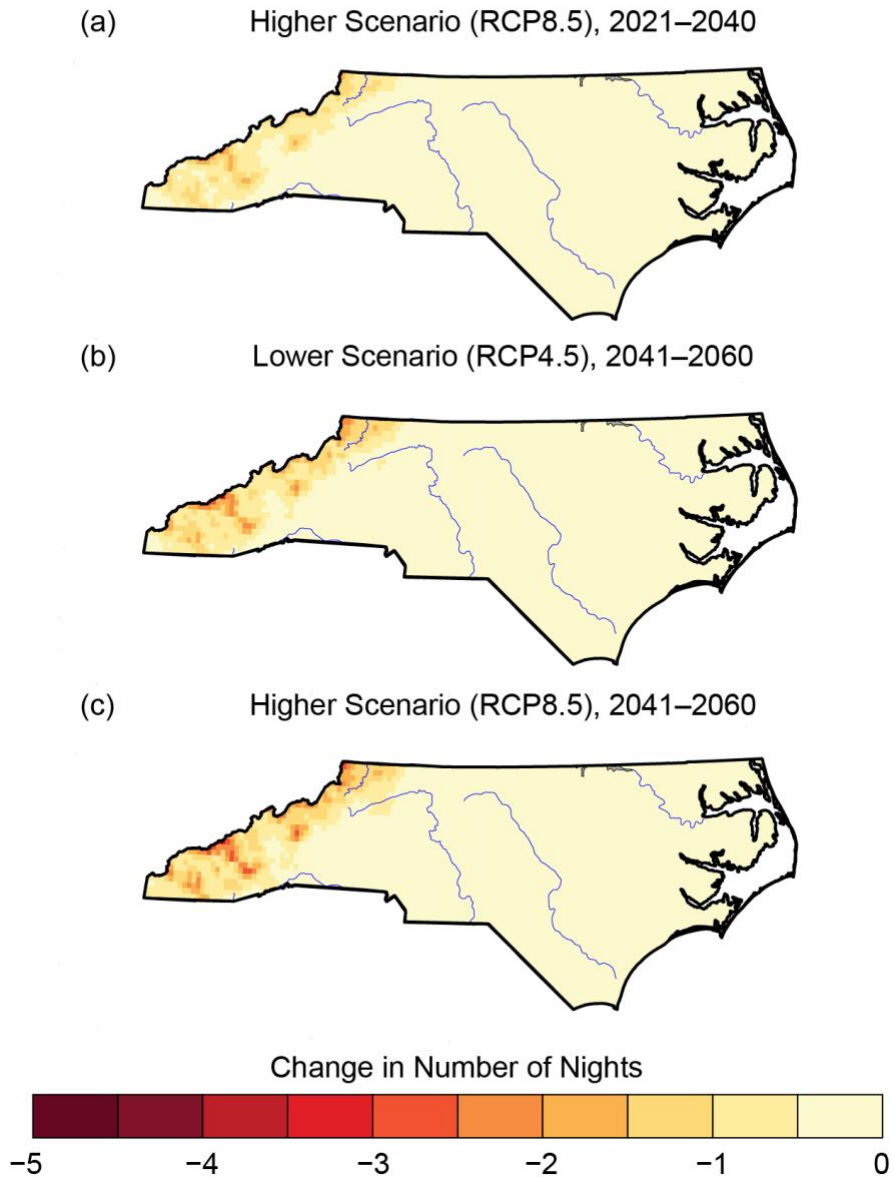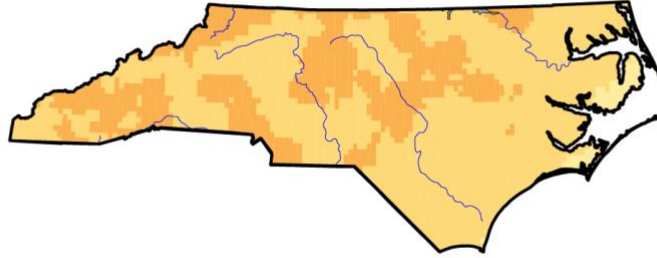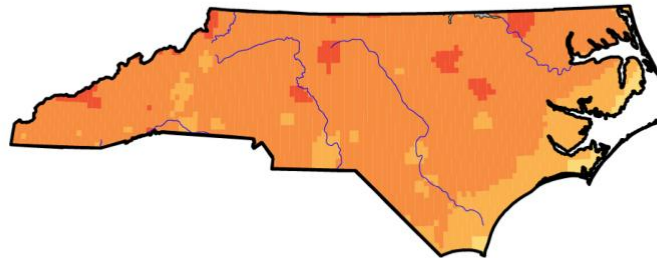

Figure 2.12. The maps show projected changes in the annual number of very cold nights (minimum temperature of 0°F or lower) for North Carolina for two mid-century time periods and two climate futures. All projected values are shown as changes compared to the 1996–2015 average. Panel (a) shows projected changes for 2021–2040 under a higher scenario (RCP8.5). Panel (b) depicts projected changes for 2041–2060 under a lower scenario (RCP4.5), and panel (c) shows projected changes under the higher scenario for the same time period. Darker shades of red indicate decreases in the number of very cold nights. Sources: NCICS and The University of Edinburgh.

Projected Changes in Annual Number of Cold Nights
Days with Minimum Temperature ≤ 32°F

(a)   Higher Scenario (RCP8.5), 2021–2040

(b)   Lower Scenario (RCP4.5), 2041–2060

(c)   Higher Scenario (RCP8.5), 2041–2060

Change in Number of Nights

−30   −27   −24   −21   −18   −15   −12   −9   −6   −3   0
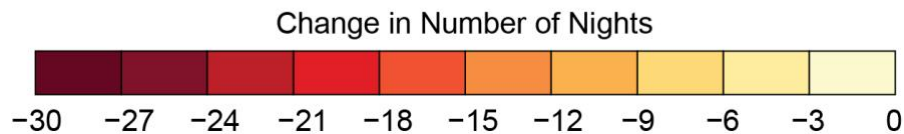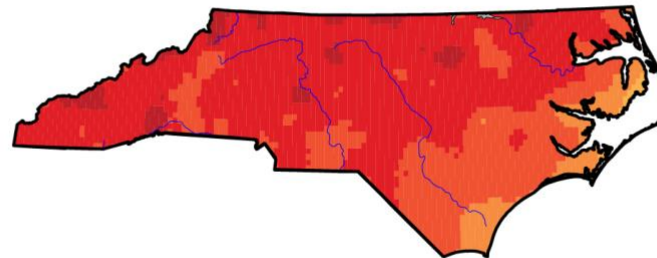
Figure 2.13. The maps show projected changes in the annual number of cold nights (minimum temperature of 32°F or lower) for North Carolina for two mid-century time periods and two climate futures. All projected values are shown as changes compared to the 1996–2015 average. Panel (a) shows projected changes for 2021–2040 under a higher scenario (RCP8.5). Panel (b) depicts projected changes for 2041–2060 under a lower scenario (RCP4.5), and panel (c) shows projected changes under the higher scenario for the same time period. Darker shades of red indicate decreases in the number of cold nights. Sources: NCICS and The University of Edinburgh.

Both the average annual hottest and coldest temperatures are projected to increase later this century. By 2021–2040, the hottest and coldest temperatures are projected to increase by 1°F to 3°F across the entire state, with the smallest changes occurring in the Coastal Plain (Figure 2.14a, b).

By 2041–2060 and under the lower scenario (RCP4.5), the annual hottest temperature is projected to increase by 2°F to 3°F in the Coastal Plain and by 3°F to 4°F throughout the Piedmont and Western Mountains regions (Figure 2.14c). The annual coldest temperature is projected to increase by 3°F to 4°F across most of the state, with a few small areas seeing increases of 4° to 5°F (Figure 2.14d). For the same time period under the higher scenario, both the hottest and coldest temperatures are projected to increase by 3°F to 5°F across most of the state, with the annual hottest temperature increasing by as much as 6°F in some areas of the Piedmont and Western Mountains regions (Figure 2.14e, f).

Projected Changes in Annual Hottest Maximum and Coldest Minimum Temperatures

Hottest Maximum   Coldest Minimum

Higher Scenario (RCP8.5), 2021–2040

(a)   (b)

Lower Scenario (RCP4.5), 2041–2060

(c)   (d)

Higher Scenario (RCP8.5), 2041–2060

(e)   (f)

Change in Temperature (°F)
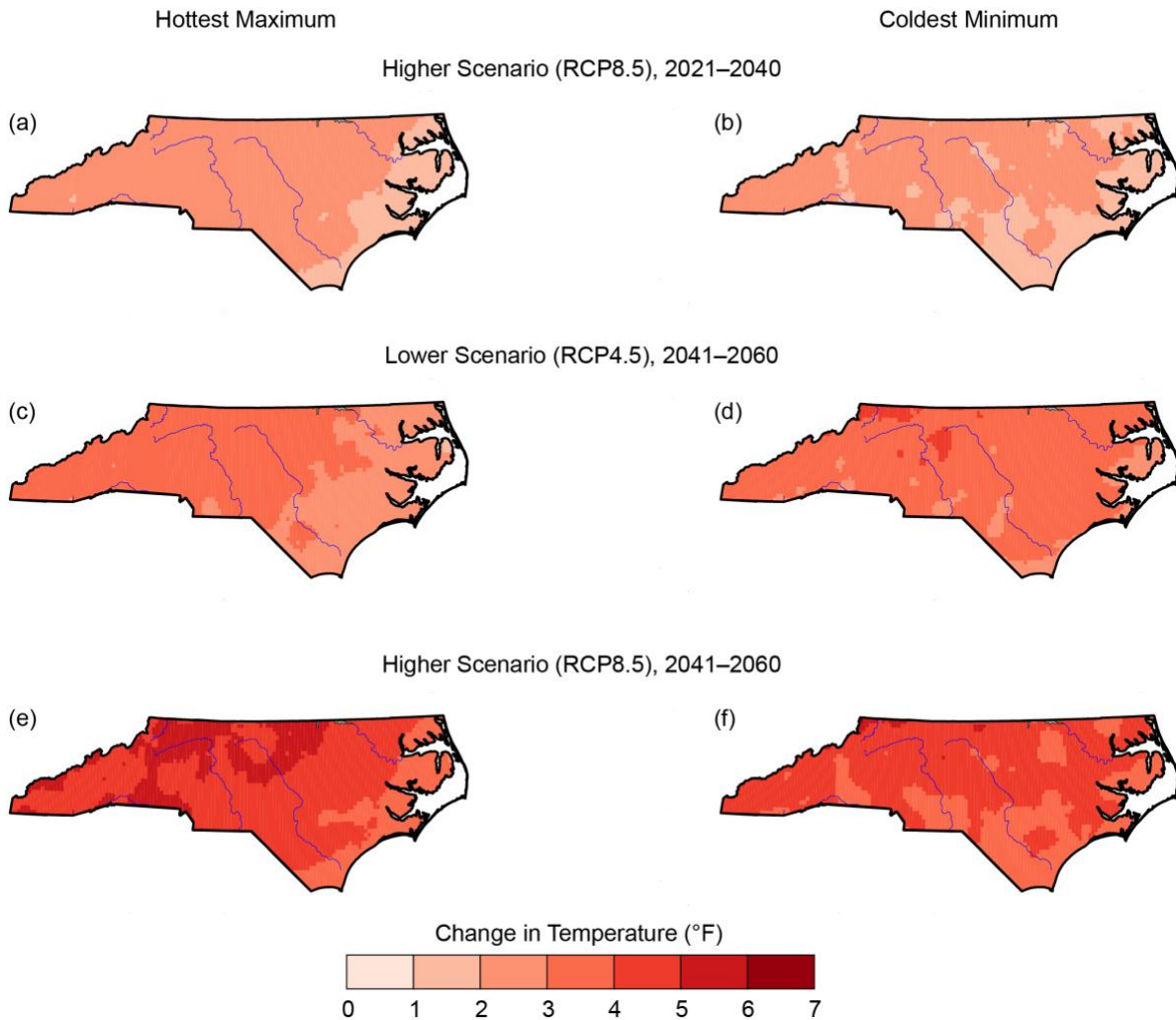
0   1   2   3   4   5   6   7

Figure 2.14. The maps show projected changes in the hottest (left column) and coldest (right column) temperatures each year for North Carolina for two mid-century time periods and two climate futures. All projected values are shown as changes compared to 1996–2015 averages. Panels (a) and (b) show projected changes for 2021–2040 under a higher scenario (RCP8.5). Panels (c) and (d) depict projected changes for 2041–2060 under a lower scenario (RCP4.5), and panels (e) and (f) show projected changes under the higher scenario for the same period. Sources: NCICS and The University of Edinburgh.

2.3 Precipitation Changes in North Carolina

2.3.1 Averages

Since 1895, statewide annual total precipitation has ranged from a low of 34.7 inches in 2007 to a high of 68.4 inches in 2018. The driest multiyear periods were in the early 1930s and early 1950s and the wettest in the late 1900s and late 2010s (Figure 2.15). The driest consecutive 5-year interval was 1930–1934, with an annual average of 44.4 inches, and the wettest was 2014–2018, with an average of 55.1 inches per year. There is no overall trend in annual total precipitation. Precipitation totals are generally highest in the summer, with a peak in July. Southwestern North Carolina is one of the wettest locations in the southeastern United States, receiving more than 90 inches of precipitation annually in a few locations.
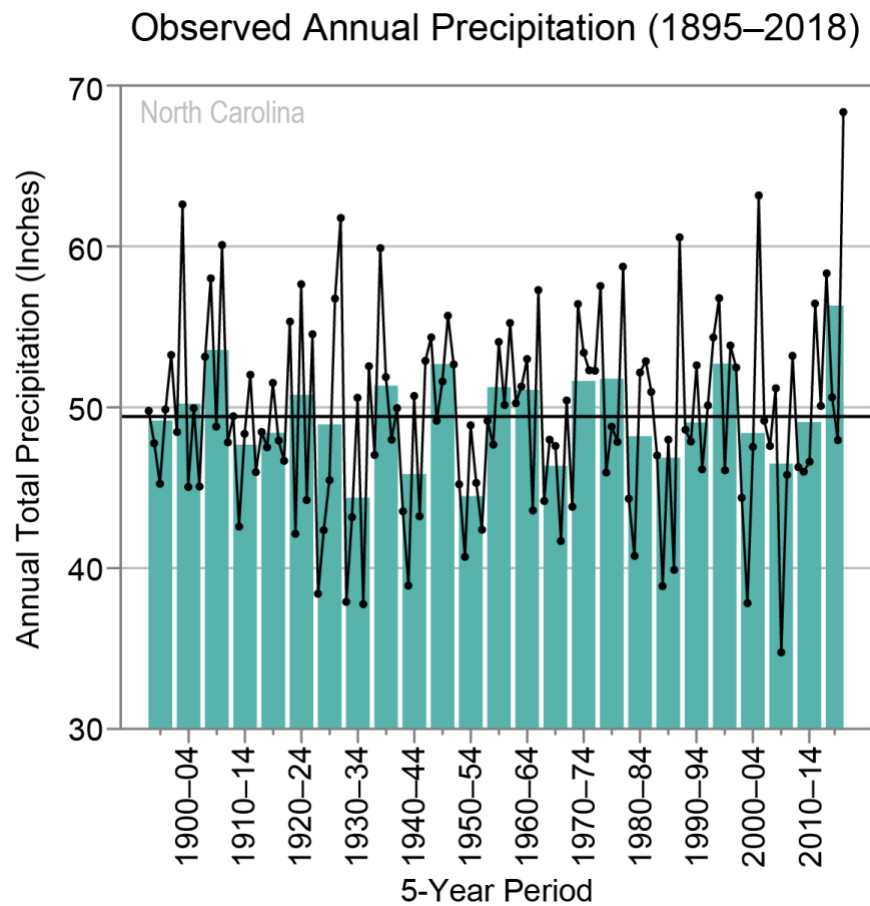

Figure 2.15. The bar graph shows the observed annual total precipitation for North Carolina for 1895–2018, as averaged over 5-year periods, with the last bar representing a 4-year period. Dots show annual values. The horizontal black line shows the long-term average of 49.4 inches per year for 1895–2018. The last 5 years (2014–2018) is the wettest consecutive 5-year interval on record. Sources: Frankson et al. 2017, 2019 update.

For scenarios in which greenhouse gas concentrations continue to increase, the majority of climate models project increases in annual total precipitation by the middle of the 21st century. The maps in Figure 2.16 show projected changes in annual total precipitation for two mid-century time periods and under two climate futures: a higher scenario (RCP8.5), in which greenhouse gas emissions continue to increase, and a lower scenario (RCP4.5), in which emissions increase at a slower rate. By 2021–2040, the two scenarios project small increases in annual total precipitation—up to about 3%, except for a small area in western North Carolina that shows slightly higher increases (only the higher scenario is shown in the figure). Projections for 2041–2060 are shown for both scenarios. The area of increases above 3% for 2041–2060 is similar to the increases for 2021–2040 under the lower scenario but increases to about half of the state (mostly in the west) under the higher scenario.

Projected Changes in Annual Total Precipitation

(a) Higher Scenario (RCP8.5), 2021–2040

(b) Lower Scenario (RCP4.5), 2041–2060

(c) Higher Scenario (RCP8.5), 2041–2060
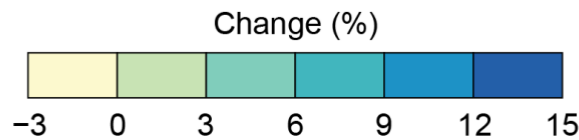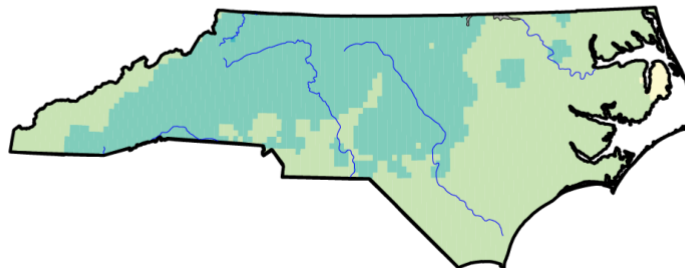
Change (%)

−3   0   3   6   9   12   15
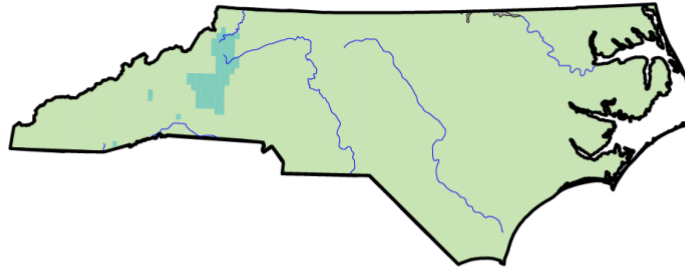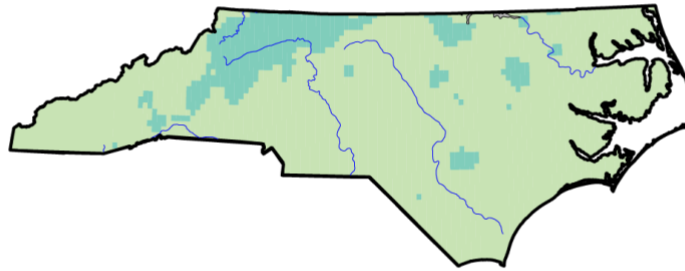
Figure 2.16. The maps show projected changes in annual total precipitation for North Carolina for two mid-century time periods and two climate futures. All projected values are shown as changes compared to the 1996–2015 average. Panel (a) shows projected changes for 2021–2040 under a higher scenario (RCP8.5). Panel (b) depicts projected changes for 2041–2060 under a lower scenario (RCP4.5), and panel (c) shows projected changes under the higher scenario for the same time period. Sources: NCICS and The University of Edinburgh.

2.3.2 Extremes

Heavy Rainfall Events

Extreme precipitation events are defined here as days on which rainfall totals 3 inches or more. The number of such events has been highly variable throughout the historical record (Figure 2.17). There is a statistically significant upward trend, with the highest number of extreme precipitation events occurring in the last 4-year period (2015–2018).

Observed Annual Number of Extreme Precipitation Events (1900–2018)

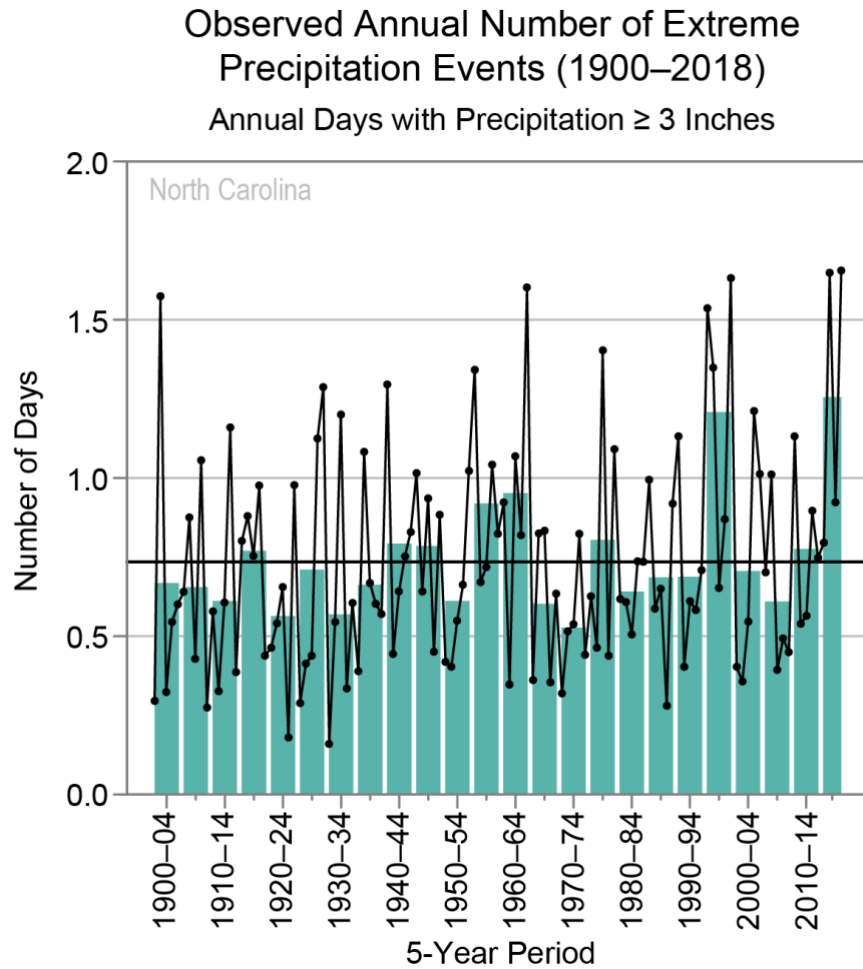### Annual Days with Precipitation ≥ 3 Inches

Figure 2.17. The bar graph shows the observed annual number of extreme precipitation events (days with precipitation of 3 inches or more) for North Carolina for 1900–2018, as averaged over 5-year periods, with the last bar representing a 4-year period. Dots show annual values. The horizontal black line shows the long-term average of 0.7 events per year for 1900–2018. The number of extreme precipitation events was well above average over the last 4-year period. Source: Frankson et al. 2017, 2019 update.

As the atmosphere continues to warm, the amount of water vapor in the atmosphere will also continue to increase. This additional water vapor then becomes available to increase heavy rainfall events. Figure 2.18 shows changes in the number of days with precipitation of 3 inches

or more for the two future time periods and scenarios shown in Figure 2.16. For both mid-century time periods, most areas are projected to see an increase in the number of days with precipitation of 3 inches or more. As is expected with more warming, the higher scenario (RCP8.5) shows the broadest areas of large increases, approaching a 100% increase in some areas of the Western Mountains. Some small areas, however, show little increase even under the higher scenario due to the high random spatial variability in the location of specific extreme events. The overall risk of future changes should be evaluated by examining averages over large regions. Based on the ***virtual certainty*** that water vapor in the atmosphere will increase as global warming occurs, it is ***very likely*** that the risk of extreme precipitation will increase everywhere in the state.
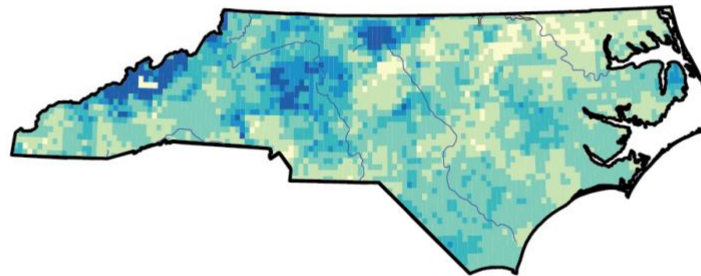
Projected Changes in Annual Number of Extreme Precipitation Events

Days with Precipitation ≥ 3 Inches

(a) Higher Scenario (RCP8.5), 2021–2040

(b) Lower Scenario (RCP4.5), 2041–2060
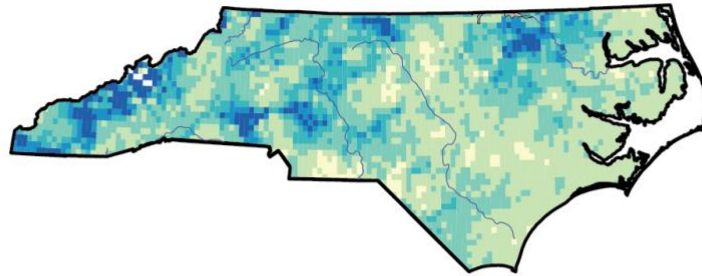
(c) Higher Scenario (RCP8.5), 2041–2060

Change (%) in Number of Days

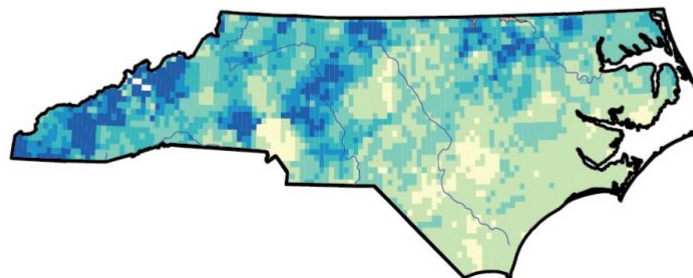−20   0   20   40   60   80   100

Figure 2.18. The maps show projected changes in the annual number of days with precipitation of 3 inches or more across North Carolina for two mid-century time periods and two climate futures. All projected values are shown as changes compared to the 1996–2015 average. Panel

(a) shows projected changes for 2021–2040 under a higher scenario (RCP8.5). Panel (b) depicts projected changes for 2041–2060 under a lower scenario (RCP4.5), and panel (c) shows projected changes under the higher scenario for the same time period. Sources: NCICS and The University of Edinburgh.
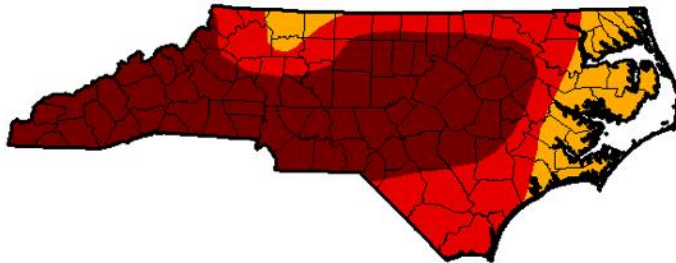
Drought

Droughts are a natural part of the climate of North Carolina. Typically, the clockwise circulation around the Bermuda High—a semipermanent high pressure system with its center off the Atlantic Coast—draws moisture northward or westward from the Atlantic Ocean and Gulf of Mexico, causing warm and moist summers with frequent thundershowers in the afternoons and evenings. Daily and weekly variations in the positioning of the Bermuda High can have a strong influence on precipitation patterns. When the Bermuda High extends northwestward into the southeastern United States, warmer and drier than normal weather occurs, which can culminate in heat waves and drought (Li et al. 2012). In 2007, as a result of a strong Bermuda High over the Southeast and a strengthening La Niña, the state experienced its driest year in the observed historical record. By the end of October of that year, most of the state was in exceptional drought (Figure 2.19).

Future droughts are projected to be warmer than historical events with a high level of confidence. The warmer conditions will lead to more rapid drying through increases in potential evapotranspiration (the amount of evaporation or transpiration that would occur if there was unlimited water on the surface or in vegetation). Also, climate model simulations indicate that extension of the Bermuda High northwestward will occur more frequently in the future (Li et al. 2013). Thus, it is *likely* that future droughts will be more severe in terms of soil moisture deficits and the impacts on rainfed agriculture and natural vegetation. See Chapter 3 for regional observations of drought (Figures 3.17, 3.33, and 3.49).

U.S. Drought Monitor
North Carolina

October 23, 2007
(Released Thursday, Oct. 25, 2007)
Valid 7 a.m. EST

Drought Conditions (Percent Area)

	None	D0-D4	D1-D4	D2-D4	D3-D4	D4
Current	0.00	100.00	100.00	100.00	84.76	56.53
Last Week 10/16/2007	0.00	100.00	100.00	100.00	84.64	54.31
3 Months Ago 7/24/2007	0.00	100.00	76.70	10.43	3.08	0.00
Start of Calendar Year 1/2/2007	98.53	1.47	0.00	0.00	0.00	0.00
Start of Water Year 9/25/2007	0.00	100.00	100.00	92.76	75.10	4.04
One Year Ago 10/24/2006	94.85	5.15	0.00	0.00	0.00	0.00

Intensity:

D0 Abnormally Dry
D1 Moderate Drought
D2 Severe Drought
D3 Extreme Drought
D4 Exceptional Drought

The Drought Monitor focuses on broad-scale conditions.
Local conditions may vary. See accompanying text summary
for forecast statements.

Author:
Mark Svoboda
National Drought Mitigation Center

USDA   National Drought Mitigation Center

http://droughtmonitor.unl.edu/

Figure 2.19. This map from the U.S. Drought Monitor shows the drought status for North Carolina on October 23, 2007. The majority of the state was in exceptional drought status, especially in the Western Mountains and central Piedmont regions. Conditions in much of the Coastal Plain and along the northern border of the state were slightly better but were still classified as severe to extreme. The U.S. Drought Monitor is jointly produced by the National Drought Mitigation Center (NDMC) at the University of Nebraska–Lincoln, the United States Department of Agriculture, and the National Oceanic and Atmospheric Administration. Map courtesy of NDMC.

2.4 Sectoral Considerations

2.4.1 Agriculture

The observed length of the freeze-free season (number of days between the last spring occurrence of daily minimum temperature below 32°F and the first fall occurrence of daily minimum temperature below 32°F) was generally shorter than normal throughout the 1960s, 70s, and 80s. However, it has been above the long-term average since 1990. For the period of 1990–2009, the freeze-free season averaged 3.5 days longer than the long-term average. Since 2010, it

has been about 12 days longer than average (Figure 2.20). The recent increases in North Carolina are part of a national trend toward longer freeze-free seasons.
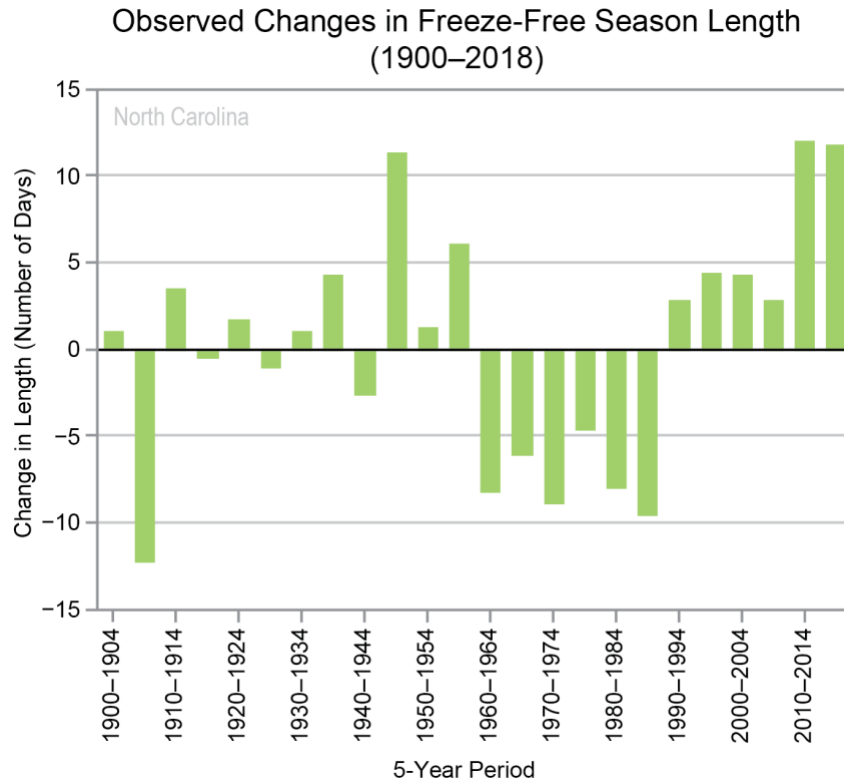

Figure 2.20. The bar graph shows the observed change in the length of the freeze-free season (number of days between the last spring occurrence of daily minimum temperature below 32°F and the first fall occurrence of daily minimum temperature below 32°F) for 1900–2018. The bars represent averages over 5-year periods, with the last bar representing a 4-year period. Sources: NCICS and NOAA NCEI.

While the observational record of soil moisture data is not long enough to reliably evaluate long-term trends, it is long enough to establish an approximate climatology. Observations of soil moisture are available from two observing networks across the state: the U.S. Climate Reference Network (USCRN) and the North Carolina ECOnet. The USCRN includes three stations—two in the Western Mountains near Asheville and one in Durham—with observations extending back to 2009 (Figure 2.21). The North Carolina ECOnet has 43 monitoring stations located around the state with variable record length. Nineteen of these stations have soil moisture observations dating back to 2001 (Figure 2.22). Figure 2.21 and Figure 2.22 show the annual cycle of soil moisture at the USCRN and regional averages of the ECOnet sites, respectively. They all exhibit a maximum in January, followed by a decrease to a minimum in summer and then an increase during fall. This seasonal pattern reflects the cycle of evaporation, which is at a minimum in winter and at a maximum in summer, and is driven by the cycles of temperature and vegetation growth.

The values in Figure 2.21 illustrate important features in the USCRN observations. The maximum winter values (0.32–0.35) are around the saturated value of soil moisture, while the minimum summer values (0.24–0.27) are well above the vegetation wilting points (0.11–0.16). Thus, vegetation usually has sufficient moisture for growth even during the hot summer months. At the two mountain stations, there is a secondary peak in soil moisture due to summer thunderstorms, which are a regular feature of the Western Mountains climate (Figure 2.21). These features are mirrored in the regional averages of the ECOnet stations, which vary from a maximum of 0.30–0.32 in January to a minimum in summer. The summer minimum for the Western Mountains sites (about 0.28) is somewhat higher than the minima in the other two regions (0.24–0.26). These seasonal variations indicate that the primary risk to vegetative growth and health is intense dry spells during the warm season, when soil moisture is at its climatological minimum and potential evapotranspiration (PET) is at its climatological peak. Projected warming will increase PET and increase the risk of adverse soil moisture conditions.
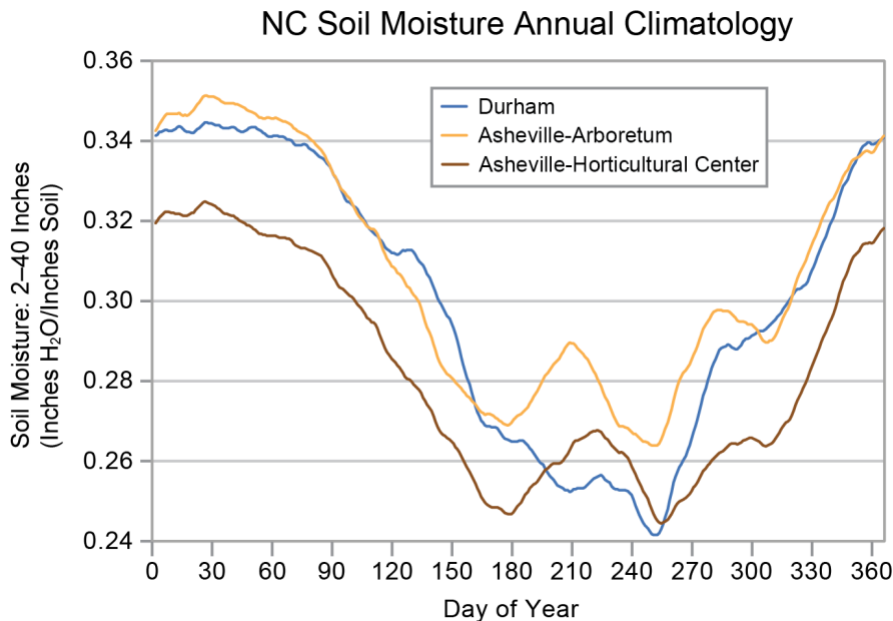

Figure 2.21. The graph shows average soil moisture by day of the year (1 = January 1; 361 = December 21), averaged over the 2–40-inch soil layer for Durham and two stations near Asheville, from the U.S. Climate Reference Network for the period 2009–2018. Sources: NOAA NCEI and NCICS.
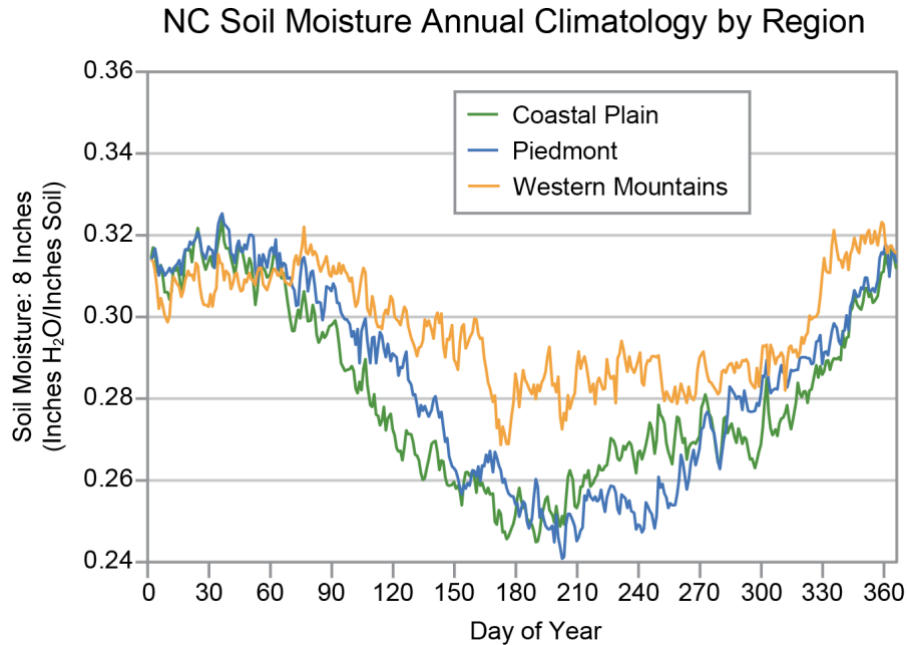
Figure 2.22. The graph shows average 8-inch soil moisture by day of year for North Carolina from ECOnet stations averaged by regions. Source: State Climate Office of North Carolina.

2.4.2 Energy Demands for Heating and Cooling

The term "heating degree days" (HDDs) refers to the number of degrees that a day's average temperature is below 65°F, while "cooling degree days" (CDDs) refers to the number of degrees that the average temperature is above 65°F. These metrics are used to quantify the energy needed to heat or cool buildings and houses. In North Carolina, annual HDDs and CDDs have varied in a manner similar to annual temperatures. Heating degree days (Figure 2.23) decreased in the first half of the 20th century to a relative minimum at mid-century, then increased to high values in the 1960s. Since 1970, there has been a decreasing trend, and the lowest 10-year average values have occurred since 2000. Cooling degree days have varied in the opposite manner (Figure 2.24), exhibiting an increasing trend in the early 20th century to moderately high values in the 1930s. Values decreased from 1940 to a minimum in the late 1960s. Since the 1970s, cooling degree days have increased to the highest 10-year average values in the observational record.

Observed Annual Heating Degree Days
(1901–2018)

Figure 2.23. The graph shows the statewide annual average heating degree days (blue) for 1901–2018 as well as the 10-year moving average (red). Sources: NCICS and NOAA NCEI.
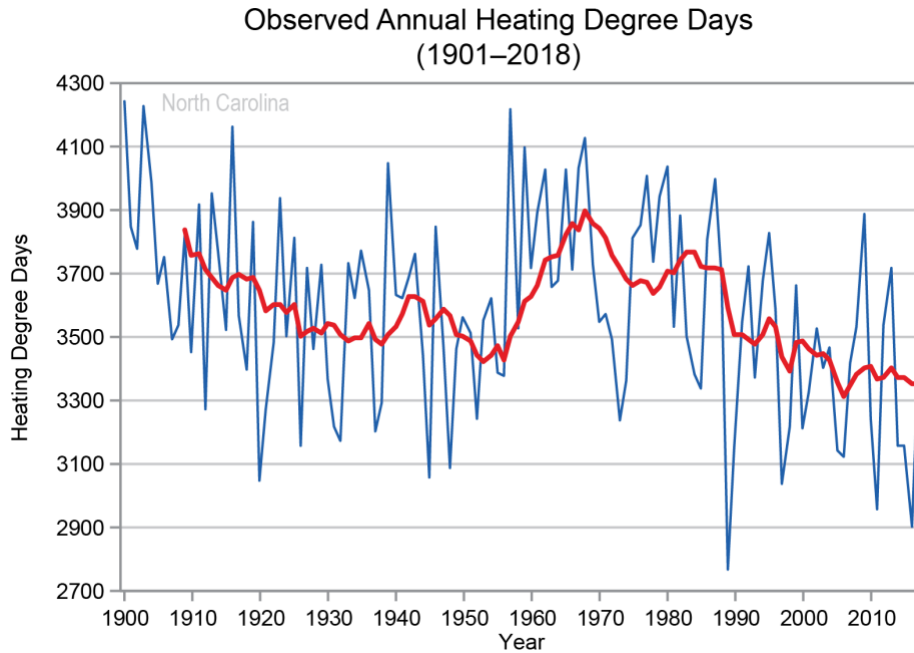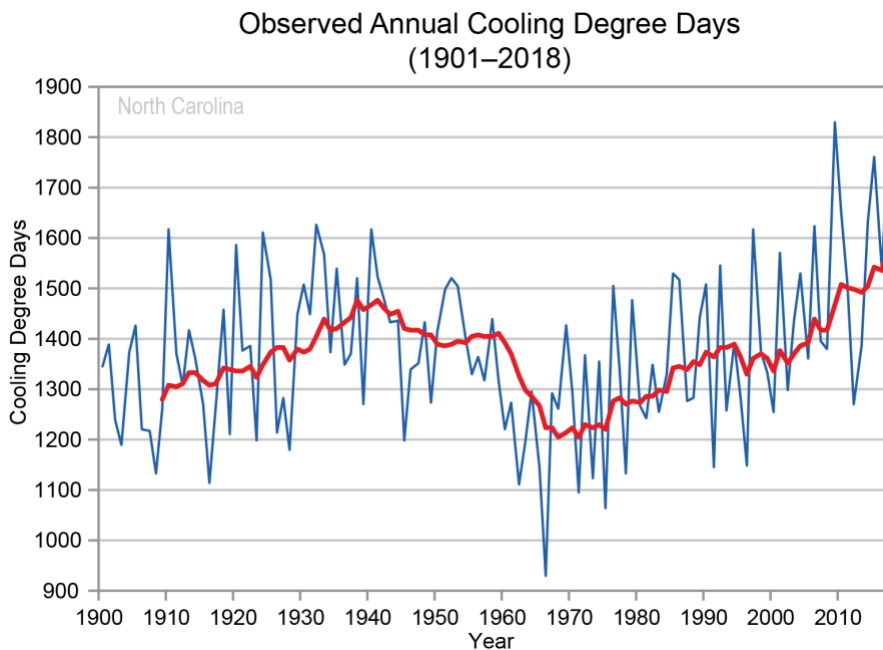
Observed Annual Cooling Degree Days
(1901–2018)

Figure 2.24. The graph shows the statewide annual average cooling degree days (blue) for 1901–2018 as well as the 10-year moving average (red). Sources: NCICS and NOAA NCEI.

The statewide annual average values for 1996–2015 are approximately 3,400 for HDDs and 1,440 for CDDs. The overall decrease in HDDs and increase in CDDs observed in North

Carolina indicate a decrease in energy needed for heating and an increase in energy needed for cooling. These trends are projected to continue throughout the century (Figure 2.25 and Figure 2.26).

By 2021–2040 and under the higher scenario (RCP8.5), HDDs are projected to decrease throughout the state, with the largest decreases occurring in the Piedmont and Western Mountains regions. Some higher mountain elevations are expected to see decreases of 500 or more HDDs per year (Figure 2.25a). Increases in CDDs for this time period are projected everywhere, with the largest increases of 300 to 400 per year occurring over most of the Piedmont and Coastal Plain (Figure 2.26a).

For 2041–2060, HDDs are projected to continue decreasing and CDDs to continue increasing under the lower scenario (RCP4.5), with the largest changes expected in the Western Mountains and Piedmont, respectively (Figure 2.25b and Figure 2.26b). Under the higher scenario, HDDs are projected to decrease by at least 500 across nearly the entire state, with decreases in the Western Mountains between 700 and 800 per year (Figure 2.25c). Cooling degree days are projected to increase by 600 to 800 per year across the Piedmont and Coastal Plain and by 400 to 700 across most of the Western Mountains region (Figure 2.26c).

Projected Changes in Annual Heating Degree Days

(a) Higher Scenario (RCP8.5), 2021–2040

(b) Lower Scenario (RCP4.5), 2041–2060

(c) Higher Scenario (RCP8.5), 2041–2060

Change in Number of Heating Degree Days

−800 −700 −600 −500 −400 −300 −200 −100

Figure 2.25. The maps show projected changes in annual heating degree days (HDDs) for North Carolina for two mid-century time periods and two climate futures. All projected values are shown as changes compared to the 1996–2015 average. Panel (a) shows projected changes for 2021–2040 under a higher scenario (RCP8.5). Panel (b) depicts projected changes for 2041–2060 under a lower scenario (RCP4.5), and panel (c) shows projected changes under the higher scenario for the same time period. Darker shades of red indicate decreases in HDDs, indicative of overall warmer conditions. Sources: NCICS and The University of Edinburgh.

Projected Changes in Annual Cooling Degree Days

(a)   Higher Scenario (RCP8.5), 2021–2040

(b)   Lower Scenario (RCP4.5), 2041–2060

(c)   Higher Scenario (RCP8.5), 2041–2060

Change in Number of Cooling Degree Days

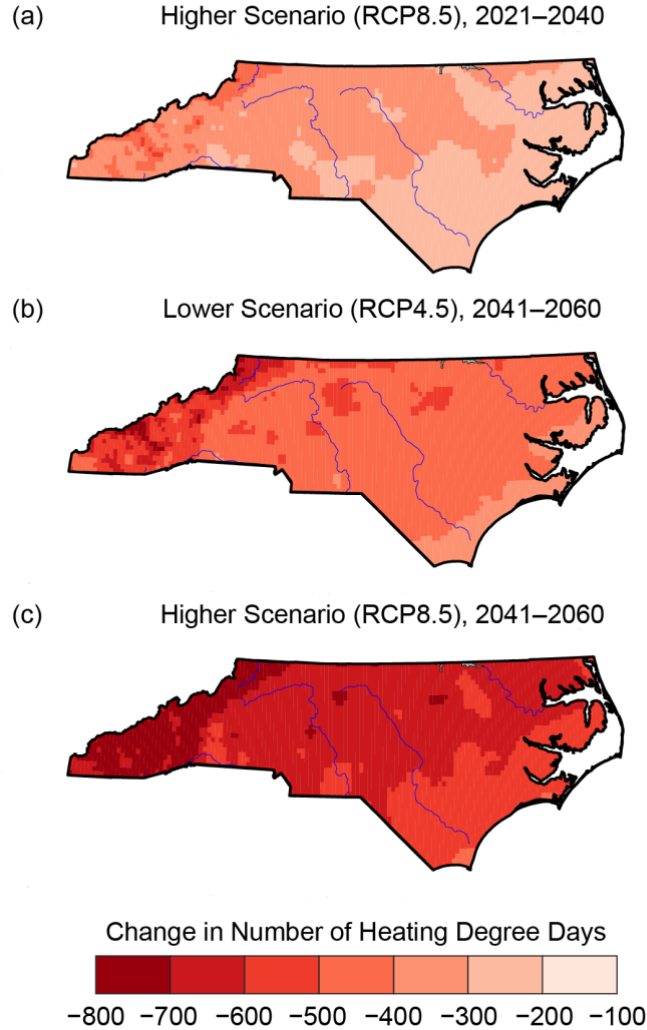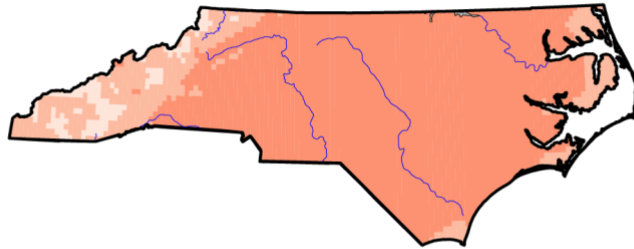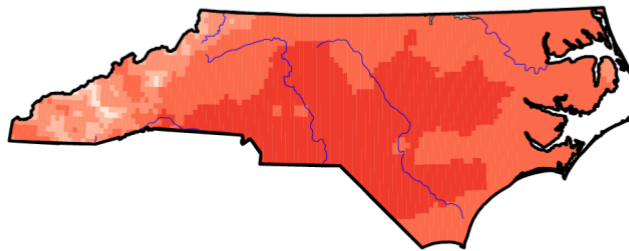100   200   300   400   500   600   700   800
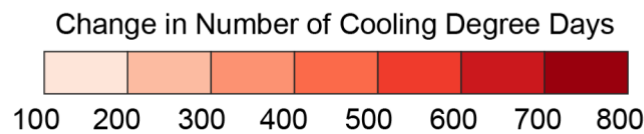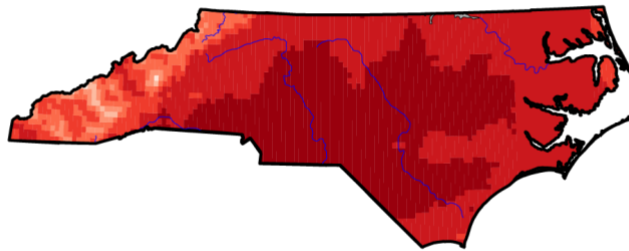
Figure 2.26. The maps show projected changes in annual cooling degree days (CDDs) for North Carolina for two mid-century time periods and two climate futures. All projected values are shown as changes compared to the 1996–2015 average. Panel (a) shows projected changes for 2021–2040 under a higher scenario (RCP8.5). Panel (b) depicts projected changes for 2041–2060 under a lower scenario (RCP4.5), and panel (c) shows projected changes under the higher scenario for the same time period. Darker shades of red indicate increases in CDDs, indicative of overall warmer conditions. Sources: NCICS and The University of Edinburgh.

2.4.3 Ski Industry

The ski industry in the Western Mountains relies on snowmaking. Snowmaking can occur when the wet-bulb temperature (the lowest temperature that can be achieved through evaporation in the local conditions) is below freezing. Figure 2.27 shows a time series, starting with the 1980–81 winter (December–February), of the percentage of hours favorable for snowmaking at an elevation of approximately 5,000 feet near Banner Elk, NC. The long-term average is about 60%. There is considerable year-to-year variability but no strong trend. The recent winters of 2015–16, 2016–17, and 2017–18 were all well below average.
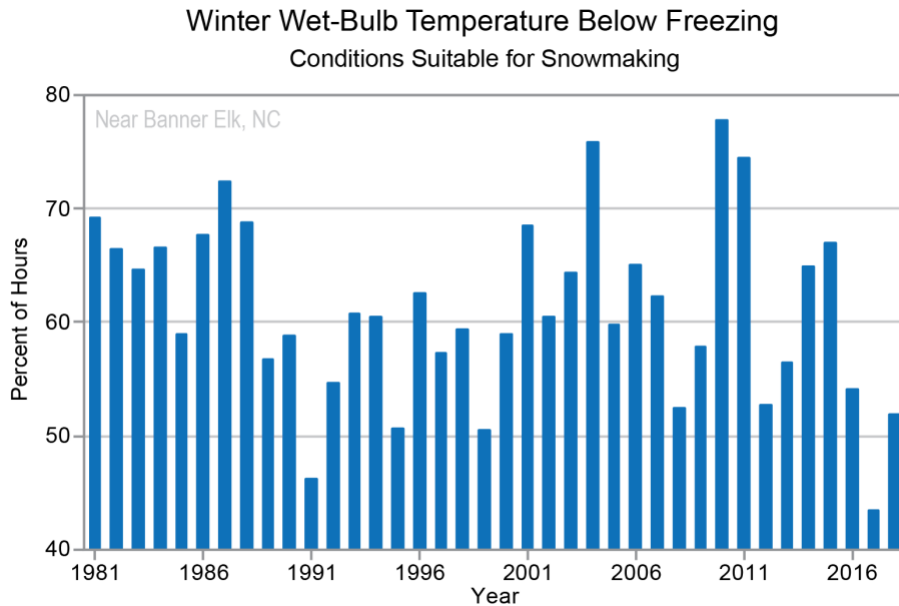
Figure 2.27. The time series shows the percentage of hours with winter (December–February) wet-bulb temperatures below freezing at an elevation of approximately 5,000 feet near Banner Elk, NC. Source: NCICS.

2.5 Changes in Storms Across North Carolina

2.5.1 Winter Storms

Extratropical cyclones are large areas of low pressure in the middle and high latitudes that are primarily distinguished by fronts separating warm and cold air masses. They often cause various types of adverse weather conditions, such as strong winds and precipitation of various types, including snow and ice. Herein, we refer to these as "winter storms" because they are most frequent and strong during the colder half of the year, although they occur in all seasons. This section discusses winter storms of all types, while the following two subsections discuss the specific instances of storms causing snow and ice.

Winter storm tracks have shifted slightly northward (by about 0.4 degrees latitude) in recent decades over the Northern Hemisphere (Bender et al. 2012). More generally, winter storm

activity is projected to change in complex ways under future climate scenarios, with increases in some regions and seasons and decreases in others. The Arctic is warming more quickly than lower latitudes (i.e., arctic amplification), due in part to sea ice loss. This reduces the lower-atmosphere temperature difference between the Arctic and the lower latitudes—this difference is an important energy source for winter storms. At the same time, the temperature difference higher up in the atmosphere is projected to increase due to a warming tropical upper troposphere and a cooling high-latitude lower stratosphere. While these two effects counteract each other with respect to a projected change in midlatitude storm tracks, the simulations indicate that the magnitude of arctic amplification may modulate some aspects (e.g., jet stream position, wave extent, and blocking frequency) of the circulation in the North Atlantic region in some seasons (Barnes and Polvani 2015).

Regional studies of trends in winter storms are challenged to provide definitive results regarding changes in the frequency or intensity of storms, but regardless of these properties, it is ***very likely*** that storms of even similar intensity will produce heavier precipitation (e.g., Marciano et al. 2015, Michaelis et al. 2017). Also, with rising sea levels, coastal flooding from storms is ***very likely*** to increase (e.g., Colle et al. 2015, Zhang and Colle 2018, Roberts et al. 2017).

Based on the available evidence, our conclusion is that there is ***low confidence*** concerning future changes in the number of winter storms.

2.5.1.1 Snowstorms and Snow Cover

In much of North Carolina, winter precipitation often falls as snow at higher elevations but as rain at lower elevations, where temperatures are warmer. Thus, winter temperatures are a critical factor in both historical and future changes in snowfall. Statewide, winter average temperatures have been above the long-term average in most winters since 1990 (Frankson et al. 2017, 2019 update). However, the foothills and mountain regions have exhibited a long-term decline in winter temperatures from 1910–2017 (Eck et al. 2019).

Analysis of snowfall at North Carolina stations with long records found decreasing trends over the period of 1930–2007 (Kunkel et al. 2009) at most stations. A more recent analysis of snowfall in the Western Mountains found no significant trends over the period 1910–2017 (Eck et al. 2019). However, an examination of the last 50 years indicates decreasing trends at many stations, particularly those located in the southern portion of the Western Mountains.

Thus, both of these studies confirm recent declines in snowfall over most areas of the state. Snowfall and anomalously low temperatures are favored by large-scale modes of climate variability, particularly the simultaneous occurrence of El Niño and the negative phase of the North Atlantic Oscillation (Eck et al. 2019).

The Fourth National Climate Assessment projects large winter warming under both moderate and higher emissions scenarios. Consistent with the projected warming, a northward shift in the rain–snow transition zone in the central and eastern United States is projected under a higher emissions scenario. By the end of this century, large areas that are currently snow dominated in

the cold season are expected to be rain dominated (Krasting et al. 2013, Ning and Bradley 2015). For North Carolina, the frequency of snowfall is projected to decrease by the end of this century and become a rare occurrence except in the Western Mountains. Even in the mountains, the frequency of snowfall is projected to decrease substantially, with snowfall increasingly confined to the higher elevations.

As noted earlier, a definitive understanding of the effects of arctic amplification on midlatitude winter weather remains elusive (Cohen et al. 2020) and this adds some uncertainty to future projections of winter climate in North Carolina. Current global climate models (CMIP5) do predict an increase in the number of winter storms over the eastern United States, including the most intense storms, under the higher emissions scenario (Colle et al. 2013). However, there are large model-to-model differences in the realism of the simulations of these storms and in the projected changes. Even if there were increases in the frequency or intensity of winter storms, the effects of warmer winters would nevertheless lead to decreases in average annual snowfall.

Another consequence of warming, however, is an expected increase in precipitation intensity. Thus, for events where air is sufficiently cold for precipitation to fall as snow, heavier totals could occur in the coming decades, before more extensive warming leads to only rare snowfall (O'Gorman 2014). However, an increase in heavy snow with warming only occurs with average temperatures colder than what occurs anywhere in North Carolina, including the mountains.

The higher elevations of the North Carolina mountains and even valley locations in counties along the Tennessee border receive substantial snowfall each year during periods of low-level wind flow from the northwest (Keighton et al. 2009). These northwest flow snow (NWFS) events frequently are associated with moisture transport extending downwind from the Great Lakes and are therefore sensitive to ice extent on the lakes (Perry et al. 2007). Ice cover effectively shuts off evaporation from the surfaces of the Great Lakes, resulting in considerably less low-level moisture downwind of the lakes.

Model simulations suggest that snowfall may increase downwind of the Great Lakes in the coming decades due to rising temperatures and decreasing seasonal ice cover (Gula and Peltier 2012). Therefore, it is possible that higher-elevation locations along the Tennessee border may see an increase in NWFS events, provided temperatures in the lower atmosphere remain sufficiently cold for snow formation.

Although snow generally melts within a few days after a snowstorm in most parts of the state, it is not uncommon for snow to persist for weeks or longer in the higher elevations of the mountains. In fact, at the highest elevations above 5,000 feet, snow may cover the ground nearly continuously some years from late fall through early spring, as was observed during the recent 2009–10 and 2013–14 snow seasons (Martin et al. 2015). The amount of water stored in the snowpack—known as the snow water equivalent (SWE)—increases with snow depth. High values of SWE increase the flood threat during rapid melting, particularly when rain falls on snow-covered ground. Nearly all model simulations suggest that future snow cover duration and SWE will decrease in the middle latitudes as a result of warming and reductions in snowfall

(Collins et al. 2013). Therefore, it is *likely* that snow cover lasting more than a few days will increasingly be limited to the highest elevations above 5,000 feet in the coming decades.

Based on the projected increase in temperature, it is *very likely* that total snowfall will decrease. It is *likely* that the number of heavy snowstorms will decrease.

2.5.1.2 Ice Storms

Ice storms occur within winter storms, the same as for snowstorms. However, icing requires a specific combination of weather conditions, most importantly precipitating conditions with a below-freezing layer near the surface and an above-freezing layer above the low-level, below-freezing layer. In this situation, snow falling from high levels melts as it falls through the above-freezing layer; it then becomes super-cooled liquid drops while falling through the near-surface freezing layer and freezes on contact with cold surface objects.

Accurately simulating this weather feature in climate models is challenging because the vertical extent of the below-freezing and above-freezing layers is often quite small and thus cannot be resolved by the current generation of climate models. Also, the horizontal resolution in models is insufficient to capture the fine spatial detail of ice-producing conditions. As a result, research on future changes in ice storm frequency and intensity is limited, and the recent Fourth National Climate Assessment did not make any statements on this weather phenomenon.

In North Carolina, the presence of the Appalachian Mountains in the western part of the state can result in a phenomenon known as cold-air damming, in which a shallow layer of cold air moves southward across the Carolinas. This setup can be accompanied by freezing rain or ice pellets. However, there is no reason why cold-air damming would be expected to change in a warmer climate, other than that the temperature of the cold air masses could moderate.

Freezing rain takes place when a layer of warm air moves over the shallow cold air near the surface, such as during cold-air damming. With warming, it may be easier for these warm layers to develop, and at least one study linked a North Carolina ice storm to warm offshore waters (Ramos de Silva et al. 2006). Thus, it is possible that warming could result in an increase of these warm layers, increasing freezing rain occurrence.

Taken together, the preceding discussion demonstrates that there is considerable uncertainty in projected changes in freezing rain in a warming climate, and more research is needed. Given the evidence currently available, our conclusion is that there is *low confidence* concerning future changes in the number of ice storms.

2.5.2 Thunderstorms and Tornadoes

Tornado and severe thunderstorm events cause significant loss of life and property: more than one-third of the $1 billion weather disasters in the United States during the past 25 years were due to such events, and, relative to other extreme weather, the damages related to severe thunderstorms have undergone the largest increase since 1980 (Smith and Katz 2013).

A particular challenge in quantifying the existence and intensity of these events arises from the data source: rather than measurements, the occurrence of tornadoes and severe thunderstorms is determined by visual sightings by eyewitnesses (such as "storm spotters" and law enforcement officials) or post-storm damage assessments. The reporting has been susceptible to changes in population density, modifications to reporting procedures and training, the introduction of video and social media, and so on. These have led to systematic, non-meteorological biases in the long-term data record.

Nonetheless, judicious use of the report database has revealed important information about tornado trends. Since the 1970s, the United States has experienced a decrease in the number of days per year on which tornadoes occur but an increase in the number of tornadoes that form on such days. One important implication is that the frequency of days with large numbers of tornadoes—tornado outbreaks—appears to be increasing (Figure 9.3 in Kossin et al. 2017). The length of the season over which such tornado activity occurs is increasing as well: although tornadoes in the United States are observed in all months of the year, an earlier calendar-day start to the season of high activity is emerging. In general, there is more interannual variability, or volatility, in tornado occurrence (Elsner et al. 2015, Tippett 2014).

Evaluations of hail and thunderstorm wind reports have thus far been less revealing. Although there is evidence of an increase in the number of hail days per year, the inherent uncertainty in reported hail size reduces the confidence in such a conclusion. Thunderstorm wind reports have proven to be even less reliable because, as compared to tornadoes and hail, there is less tangible visual evidence; thus, although the United States has lately experienced several significant thunderstorm wind events (sometimes referred to as derechos), the lack of studies that explore long-term trends in wind events and the uncertainties in the historical data preclude any robust assessment.

It is possible to bypass the use of reports by exploiting the fact that the temperature, humidity, and wind in the larger vicinity—or "environment"—of a developing thunderstorm ultimately control the intensity, structure, and hazardous tendency of the storm. Thus, the premise is that measures of temperature, humidity, and wind at various heights throughout the atmosphere can be used as a proxy for actual severe thunderstorm occurrence. In particular, a measure of the energy available for convection (known as convective available potential energy, or CAPE) and vertical wind shear (a change in wind speed or direction with a change in altitude) constitutes one widely used means of representing the frequency of severe thunderstorms. This environmental-proxy approach avoids the biases and other issues with eyewitness storm reports and is readily evaluated using the relatively coarse global datasets and global climate models. It has the disadvantage of assuming that a thunderstorm will necessarily form and then realize its environmental potential.

Global climate models consistently project an increase in the frequency of severe thunderstorm environments in the United States over the mid- to late 21st century. The most robust projected increases in frequency are over the U.S. Midwest and Plains during spring (March–May). Based

on the increased frequency of very high CAPE, increases in storm intensity are also projected over this same period (Del Genio et al. 2007).

Some studies using regional models (models that simulate a large region, such as the United States, rather than the entire globe) that can capture the details of individual severe thunderstorms support the conclusions from the preceding paragraph. The individually modeled thunderstorms are quantified and assessed in terms of severity (e.g., Trapp et al. 2011). One study also used a model that simulates individual thunderstorms to examine changes in intense hourly precipitation in the central United States, finding an increase in the most intense events and a decrease in lighter events (Prein et al. 2017). These results have thus far supported the basic findings of studies of changes in the environments conducive to severe storms, particularly in terms of the seasons and geographical regions projected to experience the largest increases in severe thunderstorm occurrence.

Based on remaining scientific uncertainties at this time, we conclude it is ***likely*** that severe thunderstorms in North Carolina will increase.

2.5.3 Hurricanes

Hurricanes and tropical storms are a frequent occurrence in North Carolina (Figure 2.28), with an average of a little more than one tropical storm or hurricane event passing near or over the state every year since 1900 (or approximately six events over a 5-year period). Hurricanes actually crossing the state occur once every 2 to 3 years (Frankson et al. 2017; 2019 update). Recent activity (since 1985) has been above the 20th-century average, with approximately eight events per 5-year period. The highest 5-year total since 1850 was 13 events, which occurred in 2000–2004. The latter half of the 19th century was also a period of above average activity. This indicates that future changes will be a combination of largely unpredictable natural variations and the physics-based changes from a warmer world.
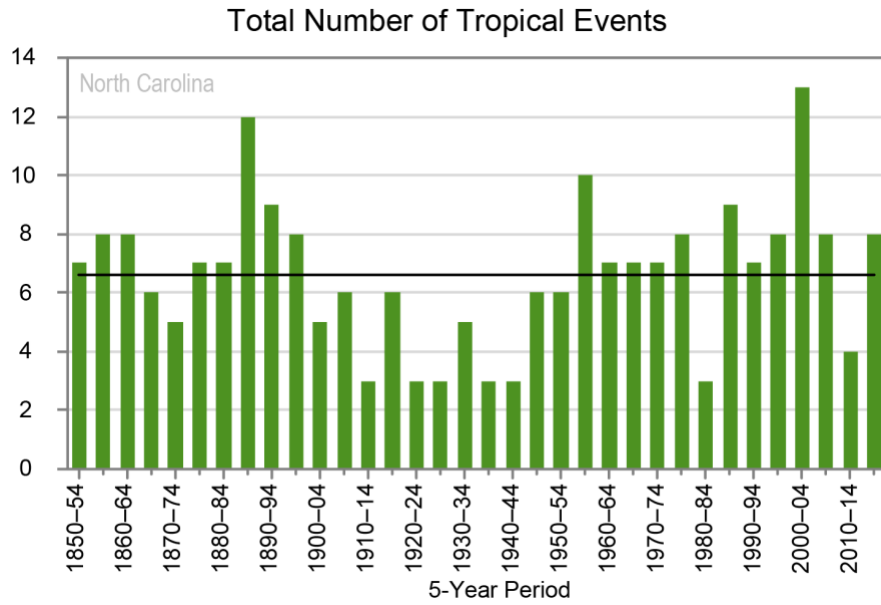
Total Number of Tropical Events

Figure 2.28. The bar graph shows the total number of tropical events (tropical storms or hurricanes) passing near or over North Carolina for 5-year periods since 1850. The last bar shows the 4-year period of 2015–2018. The long-term average (for 1850–2018) is six tropical events per 5-year period, or slightly more than one per year. The last half of the 19th century was characterized by above average activity followed by below average activity in the first half of the 20th century. Sources: U.S. Geological Survey, NCICS, and NOAA NCEI.

While the tremendous costs of hurricanes are most visible, there are benefits to society as well. In particular, heavy precipitation accompanying hurricanes can be beneficial in the form of a tropical storm-level disturbance that brings soaking rain to a drought-stricken area. More commonly, however, hurricanes can produce flooding rainfall. The recent destructive flooding impacts from Hurricane Matthew in 2016 and Hurricane Florence in 2018 have highlighted the exposure and risks the state faces from these powerful storms. But understanding and predicting how climate change could affect the frequency, intensity, and rainfall characteristics of hurricanes is difficult because of the complex response of these short-lived events to the changing background environmental conditions (Kossin et al. 2017).

Historical trends in hurricanes reveal significant changes due to natural variability, and these year-to-year variations may obscure the more gradual changes in hurricane characteristics due to climate change. The amount of influence that human-induced warming has had on hurricanes to date is believed to be relatively small, and this, in conjunction with observational limitations and large natural variations, makes it difficult to establish whether there are as yet any clear trends in hurricanes that can be attributed to human-induced warming (e.g., Knutson et al. 2019a).

In numerous previous studies of hurricanes and climate change, a consistent finding is that the strongest storms will become stronger as the climate continues to warm. There is less consistency regarding how hurricane frequency will change. Many previous studies have

suggested a *decrease* in the frequency of hurricanes as the climate warms (e.g., review paper by Knutson et al. 2019b). These findings imply a shift towards increased average hurricane intensity. However, in recent years several studies have suggested that there will be either little change in frequency with warming or even increases in hurricane frequency (e.g., Bhatia et al. 2018). The result that the strongest storms will get stronger still holds, but there is lessened confidence that hurricane frequency will decrease. The most recent studies tend to use higher model resolution (e.g., Bhatia et al. 2018) and are thus better able to represent the process of hurricane formation and intensification. Generally, the most important factors affecting the occurrence and intensity of hurricanes are ocean temperatures, atmospheric moisture, and changing wind speeds at higher levels in the atmosphere (i.e., vertical wind shear).

Ocean Temperatures: Warm ocean water is required for hurricane formation, and sea surface temperatures (SSTs) are warming in response to greenhouse gas emissions. This alone motivated initial research into the possibility of increased future hurricane intensity with warming (e.g., Emanuel 1987). However, climate models also show warming aloft in the tropics, which works against the strengthening of hurricanes and thus mitigates the strengthening to some extent. In other words, if both the ocean and the atmosphere warmed uniformly, there would be a very large increase in hurricane intensity. However, with greater warming at upper levels of the atmosphere in the tropics compared to warming SSTs, hurricane intensity still increases, but the increase is lessened (e.g., Shen et al. 2000, Hill and Lackmann 2011, Tuleya et al. 2016).

Atmospheric Moisture: Dry air inhibits hurricane formation. A consequence of warming is an increase in the amount of moistening (humidity) needed to bring air to saturation. This means that it is more difficult for initial disturbances to develop into mature hurricanes in dry environments. However, humidity limits hurricane formation in only some situations. While the amount of moistening needed to reach saturation will increase as temperature increases in the future, which works against hurricane formation, there are other factors that may dominate this effect.

Wind Shear: Strong vertical wind shear (the change in wind speed and/or direction with height) is detrimental to hurricane formation and intensity. Climate model projections of changes in vertical wind shear across the Atlantic basin exhibit considerable variability, but there is some degree of consensus that the subtropical Atlantic would experience a decrease in shear, which could favor increased hurricane activity in this region (Vecchi and Soden 2007). Other recent studies suggest that increased wind shear near the U.S. East Coast in the current climate, which helps to reduce hurricane impacts there, could weaken in a warming climate, further increasing risks (Ting et al. 2019).

A known consequence of warming is an increase in atmospheric water vapor content, meaning that a hurricane in a warmer environment will ***likely*** produce heavier precipitation (Knutson et al. 2010, 2019b). A survey of recent literature indicates ***medium to high confidence*** that precipitation rates will increase with warming; a median increase of 14% was found for studies examining the effects of a 3.6°F (2°C) global warming (Knutson et al. 2019). With continued

warming, increased freshwater flooding from hurricanes will **_likely_** take place. This will be exacerbated by increasing urbanization that adds impervious surfaces and development in low-lying areas.

Damage from severe winds and storm surge are also significant threats with landfalling hurricanes. With **_medium to high confidence_** for expected increases in the intensity of the strongest hurricanes, there is a corresponding **_medium to high confidence_** in future increases in the likelihood of damaging storm surge and severe winds with future hurricanes. Hurricanes can also spawn tornadoes, as was recently experienced with Hurricane Dorian (occurred in 2019), which was accompanied by more than 20 tornadoes in North Carolina and South Carolina. Stronger hurricanes would, all else being equal, be more prone to produce tornadoes due to a stronger wind field, but there is **_very low confidence_** in this projection due to the limited research results to date.

Even hurricanes that make landfall far from North Carolina, such as along the U.S. Gulf Coast, can cause significant damage to the state. Hurricane Ivan (occurred in 2004), for example, led to flooding along the French Broad, Swannanoa, and Pigeon Rivers, in addition to debris flows, in western North Carolina. When hurricanes move out of the tropics, their structure and size change. The process through which a tropical system transforms into one that has characteristics of midlatitude low pressure systems is called extratropical transition. In North Carolina, several impactful events have accompanied hurricanes that were undergoing this transition at the time, such as Hurricane Floyd (occurred in 1999). Recent research on how climate change would influence these transitioning systems indicates that they will **_likely_** retain greater intensity and be accompanied by heavier precipitation in a warmer climate (e.g., Jung and Lackmann 2019, Michaelis and Lackmann 2019). Note that there have been very few studies of extratropical transition and climate change to date, so **_confidence_** in these results will remain **_low_** until they are corroborated by additional research.

Based on the assessment above, we conclude the following:

1. The intensity of the strongest hurricanes is **_likely_** to increase with warming, and this could result in stronger hurricanes impacting North Carolina. **_Confidence_** in this result is **_high_** for changes in tropical storms (including hurricanes) globally, but lower for individual regions such as North Carolina.

2. Heavy precipitation accompanying hurricanes is **_very likely_** to increase, increasing freshwater flood potential.

3. The frequency of hurricane impacts on North Carolina in the future is not clear at this time, but earlier projections of decreases in hurricane activity now appear less confident in light of recent high-resolution modeling studies.

Box 2.1: Hurricane Florence

Hurricane Florence made landfall on the North Carolina coast on September 14, 2018, as a Category 1 storm. Florence's forward speed slowed at about the time of landfall, and it meandered over the eastern portions of North Carolina and South Carolina for several days. The result was torrential rainfall accumulations, in the range of 20 to 36 inches in eastern North Carolina (Figure 2.29), causing widespread destruction with losses in excess of $22 billion (in 2019 dollars), more than the combined losses from Hurricanes Floyd (occurred in 1999) and Matthew (occurred in 2016). At Wilmington, most of the rain fell on September 14, 15, and 16, with 9.58, 7.44, and 4.50 inches, respectively (Figure 2.30). Rainfall amounts on September 14 and 16 were records for those dates. September 2018 was also the wettest month on record at Wilmington, with 24.13 inches, almost all of that falling during Hurricane Florence.

Sea surface temperatures off the coast of North Carolina were about 3°F above the 1981–2010 average during early September 2018 (Figure 2.31). As air temperature rises, the proportion of water vapor in the atmosphere increases at about 3.5% per °F, so it is ***very likely*** that the high sea surface temperatures contributed to the excessive rainfall. Analysis of historical rainfall statistics for the United States indicates that Hurricane Florence rainfall totals were among the highest multiday, area-averaged amounts in U.S. history for rainfall area sizes of up to 20,000 square miles.

Hurricane Matthew caused torrential rainfall in eastern North Carolina in October 2016. Rainfall amounts of up to 18.95 inches were reported (Stewart 2017). Maximum rainfall amounts were less than Florence amounts because Matthew did not slow down and rainfall was mostly restricted to a 1- to 2-day period. While global warming is ***likely*** to lead to heavier rainfall rates in hurricanes, there is no scientific evidence that future landfalling hurricanes are more likely to slow down after landfall.
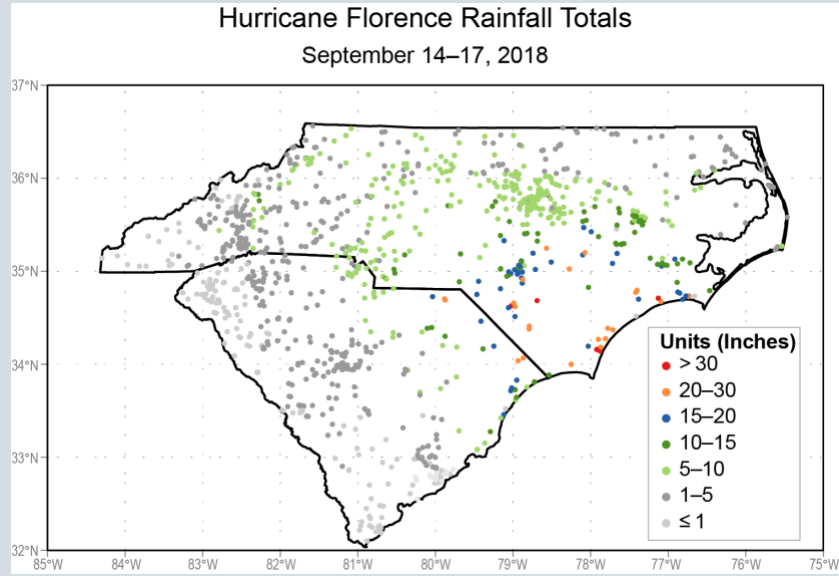
Figure 2.29. The map shows total rainfall (inches) for September 14–17, 2018, for North Carolina and South Carolina. Source: adapted from Kunkel and Champion 2019.
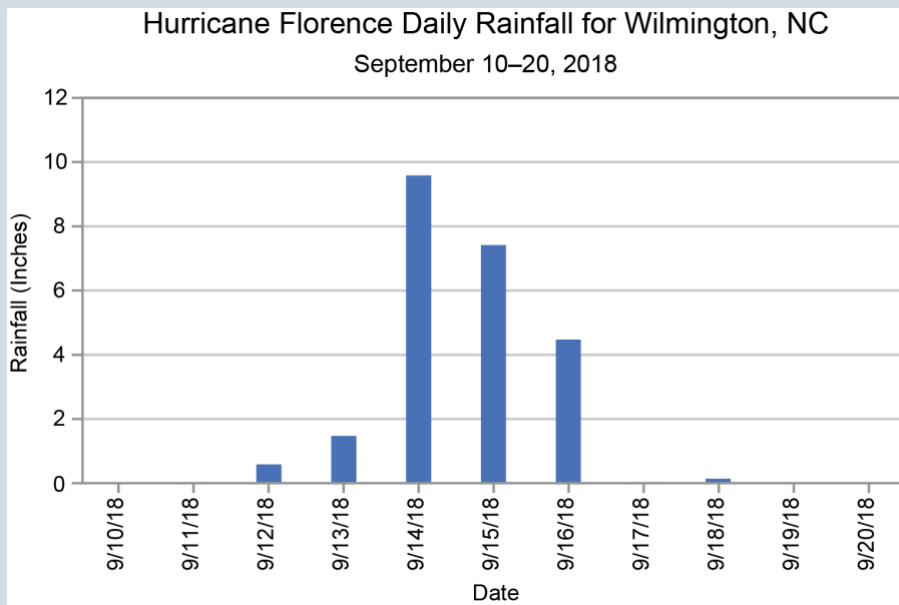

Figure 2.30. The figure shows daily rainfall totals at Wilmington, NC, from Hurricane Florence for September 10–20, 2018. Sources: NCICS and NOAA NCEI.
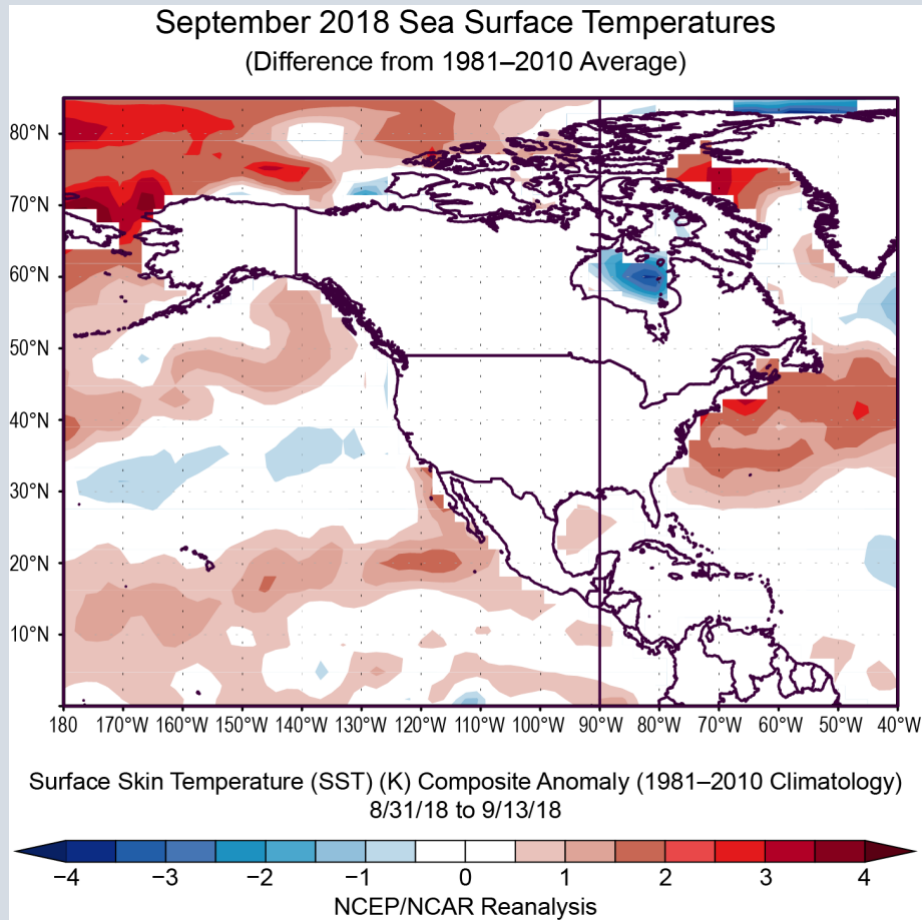
Figure 2.31. The map shows sea surface temperature anomalies for early September 2018 compared to the 1981–2010 averages. Values off the coast of North Carolina are in the range of 0.5–2.0 K (0.9°–3.6°F) warmer than average. Sources: Image provided by NOAA ESRL Physical Sciences Division, Boulder, Colorado, from their website http://www.esrl.noaa.gov/psd/; Kalnay et al. 1996.

2.6 References

Barnes, E.A. and L.M. Polvani, 2015: CMIP5 projections of Arctic amplification, of the North American/North Atlantic circulation, and of their relationship. *Journal of Climate,* **28** (13), 5254–5271. http://dx.doi.org/10.1175/JCLI-D-14-00589.1

Bender, F.A.-M., V. Ramanathan, and G. Tselioudis, 2012: Changes in extratropical storm track cloudiness 1983–2008: Observational support for a poleward shift. *Climate Dynamics,* **38** (9), 2037–2053. http://dx.doi.org/10.1007/s00382-011-1065-6

Bhatia, K., G. Vecchi, H. Murakami, S. Underwood, and J. Kossin, 2018: Projected response of tropical cyclone intensity and intensification in a global climate model. *Journal of Climate,* **31**, 8281–8303. http://dx.doi.org/10.1175/JCLI-D-17-0898.1

Cohen, J., X. Zhang, J. Francis, T. Jung, R. Kwok, J. Overland, T.J. Ballinger, U.S. Bhatt, H.W. Chen, D. Coumou, S. Feldstein, H. Gu, D. Handorf, G. Henderson, M. Ionita, M. Kretschmer, F. Laliberte, S. Lee, H.W. Linderholm, W. Maslowski, Y. Peings, K. Pfeiffer, I. Rigor, T. Semmler, J. Stroeve, P.C. Taylor, S. Vavrus, T. Vihma, S. Wang, M. Wendisch, Y. Wu, and J. Yoon, 2020: Divergent consensuses on Arctic amplification influence on midlatitude severe winter weather. *Nature Climate Change,* **10** (1), 20–29. http://dx.doi.org/10.1038/s41558-019-0662-y

Colle, B.A., Z. Zhang, K.A. Lombardo, E. Chang, P. Liu, and M. Zhang, 2013: Historical evaluation and future prediction of eastern North American and western Atlantic extratropical cyclones in the CMIP5 models during the cool season. *Journal of Climate,* **26** (18), 6882–6903. http://dx.doi.org/10.1175/JCLI-D-12-00498.1

Colle, B.A., J.F. Booth, and E.K.M. Chang, 2015: A review of historical and future changes of extratropical cyclones and associated impacts along the US East Coast. *Current Climate Change Reports,* **1** (3), 125–143. http://dx.doi.org/10.1007/s40641-015-0013-7

Collins, M., R. Knutti, J. Arblaster, J.-L. Dufresne, T. Fichefet, P. Friedlingstein, X. Gao, W.J. Gutowski, T. Johns, G. Krinner, M. Shongwe, C. Tebaldi, A.J. Weaver, and M. Wehner, 2013: Long-term climate change: Projections, commitments and irreversibility. *Climate Change 2013: The Physical Science Basis. Contribution of Working Group I to the Fifth Assessment Report of the Intergovernmental Panel on Climate Change*. Stocker, T.F., D. Qin, G.-K. Plattner, M. Tignor, S.K. Allen, J. Boschung, A. Nauels, Y. Xia, V. Bex, and P.M. Midgley, Eds. Cambridge University Press, Cambridge, United Kingdom and New York, NY, USA, 1029–1136. https://www.ipcc.ch/report/ar5/wg1/

Del Genio, A.D., M.S. Yao, and J. Jonas, 2007: Will moist convection be stronger in a warmer climate? *Geophysical Research Letters,* **34** (16), L16703. http://dx.doi.org/10.1029/2007GL030525

Eck, M.A., L.B. Perry, P.T. Soulé, J.W. Sugg, and D.K. Miller, 2019: Winter climate variability in the southern Appalachian Mountains, 1910–2017. *International Journal of Climatology,* **39** (1), 206–217. http://dx.doi.org/10.1002/joc.5795

Elsner, J.B., S.C. Elsner, and T.H. Jagger, 2015: The increasing efficiency of tornado days in the United States. *Climate Dynamics,* **45** (3), 651–659. http://dx.doi.org/10.1007/s00382-014-2277-3

Emanuel, K.A., 1987: The dependence of hurricane intensity on climate. *Nature,* **326** (6112), 483–485. http://dx.doi.org/10.1038/326483a0

Frankson, R., K. Kunkel, L. Stevens, D. Easterling, W. Sweet, A. Wootten, and R. Boyles, 2017: North Carolina State Climate Summary. NOAA Technical Report NESDIS 149-NC, May 2019 Revision. 4 pp. https://statesummaries.ncics.org/chapter/nc/

Gula, J. and W. Peltier, 2012: Dynamical downscaling over the Great Lakes Basin of North America using the WRF regional climate model: The impact of the Great Lakes system on regional greenhouse warming. *Journal of Climate,* **25**, 7723–7742. http://dx.doi.org/10.1175/JCLI-D-11-00388.1

Hill, K. and G. Lackmann, 2011: The impact of future climate change on TC intensity and structure: A downscaling approach. *Journal of Climate,* **24**, 4644–4661. http://dx.doi.org/10.1175/2011JCLI3761.1

Jung, C. and G. Lackmann, 2019: Extratropical transition of Hurricane Irene (2011) in a changing climate. *Journal of Climate,* **32** (15), 4847–4871. http://dx.doi.org/10.1175/JCLI-D-18-0558.1

Kalnay, E., M. Kanamitsu, R. Kistler, W. Collins, D. Deaven, L. Gandin, M. Iredell, S. Saha, G. White, J. Woollen, Y. Zhu, M. Chelliah, W. Ebisuzaki, W. Higgins, J. Janowiak, K.C. Mo, C. Ropelewski, J. Wang, A. Leetmaa, R. Reynolds, R. Jenne, and D. Joseph, 1996: The NCEP/NCAR 40-Year Reanalysis Project. *Bulletin of the American*

Meteorological Society, **77** (3), 437–472. http://dx.doi.org/10.1175/1520-0477(1996)077<0437:TNYRP>2.0.CO;2

Keighton, S., L. Lee, B. Holloway, D. Hotz, S. Zubrick, J. Hovis, G. Votaw, L.B. Perry, G. Lackmann, S.E. Yuter, C. Konrad, D. Miller, and B. Etherton, 2009: A collaborative approach to study northwest flow snow in the southern Appalachians. *Bulletin of the American Meteorological Society,* **90** (7), 979–992. http://dx.doi.org/10.1175/2009BAMS2591.1

Knutson, T., S.J. Camargo, J.C.L. Chan, K. Emanuel, C.-H. Ho, J. Kossin, M. Mohapatra, M. Satoh, M. Sugi, K. Walsh, and L. Wu, 2019a: Tropical cyclones and climate change assessment: Part I. Detection and attribution. *Bulletin of the American Meteorological Society*. http://dx.doi.org/10.1175/BAMS-D-18-0189.1

Knutson, T., S.J. Camargo, J.C.L. Chan, K. Emanuel, C.-H. Ho, J. Kossin, M. Mohapatra, M. Satoh, M. Sugi, K. Walsh, and L. Wu, 2019b: Tropical cyclones and climate change assessment: Part II. Projected response to anthropogenic warming. *Bulletin of the American Meteorological Society*. http://dx.doi.org/10.1175/BAMS-D-18-0194.1

Knutson, T.R., J.L. McBride, J. Chan, K. Emanuel, G. Holland, C. Landsea, I. Held, J.P. Kossin, A.K. Srivastava, and M. Sugi, 2010: Tropical cyclones and climate change. *Nature Geoscience,* **3** (3), 157–163. http://dx.doi.org/10.1038/ngeo779

Kossin, J.P., T. Hall, T. Knutson, K.E. Kunkel, R.J. Trapp, D.E. Waliser, and M.F. Wehner, 2017: Extreme storms. *Climate Science Special Report: Fourth National Climate Assessment, Volume I*. Wuebbles, D.J., D.W. Fahey, K.A. Hibbard, D.J. Dokken, B.C. Stewart, and T.K. Maycock, Eds. U.S. Global Change Research Program, Washington, DC, USA, 257–276. http://dx.doi.org/10.7930/J07S7KXX

Krasting, J.P., A.J. Broccoli, K.W. Dixon, and J.R. Lanzante, 2013: Future changes in Northern Hemisphere snowfall. *Journal of Climate,* **26** (20), 7813–7828. http://dx.doi.org/10.1175/JCLI-D-12-00832.1

Kunkel, K.E., M. Palecki, L. Ensor, K.G. Hubbard, D. Robinson, K. Redmond, and D. Easterling, 2009: Trends in twentieth-century U.S. snowfall using a quality-controlled dataset. *Journal of Atmospheric and Oceanic Technology,* **26**, 33–44. http://dx.doi.org/10.1175/2008JTECHA1138.1

Kunkel, K.E. and S.M. Champion, 2019: An assessment of rainfall from Hurricanes Harvey and Florence relative to other extremely wet storms in the United States. *Geophysical Research Letters,* **46** (22), 13500–13506. http://dx.doi.org/10.1029/2019GL085034

Li, L., W. Li, and Y. Kushnir, 2012: Variation of the North Atlantic subtropical high western ridge and its implication to Southeastern US summer precipitation. *Climate Dynamics,* **39** (6), 1401–1412. http://dx.doi.org/10.1007/s00382-011-1214-y

Li, L., W. Li, and Y. Deng, 2013: Summer rainfall variability over the Southeastern United States and its intensification in the 21st century as assessed by CMIP5 models. *Journal of Geophysical Research: Atmospheres,* **118** (2), 340–354. http://dx.doi.org/doi:10.1002/jgrd.50136

Marciano, C.G., G.M. Lackmann, and W.A. Robinson, 2015: Changes in U.S. East Coast Cyclone Dynamics with Climate Change. *Journal of Climate,* **28** (2), 468–484. https://doi.org/10.1175/JCLI-D-14-00418.1

Martin, D.T., L.B. Perry, D.K. Miller, and P.T. Soulé, 2015: Snowfall event characteristics from a high-elevation site in the Southern Appalachian Mountains, USA. *Climate Research,* **63** (3), 171–190. https://www.int-res.com/abstracts/cr/v63/n3/p171-190/

Michaelis, A., J. Willison, G. Lackmann, and W. Robinson, 2017: Changes in winter North Atlantic extratropical cyclones in high-resolution regional pseudo-global warming simulations. **30** (17), 6905–6925. http://dx.doi.org/10.1175/JCLI-D-16-0697.1

Michaelis, A.C. and G.M. Lackmann, 2019: Climatological changes in the extratropical transition of tropical cyclones in high-resolution global simulations. *Journal of Climate*. http://dx.doi.org/10.1175/JCLI-D-19-0259.1

Ning, L. and R.S. Bradley, 2015: Snow occurrence changes over the central and eastern United States under future warming scenarios. *Scientific Reports,* **5**, 17073. http://dx.doi.org/10.1038/srep17073

O'Gorman, P.A., 2014: Contrasting responses of mean and extreme snowfall to climate change. *Nature,* **512** (7515), 416–418. http://dx.doi.org/10.1038/nature13625

Perry, L.B., C.E. Konrad, and T.W. Schmidlin, 2007: Antecedent upstream air trajectories associated with northwest flow snowfall in the southern Appalachians. *Weather and Forecasting,* **22** (2), 334–352. http://dx.doi.org/10.1175/waf978.1

Prein, A.F., C. Liu, K. Ikeda, S.B. Trier, R.M. Rasmussen, G.J. Holland, and M.P. Clark, 2017: Increased rainfall volume from future convective storms in the US. **7** (12), 880–884. http://dx.doi.org/10.1038/s41558-017-0007-7

Ramos da Silva, R., G. Bohrer, D. Werth, M.J. Otte, and R. Avissar, 2006: Sensitivity of ice storms in the southeastern United States to Atlantic SST—Insights from a case study of the December 2002 storm. *Monthly Weather Review,* **134** (5), 1454–1464. http://dx.doi.org/10.1175/MWR3127.1

Roberts, K.J., B.A. Colle, and N. Korfe, 2017: Impact of simulated twenty-first-century changes in extratropical cyclones on coastal flooding at the Battery, New York City. *Journal of Applied Meteorology and Climatology,* **56** (2), 415–432. http://dx.doi.org/10.1175/JAMC-D-16-0088.1

Shen, W., R.E. Tuleya, and I. Ginis, 2000: A sensitivity study of the thermodynamic environment on GFDL model hurricane intensity: Implications for global warming. *Journal of Climate,* **13** (1), 109–121. http://dx.doi.org/10.1175/1520-0442(2000)013<0109:ASSOTT>2.0.CO;2

Smith, A.B. and R.W. Katz, 2013: U.S. billion-dollar weather and climate disasters: Data sources, trends, accuracy and biases. *Natural Hazards,* **67** (2), 387–410. http://dx.doi.org/10.1007/s11069-013-0566-5

State Climate Office of North Carolina, n.d.: NC Climate Synopsis, accessed October 29, 2019. http://climate.ncsu.edu/climate/synopsis

Stewart, S.R., 2017: Hurricane Matthew (AL143016) 28 September–9 October 2019. National Hurricane Center Tropical Cyclone Report. 96 pp. https://www.nhc.noaa.gov/data/tcr/AL142016_Matthew.pdf

Ting, M., J.P. Kossin, S.J. Camargo, and C. Li, 2019: Past and future hurricane intensity change along the U.S. East Coast. **9** (1), 7795. http://dx.doi.org/10.1038/s41598-019-44252-w

Tippett, M.K., 2014: Changing volatility of U.S. annual tornado reports. *Geophysical Research Letters,* **41** (19), 6956–6961. http://dx.doi.org/10.1002/2014GL061347

Trapp, R.J., E.D. Robinson, M.E. Baldwin, N.S. Diffenbaugh, and B.R.J. Schwedler, 2011: Regional climate of hazardous convective weather through high-resolution dynamical downscaling. *Climate Dynamics,* **37** (3), 677–688. http://dx.doi.org/10.1007/s00382-010-0826-y

Tuleya, R.E., M. Bender, T.R. Knutson, J.J. Sirutis, B. Thomas, and I. Ginis, 2016: Impact of upper-tropospheric temperature anomalies and vertical wind shear on tropical cyclone evolution using an idealized version of the

operational GFDL hurricane model. *Journal of the Atmospheric Sciences,* **73** (10), 3803–3820. http://dx.doi.org/10.1175/JAS-D-16-0045.1

Vecchi, G.A. and B.J.C.L. Soden, 2007: Increased tropical Atlantic wind shear in model projections of global warming. **34** (8). http://dx.doi.org/10.1029/2006GL028905

Zhang, Z. and B.A. Colle, 2018: Impact of dynamically downscaling two CMIP5 models on the historical and future changes in winter extratropical cyclones along the East Coast of North America. *Journal of Climate,* **31** (20), 8499–8525. http://dx.doi.org/10.1175/JCLI-D-18-0178.1

3. Regional Changes in Temperature, Precipitation, and Storms

3.1 Introduction

The climate conditions across the state are influenced by two major geographic features, the Atlantic Ocean to the east and the mountains in the western part of the state. Air over the ocean is usually more humid and experiences smaller day-to-night temperature variations than air over land. As a result, the coastal areas of the state experience more humid conditions and smaller day-to-night temperature differences, particularly when the air flow is onshore, than areas to the west. This oceanic influence on the climate diminishes as distance from the coast increases. The higher elevations in the Western Mountains have a direct influence on temperature. On average, temperature decreases about 3.5°F per 1,000 feet of elevation, simply due to lower atmospheric pressure. The higher elevations also provide a barrier to wind flow, forcing air upward and increasing precipitation on the windward slopes of the mountains.

Because of the differences in certain aspects of the average climate conditions that derive from these geographic features, this chapter examines climate trends and projections by region. Three broad regions were defined for this study: Coastal Plain, Piedmont, and Western Mountains (Figure 3.1). Because the influence of oceanic air characteristics diminishes gradually with distance from the coast, the boundary between the Coastal Plain and the Piedmont is somewhat arbitrary and was chosen such that the two regions have an approximately equal east–west extent. By contrast, the effects of elevation on climate are abrupt, so the boundary between the Piedmont and the Western Mountains consists of the eastern boundaries of counties that include elevations above 2,000 feet.
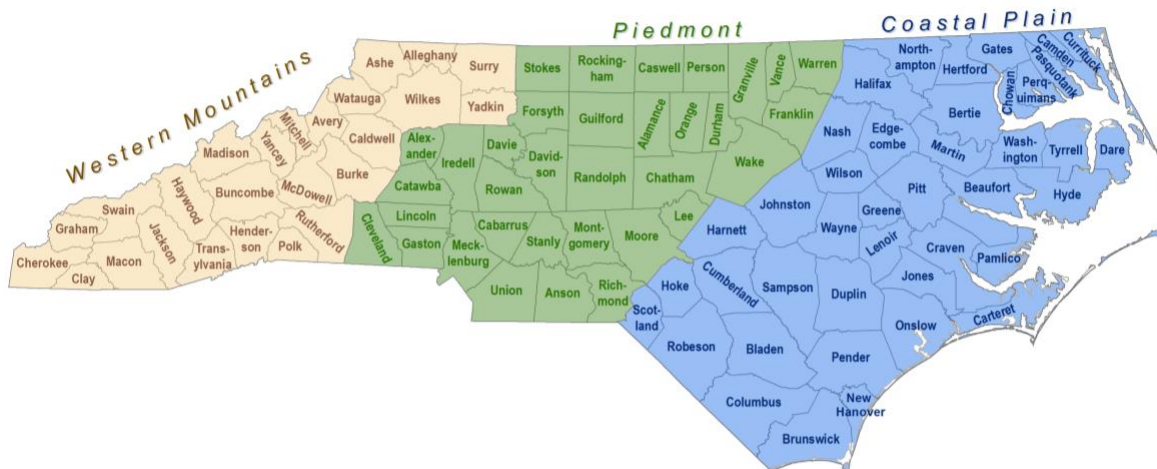
Figure 3.1. The map of North Carolina shows the counties in each of the three regions used in this report: Western Mountains, Piedmont, and Coastal Plain. Source: NCICS.

See Appendix A for details on the datasets and scenarios used in this chapter.

3.2 Coastal Plain

3.2.1 Average Temperature

Trends in annual average temperatures in the Coastal Plain (Figure 3.2) are similar to statewide trends (see Figure 2.1). Temperatures were below the long-term average through 1920, generally above average in both the 1930s and 1940s, then well below average in the 1960s. They have been increasing since then and have remained consistently above average since the 1990s. Each of the last 4 years (2015–2018) has been one of the 8 warmest on record, while 16 of the last 18 years have been above the long-term average of about 61°F degrees for the Coastal Plain region.

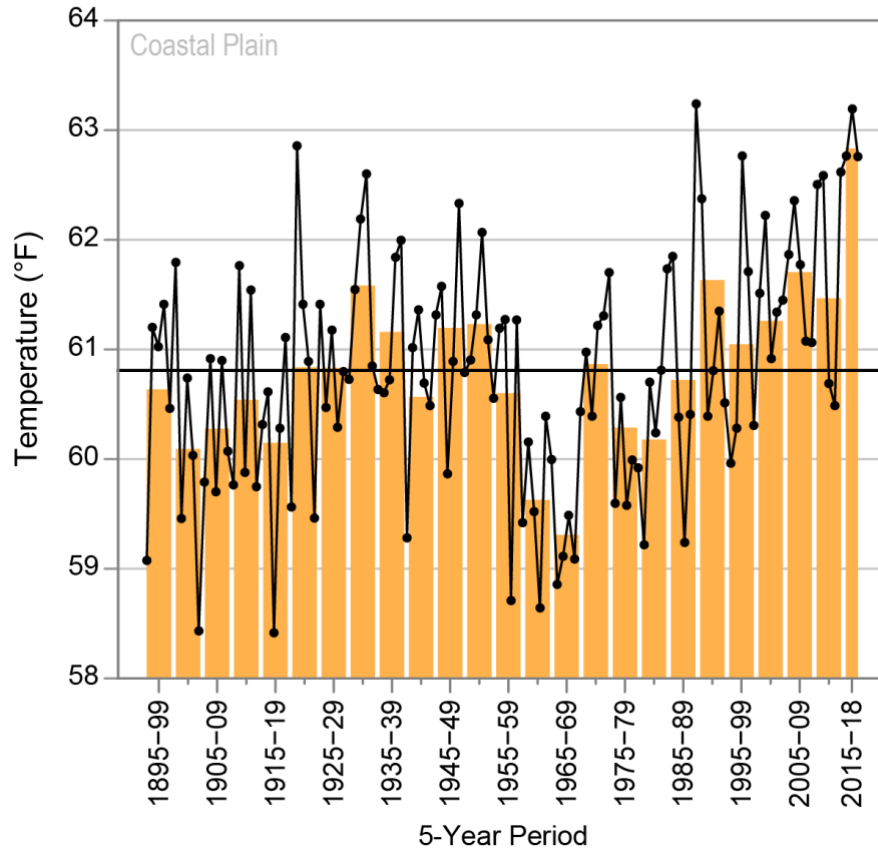## Observed Annual Average Temperature: Coastal Plain (1895–2018)

Figure 3.2. The bar graph shows the observed annual average temperature for the Coastal Plain region of North Carolina for 1895–2018, as averaged over 5-year periods, with the last bar representing a 4-year period (2015–2018). Dots show annual values. The horizontal black line shows the long-term average of 60.8°F for 1895–2018. Source: NCICS, NOAA NCEI, and the State Climate Office of North Carolina.

By the end of the century, the average temperature is projected to increase by 2°–5°F under the lower scenario (RCP 4.5) and by 6°–10°F under the higher scenario (RCP 8.5; Figure 3.3), compared to the average temperature for 1996–2015. Figure 3.3 also shows the observed average temperature value for the period 1970–2013. Here, the Livneh observational dataset is used (see Appendix A for a description of datasets).

The observed temperatures have tended to be on the lower end of the range of historical model simulations (not shown), similar to the statewide average temperature (Frankson et al. 2017; 2019 update). This suggests that the lower end of the projected values is a more likely outcome for the future. However, since the causes of the lesser warming observed in the Southeast are not yet fully understood and recent years have exhibited substantial warming, the higher end of the projected values should not be discounted as a possibility.
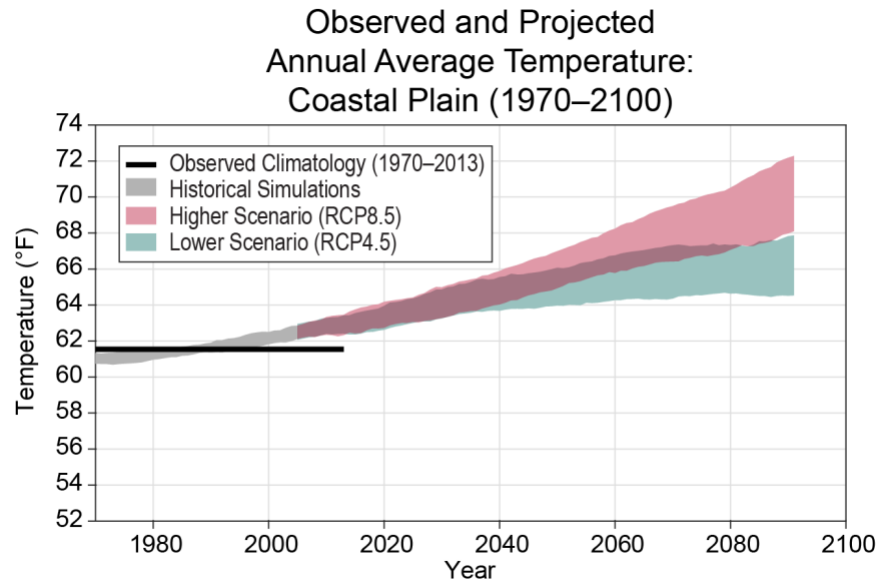
Figure 3.3. These time series show the simulated historical and projected annual average temperature for the Coastal Plain region of North Carolina from the LOCA data and the observed climatological value averaged for the period 1970–2013 (black line). Historical simulations (gray shading) are shown for 1970–2005. Projected changes for 2006–2100 are shown for a higher scenario (RCP8.5; red shading) and a lower scenario (RCP4.5; green shading). The shaded ranges indicate the 10% to 90% confidence intervals of 20-year running averages from the set of climate models. Sources: NCICS and The University of Edinburgh.

3.2.2 Hot Days and Warm Nights

The Coastal Plain region has not experienced an overall increase in the frequency of very hot days (maximum temperature of 95°F or higher; Figure 3.4) over the period 1970–2013, though there has been an increasing trend in the number of very warm nights (minimum temperature of 75°F or higher; Figure 3.5) over the same period.

On average, the Coastal Plain region sees about 13 very hot days per year. Changes in the annual number of such days have not followed the same pattern as annual average temperatures (Figure 3.2). In fact, there were more instances of very hot days earlier in the first half of the 20th century compared to recent years. The highest average—23 days per year—occurred in 1930–1934. The higher frequencies of such days during the late 1920s through the early 1950s correspond to periods of exceptionally dry weather.
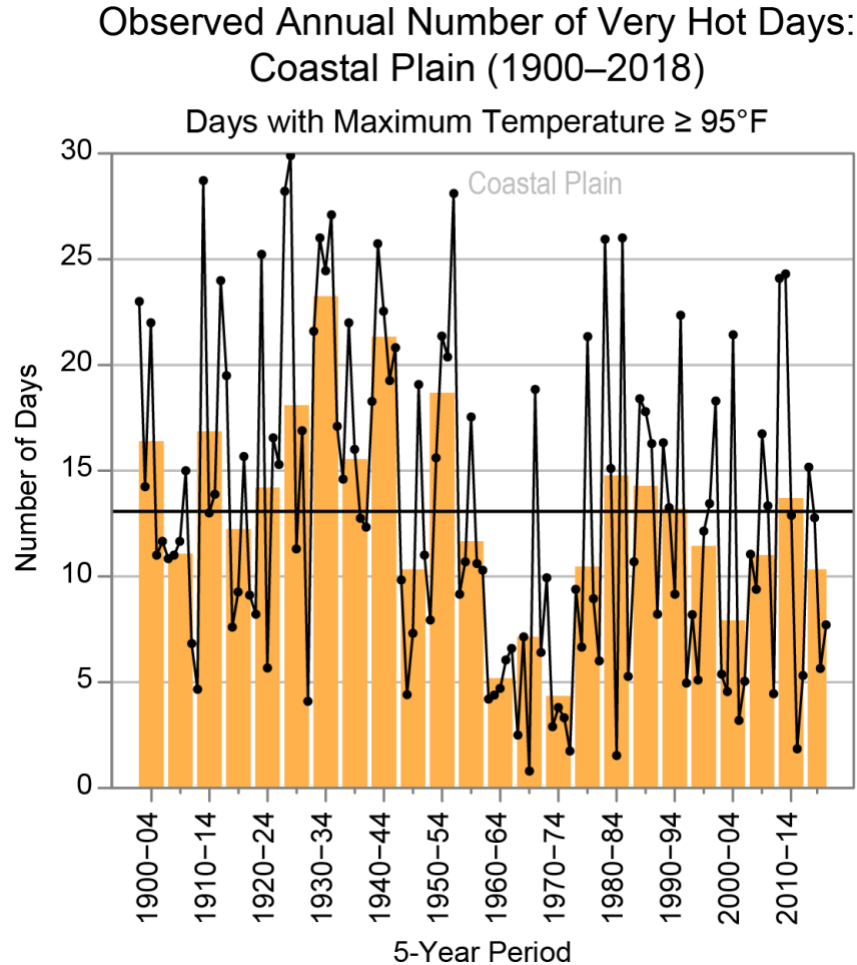
Observed Annual Number of Very Hot Days: Coastal Plain (1900–2018)

Days with Maximum Temperature ≥ 95°F

Figure 3.4. The bar graph shows the observed annual number of very hot days (maximum temperature of 95°F or higher) for the Coastal Plain region of North Carolina for 1900–2018, as averaged over 5-year periods, with the last bar representing a 4-year period (2015–2018). Dots show annual values. The horizontal black line shows the long-term average of 13 very hot days per year for 1900–2018. Source: NCICS, NOAA NCEI, and the State Climate Office of North Carolina.

The region sees a long-term average of about 8 very warm nights per year. The changes over the period of record (Figure 3.5) have been similar to the pattern in annual average temperatures (Figure 3.2), with an increasing trend since 1970. The average annual number of very warm nights was well above the long-term average during the very first period (1900–1904), which included the highest annual value of about 23 days in 1900. Most years since 2005 have been at or above the long-term average, and this period includes the 2nd (2010), 3rd (2016), and 4th (2017) highest years.
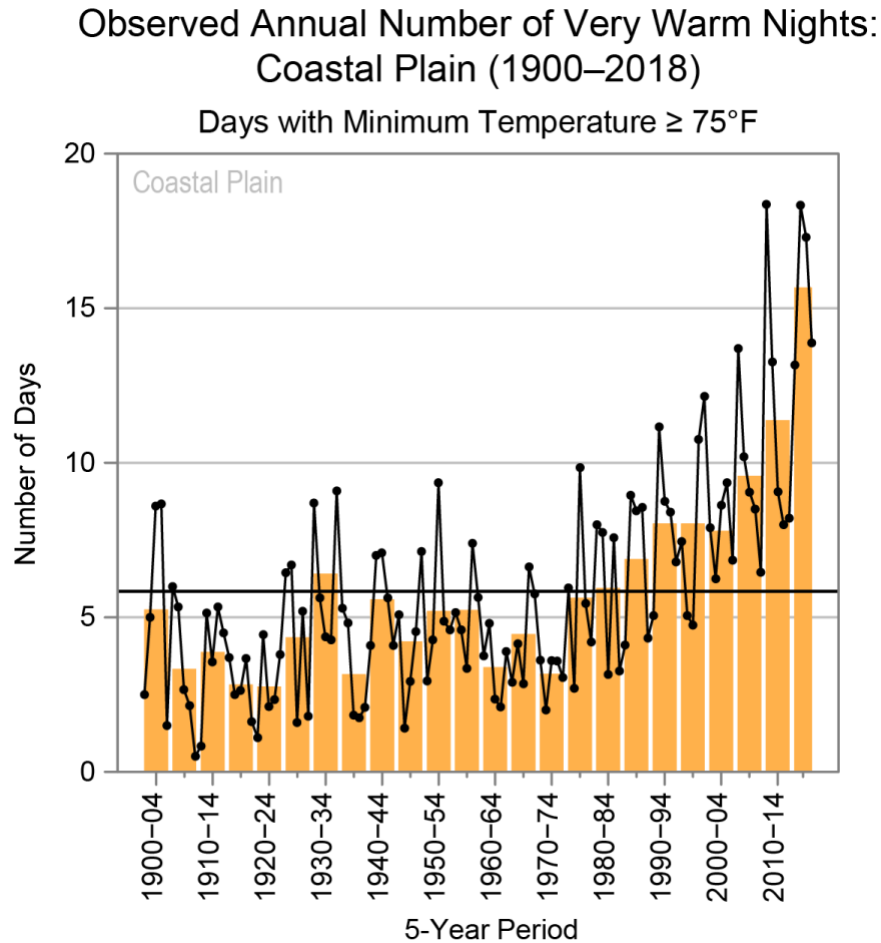
Observed Annual Number of Very Warm Nights: Coastal Plain (1900–2018)

Days with Minimum Temperature ≥ 75°F

Figure 3.5. The bar graph shows the observed annual number of very warm nights (minimum temperature of 75°F or higher) for the North Carolina Coastal Plain region for 1900–2018, as averaged over 5-year periods, with the last bar representing a 4-year period (2015–2018). Dots show annual values. The horizontal black line shows the long-term average of 8 very warm nights per year for 1900–2018. Source: NCICS, NOAA NCEI, and the State Climate Office of North Carolina.

Climate models project a substantial increase in the number of these very hot days and very warm nights by mid- to late century under both scenarios. By the end of the century, the number of very hot days is projected to increase by 11–49 under the lower scenario and 42–94 under the higher scenario, compared to the 1996–2015 average. The number of very warm nights is projected to increase by 14–45 under the lower scenario and 48–87 under the higher scenario.

The projections for increases in the number of very warm nights (Figure 3.6) is consistent with recent observations (Figure 3.5). Because of this consistency, it is *very likely* that the model-projected increases in the number of very warm nights will occur.

However, the projected increase in the number of very hot days (Figure 3.6) is not consistent with the lack of an observed trend (Figure 3.4). Since the causes of the lack of an increase in the

99

number of very hot days are not yet fully understood, our level of confidence in the projections is lessened. However, summers have become warmer, and that warming is projected to continue. Thus, it is *likely* that the number of very hot days will eventually increase.
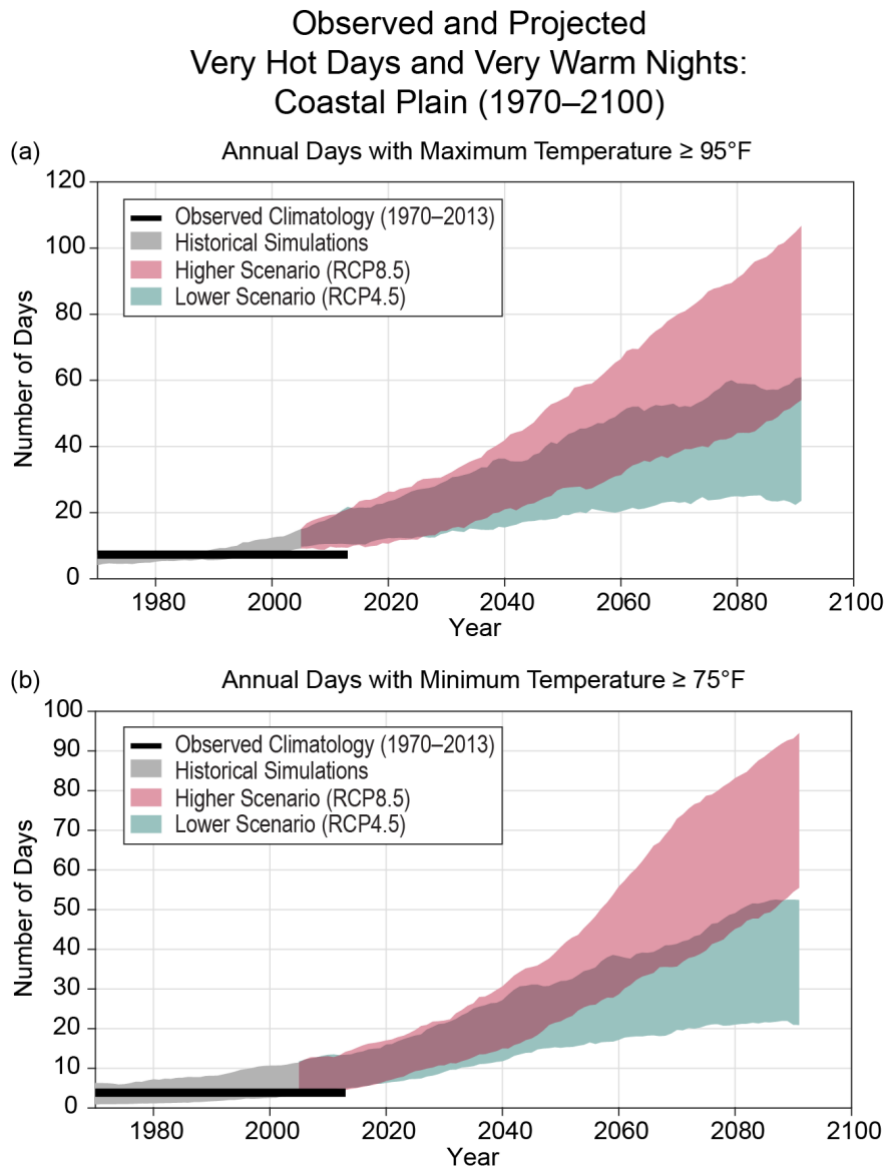
Observed and Projected
Very Hot Days and Very Warm Nights:
Coastal Plain (1970–2100)

(a)

Annual Days with Maximum Temperature ≥ 95°F

(b)

Annual Days with Minimum Temperature ≥ 75°F

Figure 3.6. These time series show the simulated historical and projected number of days per year on which (a) the maximum temperature is 95°F or higher and (b) the minimum temperature is 75°F or higher for the Coastal Plain region of North Carolina from the LOCA data and the observed climatological values averaged for the period 1970–2013 (black line). Historical simulations (gray shading) are shown for 1970–2005. Projected changes for 2006–2100 are shown for a higher scenario (RCP8.5; red shading) and a lower scenario (RCP4.5; green shading). The shaded ranges indicate the 10% to 90% confidence intervals of 20-year running averages from the set of climate models. Source: NCICS and The University of Edinburgh.

3.2.3 Cold Days

Occurrences of cold days (maximum temperature of 32˚F or below) are rare in the Coastal Plain, with a long-term average of about 1–2 days per year (Figure 3.7). There is no overall trend, but the number has been above average since 2014, including the 6th (2015) and 7th (2018) highest number of days on record. The highest annual value of 5.5 days occurred in 1917. The relatively high values in recent years were caused in part by occurrences of a winter weather pattern popularly known as the polar vortex—an area of upper-level low pressure that is nearly always present over the North and South Poles. Occasionally, the arctic vortex is displaced southward over eastern North America and becomes nearly stationary, bringing unusually cold weather to the eastern United States. While the sporadic southward displacement of the vortex is a natural feature of the winter climate, some recent years have featured unusually persistent patterns, resulting in episodes of extended cold and stormy weather in the eastern United States, notably in the winters of 2009–10, 2010–11, 2013–14, and 2014–15. A number of research studies have found empirical evidence of a link between cold winters and the fact that the Arctic is warming more rapidly than lower latitudes (a phenomenon referred to as arctic amplification). The current scientific consensus is that observed winter temperature trends, including the lack of recent warming in the eastern United States, cannot be explained without including the potential effects of Arctic warming (Cohen et al. 2020).
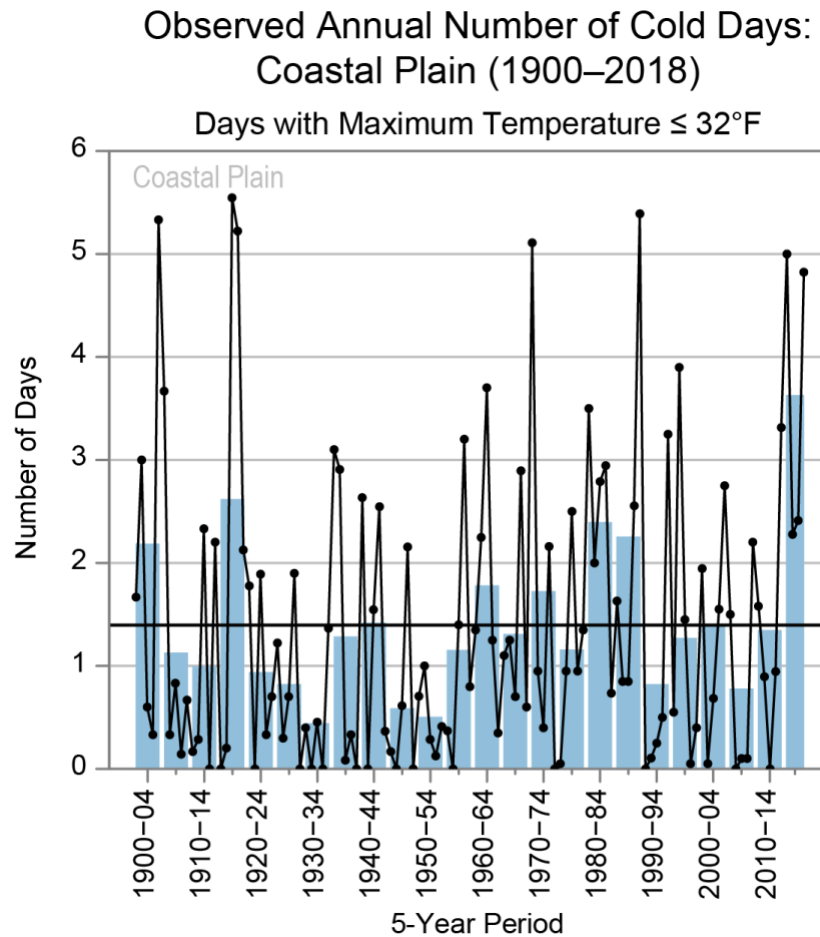
Observed Annual Number of Cold Days: Coastal Plain (1900–2018)

Figure 3.7. The bar graph shows the observed annual number of cold days (maximum temperature of 32°F or below) for the North Carolina Coastal Plain region for 1900–2018, as averaged over 5-year periods, with the last bar representing a 4-year period (2015–2018). Dots show annual values. The horizontal black line shows the long-term average of 1.4 cold days per year for 1900–2018. Source: NCICS, NOAA NCEI, and the State Climate Office of North Carolina.

By the end of the century, climate models project that the annual number of cold days will be at or close to zero under both scenarios. There has not been a strong trend in the number of cold nights (days with a minimum temperature of 32°F or below) in recent years. However, by the end of the century, the number of cold nights is projected to decrease by 10–26 under the lower scenario and 24–39 under the higher scenario, compared to the 1996–2015 average (Figure 3.8).

The projected decrease in cold days (Figure 3.8) is not consistent with the lack of an observed trend (Figure 3.7). As noted above, one reason for the lack of an observed trend is the recent occurrences of an unusually persistent southward-displaced polar vortex over eastern North America. However, there is no scientific consensus that continued Arctic warming will lead to an increase in polar vortex occurrences over eastern North America (Cohen et al. 2020). Thus, it is *likely* that the number of cold days and cold nights will eventually decrease.

Observed and Projected Cold Days and Nights:
Coastal Plain (1970–2100)

(a)

Annual Days with Maximum Temperature ≤ 32°F

Legend:
- Observed Climatology (1970–2013)
- Historical Simulations
- Higher Scenario (RCP8.5)
- Lower Scenario (RCP4.5)

Y-axis: Number of Days (0–9)
X-axis: Year (1980–2100)

(b)

Annual Days with Minimum Temperature ≤ 32°F

Legend:
- Observed Climatology (1970–2013)
- Historical Simulations
- Higher Scenario (RCP8.5)
- Lower Scenario (RCP4.5)

Y-axis: Number of Days (10–120)
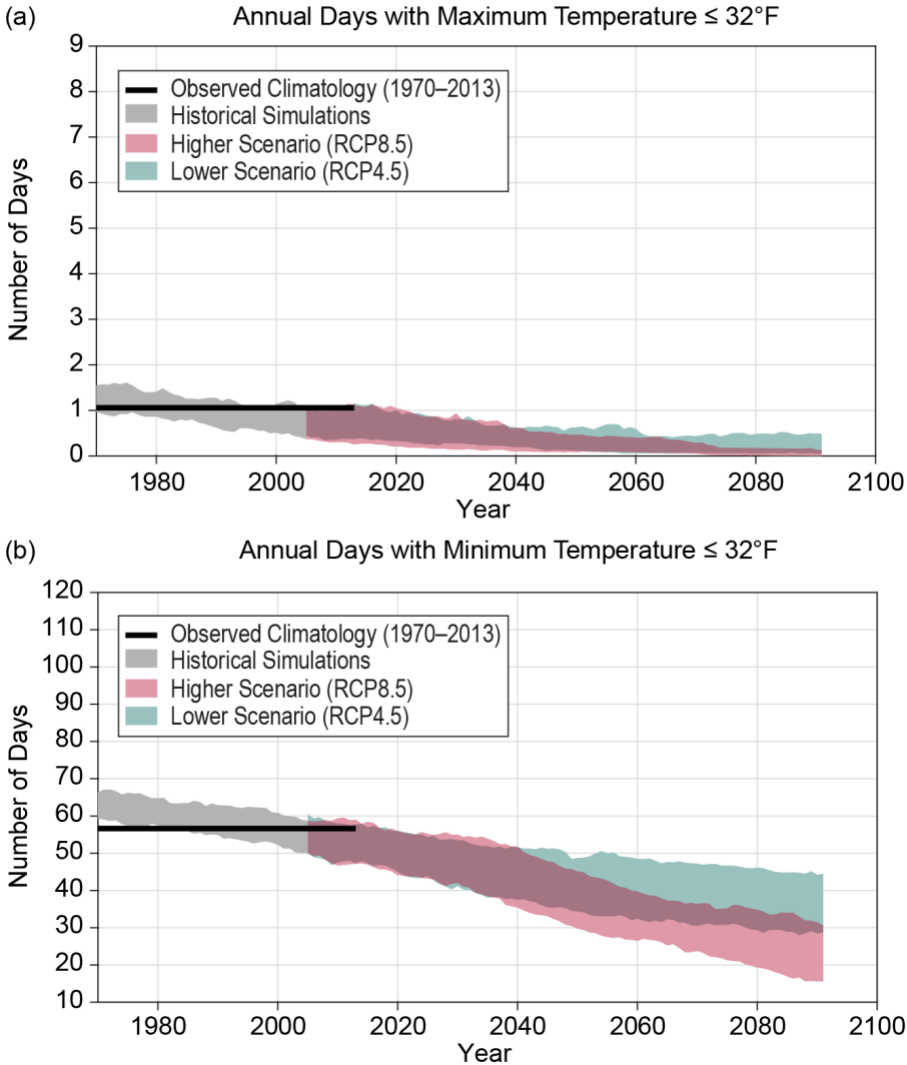X-axis: Year (1980–2100)

Figure 3.8. These time series show the simulated historical and projected number of days per year on which the (a) maximum temperature and (b) minimum temperature is 32°F or lower for the Coastal Plain region of North Carolina from the LOCA data and the observed climatological values averaged for the period 1970–2013 (black line). Historical simulations (gray shading) are shown for 1970–2005. Projected changes for 2006–2100 are shown for a higher scenario (RCP8.5; red shading) and a lower scenario (RCP4.5; green shading). The shaded ranges indicate the 10% to 90% confidence intervals of 20-year running averages from the set of climate models. Sources: NCICS and The University of Edinburgh.

3.2.4 Annual Hottest / Coldest Temperatures

The annual hottest maximum temperature, averaged over the Coastal Plain region, has shown no strong trend since 1970. However, there has been a notable increase in the annual coldest minimum temperature since the late 1990s. By the end of the century, the annual hottest temperature is projected to increase by 2°–6°F under the lower scenario and 5°–12°F under the higher scenario, compared to the 1996–2015 average. The annual coldest temperature is projected to increase by 2°–7°F under the lower scenario and 6°–10°F under the higher scenario (Figure 3.9).

The projections for increases in annual coldest temperature are consistent with recent observations. Because of this consistency, it is *very likely* that the model-projected increases in annual coldest temperature will occur. However, the projected increase in annual hottest temperature is not consistent with the lack of an observed trend. Since the causes of the lack of an increase in annual hottest temperature are not yet fully understood, our level of confidence in the projections is lessened. However, summers have become warmer, and that warming is projected to continue. Thus, it is *likely* that the annual hottest temperature will eventually increase.

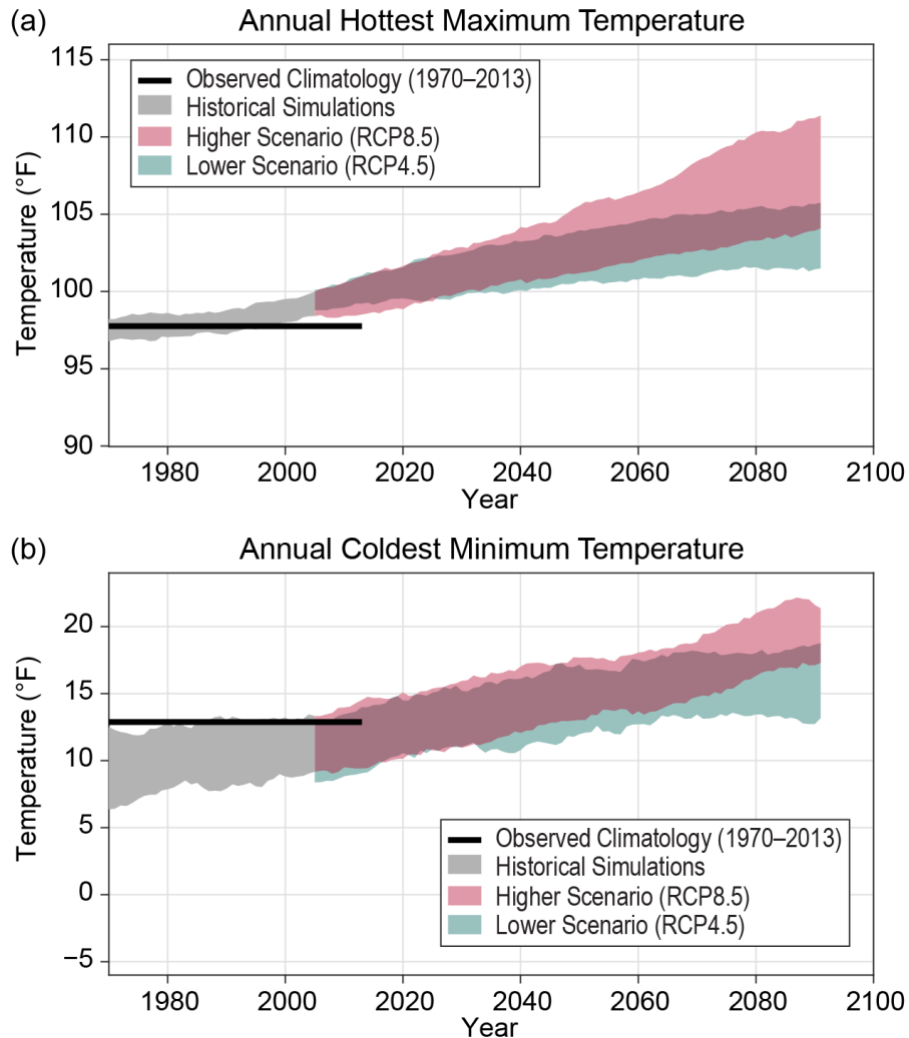## Observed and Projected Maximum and Minimum Temperatures: Coastal Plain (1970–2100)

Figure 3.9. These time series show the simulated historical and projected (a) hottest maximum and (b) coldest minimum temperatures each year averaged over the Coastal Plain region of North Carolina from the LOCA data and the observed climatological values averaged for the period 1970–2013 (black line). Historical simulations (gray shading) are shown for 1970–2005. Projected changes for 2006–2100 are shown for a higher scenario (RCP8.5; red shading) and a lower scenario (RCP4.5; green shading). The shaded ranges indicate the 10% to 90% confidence intervals of 20-year running averages from the set of climate models. Sources: NCICS and The University of Edinburgh.

3.2.5 Heating and Cooling Degree Days

The term "heating degree days" (HDDs) refers to the number of degrees that a day's average temperature is below 65°F, while "cooling degree days" (CDDs) refers to the number of degrees that the average temperature is above 65°F. These metrics are used to quantify the energy needed to heat or cool buildings and houses. HDDs and CDDs in the Coastal Plain region have varied in concert with the region's annual average temperature. As average temperature (Figure 3.2) increased in the first half of the 20th century, HDDs (Figure 3.10) decreased, reaching a relative minimum around mid-century, while CDDs (Figure 3.11) exhibited little overall trend. HDDs then increased to relatively higher values by the 1960s, as the region's average temperature and CDDs reached their lowest values in decades. Coincident with an upward trend in annual average temperature, there has been a decreasing trend in HDDs since the 1980s, and all but two years have been below the long-term average since 2000. At the same time, there has been an increasing trend in CDDs, with the highest values on record occurring since 2010.

Overall warming is projected to lead to decreases in HDDs and increases in CDDs in the Coastal Plain (Figure 3.12). This indicates a decrease in energy needed for heating and an increase in energy needed for cooling. By the end of the century, HDDs are projected to decrease by 400–900 under the lower scenario and 800–1,400 under the higher scenario, compared to the 1996–2015 average. CDDs are projected to increase by 400–1,100 under the lower scenario and 1,100–2,100 under the higher scenario. These projections are consistent with recent trends. For this reason, it is *very likely* that HDDs will decrease and CDDs will increase in the future.
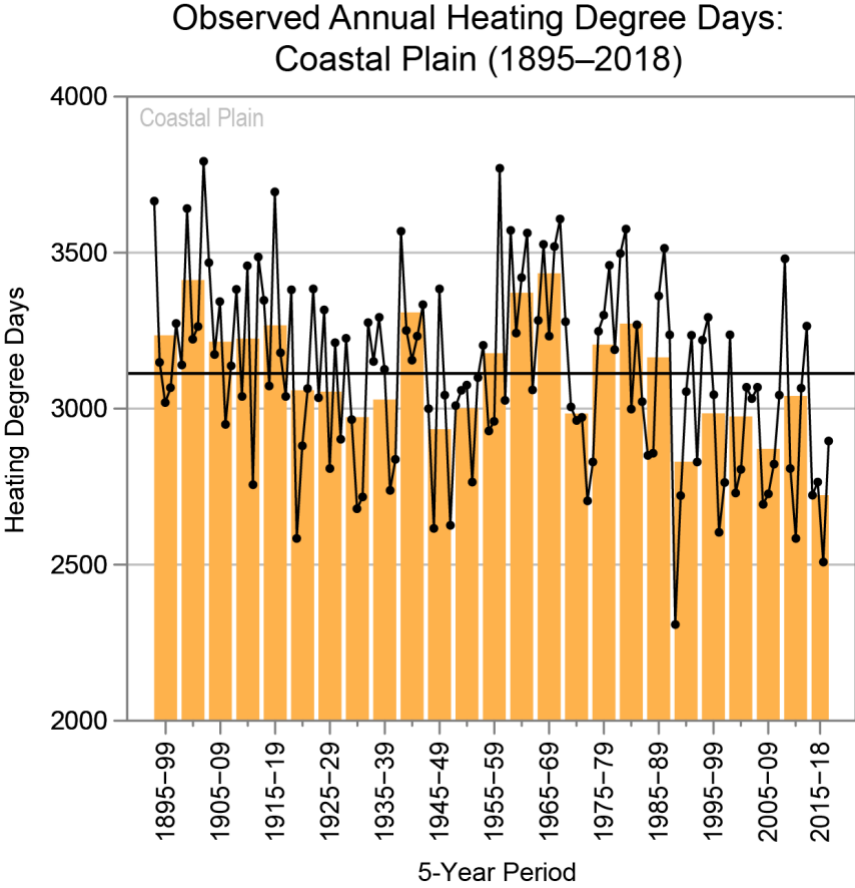
Figure 3.10. The bar graph shows the observed annual heating degree days for the Coastal Plain region of North Carolina for 1895–2018, as averaged over 5-year periods, with the last bar representing a 4-year period (2015–2018). Dots show annual values. The horizontal black line shows the long-term average of 3,110 heating degree days per year for 1895–2018. There has been a decreasing trend in heating degree days since the 1980s, and all but two years have been below the long-term average since 2000. Sources: NCICS, NOAA NCEI, and the State Climate Office of North Carolina.

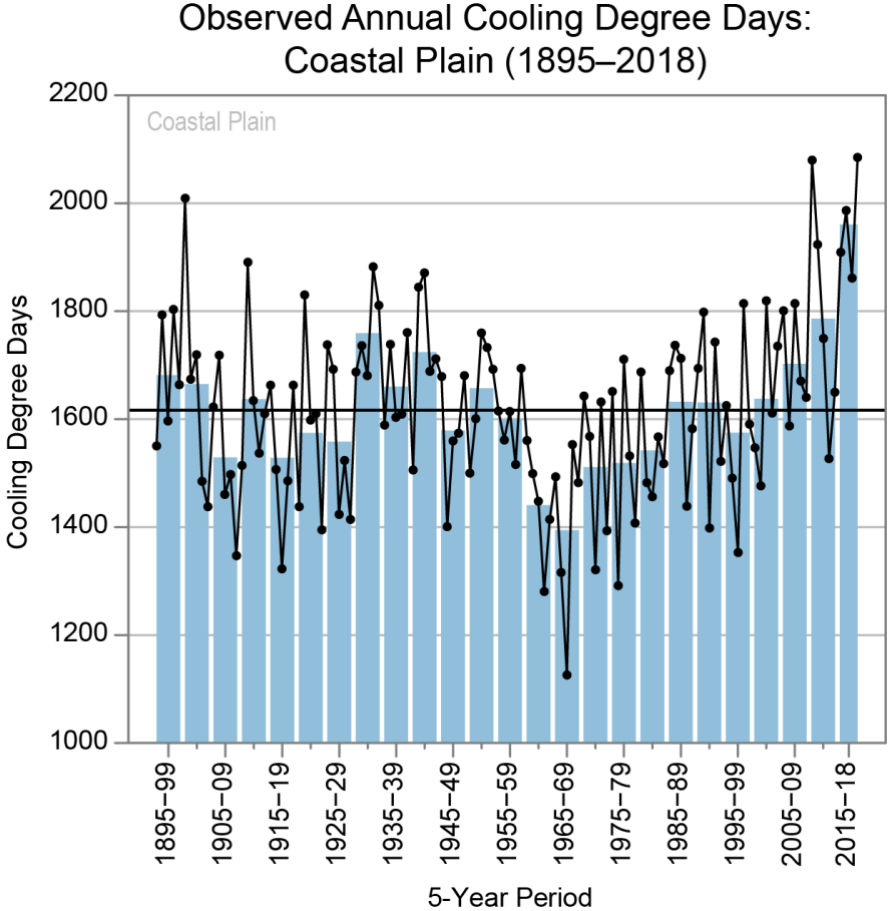## Observed Annual Cooling Degree Days: Coastal Plain (1895–2018)

Figure 3.11. The bar graph shows the observed annual cooling degree days for the Coastal Plain region of North Carolina for 1895–2018, as averaged over 5-year periods, with the last bar representing a 4-year period (2015–2018). Dots show annual values. The horizontal black line shows the long-term average of 1,620 cooling degree days per year for 1895–2018. There has been an increasing trend in cooling degree days since the 1990s, and the highest values on record have occurred since 2010. Sources: NCICS, NOAA NCEI, and the State Climate Office of North Carolina.

Observed and Projected Heating and Cooling Degree Days: Coastal Plain (1970–2100)

(a)

Annual Heating Degree Days
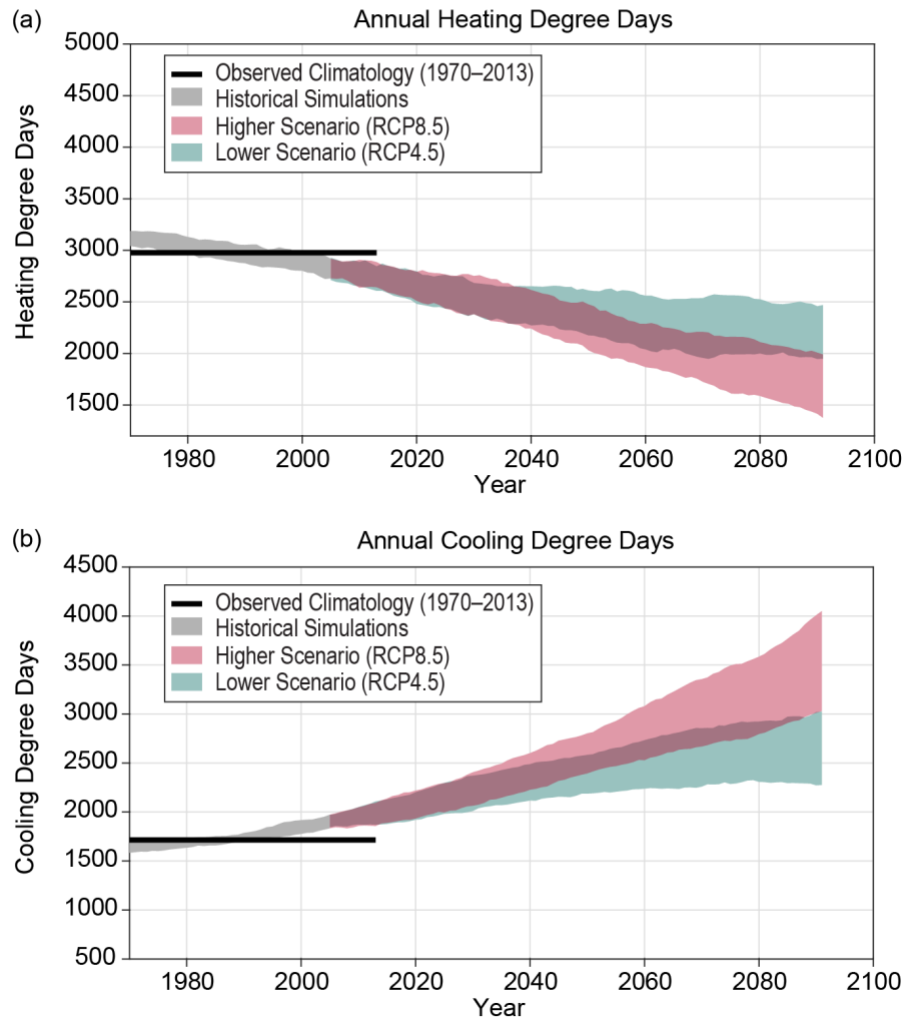

(b)

Annual Cooling Degree Days

Figure 3.12. These time series show simulated historical and projected values for (a) annual heating degree days and (b) annual cooling degree days for the Coastal Plain region of North Carolina from the LOCA data and the observed climatological values averaged for the period 1970–2013 (black line). Historical simulations (gray shading) are shown for 1970–2005. Projected changes for 2006–2100 are shown for a higher scenario (RCP8.5; red shading) and a lower scenario (RCP4.5; green shading). The shaded ranges indicate the 10% to 90% confidence intervals of 20-year running averages from the set of climate models. Sources: NCICS and The University of Edinburgh.

3.2.6 Annual Precipitation

The variations in annual precipitation for the Coastal Plain (Figure 3.13) are similar to those for the statewide average annual precipitation (see Figure 2.15). There is substantial year-to-year

variability but no discernible overall trend. Dominant physical mechanisms driving precipitation in this region are tropical systems, daytime thunderstorms, and winter coastal storms. The 2015–2018 period was the wettest period on record in the Coastal Plain, averaging about 10 inches above the long-term average of 49 inches. The wettest year on record (67 inches) was 2018, boosted in part by Hurricane Florence rainfall, which contributed about 12 inches to the annual total. The driest year on record was 2007, with about 35 inches. The 1995–1999 period was the second wettest 5-year period (annual average of 54 inches). The driest 5-year period in the Coastal Plain was 1930–1934, with an annual average of 42 inches (this was also the driest statewide period on record; see Figure 2.15).
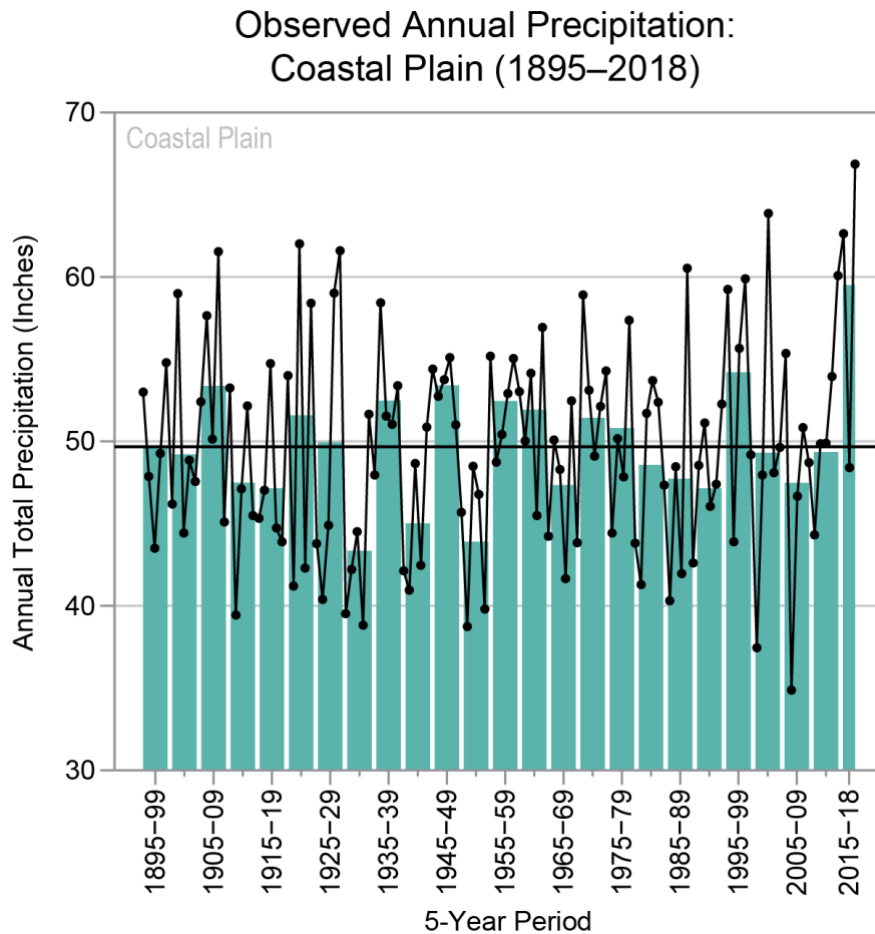

Figure 3.13. The bar graph shows the observed annual total precipitation for the Coastal Plain region of North Carolina for 1895–2018, as averaged over 5-year periods, with the last bar representing a 4-year period (2015–2018). Dots show annual values. The horizontal black line shows the long-term average of 49.6 inches per year for 1895–2018. Sources: NCICS, NOAA NCEI, and the State Climate Office of North Carolina.

By the end of the century, climate models project a wide range of potential outcomes, from drier to wetter conditions. While the average of the model projections shows small increases in annual total precipitation compared to the current climate (see Figure 2.16), the models range from

110

decreases of 3 inches to increases of 6 inches under the lower scenario and decreases of 3 inches to increases of 8 inches under the higher scenario, compared to the 1996–2015 average (Figure 3.14). Based on the greater number of models showing increases, it is likely that annual precipitation will increase.

Observed and Projected Annual Total Precipitation: Coastal Plain (1970–2100)
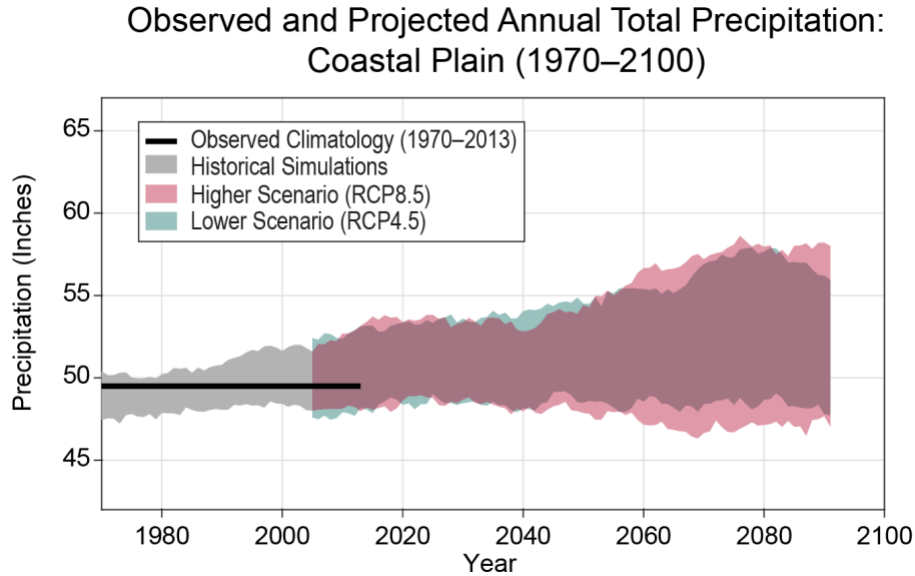

Figure 3.14. These time series show the simulated historical and projected annual total precipitation for the Coastal Plain region of North Carolina from the LOCA data and the observed climatological value averaged for the period 1970–2013 (black line). Historical simulations (gray shading) are shown for 1970–2005. Projected changes for 2006–2100 are shown for a higher scenario (RCP8.5; red shading) and a lower scenario (RCP4.5; green shading). The shaded ranges indicate the 10% to 90% confidence intervals of 20-year running averages from the set of climate models. Sources: NCICS and The University of Edinburgh.

3.2.7 Heavy Precipitation

Extreme precipitation is highly variable across the historical record, especially from year to year (Figure 3.15). Days with precipitation amounts of 3 inches or more are rare, with slightly fewer than 1 day per year expected on average at any individual location. There is an upward trend: since 1995, the average number of 3-inch days has been about 35% above the long-term average. The years 1995, 1998, 2009, and 2016 are 4 of the 5 highest years on record.

Observed Annual Number of Extreme Precipitation Events: Coastal Plain (1900–2018)
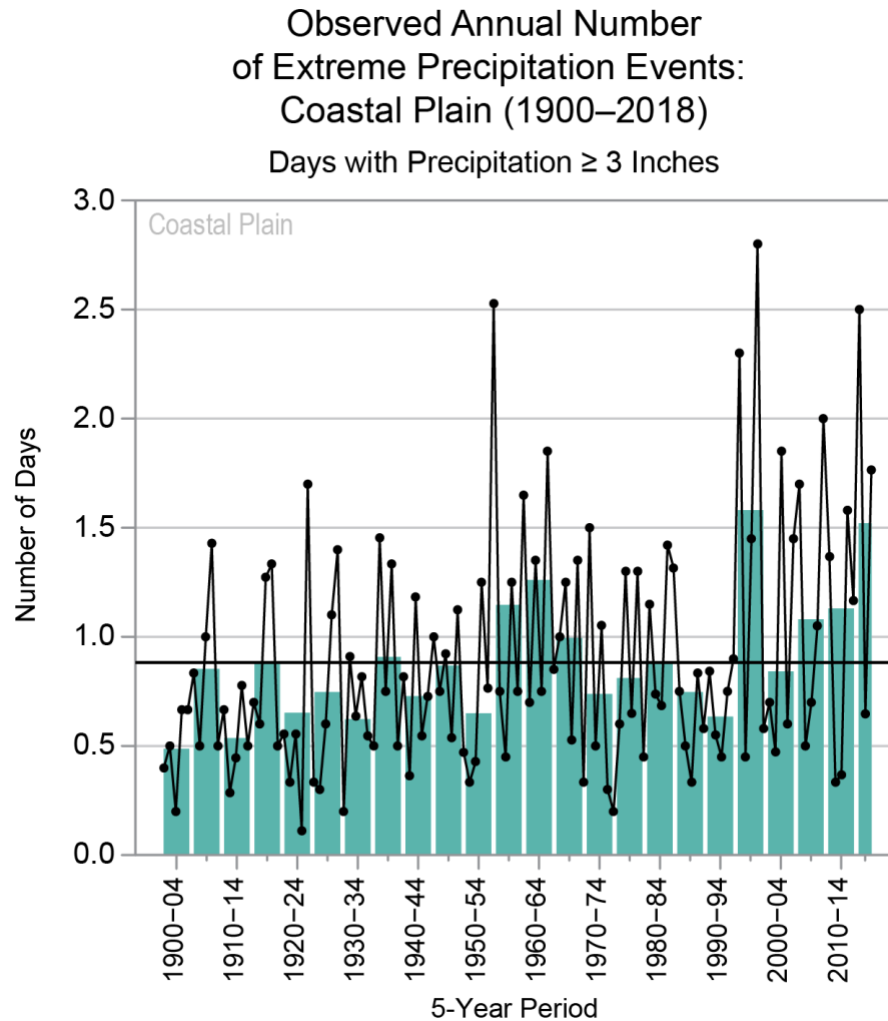
Days with Precipitation ≥ 3 Inches

Figure 3.15. The bar graph shows the observed annual number of extreme precipitation events (days with precipitation of 3 inches or more) for the Coastal Plain region of North Carolina for 1900–2018, as averaged over 5-year periods, with the last bar representing a 4-year period (2015–2018). Dots show annual values. The horizontal black line shows the long-term average of 0.9 extreme precipitation days per year for 1900–2018. Sources: NCICS, NOAA NCEI, and the State Climate Office of North Carolina.

By the end of the century, climate models project a large range of potential changes. This large range is mainly a result of the random nature of extreme rainfall. However, the models show an overall increase in the number of extreme precipitation days in the Coastal Plain region. By the end of the century, the annual number of days with precipitation of 3 inches or more is projected to increase by up to 0.2 (78%) under the lower scenario and 0.3 (130%) under the higher scenario, compared to the 1996–2015 average (Figure 3.16). Note that the current value of 0.3 days per year from the Livneh dataset is lower than the station average of 0.9 days per year (Figure 3.15). The Livneh dataset consists of spatially averaged data, which have lower values of extreme rainfall.

Based on the virtual certainty that water vapor in the atmosphere will increase as global warming occurs, it is ***very likely*** that the risk of extreme precipitation will increase everywhere in the Coastal Plain.

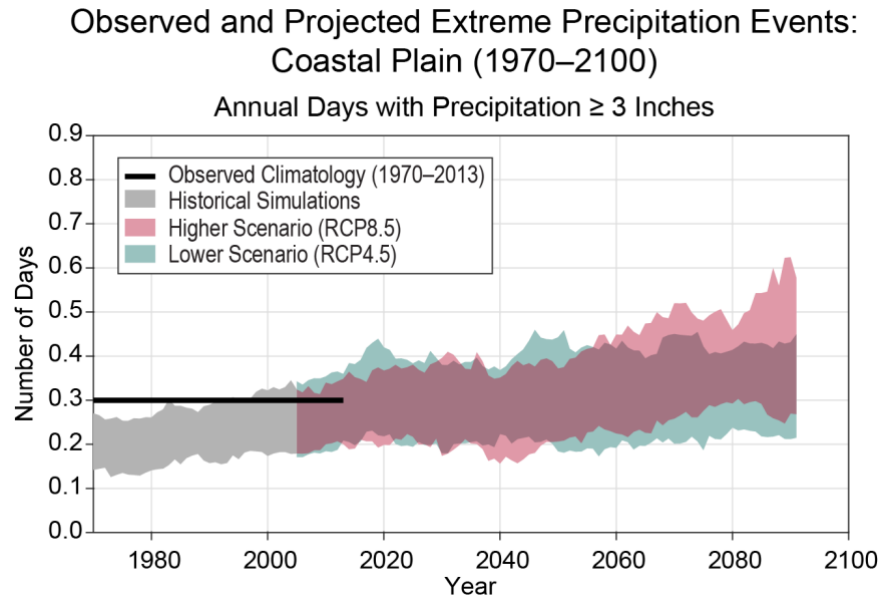**Observed and Projected Extreme Precipitation Events: Coastal Plain (1970–2100)**

Figure 3.16. These time series show the simulated historical and projected annual number of days with precipitation of 3 inches or more⬚ for the Coastal Plain region of North Carolina from the LOCA data and the observed climatological value averaged for the period 1970–2013 (black line). Historical simulations (gray shading) are shown for 1970–2005. Projected changes for 2006–2100 are shown for a higher scenario (RCP8.5; red shading) and a lower scenario (RCP4.5; green shading). The shaded ranges indicate the 10% to 90% confidence intervals of 20-year running averages from the set of climate models. Sources: NCICS and The University of Edinburgh.

3.2.8 Drought

Drought can be measured using the Palmer Drought Severity Index (PDSI), which uses temperature and precipitation data to calculate the severity of drought at a location by estimating the relative dryness. The values calculated for PDSI range from −10 (dry) to +10 (wet). This metric captures medium- to long-term drought in North Carolina and is used by water managers and climate scientists to quantify and compare droughts throughout recorded history. Figure 3.17 shows the number of months per year with a PDSI value less than or equal to −2 (moderate, severe, or extreme drought). In the Coastal Plain, the period of 1930–1934 experienced the highest number of months in drought of at least moderate severity, with an average of 6 months per year. More recently, a drought during 2007–2009 was the most severe since the 1930s. Moderate or worse drought conditions have not occurred since 2013.

Observed Annual Number of Drought Months:
Coastal Plain (1895–2018)

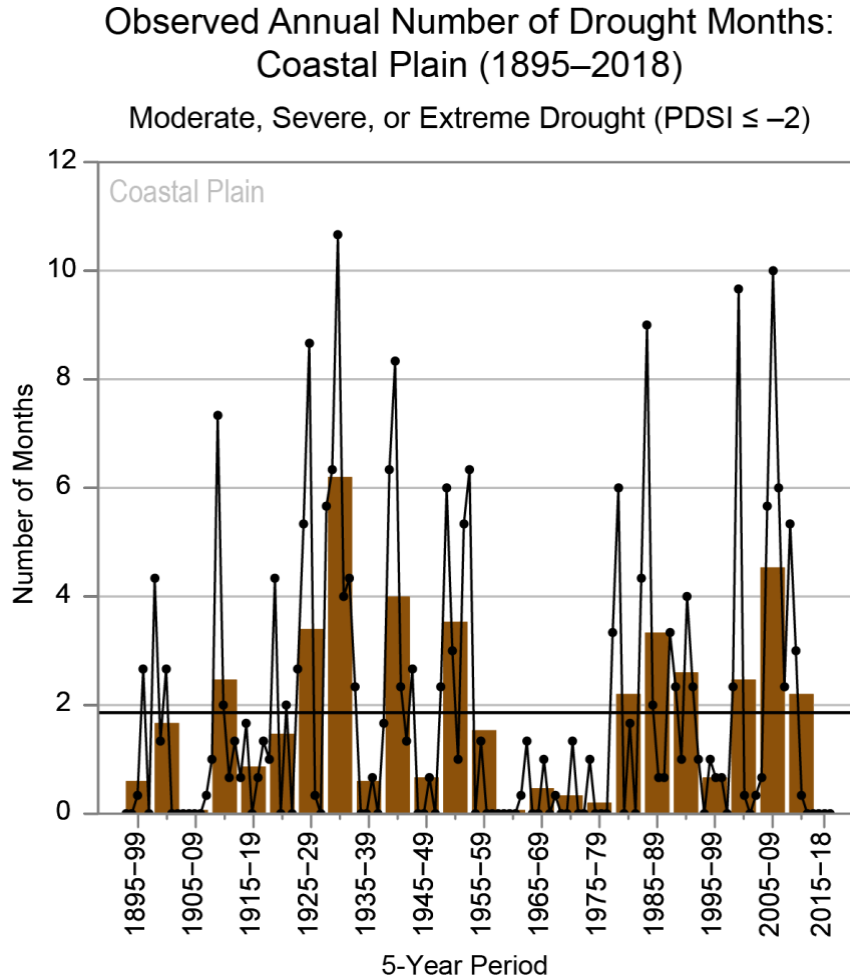### Moderate, Severe, or Extreme Drought (PDSI ≤ –2)

Figure 3.17. The bar graph shows the observed annual number of months in drought of moderate or worse severity (Palmer Drought Severity Index values less than or equal to –2) for the Coastal Plain region of North Carolina for 1895–2018, as averaged over 5-year periods, with the last bar representing a 4-year period (2015–2018). Dots show annual values. The horizontal black line shows the long-term average of 1.9 drought months per year for 1895–2018. Sources: NCICS, NOAA NCEI, and the State Climate Office of North Carolina.

Droughts are a natural part of the climate of North Carolina. Future droughts are projected to be warmer than historical events with a high level of confidence. The warmer conditions will lead to more rapid drying through increases in potential evapotranspiration. Thus, it is *likely* that future droughts will be more severe in terms of soil moisture deficits and the impacts on rainfed agriculture and natural vegetation.

3.2.9 Winter Storms

Winter storms are large areas of low pressure in the middle and high latitudes that are primarily distinguished by fronts separating warm and cold air masses. They often cause various types of adverse weather conditions, such as strong winds and precipitation of various types, including

snow and ice. This section discusses winter storms of all types, while the following two subsections discuss the specific instances of storms causing snow and ice.

Winter storm tracks have shifted slightly northward (by about 0.4 degrees latitude) in recent decades over the Northern Hemisphere (Bender et al. 2012). More generally, winter storm activity is projected to change in complex ways under future climate scenarios, with increases in some regions and seasons and decreases in others. The Arctic is warming more quickly than lower latitudes (i.e., arctic amplification), due in part to sea ice loss. This reduces the lower-atmosphere temperature difference between the Arctic and the lower latitudes—this difference is an important energy source for winter storms. At the same time, the temperature difference higher up in the atmosphere is projected to increase due to a warming tropical upper troposphere and a cooling high-latitude lower stratosphere. While these two effects counteract each other with respect to a projected change in midlatitude storm tracks, the simulations indicate that the magnitude of arctic amplification may modulate some aspects (e.g., jet stream position, wave extent, and blocking frequency) of the circulation in the North Atlantic region in some seasons (Barnes and Polvani 2015).

Regional studies of trends in cyclones are challenged to provide definitive results regarding changes in the frequency or intensity of storms, but regardless of these properties, it is ***very likely*** that cyclones of even similar intensity will produce heavier precipitation (e.g., Marciano et al. 2015, Michaelis et al. 2017). Also, with rising sea levels, coastal flooding from cyclones is ***very likely*** to increase (e.g., Colle et al. 2015, Zhang and Colle 2018, Roberts et al. 2017).

Based on the available evidence, our conclusion is that there is ***low confidence*** concerning future changes in the number of winter storms.

3.2.9.1 Snowstorms and Snow Cover
In the North Carolina Coastal Plain, winter precipitation mostly falls as rain because temperatures are above freezing near the surface. Winter temperatures are a critical factor in both historical and future changes in snowfall. Winter temperatures have been above the long-term average in most winters since 1990. Analysis of snowfall at eastern North Carolina stations with long records found decreasing trends over the period of 1930–2007 (Kunkel et al. 2009) at most stations.

The Fourth National Climate Assessment projects large winter warming under both moderate and higher emissions scenarios. Consistent with the projected warming, a northward shift in the rain–snow transition zone in the central and eastern United States is projected under a higher emissions scenario. For the Coastal Plain, the frequency of snowfall is projected to decrease and become an even rarer occurrence than it is today.

As noted earlier, a definitive understanding of the effects of arctic amplification on midlatitude winter weather remains elusive (Cohen et al. 2020), and this adds some uncertainty to future projections of winter climate in North Carolina. Current global climate models (CMIP5) do predict an increase in the frequency of winter storms over the eastern United States, including the

most intense storms, under the higher emissions scenario (Colle et al. 2013). However, there are large model-to-model differences in the realism of historical simulations and in the projected changes. Even if there were increases in the frequency or intensity of winter storms, the effects of warmer winters would nevertheless lead to decreases in average annual snowfall.

Based on the projected increase in temperature, it is ***very likely*** that total snowfall will decrease. It is ***likely*** that the number of heavy snowstorms will decrease.

3.2.9.2 Ice Storms

Ice storms occur within winter storms, the same as for snowstorms. However, icing requires a specific combination of weather conditions, most importantly precipitating conditions with a below-freezing layer near the surface and an above-freezing layer above the low-level freezing layer. In this situation, snow falling from high levels melts as it falls through the above-freezing layer; it then becomes super-cooled liquid drops while falling through the near-surface freezing layer and freezes on contact with cold surface objects.

The accurate simulation of this weather feature by climate models is challenging because the vertical extent of the below-freezing and above-freezing layers is often quite small and thus non-resolvable by the current generation of climate models. Also, the horizontal resolution in models is insufficient to capture the fine spatial detail of ice-producing conditions. As a result, research on future changes in ice storm frequency and intensity is limited, and the recent Fourth National Climate Assessment did not make any statements on this weather phenomenon.

In North Carolina, the presence of the Appalachian Mountains in the western part of the state can result in a phenomenon known as cold-air damming, in which a shallow layer of cold air moves southward across the Carolinas. This setup can be accompanied by freezing rain or ice pellets. However, there is no reason why cold-air damming would be expected to change in a warmer climate, other than that the temperature of the cold air masses could moderate.

Freezing rain takes place when a layer of warm air moves over the shallow cold air near the surface, such as during cold-air damming. With warming, it may be easier for these warm layers to develop, and at least one study linked a North Carolina ice storm to warm offshore waters (Ramos de Silva et al. 2006). Thus, it is possible that warming could result in an increase of these warm layers, increasing freezing rain occurrence.

Taken together, the preceding discussion demonstrates that there is considerable uncertainty in projected changes in freezing rain in a warming climate, and more research is needed. Given the evidence currently available, our conclusion is that there is ***low confidence*** concerning future changes in the number of ice storms.

3.2.10 Thunderstorms and Tornadoes

Tornado and severe thunderstorm events cause significant loss of life and property: more than one-third of the $1 billion weather disasters in the United States during the past 25 years were due to such events, and, relative to other extreme weather, the damages from convective weather

hazards have undergone the largest increase since 1980 (Smith and Katz 2013). A particular challenge in quantifying the existence and intensity of these events arises from the data source: rather than measurements, the occurrence of tornadoes and severe thunderstorms is determined by visual sightings by eyewitnesses (such as "storm spotters" and law enforcement officials) or post-storm damage assessments. The reporting has been susceptible to changes in population density, modifications to reporting procedures and training, the introduction of video and social media, and so on. These have led to systematic, non-meteorological biases in the long-term data record.

Nonetheless, judicious use of the report database has revealed important information about tornado trends. Since the 1970s, the United States has experienced a decrease in the number of days per year on which tornadoes occur but an increase in the number of tornadoes that form on such days. One important implication is that the frequency of days with large numbers of tornadoes—tornado outbreaks—appears to be increasing (Figure 9.3 in Kossin et al. 2017). The length of the season over which such tornado activity occurs is increasing as well: although tornadoes in the United States are observed in all months of the year, an earlier calendar-day start to the season of high activity is emerging. In general, there is more interannual variability, or volatility, in tornado occurrence (Elsner et al. 2015, Tippett, 2014).

Evaluations of hail and thunderstorm wind reports have thus far been less revealing. Although there is evidence of an increase in the number of hail days per year, the inherent uncertainty in reported hail size reduces the confidence in such a conclusion. Thunderstorm wind reports have proven to be even less reliable because, as compared to tornadoes and hail, there is less tangible visual evidence; thus, although the United States has lately experienced several significant thunderstorm wind events (sometimes referred to as derechos), the lack of studies that explore long-term trends in wind events and the uncertainties in the historical data preclude any robust assessment.

It is possible to bypass the use of reports by exploiting the fact that the temperature, humidity, and wind in the larger vicinity—or "environment"—of a developing thunderstorm ultimately control the intensity, structure, and hazardous tendency of the storm. Thus, the premise is that measures of temperature, humidity, and wind at various heights throughout the atmosphere can be used as a proxy for actual severe thunderstorm occurrence. In particular, a measure of the energy available for convection (known as convective available potential energy, or CAPE) and vertical wind shear (a change in wind speed or direction with change in altitude) constitutes one widely used means of representing the frequency of severe thunderstorms. This environmental-proxy approach avoids the biases and other issues with eyewitness storm reports and is readily evaluated using the relatively coarse global datasets and global climate models. It has the disadvantage of assuming that a thunderstorm will necessarily form and then realize its environmental potential.

Global climate models consistently project an increase in the frequency of severe thunderstorm environments in the United States over the mid- to late 21st century. The most robust projected

increases in frequency are over the U.S. Midwest and Southern Great Plains during spring (March–May). Based on the increased frequency of very high CAPE, increases in storm intensity are also projected over this same period (Del Genio et al. 2007).

Key limitations of the environmental-proxy approach are being addressed through the applications of high-resolution dynamical downscaling, wherein sufficiently fine model grids are used so that individual thunderstorms are explicitly represented, rather than implicitly represented (as through environmental proxies). The individually modeled thunderstorms can then be quantified and assessed in terms of severity (e.g., Trapp et al. 2011). Prein et al. (2017) used a convection-permitting model to examine changes in intense hourly precipitation in the central United States, finding an increase in the most intense events and a decrease in lighter events. The dynamical-downscaling results have thus far supported the basic findings of the environmental-proxy studies, particularly in terms of the seasons and geographical regions projected to experience the largest increases in severe thunderstorm occurrence.

Based on these studies, we conclude it is ***likely*** that severe thunderstorms in the Coastal Plain will increase in frequency.

3.3 Piedmont

3.3.1 Average Temperature

Trends in annual average temperatures in the Piedmont (Figure 3.18) are similar to statewide trends (see Figure 2.1). Temperatures were generally below the long-term average until about 1920 and generally above average in the 1930s through the middle 1950s. Below average temperatures were the norm from the late 1950s through the 1970s. Temperatures have been increasing since the 1970s and have remained consistently above average since the 1990s. The most recent 4-year period (2015–2018) was well above average and is the warmest 4-year period on record, and 15 of the last 18 years have been above the long-term average of about 59°F for the Piedmont region.
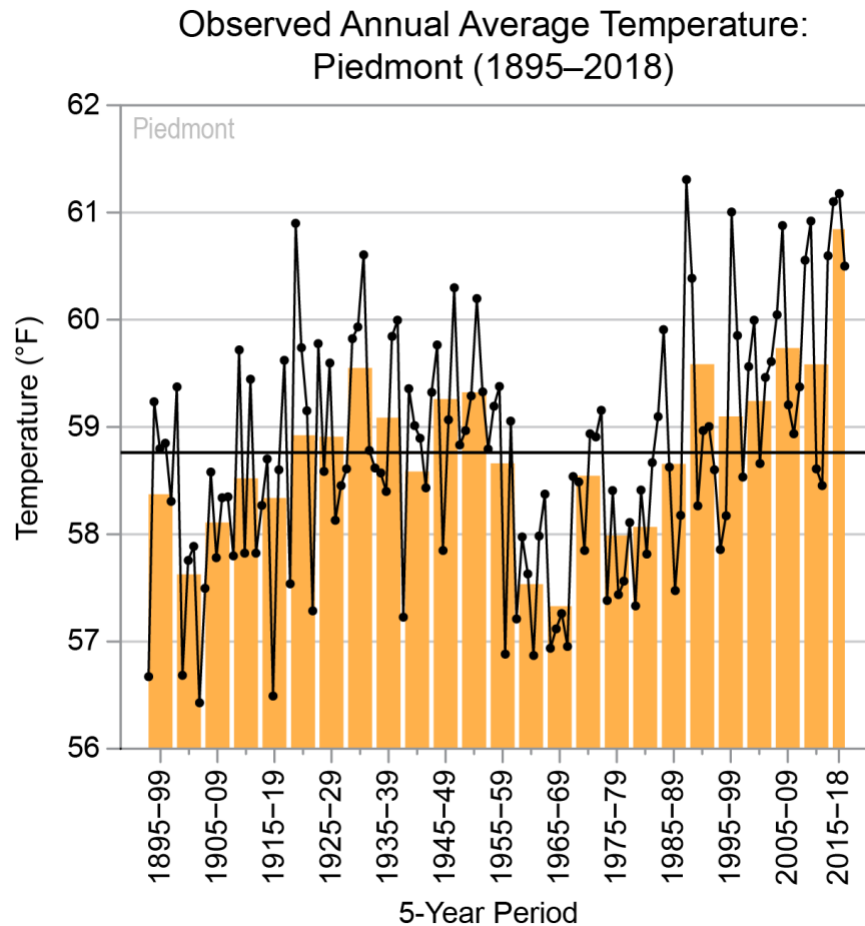
Figure 3.18. The bar graph shows the observed annual average temperature for the Piedmont region of North Carolina for 1895–2018, as averaged over 5-year periods, with the last bar representing a 4-year period (2015–2018). Dots show annual values. The horizontal black line shows the long-term average of 58.8°F for 1895–2018. Sources: NCICS, NOAA NCEI, and the State Climate Office of North Carolina.

By the end of the century, the average temperature is projected to increase by 2°–6°F under the lower scenario (RCP 4.5) and by 6°–10°F under the higher scenario (RCP 8.5; Figure 3.19), compared to the average temperature for 1996–2015. Figure 3.19 also shows the observed average temperature value for the period 1970–2013. Here, the Livneh observational dataset is used (see Appendix A for a description of datasets).

The observed temperatures have tended to be on the lower end of the range of historical model simulations (not shown), similar to the statewide average temperature (Frankson et al. 2017; 2019 update). This suggests that the lower end of the projected values is a more likely outcome for the future. However, since the causes of the lesser warming observed in the Southeast are not yet fully understood and recent years have exhibited substantial warming, the higher end of the projected values should not be discounted as a possibility.

Observed and Projected
Annual Average Temperature:
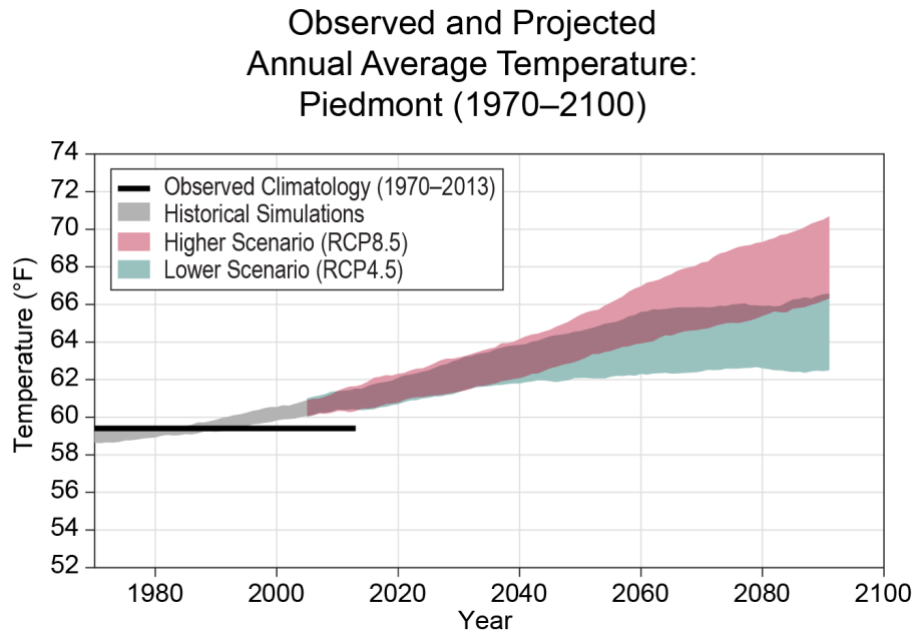Piedmont (1970–2100)

Figure 3.19. These time series show the simulated historical and projected annual average temperature for the Piedmont region of North Carolina from the LOCA data and the observed climatological value averaged for the period 1970–2013 (black line). Historical simulations (gray shading) are shown for 1970–2005. Projected changes for 2006–2100 are shown for a higher scenario (RCP8.5; red shading) and a lower scenario (RCP4.5; green shading). The shaded ranges indicate the 10% to 90% confidence intervals of 20-year running averages from the set of climate models. Sources: NCICS and The University of Edinburgh.

3.3.2 Hot Days and Warm Nights

The Piedmont region has not experienced an overall increase in the number of very hot days (maximum temperature of 95°F or higher; Figure 3.20), though there has been an increase in the number of very warm nights (minimum temperature of 75°F or higher; Figure 3.21) in recent years.

On average, the Piedmont region sees about 13 days per year at or above 95°F. Changes in the annual number of very hot days have not followed the same pattern as annual average temperatures (Figure 3.18). As in the Coastal Plain, there were more occurrences earlier in the first half of the 20th century, and the highest average of 25 days per year occurred in the 1930–1934 period. The higher frequencies of such days during the 1930s through the 1950s correspond to periods of exceptionally dry weather.
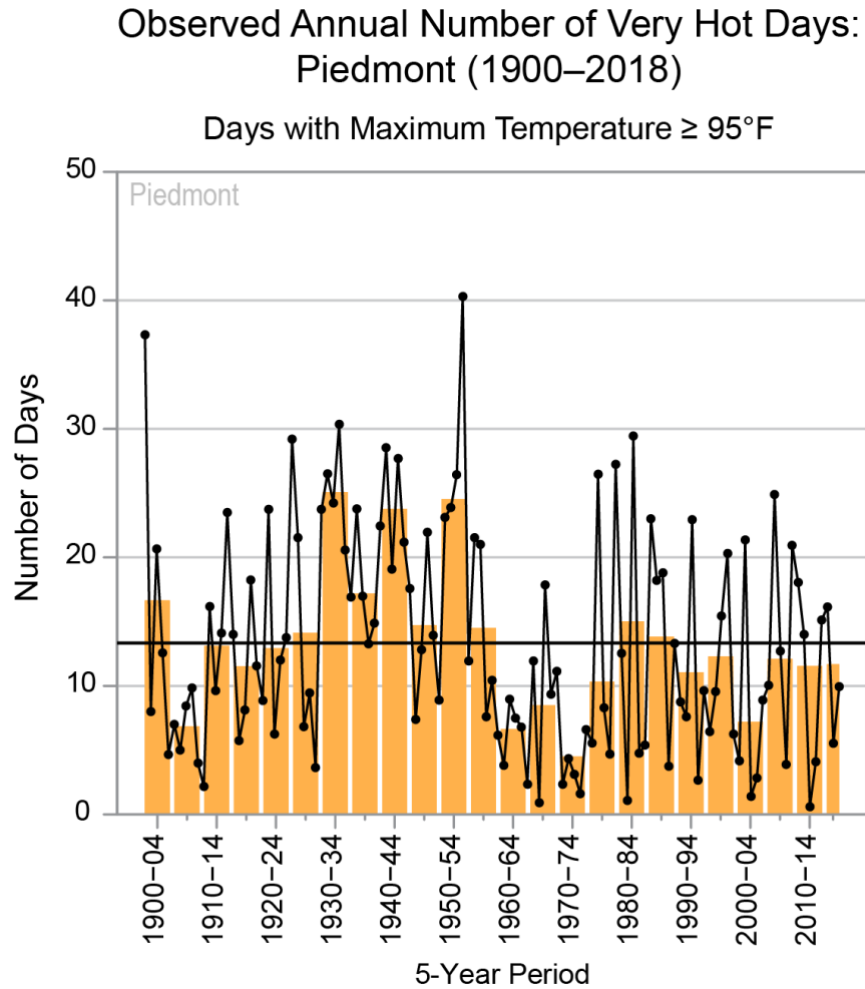
Observed Annual Number of Very Hot Days: Piedmont (1900–2018)

Days with Maximum Temperature ≥ 95°F

Figure 3.20. The bar graph shows the observed annual number of very hot days (maximum temperature of 95°F or higher) for the Piedmont region of North Carolina for 1900–2018, as averaged over 5-year periods, with the last bar representing a 4-year period (2015–2018). Dots show annual values. The horizontal black line shows the long-term average of 13 very hot days per year for 1900–2018. Sources: NCICS, NOAA NCEI, and the State Climate Office of North Carolina.

Very warm nights are less common in the Piedmont than in the Coastal Plain, with about 2 per year on average. The changes in warm nighttime temperatures over time are similar to those for annual average temperatures (Figure 3.18), including an increase over the most recent 14 years. The average annual number of days during the very first period (1900–1904) was well above the long-term average. Since 2005, the average number of very warm nights has been above the long-term average, and this period includes the highest year on record (2010), with 9 very warm nights.
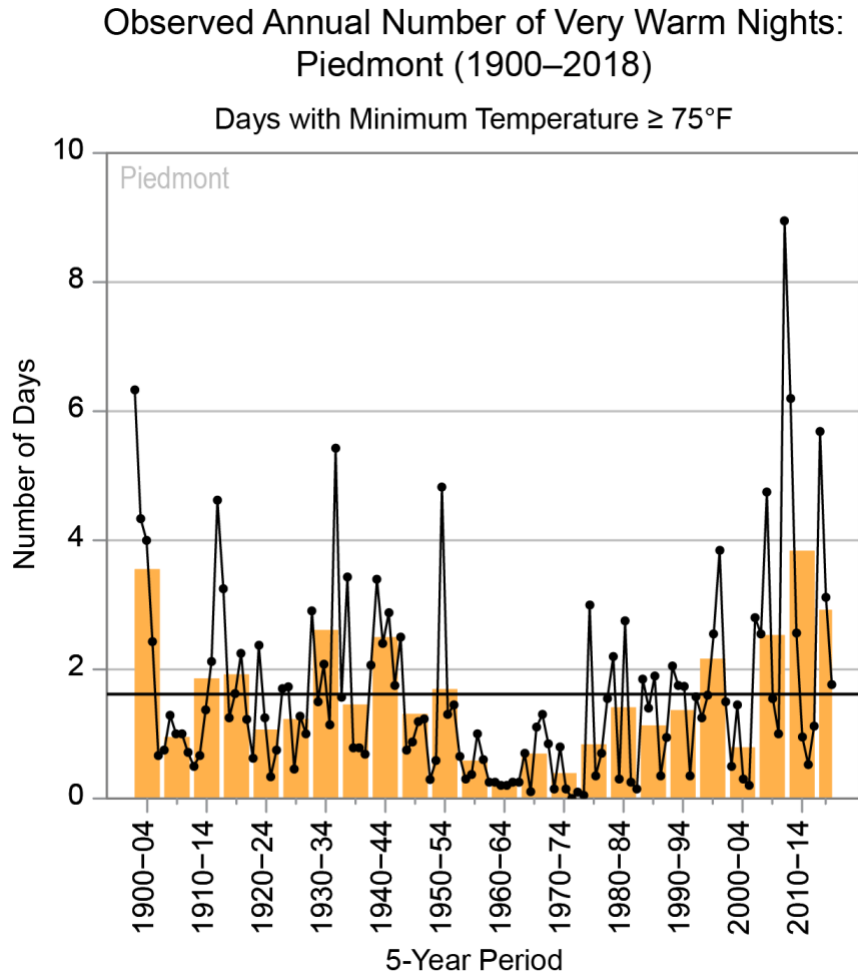
Observed Annual Number of Very Warm Nights: Piedmont (1900–2018)

Days with Minimum Temperature ≥ 75°F

Figure 3.21. The bar graph shows the observed annual number of very warm nights (minimum temperature of 75°F or higher) for the Piedmont region of North Carolina for 1900–2018, as averaged over 5-year periods, with the last bar representing a 4-year period (2015–2018). Dots show annual values. The horizontal black line shows the long-term average of 1.6 very warm nights per year for 1900–2018. Sources: NCICS, NOAA NCEI, and the State Climate Office of North Carolina.

Climate models project a substantial increase in the number of these very hot days and very warm nights by mid- to-late century under both scenarios. By the end of the century, the number of very hot days is projected to increase by 9–52 under the lower scenario and 40–99 under the higher scenario, compared to the 1996–2015 average. The number of very warm nights is projected to increase by 7–34 under the lower scenario and 36–79 under the higher scenario (Figure 3.22).

The projections for increases in the number of very warm nights (Figure 3.22) are consistent with recent observations (Figure 3.21). Because of this consistency, it is ***very likely*** that the model-projected increases in the number of very warm nights will occur. However, the projected increase in the number of very hot days (Figure 3.22) is not consistent with the lack of an

122

observed trend (Figure 3.20). Since the causes of the lack of an increase in the number of very hot days are not yet fully understood, our level of confidence in the projections is lessened. However, summers have become warmer, and that warming is projected to continue. Thus, it is *likely* that the number of very hot days will eventually increase.

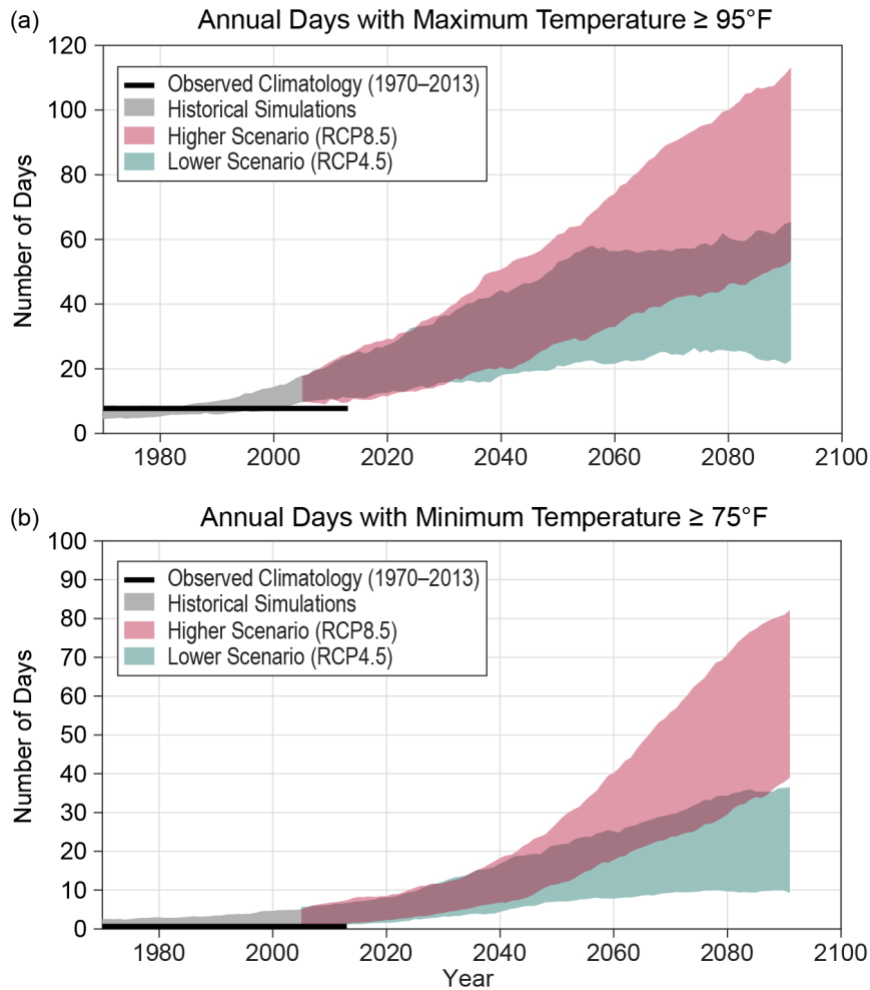## Observed and Projected Very Hot Days and Very Warm Nights: Piedmont (1970–2100)

Figure 3.22. These time series show the simulated historical and projected number of days per year on which (a) the maximum temperature is 95°F or higher and (b) the minimum temperature is 75°F or higher for the Piedmont region of North Carolina from the LOCA data and the observed climatological values averaged for the period 1970–2013 (black line). Historical simulations (gray shading) are shown for 1970–2005. Projected changes for 2006–2100 are shown for a higher scenario (RCP8.5; red shading) and a lower scenario (RCP4.5; green shading). The shaded ranges indicate the 10% to 90% confidence intervals of 20-year running averages from the set of climate models. Sources: NCICS and The University of Edinburgh.

3.3.3 Cold Days

Occurrences of cold days (maximum temperature of 32˚F or lower) are relatively infrequent, with just over 2 days per year on average (Figure 3.23). There is no overall trend, but the number has been above the long-term average since 2014. The highest value of about 10 days occurred in 1917. The relatively high values in recent years were caused in part by occurrences of a winter weather pattern popularly known as the polar vortex—an area of upper-level low pressure that is nearly always present over the North and South Poles. Occasionally, the arctic vortex is displaced southward over eastern North America and becomes nearly stationary, bringing unusually cold weather to the eastern United States. While the sporadic southward displacement of the vortex is a natural feature of the winter climate, some recent years have featured unusually persistent patterns, resulting in episodes of extended cold and stormy weather in the eastern United States, notably in the winters of 2009–10, 2010–11, 2013–14, and 2014–15. A number of research studies have found empirical evidence of a link between cold winters and the fact that the Arctic is warming more rapidly than lower latitudes (a phenomenon referred to as arctic amplification). The current scientific consensus is that observed winter temperature trends, including the lack of recent warming in the eastern United States, cannot be explained without including the potential effects of Arctic warming (Cohen et al. 2020).
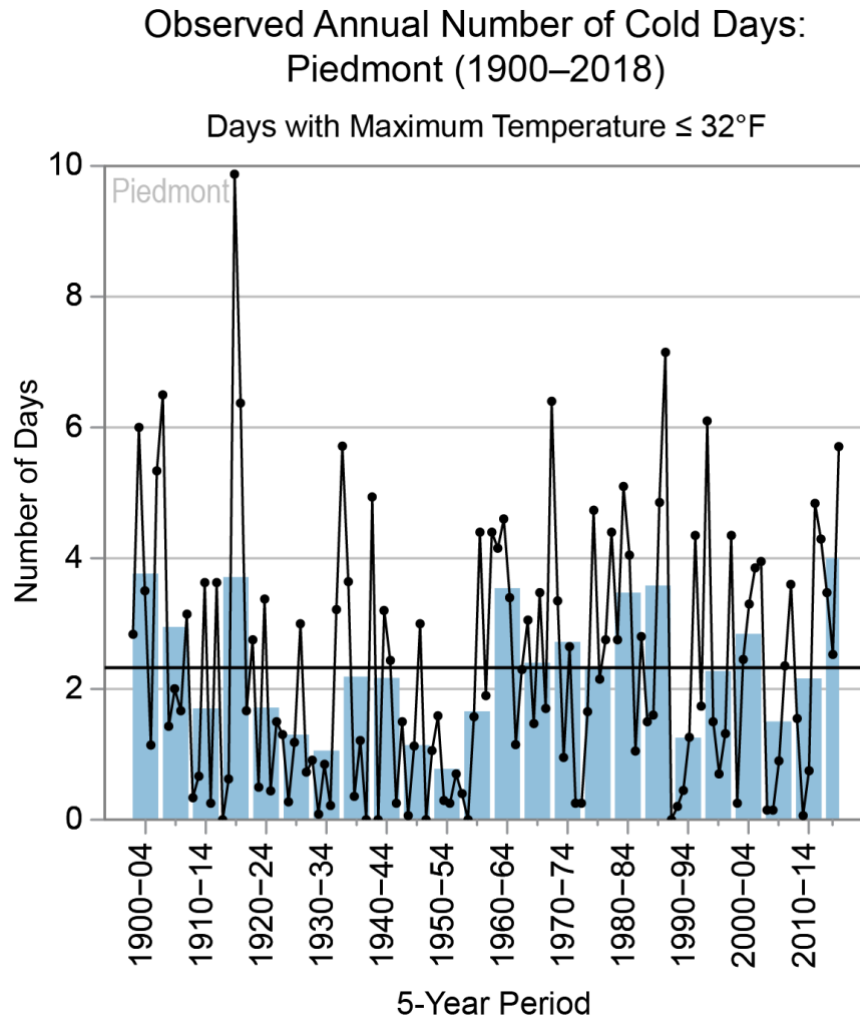
Observed Annual Number of Cold Days: Piedmont (1900–2018)

Days with Maximum Temperature ≤ 32°F

Figure 3.23. The bar graph shows the observed annual number of cold days (maximum temperature of 32°F or lower) for the Piedmont region of North Carolina for 1900–2018, as averaged over 5-year periods, with the last bar representing a 4-year period (2015–2018). Dots show annual values. The horizontal black line shows the long-term average of 2.4 cold days per year for 1900–2018. Sources: NCICS, NOAA NCEI, and the State Climate Office of North Carolina.

By the end of the century, climate models project that the annual number of cold days will be at or close to zero under both scenarios. There has not been a strong trend in the number of cold nights (minimum temperature of 32°F or lower) in recent years. However, by the end of the century, the number of cold nights is projected to decrease by 11–29 under the lower scenario and 25–46 under the higher scenario (Figure 3.24).

The projected decrease in cold days (Figure 3.24) is not consistent with the lack of an observed trend (Figure 3.23). As noted above, one reason for the lack of an observed trend is the recent occurrences of an unusually persistent southward-displaced polar vortex over eastern North America. However, there is no scientific consensus that continued polar warming will lead to an

increase in polar vortex occurrences over eastern North America (Cohen et al. 2020). Thus, it is ***likely*** that the number of cold days and cold nights will eventually decrease.

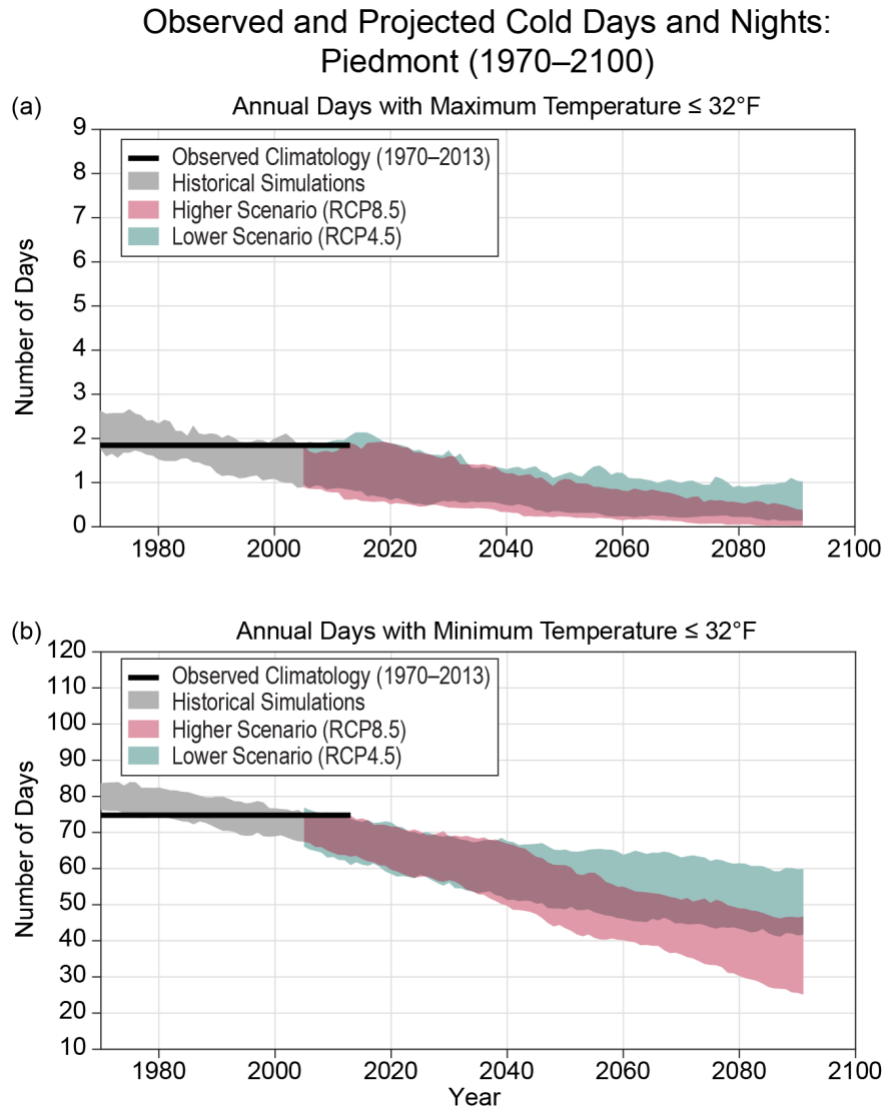## Observed and Projected Cold Days and Nights: Piedmont (1970–2100)

Figure 3.24. These time series show the simulated historical and projected number of days per year on which the (a) maximum temperature and (b) minimum temperature is 32°F or lower for the Piedmont region of North Carolina from the LOCA data and the observed climatological values averaged for the period 1970–2013 (black line). Historical simulations (gray shading) are shown for 1970–2005. Projected changes for 2006–2100 are shown for a higher scenario (RCP8.5; red shading) and a lower scenario (RCP4.5; green shading). The shaded ranges indicate the 10% to 90% confidence intervals of 20-year running averages from the set of climate models. Sources: NCICS and The University of Edinburgh.

3.3.4 Annual Hottest / Coldest Temperatures

Since 1970, there has been no strong trend in the annual hottest temperatures averaged over the Piedmont region, but there has been an increase in the annual coldest temperatures. By the end of the century, the annual hottest temperature is projected to increase by 2°–9°F under the lower scenario and 4°–15°F under the higher scenario, compared to the 1996–2015 average. The annual coldest temperature is projected to increase by 1°–8°F under the lower scenario and 6°–11°F under the higher scenario (Figure 3.25).

The projections for increases in annual coldest temperature are consistent with recent observations. Because of this consistency, it is *very likely* that the model-projected increases in annual coldest temperature will occur. However, the projected increase in annual hottest temperature is not consistent with the lack of an observed trend. Since the causes of the lack of an increase in annual hottest temperature are not yet fully understood, our level of confidence in the projections is lessened. However, summers have become warmer, and that warming is projected to continue. Thus, it is *likely* that the annual hottest temperature will eventually increase.

Observed and Projected Maximum and Minimum Temperatures: Piedmont (1970–2100)
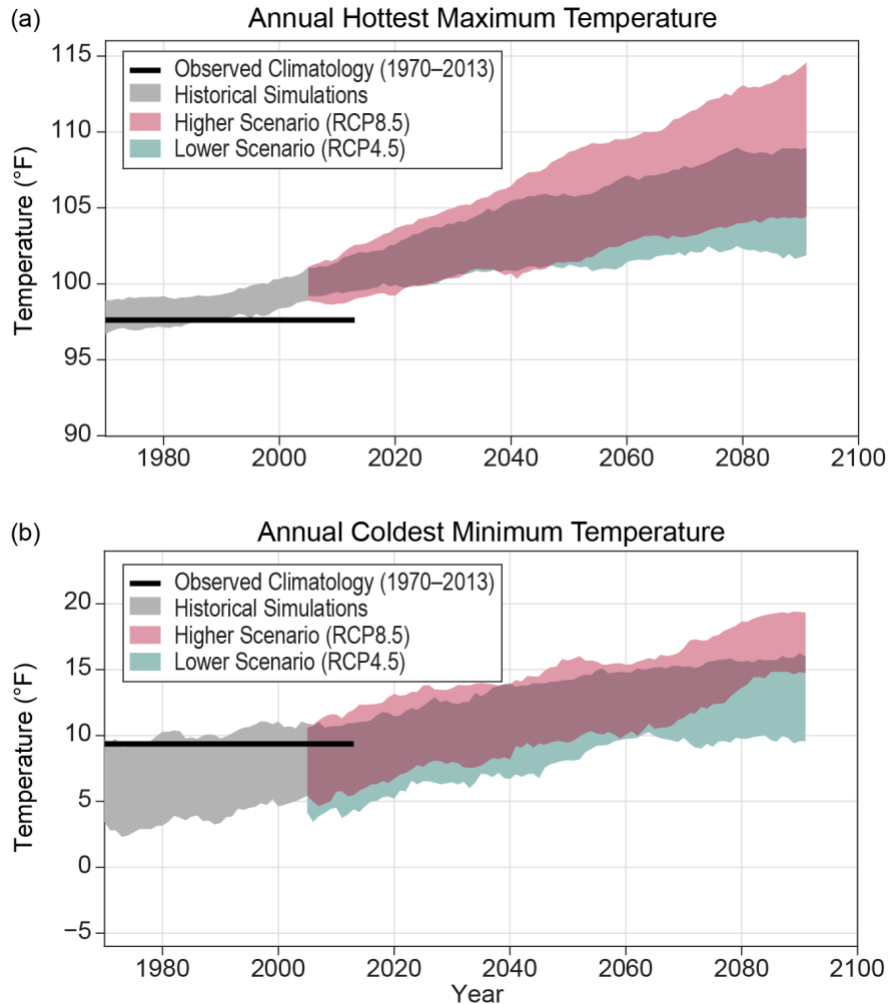

Figure 3.25. These time series show the simulated historical and projected (a) hottest maximum and (b) coldest minimum temperatures each year averaged over the Piedmont region of North Carolina from the LOCA data and the observed climatological values averaged for the period 1970–2013 (black line). Historical simulations (gray shading) are shown for 1970–2005. Projected changes for 2006–2100 are shown for a higher scenario (RCP8.5; red shading) and a lower scenario (RCP4.5; green shading). The shaded ranges indicate the 10% to 90% confidence intervals of 20-year running averages from the set of climate models. Sources: NCICS and The University of Edinburgh.

3.3.5 Heating and Cooling Degree Days

The term "heating degree days" (HDDs) refers to the number of degrees that a day's average temperature is below 65°F, while "cooling degree days" (CDDs) refers to the number of degrees that the average temperature is above 65°F. These metrics are used to quantify the energy needed

to heat or cool buildings and houses. HDDs and CDDs in the Piedmont region have varied in concert with the region's annual average temperature. As average temperature (Figure 3.18) increased in the first half of the 20th century, HDDs (Figure 3.26) decreased, reaching a relative minimum around mid-century, while CDDs (Figure 3.27) exhibited little overall trend. HDDs then increased to relatively higher values by the 1960s, as the region's average temperature and CDDs reached their lowest values in decades. Coincident with an upward trend in annual average temperature, there has been a decreasing trend in HDDs since the 1980s, and all but two years have been below the long-term average since 2000. At the same time, there has been an increasing trend in CDDs, with the highest values on record occurring since 2010.

Overall warming is projected to lead to decreases in HDDs and increases in CDDs in the Piedmont (Figure 3.28). This indicates a decrease in energy needed for heating and an increase in energy needed for cooling. By the end of the century, HDDs are projected to decrease by 400–1,000 under the lower scenario and 900–1,600 under the higher scenario, compared to the 1996–2015 average. CDDs are projected to increase by 300–1,200 under the lower scenario and 1,100–2,200 under the higher scenario. These trends are projected to continue throughout the century. These projections are consistent with recent trends. For this reason, it is ***very likely*** that HDDs will decrease and CDDs will increase in the future.

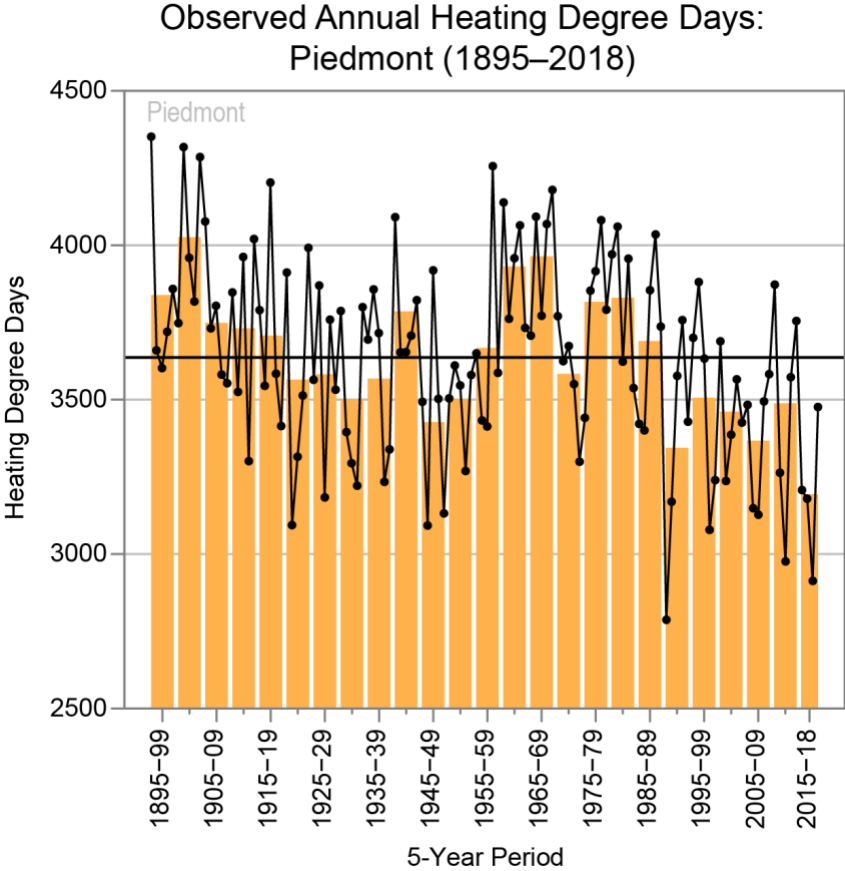**Observed Annual Heating Degree Days: Piedmont (1895–2018)**

Figure 3.26. The bar graph shows the observed annual heating degree days for the Piedmont region of North Carolina for 1895–2018, as averaged over 5-year periods, with the last bar representing a 4-year period (2015–2018). Dots show annual values. The horizontal black line shows the long-term average of 3,635 heating degree days per year for 1895–2018. There has been a decreasing trend in heating degree days since the 1980s, and all but two years have been below the long-term average since 2000. Sources: NCICS, NOAA NCEI, and the State Climate Office of North Carolina.
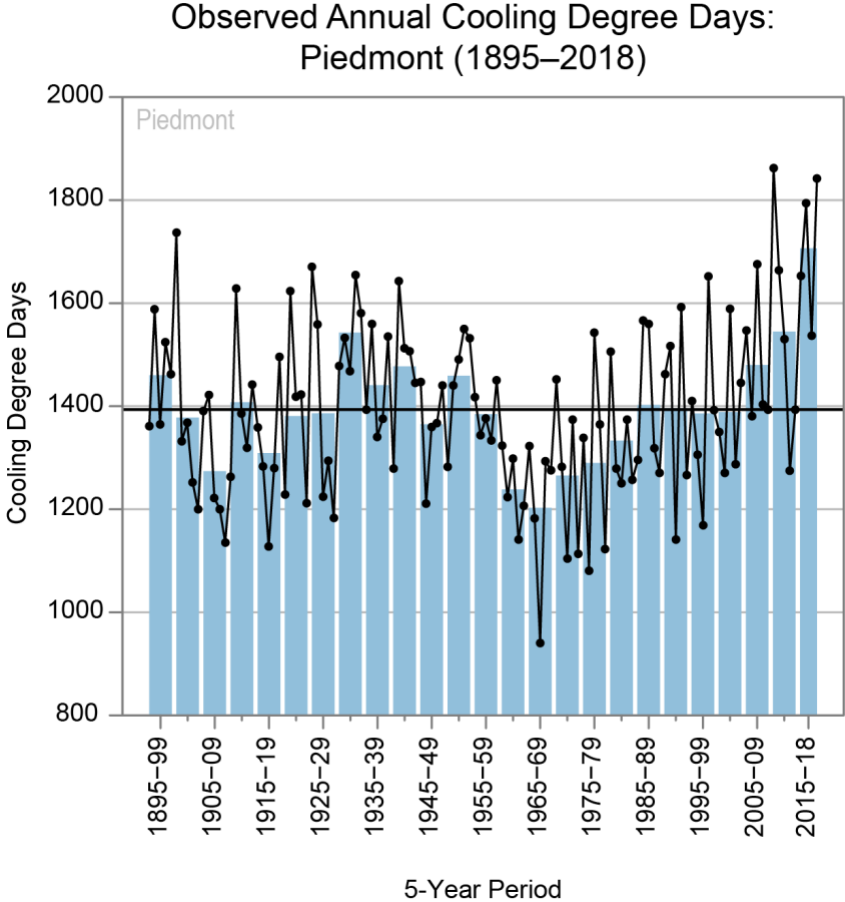
Figure 3.27. The bar graph shows the observed annual cooling degree days for the Piedmont region of North Carolina for 1895–2018, as averaged over 5-year periods, with the last bar representing a 4-year period (2015–2018). Dots show annual values. The horizontal black line shows the long-term average of 1,395 cooling degree days per year for 1895–2018. There has been an increasing trend in cooling degree days since the 1990s, and the highest values on record have occurred since 2010. Sources: NCICS, NOAA NCEI, and the State Climate Office of North Carolina.

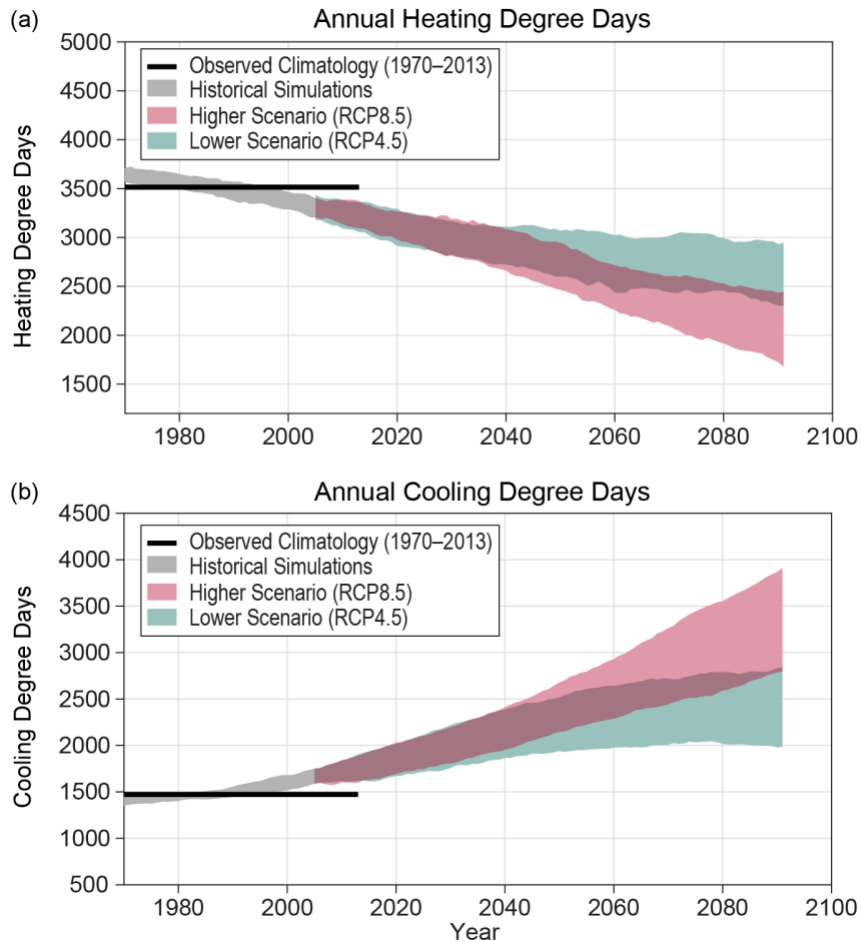## Observed and Projected Heating and Cooling Degree Days: Piedmont (1970–2100)

Figure 3.28. These time series show simulated historical and projected values for (a) annual heating degree days and (b) annual cooling degree days for the Piedmont region of North Carolina from the LOCA data and the observed climatological values averaged for the period 1970–2013 (black line). Historical simulations (gray shading) are shown for 1970–2005. Projected changes for 2006–2100 are shown for a higher scenario (RCP8.5; red shading) and a lower scenario (RCP4.5; green shading). The shaded ranges indicate the 10% to 90% confidence intervals of 20-year running averages from the set of climate models. Sources: NCICS and The University of Edinburgh.

3.3.6 Annual Precipitation

The Piedmont is the driest of the three regions in North Carolina, with a long-term average of 46 inches of precipitation per year compared to 49 and 54 inches per year in the Coastal Plain and Mountains, respectively (Figure 3.29). Precipitation in the Mountains is enhanced by forced uplift of moist air masses, while precipitation along the Coast is enhanced by warm-season thunderstorms caused by the sea breeze. Neither of these mechanisms occurs in the Piedmont.

The 5-year period of 1965–1969 was the driest such period in the Piedmont. The driest years on record were 1925, 1933, and 2006, with about 32 inches in each of those years. The 1905–1909 period is the wettest 5-year period on record, while 2018 was the wettest year on record, receiving 63 inches, 17 inches above average. Hurricane Florence contributed about 9 inches to the annual total for the Piedmont.
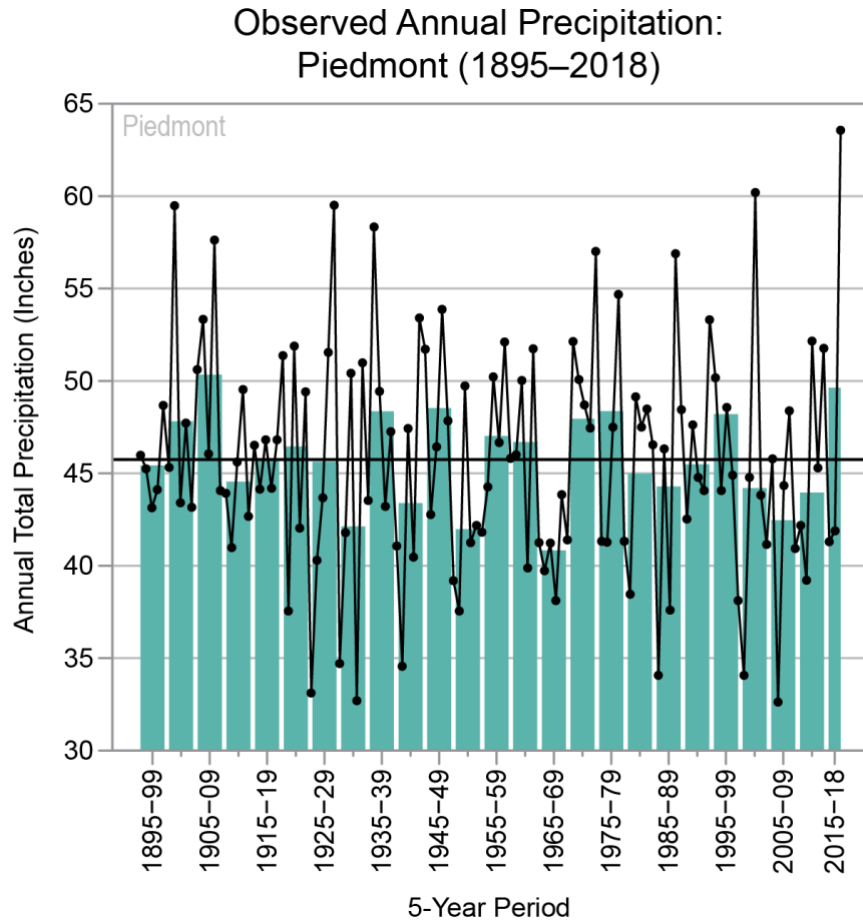

Figure 3.29. The bar graph shows the observed annual total precipitation for the Piedmont region of North Carolina for 1895–2018, as averaged over 5-year periods, with the last bar representing a 4-year period (2015–2018). Dots show annual. The horizontal black line shows the long-term average of 45.7 inches per year for 1895–2018. Sources: NCICS, NOAA NCEI, and the State Climate Office of North Carolina.

By the end of the century, climate models project a wide range in potential outcomes, from drier to wetter conditions. While the average of the model projections shows small increases in annual total precipitation compared to the current climate (see Figure 2.16), the models range from decreases of 2 inches to increases of 5 inches under the lower scenario and decreases of 2 inches to increases of 9 inches under the higher scenario, compared to the 1996–2015 average (Figure 3.30). Based on the greater number of models showing increases, it is ***likely*** that annual precipitation will increase.

Observed and Projected Annual Total Precipitation:
Piedmont (1970–2100)
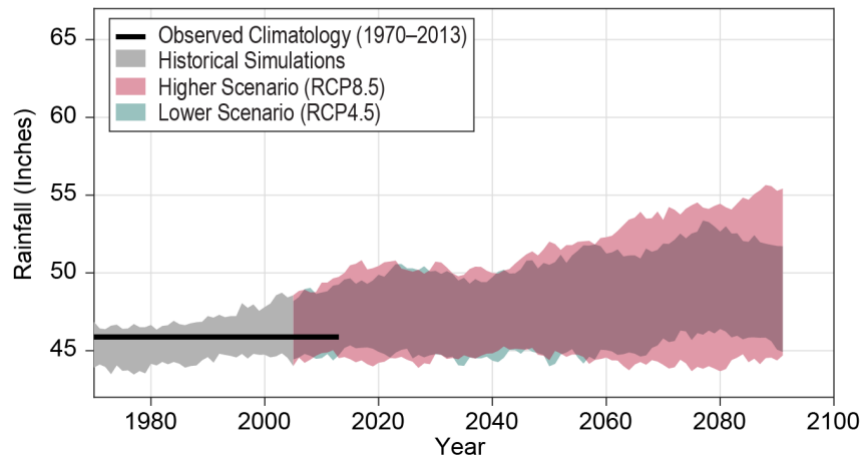

Figure 3.30. These time series show the simulated historical and projected annual total precipitation for the Piedmont region of North Carolina from the LOCA data and the observed climatological value averaged for the period 1970–2013 (black line). Historical simulations (gray shading) are shown for 1970–2005. Projected changes for 2006–2100 are shown for a higher scenario (RCP8.5; red shading) and a lower scenario (RCP4.5; green shading). The shaded ranges indicate the 10% to 90% confidence intervals of 20-year running averages from the set of climate models. Sources: NCICS and The University of Edinburgh.

3.3.7 Heavy Precipitation

Extreme precipitation is highly variable across the historical record, especially from year to year (Figure 3.31). Days with precipitation amounts of 3 inches or more are rare, with fewer than 1 such day per year expected on average at any individual location. The most recent six years have all been near or above the long-term average, and 2018 had the third highest number of days with 3 inches or more on record.
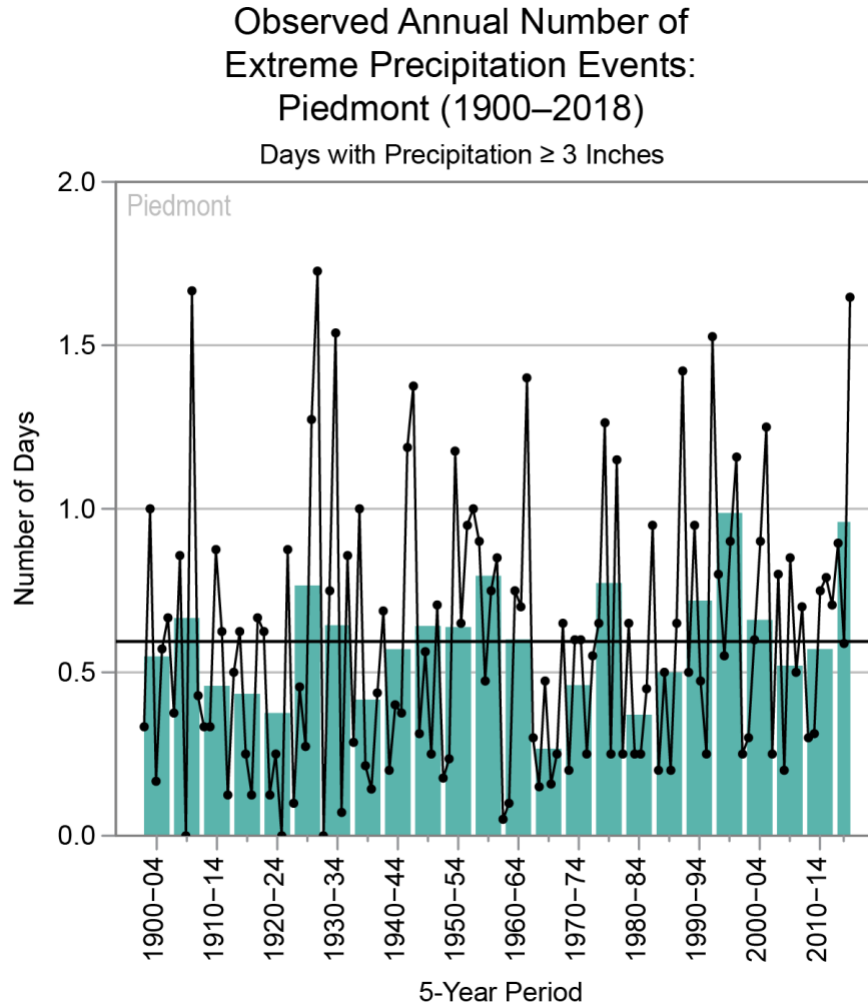
Figure 3.31. The bar graph shows the observed annual number of extreme precipitation events (days with precipitation of 3 inches or more) for the Piedmont region of North Carolina for 1900–2018, as averaged over 5-year periods, with the last bar representing a 4-year period (2015–2018). Dots show annual values. The horizontal black line shows the long-term average of 0.6 extreme precipitation days per year for 1900–2018. Sources: NCICS, NOAA NCEI, and the State Climate Office of North Carolina.

By the end of the century, climate models project a large range of potential changes. This large range is mainly a result of the random nature of extreme rainfall. However, the models show an overall increase in the number of extreme precipitation days in the Piedmont region.

By the end of the century, the annual number of days with precipitation of 3 inches or more will increase by up to 0.1 (115%) under the lower scenario and 0.3 (200%) under the higher scenario, compared to the 1996–2015 average (Figure 3.32). Note that the current value of 0.1 days per year from the Livneh dataset is lower than the station average of 0.6 days per year (Figure 3.31). The Livneh dataset consists of spatially averaged data, which have lower values of extreme rainfall.

Based on the virtual certainty that water vapor in the atmosphere will increase as global warming occurs, it is ***very likely*** that the risk of extreme precipitation will increase everywhere in the Piedmont.
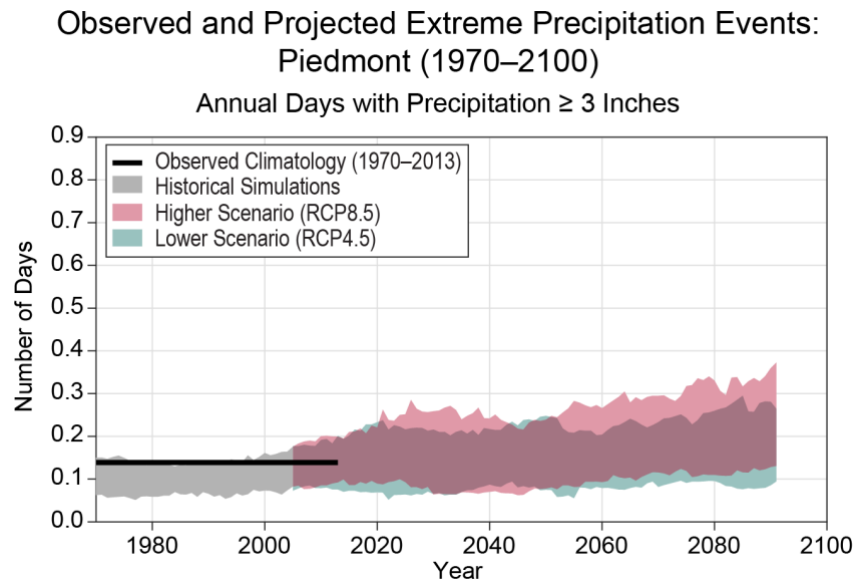

Figure 3.32. These time series show the simulated historical and projected annual number of days with precipitation of 3 inches or more⌷ for the Piedmont region of North Carolina from the LOCA data and the observed climatological value averaged for the period 1970–2013 (black line). Historical simulations (gray shading) are shown for 1970–2005. Projected changes for 2006–2100 are shown for a higher scenario (RCP8.5; red shading) and a lower scenario (RCP4.5; green shading). The shaded ranges indicate the 10% to 90% confidence intervals of 20-year running averages from the set of climate models. Sources: NCICS and The University of Edinburgh.

3.3.8 Drought

Drought can be measured using the Palmer Drought Severity Index (PDSI), which uses temperature and precipitation data to calculate the severity of drought at a location by estimating the relative dryness. The values calculated for PDSI range from −10 (dry) to +10 (wet). This metric captures medium- to long-term drought in North Carolina and is a metric used by water managers and climate scientists to quantify and compare droughts across recorded history. Figure 3.33 shows the number of months with a PDSI value less than or equal to −2 (moderate, severe, or extreme drought). In the Piedmont, the periods of 1925–1929, 1985–1989, 2000–2004, and 2010–2014 experienced the most frequent drought, with an average of about 5 months per year with moderate or more severe drought conditions. The years 1926, 2010, and 2011 each experienced 10 or more months with drought conditions.
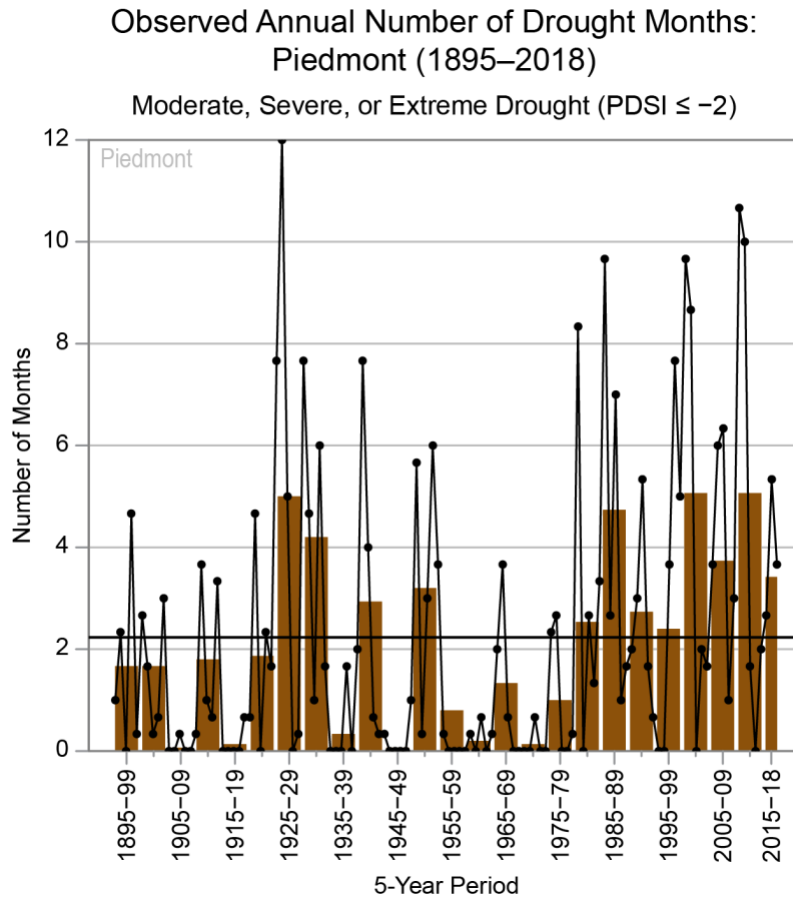
Figure 3.33. The bar graph shows the observed annual number of months in drought of moderate or worse severity (PDSI values less than or equal to −2) for the Piedmont region of North Carolina for 1895–2018, as averaged over 5-year periods, with the last bar representing a 4-year period (2015–2018). Dots show annual values. The horizontal black line shows the long-term average of 2.2 drought months per year for 1895–2018. Sources: NCICS, NOAA NCEI, and the State Climate Office of North Carolina.

Droughts are a natural part of the climate of North Carolina. Future droughts are projected to be warmer than historical events with a high level of confidence. The warmer conditions will lead to more rapid drying through increases in potential evapotranspiration. Thus, it is *likely* that future droughts will be more severe in terms of soil moisture deficits and the impacts on rainfed agriculture and natural vegetation.

3.3.9 Winter Storms

Winter storms are large areas of low pressure in the middle and high latitudes that are primarily distinguished by fronts separating warm and cold air masses. They often cause various types of adverse weather conditions, such as strong winds and precipitation of various types, including snow and ice. This section discusses winter storms of all types, while the following two subsections discuss the specific instances of storms causing snow and ice.

Winter storm tracks have shifted slightly northward (by about 0.4 degrees latitude) in recent decades over the Northern Hemisphere (Bender et al. 2012). More generally, winter storm activity is projected to change in complex ways under future climate scenarios, with increases in some regions and seasons and decreases in others.

The Arctic is warming more quickly than lower latitudes (i.e., arctic amplification), due in part to sea ice loss. This reduces the lower-atmosphere temperature difference between the Arctic and the lower latitudes—this difference is an important energy source for winter storms. At the same time, the temperature difference higher up in the atmosphere is projected to increase due to a warming tropical upper troposphere and a cooling high-latitude lower stratosphere. While these two effects counteract each other with respect to a projected change in midlatitude storm tracks, the simulations indicate that the magnitude of arctic amplification may modulate some aspects (e.g., jet stream position, wave extent, and blocking frequency) of the circulation in the North Atlantic region in some seasons (Barnes and Polvani 2015).

Regional studies of trends in cyclones are challenged to provide definitive results regarding changes in the frequency or intensity of storms, but regardless of these properties, it is ***very likely*** that cyclones of even similar intensity will produce heavier precipitation (e.g., Marciano et al. 2015, Michaelis et al. 2017).

Based on the available evidence, our conclusion is that there is ***low confidence*** concerning future changes in the number of winter storms.

3.3.9.1 Snowstorms and Snow Cover
In the Piedmont of North Carolina, winter precipitation usually falls as rain because temperatures are above freezing near the surface. Thus, winter temperatures are a critical factor in both historical and future changes in snowfall. Central North Carolina winter temperatures have been above the long-term average in most winters since 1990. Analysis of snowfall at central North Carolina stations with long records found decreasing trends over the period of 1930–2007 (Kunkel et al. 2009) at most stations.

The Fourth National Climate Assessment projects large winter warming under both moderate and higher emissions scenarios. Consistent with the projected warming, a northward shift in the rain–snow transition zone in the central and eastern United States is projected under a higher emissions scenario. By the end of the 21st century, large areas that are currently snow dominated in the cold season are expected to be rain dominated (Krasting et al. 2013, Ning and Bradley 2015). For the Piedmont of North Carolina, the frequency of snowfall is projected to decrease and become a rare occurrence.

As noted earlier, a definitive understanding of the effects of arctic amplification on midlatitude winter weather remains elusive (Cohen et al. 2020) suggest a linkage between such episodes and enhanced Arctic warming (referred to as arctic amplification), and this adds some uncertainty to future projections of winter climate in North Carolina. Current global climate models (CMIP5) do predict an increase in the frequency of winter storms over the eastern United States, including

the most intense storms, under the higher emissions scenario (Colle et al. 2013). However, there are large model-to-model differences in the realism of historical simulations and in the projected changes. Even if there were increases in the frequency or intensity of winter storms, the effects of warmer winters would nevertheless lead to decreases in average annual snowfall.

Another consequence of warming, however, is an expected increase in precipitation intensity. Thus, for events where air is sufficiently cold for precipitation to fall as snow, heavier totals could occur in the coming decades, before more extensive warming leads to only rare snowfall (O'Gorman 2014). However, an increase in heavy snow with warming only occurs with average temperatures colder than what occurs anywhere in North Carolina, including the mountains.

Based on the projected increase in temperature, it is ***very likely*** that total snowfall will decrease. It is ***likely*** that the number of heavy snowstorms will decrease.

3.3.9.2 Ice Storms
Ice storms occur within winter storms, the same as for snowstorms. However, icing requires a specific combination of weather conditions, most importantly precipitating conditions with a below-freezing layer near the surface and an above-freezing layer above the low-level freezing layer. In this situation, snow falling from high levels melts as it falls through the above-freezing layer; it then becomes super-cooled liquid drops while falling through the near-surface freezing layer and freezes on contact with cold surface objects.

The accurate simulation of this weather feature by climate models is challenging because the vertical extent of the below-freezing and above-freezing layers is often quite small and thus non-resolvable by the current generation of climate models. Also, the horizontal resolution in models is insufficient to capture the fine spatial detail of ice-producing conditions. As a result, research on future changes in ice storm frequency and intensity is limited, and the recent Fourth National Climate Assessment did not make any statements on this weather phenomenon.

In the Piedmont of North Carolina, the presence of the Appalachian Mountains to the west can result in a phenomenon known as cold-air damming, in which a shallow layer of cold air moves southward across the Carolinas. This setup can be accompanied by freezing rain or ice pellets. However, there is no reason why cold-air damming would be expected to change in a warmer climate, other than that the temperature of the cold air masses could moderate.

Freezing rain takes place when a layer of warm air moves over the shallow cold air near the surface, such as during cold-air damming. With warming, it may be easier for these warm layers to develop, and at least one study linked a North Carolina ice storm to warm offshore waters (Ramos de Silva et al. 2006). Thus, it is possible that warming could result in an increase of these warm layers, increasing freezing rain occurrence.

Taken together, the preceding discussion demonstrates that there is considerable uncertainty in projected changes in freezing rain in a warming climate. More research is needed. Our conclusion is that there is ***low confidence*** concerning future changes in the number of ice storms.

3.3.10 Thunderstorms and Tornadoes

Tornado and severe thunderstorm events cause significant loss of life and property: more than one-third of the $1 billion weather disasters in the United States during the past 25 years were due to such events, and, relative to other extreme weather, the damages from convective weather hazards have undergone the largest increase since 1980 (Smith and Katz 2013). A particular challenge in quantifying the existence and intensity of these events arises from the data source: rather than measurements, the occurrence of tornadoes and severe thunderstorms is determined by visual sightings by eyewitnesses (such as "storm spotters" and law enforcement officials) or post-storm damage assessments. The reporting has been susceptible to changes in population density, modifications to reporting procedures and training, the introduction of video and social media, and so on. These have led to systematic, non-meteorological biases in the long-term data record.

Nonetheless, judicious use of the report database has revealed important information about tornado trends. Since the 1970s, the United States has experienced a decrease in the number of days per year on which tornadoes occur but an increase in the number of tornadoes that form on such days. One important implication is that the frequency of days with large numbers of tornadoes—tornado outbreaks—appears to be increasing (Figure 9.3 in Kossin et al. 2017). The length of the season over which such tornado activity occurs is increasing as well: although tornadoes in the United States are observed in all months of the year, an earlier calendar-day start to the season of high activity is emerging. In general, there is more interannual variability, or volatility, in tornado occurrence (Elsner et al. 2015, Tippett 2014).

Evaluations of hail and thunderstorm wind reports have thus far been less revealing. Although there is evidence of an increase in the number of hail days per year, the inherent uncertainty in reported hail size reduces the confidence in such a conclusion. Thunderstorm wind reports have proven to be even less reliable because, as compared to tornadoes and hail, there is less tangible visual evidence; thus, although the United States has lately experienced several significant thunderstorm wind events (sometimes referred to as derechos), the lack of studies that explore long-term trends in wind events and the uncertainties in the historical data preclude any robust assessment.

It is possible to bypass the use of reports by exploiting the fact that the temperature, humidity, and wind in the larger vicinity—or "environment"—of a developing thunderstorm ultimately control the intensity, structure, and hazardous tendency of the storm. Thus, the premise is that measures of temperature, humidity, and wind at various heights throughout the atmosphere can be used as a proxy for actual severe thunderstorm occurrence. In particular, a measure of the energy available for convection (known as convective available potential energy or CAPE) and vertical wind shear (a change in wind speed or direction with change in altitude) constitutes one widely used means of representing the frequency of severe thunderstorms. This environmental-proxy approach avoids the biases and other issues with eyewitness storm reports and is readily evaluated using the relatively coarse global datasets and global climate models. It has the

disadvantage of assuming that a thunderstorm will necessarily form and then realize its environmental potential.

Global climate models consistently project an increase in the frequency of severe thunderstorm environments in the United States over the mid- to late 21st century. The most robust projected increases in frequency are over the U.S. Midwest and Southern Great Plains during spring (March–May). Based on the increased frequency of very high CAPE, increases in storm intensity are also projected over this same period (Del Genio et al. 2007).

Key limitations of the environmental-proxy approach are being addressed through the applications of high-resolution dynamical downscaling, wherein sufficiently fine model grids are used so that individual thunderstorms are explicitly represented, rather than implicitly represented (as through environmental proxies). The individually modeled thunderstorms can then be quantified and assessed in terms of severity (e.g., Trapp et al. 2011). Prein et al. (2017) used a convection-permitting model to examine changes in intense hourly precipitation in the central United States, finding an increase in the most intense events and a decrease in lighter events. The dynamical-downscaling results have thus far supported the basic findings of the environmental-proxy studies, particularly in terms of the seasons and geographical regions projected to experience the largest increases in severe thunderstorm occurrence.

Based on these studies, we conclude it is ***likely*** that severe thunderstorms in the Piedmont will increase in frequency.

3.4 Western Mountains

3.4.1 Average Temperature

The Western Mountains region is the coolest of the three regions in North Carolina, with a long-term annual average temperature of about 54˚F, compared to about 59˚F in the Piedmont and about 61°F in the Coastal Plain. Trends in annual average temperatures in the Mountains (Figure 3.34) are similar to statewide trends (see Figure 2.1). Temperatures were generally below the long-term average through 1920 and mostly above average from the 1930s through the mid-1950s. Below average temperatures were the norm from the 1960s through the 1980s. Temperatures have been increasing since then, and have remained consistently above average since the 1990s. The most recent 4-year period (2015–2018) was well above average and was the warmest on record, and 16 of the last 18 years have been above the long-term average.

Observed Annual Average Temperature: Western Mountains (1895–2018)
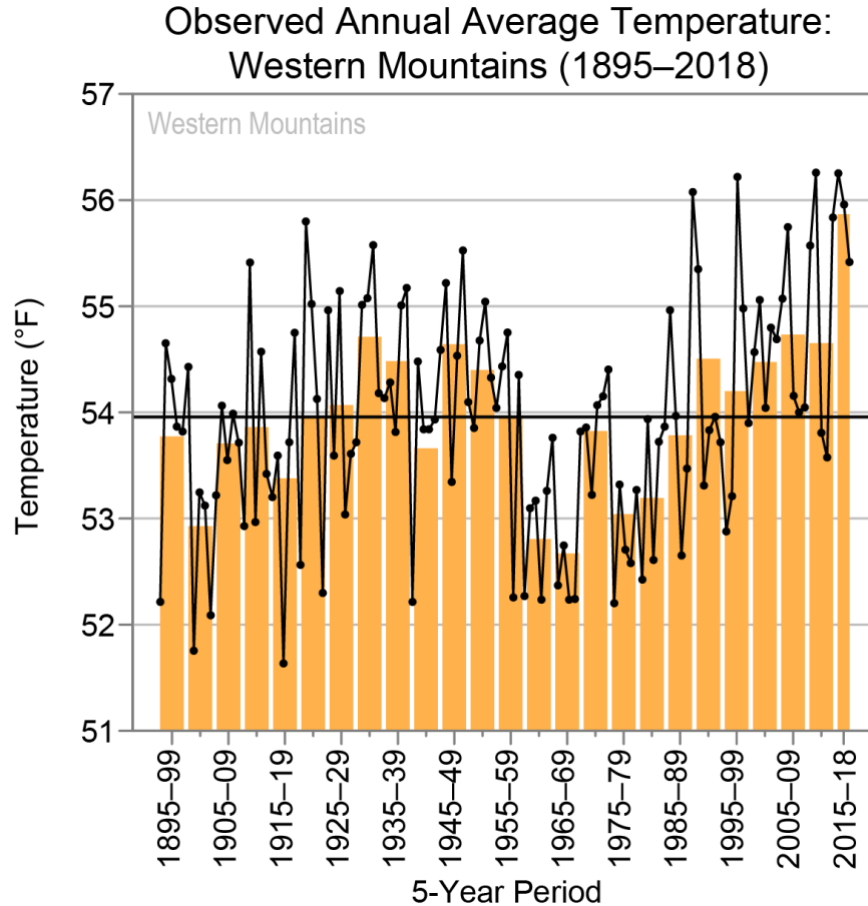

Figure 3.34. The bar graph shows the observed annual average temperature for the Western Mountains of North Carolina for 1895–2018, as averaged over 5-year periods, with the last bar representing a 4-year period (2015–2018). Dots show annual values. The horizontal black line shows the long-term average of 53.9°F for 1895–2018. Sources: NCICS, NOAA NCEI, and the State Climate Office of North Carolina.

By the end of the century, the average temperature is projected to increase by 2°–6°F under the lower scenario (RCP 4.5) and by 5°–10°F under the higher scenario (RCP 8.5; Figure 3.35), compared to the average temperature for 1996–2015. Figure 3.35 also shows the observed average temperature value for the period 1970–2013. Here, the Livneh observational dataset is used (see Appendix A for a description of datasets).

The observed temperatures have tended to be on the lower end of the range of historical model simulations (not shown), similar to the statewide average temperature (Frankson et al. 2017; 2019 update). This suggests that the lower end of the projected values is a more likely outcome for the future. However, since the causes of the lesser warming observed in the Southeast are not yet fully understood and recent years have exhibited substantial warming, the higher end of the projected values should not be discounted as a possibility.

Observed and Projected Annual Average Temperature: Western Mountains (1970–2100)
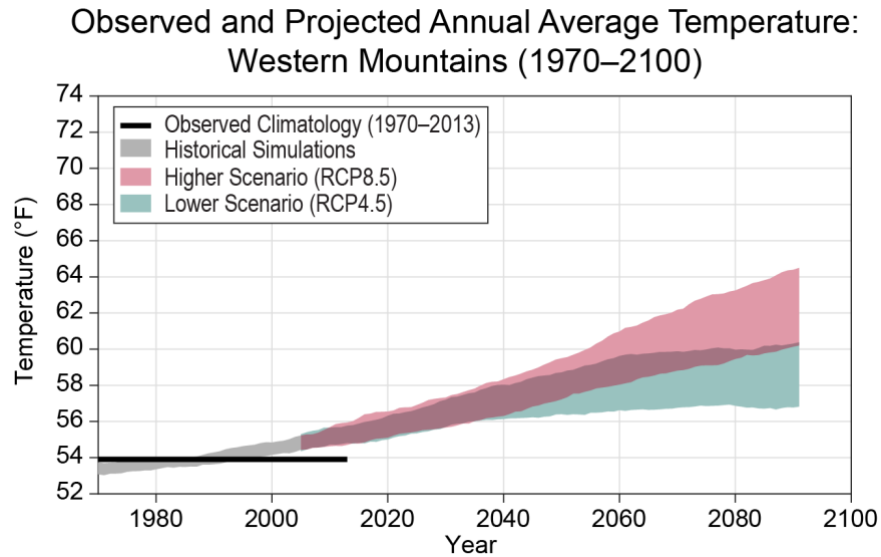
Figure 3.35. These time series show the simulated historical and projected annual average temperature for the Western Mountains of North Carolina from the LOCA data and the observed climatological value averaged for the period 1970–2013 (black line). Historical simulations (gray shading) are shown for 1970–2005. Projected changes for 2006–2100 are shown for a higher scenario (RCP8.5; red shading) and a lower scenario (RCP4.5; green shading). The shaded ranges indicate the 10% to 90% confidence intervals of 20-year running averages from the set of climate models. Source: NCICS and The University of Edinburgh.

3.4.2 Hot Days and Warm Nights

The Western Mountains region has not experienced an overall increase in the frequency of hot days (maximum temperature of 90°F or higher; Figure 3.36), though there has been a recent increase in the number of warm nights (minimum temperature of 70°F or higher; Figure 3.37). Because the cooler Western Mountains region rarely sees days above 95°F or nights above 75°F, the analysis presented here is for "hot days" and "warm nights" (thresholds of 90°F and 70°F, respectively) rather than the "very hot days" and "very warm nights."

On average, the Western Mountains experience about 12 days per year at or above 90°F. Changes in the annual number of hot days have not followed the same pattern as the annual average temperatures in the Western Mountains (Figure 3.34); as in the Coastal Plain and Piedmont regions, there were more occurrences of hot days earlier in the historical record than in recent periods, and the highest average of 22 days per year occurred in the 1930–1934 period. The higher frequencies of such days during the 1930s through the 1950s correspond to periods of exceptionally dry weather.
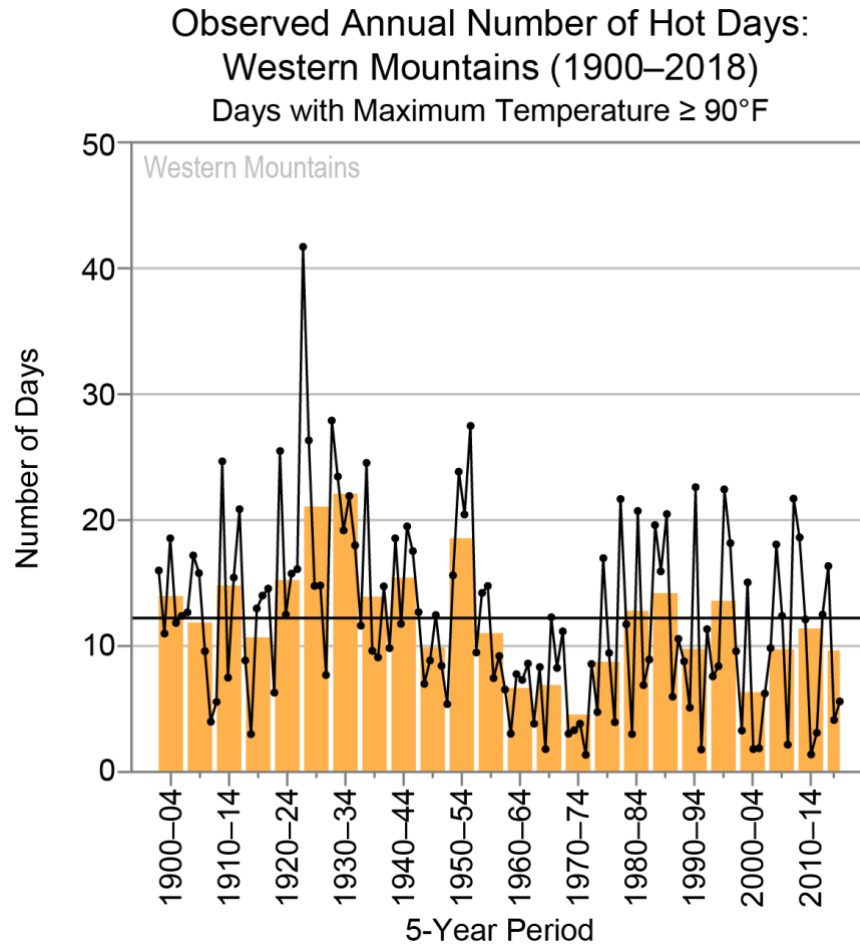
Figure 3.36. The bar graph shows the observed annual number of hot days (maximum temperature of 90˚F or higher) for the Western Mountains of North Carolina for 1900–2018, as averaged over 5-year periods, with the last bar representing a 4-year period (2015–2018). Dots show annual values. The horizontal black line shows the long-term average of 12 hot days per year for 1900–2018. Sources: NCICS, NOAA NCEI, and the State Climate Office of North Carolina.

Warm nights are rare in the Western Mountains, occurring on average about once per year. Changes in warm nighttime temperatures in the Western Mountains have been similar to the changes in annual average temperatures (Figure 3.34), with an increase in recent years. The 2010–2014 period (with an annual average of more than 3 nights per year) and the year 2010 in particular (with an average of about 8 nights) experienced the highest number of warm nights.
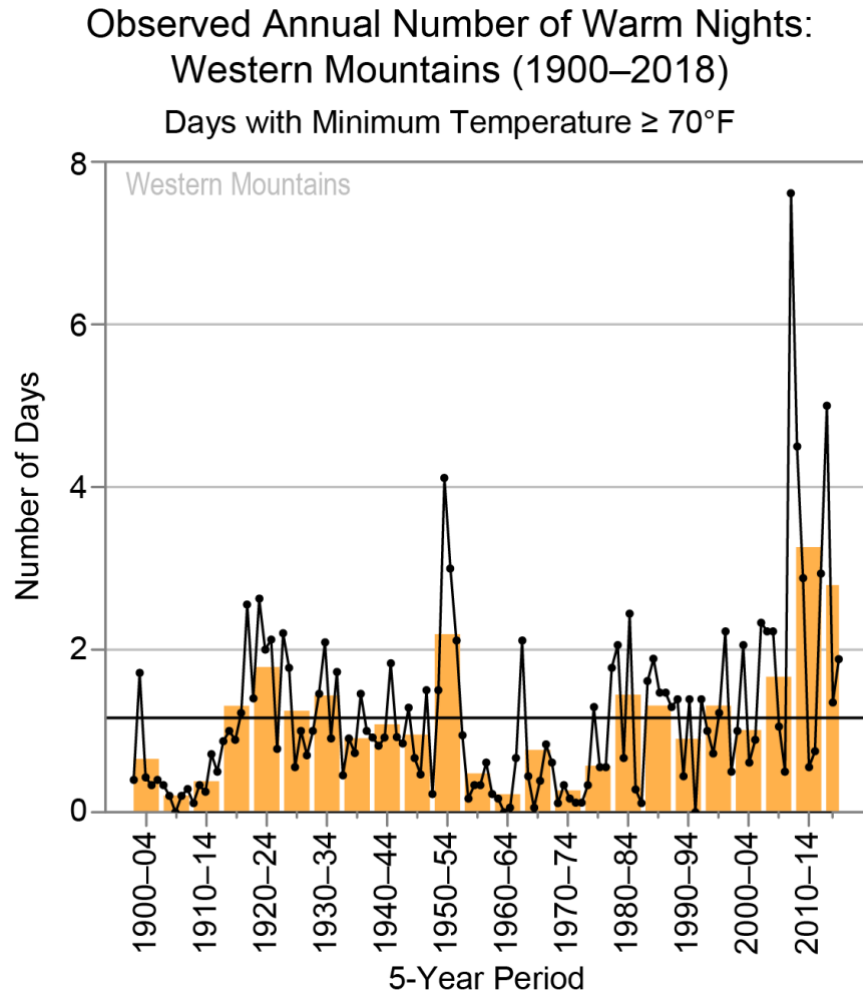
Observed Annual Number of Warm Nights: Western Mountains (1900–2018)

Days with Minimum Temperature ≥ 70°F

Figure 3.37. The bar graph shows the observed annual number of warm nights (minimum temperature of 70°F or higher) for the Western Mountains of North Carolina for 1900–2018, as averaged over 5-year periods, with the last bar representing a 4-year period (2015–2018). Dots show annual values. The horizontal black line shows the long-term average of 1.2 warm nights per year for 1900–2018. Sources: NCICS, NOAA NCEI, and the State Climate Office of North Carolina.

Climate models project a substantial increase in the number of these hot days and warm nights by mid- to late century under both scenarios. By the end of the century, the number of hot days is projected to increase by 9–44 under the lower scenario and 31–91 under the higher scenario, compared to the 1996–2015 average. The number of warm nights is projected to increase by 7–23 under the lower scenario and 27–58 under the higher scenario (Figure 3.38).

The projections for increases in the number of warm nights (Figure 3.38) are consistent with recent observations (Figure 3.37). Because of this consistency, it is ***very likely*** that the model-projected increases in the number of warm nights will occur. However, the projected increase in hot days (Figure 3.38) is not consistent with the lack of an observed trend (Figure 3.36). Since

the causes of the lack of an increase in the number of hot days are not yet fully understood, our level of confidence in the projections is lessened. However, summers have become warmer, and that warming is projected to continue. Thus, it is ***likely*** that the number of hot days will eventually increase.
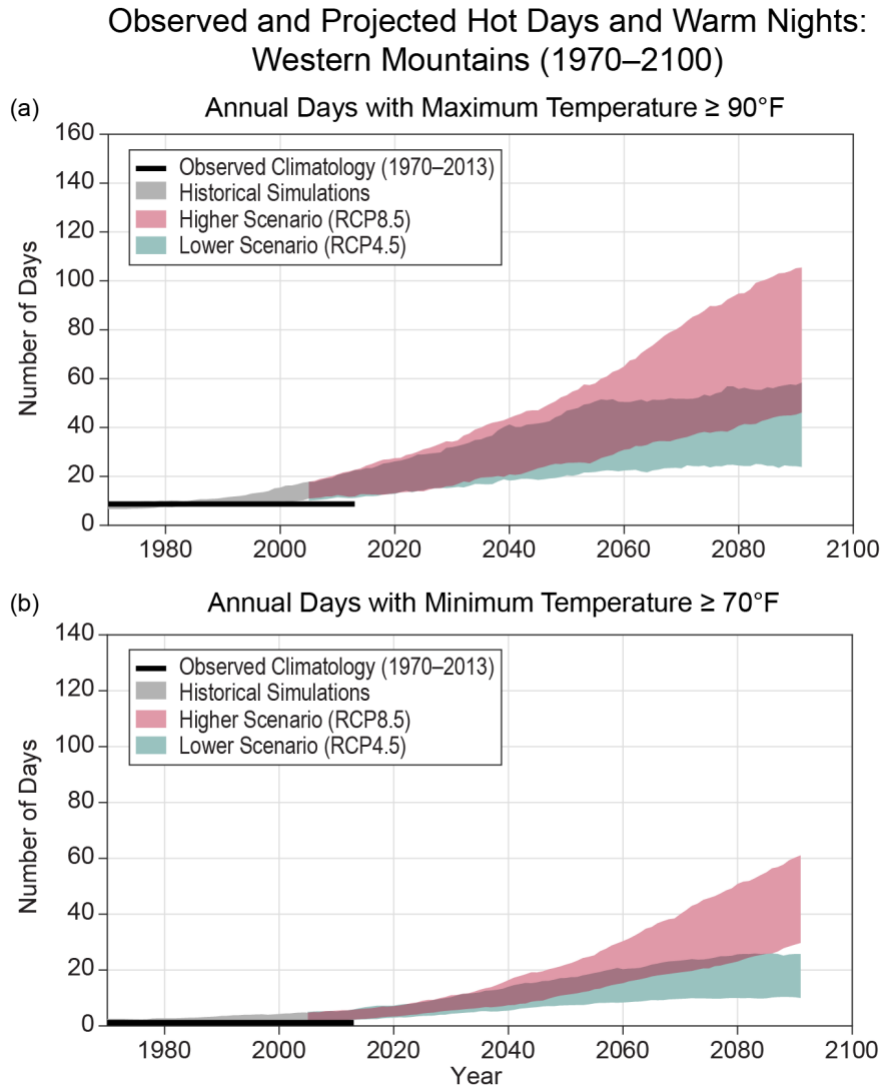

Figure 3.38. These time series show the simulated historical and projected number of days per year on which (a) the maximum temperature is 90°F or higher and (b) the minimum temperature is 70°F or higher for the Western Mountains of North Carolina from the LOCA data and the observed climatological values averaged for the period 1970–2013 (black line). Historical simulations (gray shading) are shown for 1970–2005. Projected changes for 2006–2100 are shown for a higher scenario (RCP8.5; red shading) and a lower scenario (RCP4.5; green shading). The shaded ranges indicate the 10% to 90% confidence intervals of 20-year running averages from the set of climate models. Sources: NCICS and The University of Edinburgh.

3.4.3 Cold Days

The Western Mountains experience a higher number of cold days (maximum temperature of 32°F or lower) than the other two regions, with a long-term average of approximately 5 days per year (Figure 3.39). There is no trend in the number of days below freezing in this region; however, the period since 2010 has averaged about 8 days per year. The relatively high values in recent years were caused in part by occurrences of a winter weather pattern popularly known as the polar vortex—an area of upper-level low pressure that is nearly always present over the North and South Poles. Occasionally, the arctic vortex is displaced southward over eastern North America and becomes nearly stationary, bringing unusually cold weather to the eastern United States. While the sporadic southward displacement of the vortex is a natural feature of the winter climate, some recent years have featured unusually persistent patterns, resulting in episodes of extended cold and stormy weather in the eastern United States, notably in the winters of 2009–10, 2010–11, 2013–14, and 2014–15. A number of research studies have found empirical evidence of a link between cold winters and the fact that the Arctic is warming more rapidly than lower latitudes (a phenomenon referred to as arctic amplification). The current scientific consensus is that observed winter temperature trends, including the lack of recent warming in the eastern United States, cannot be explained without including the potential effects of Arctic warming (Cohen et al. 2020).
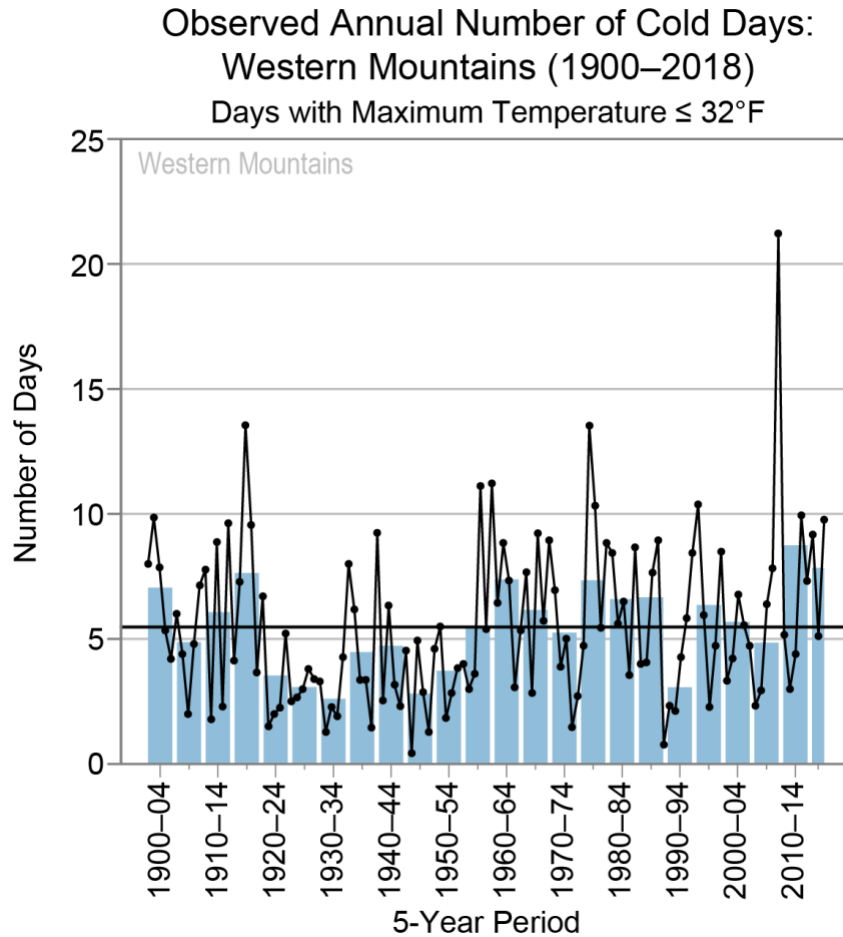
Figure 3.39. The bar graph shows the observed annual number of cold days (maximum temperature of 32°F or lower) for the Western Mountains of North Carolina for 1900–2018, as averaged over 5-year periods, with the last bar representing a 4-year period (2015–2018). Dots show annual values. The horizontal black line shows the long-term average of 5.5 cold days per year for 1900–2018. Sources: NCICS, NOAA NCEI, and the State Climate Office of North Carolina.

By the end of the century, the number of cold days is projected to decrease by 1–4 under the lower scenario and 3–5 under the higher scenario, compared to the 1996–2015 average. There has not been a strong trend in the number of cold nights (minimum temperature of 32°F or lower) in recent years. However, by the end of the century, the number of cold nights is projected to decrease by 8–31 under the lower scenario and 25–50 under the higher scenario.

Despite large year-to-year variability, the number of very cold nights (minimum temperature of 0°F or lower) has decreased in recent years, occurring on average less than once per year since 1997. Under the higher scenario, nights below 0°F are projected to be very rare or nonexistent by the end of the century (Figure 3.40).

The projected decrease in the number of cold days (Figure 3.40) is not consistent with the lack of an observed trend (Figure 3.39). As noted above, one reason for the lack of an observed trend is the recent occurrences of an unusually persistent southward-displaced polar vortex over eastern North America. However, there is no scientific consensus that continued polar warming will lead to an increase in polar vortex occurrences over eastern North America (Cohen et al. 2020). Thus, it is *likely* that the number of cold days and cold nights will eventually decrease.

Observed and Projected Cold Days and Nights: Western Mountains (1970–2100)

(a) Annual Days with Maximum Temperature ≤ 32°F

(b) Annual Days with Minimum Temperature ≤ 32°F
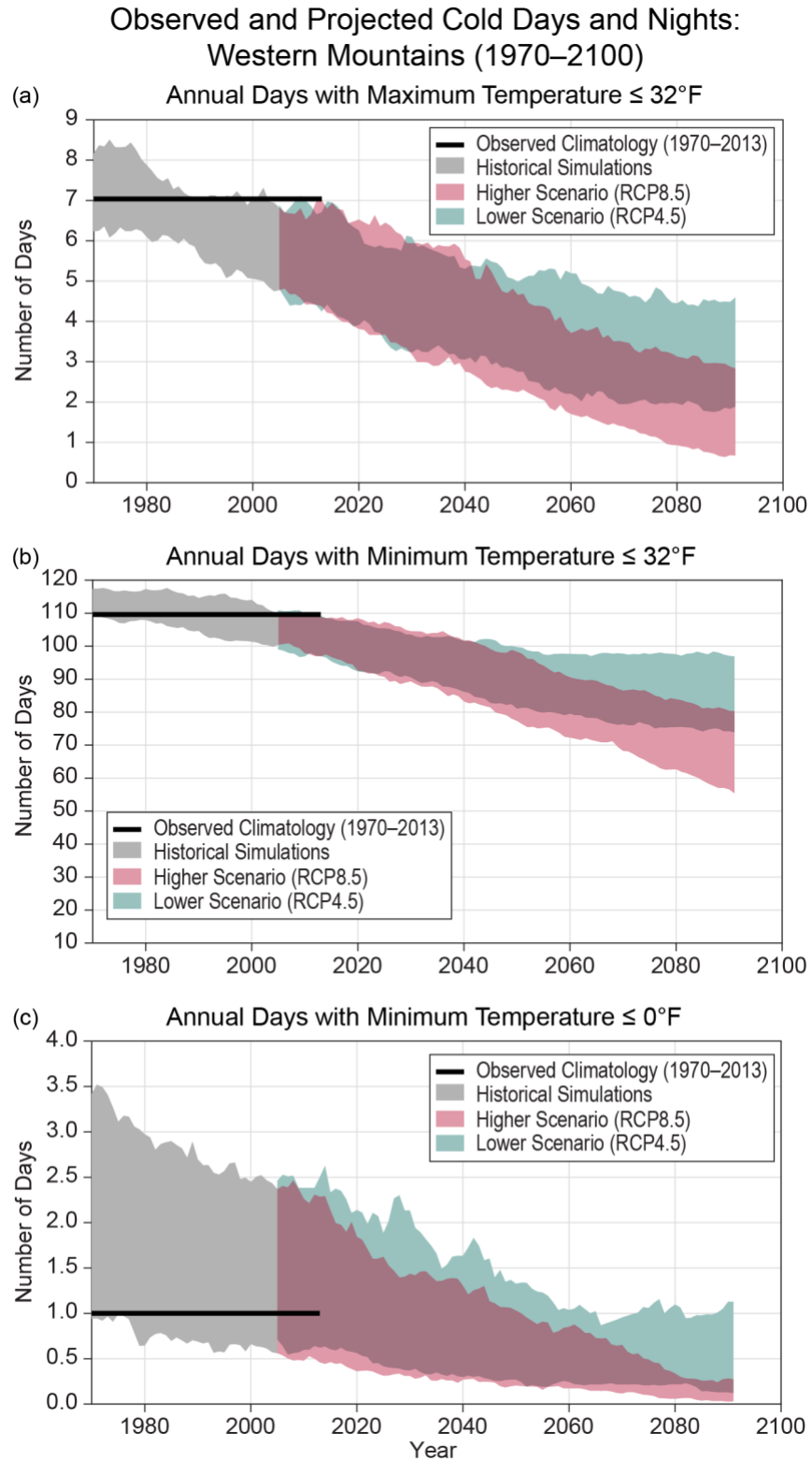
(c) Annual Days with Minimum Temperature ≤ 0°F

Figure 3.40. These time series show the simulated historical and projected number of days per year on which the (a) maximum temperature and (b) minimum temperature is 32°F or lower, and days on which (c) the minimum temperature is 0°F or lower for the Western Mountains of

North Carolina from the LOCA data and the observed climatological values averaged for the period 1970–2013 (black line). Historical simulations (gray shading) are shown for 1970–2005. Projected changes for 2006–2100 are shown for a higher scenario (RCP8.5; red shading) and a lower scenario (RCP4.5; green shading). The shaded ranges indicate the 10% to 90% confidence intervals of 20-year running averages from the set of climate models. Sources: NCICS and The University of Edinburgh.

3.4.4 Annual Hottest / Coldest Temperatures

Since 1970, there has been no strong trend in the annual hottest temperatures averaged over the Western Mountains region, but there has been an increase in the annual coldest temperatures. By the end of the century, the annual hottest temperature is projected to increase by 2°–9°F under the lower scenario and 4°–15°F under the higher scenario, compared to the 1996–2015 average. The annual coldest temperature is projected to increase by 0°–8°F under the lower scenario and 7°–12°F under the higher scenario (Figure 3.41).

The projections for increases in annual coldest temperature are consistent with recent observations. Because of this consistency, it is *very likely* that the model-projected increases in annual coldest temperature will occur. However, the projected increase in annual hottest temperature is not consistent with the lack of an observed trend. Since the causes of the lack of an increase in annual hottest temperature are not yet fully understood, our level of confidence in the projections is lessened. However, summers have become warmer, and that warming is projected to continue. Thus, it is *likely* that the annual hottest temperature will eventually increase.

Observed and Projected Maximum and Minimum Temperatures: Western Mountains (1970–2100)
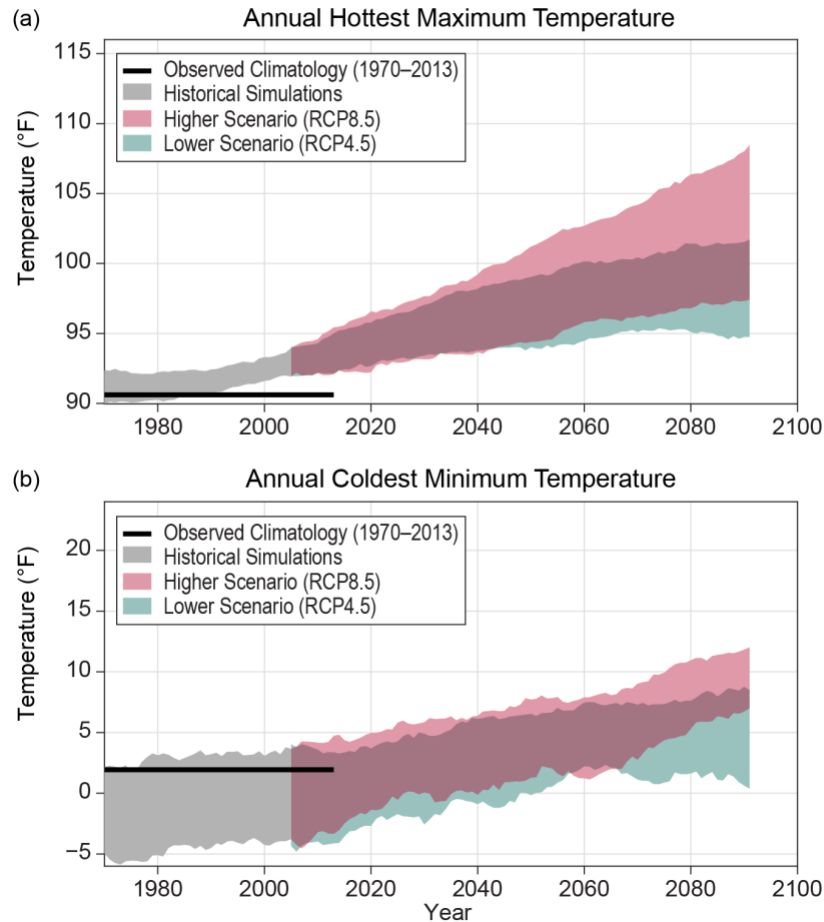

Figure 3.41. These time series show the simulated historical and projected (a) hottest maximum and (b) coldest minimum temperatures each year averaged over the Western Mountains of North Carolina from the LOCA data and the observed climatological values averaged for the period 1970–2013 (black line). Historical simulations (gray shading) are shown for 1970–2005. Projected changes for 2006–2100 are shown for a higher scenario (RCP8.5; red shading) and a lower scenario (RCP4.5; green shading). The shaded ranges indicate the 10% to 90% confidence intervals of 20-year running averages from the set of climate models. Sources: NCICS and The University of Edinburgh.

3.4.5 Heating and Cooling Degree Days

The term "heating degree days" (HDDs) refers to the number of degrees that a day's average temperature is below 65°F, while "cooling degree days" (CDDs) refers to the number of degrees that the average temperature is above 65°F. These metrics are used to quantify the energy needed to heat or cool buildings and houses. HDDs and CDDs in the Western Mountains have varied in concert with the region's annual average temperature. As average temperature (Figure 3.34)

152

increased in the first half of the 20th century, HDDs (Figure 3.42) decreased, reaching a relative minimum around mid-century, while CDDs (Figure 3.43) exhibited little overall trend. HDDs then increased to relatively higher values by the 1960s, as the region's average temperature and CDDs reached their lowest values in decades. Coincident with an upward trend in annual average temperature, there has been a decreasing trend in HDDs since the 1980s, and all but three years have been below the long-term average since 2000. At the same time, there has been an increasing trend in CDDs, with the highest values on record occurring since 2010.

Overall warming is projected to lead to decreases in HDDs and increases in CDDs in the Western Mountains (Figure 3.44). This indicates a decrease in energy needed for heating and an increase in energy needed for cooling. By the end of the century, HDDs are projected to decrease by 400–1,200 under the lower scenario and 1,000–1,900 under the higher scenario, compared to the 1996–2015 average. CDDs are projected to increase by 200–900 under the lower scenario and 800–1,800 under the higher scenario. These trends are projected to continue throughout the century. These projections are consistent with recent trends. For this reason, it is ***very likely*** that HDDs will decrease and CDDs will increase in the future.
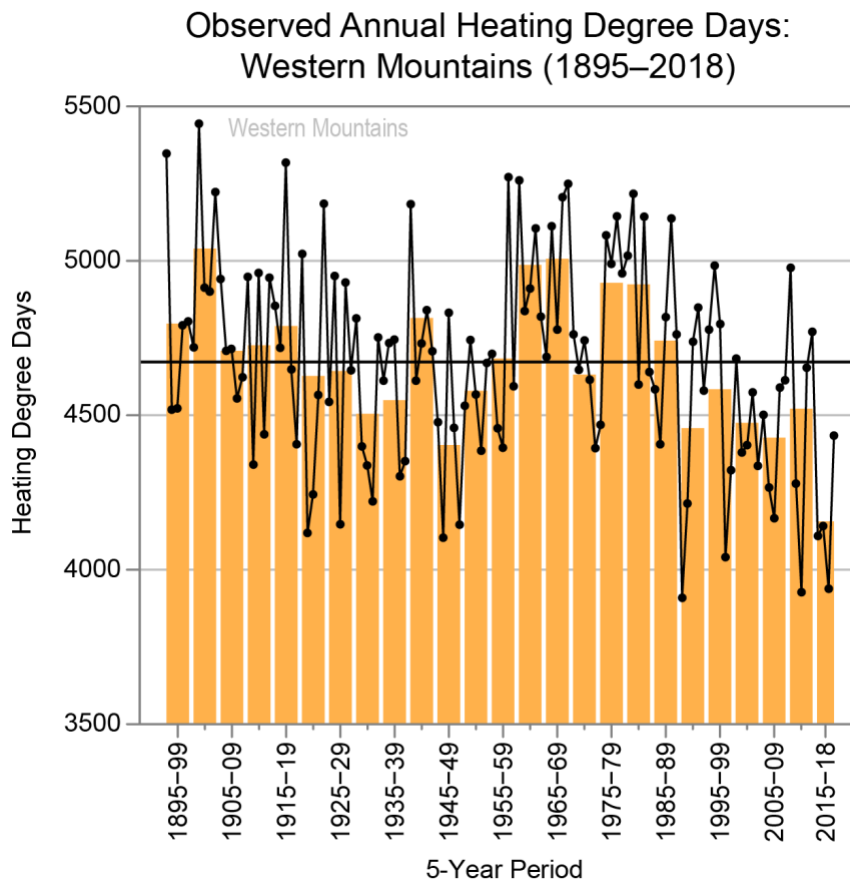

Figure 3.42. The bar graph shows the observed annual heating degree days for the Western Mountains of North Carolina for 1895–2018, as averaged over 5-year periods, with the last bar representing a 4-year period (2015–2018). Dots show annual values. The horizontal black line

shows the long-term average of 4,670 heating degree days per year for 1895–2018. There has been a decreasing trend in heating degree days since the 1980s, and all but three years have been below the long-term average since 2000. Sources: NCICS, NOAA NCEI, and the State Climate Office of North Carolina.
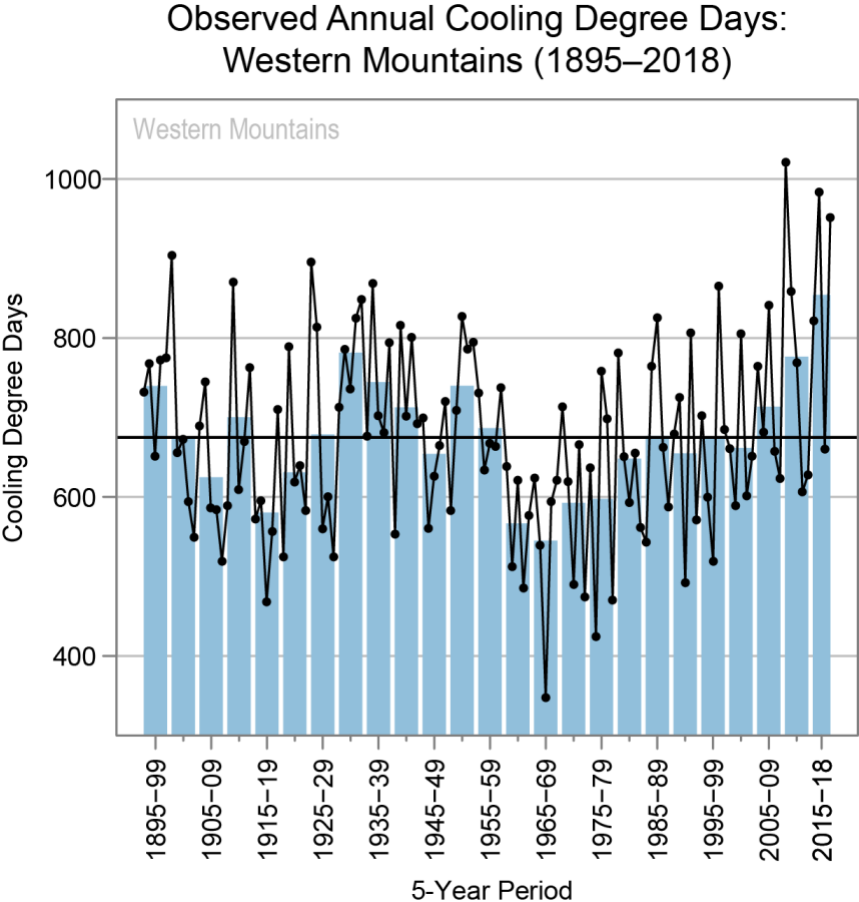

Figure 3.43. The bar graph shows the observed annual cooling degree days for the Western Mountains of North Carolina for 1895–2018, as averaged over 5-year periods, with the last bar representing a 4-year period (2015–2018). Dots show annual values. The horizontal black line shows the long-term average of 675 cooling degree days per year for 1895–2018. There has been an increasing trend in cooling degree days since the 1990s, and the highest values on record have occurred since 2010. Sources: NCICS, NOAA NCEI, and the State Climate Office of North Carolina.

Observed and Projected Heating and Cooling Degree Days: Western Mountains (1970–2100)
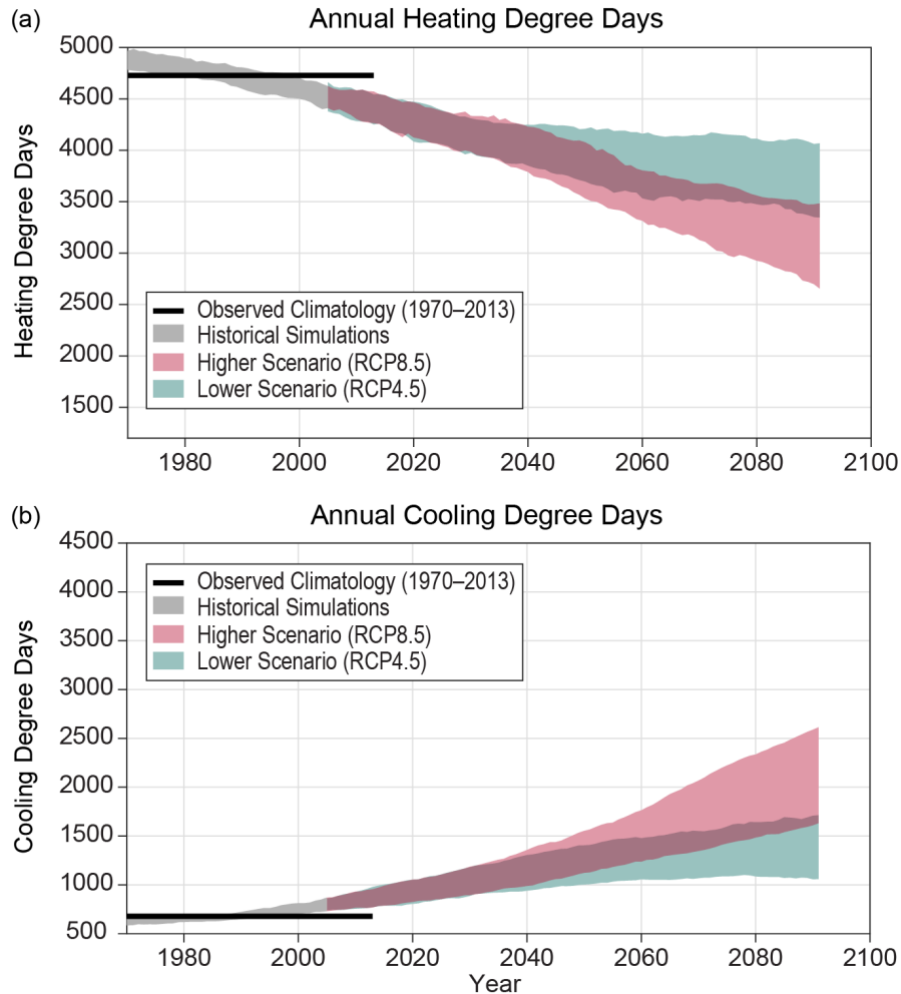

Figure 3.44. These time series show simulated historical and projected values for (a) annual heating degree days and (b) annual cooling degree days for the Western Mountains of North Carolina from the LOCA data and the observed climatological values averaged for the period 1970–2013 (black line). Historical simulations (gray shading) are shown for 1970–2005. Projected changes for 2006–2100 are shown for a higher scenario (RCP8.5; red shading) and a lower scenario (RCP4.5; green shading). The shaded ranges indicate the 10% to 90% confidence intervals of 20-year running averages from the set of climate models. Sources: NCICS and The University of Edinburgh.

3.4.6 Annual Precipitation

The Western Mountains of North Carolina tend to be the wettest of the three regions in the state, with a long-term average of about 54 inches of precipitation per year. Consistent with the other two regions, the 2015–2018 period was the wettest period on record for the Mountains (Figure 3.45). The Mt. Mitchell National Weather Service Cooperative Observer Network site measured

139.94 inches of precipitation in 2018, setting a new state record for the most precipitation at a single North Carolina weather station in a year. The 1950–1954 and 1985–1989 periods were the driest intervals for the region, with averages of about 49 inches per year, while 1925 was the driest year, with about 35 inches.
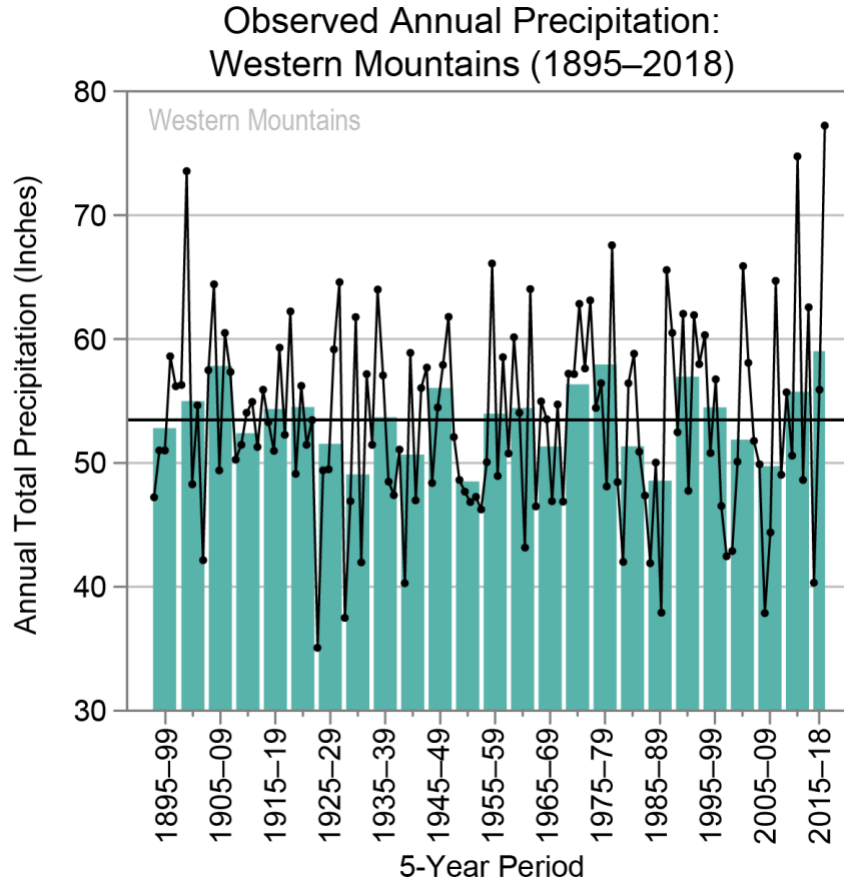

Figure 3.45. The bar graph shows the observed annual total precipitation for 1895–2018 for the Western Mountains of North Carolina, as averaged over 5-year periods, with the last bar representing a 4-year period (2015–2018). Dots show annual values. The horizontal black line shows the long-term average of 53.4 inches per year for 1895–2018. Sources: NCICS, NOAA NCEI, and the State Climate Office of North Carolina.

By the end of the century, climate models project a wide range of potential outcomes, from drier to wetter conditions. While the average of the model projections shows small increases in annual total precipitation compared to the current climate (see Figure 2.16), the models range from decreases of 1 inch to increases of 6 inches under the lower scenario and decreases of 2 inches to increases of 10 inches under the higher scenario, compared to the 1996–2015 average (Figure 3.46). Based on the greater number of models showing increases, it is *likely* that annual precipitation will increase.
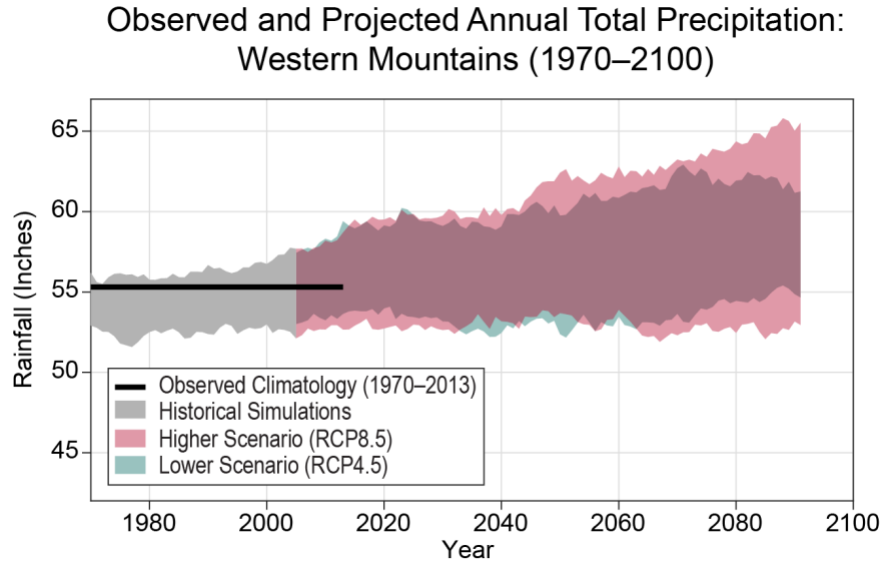
Observed and Projected Annual Total Precipitation: Western Mountains (1970–2100)

Figure 3.46. These time series show the simulated historical and projected annual total precipitation⬚ for the Western Mountains of North Carolina from the LOCA data and the observed climatological value averaged for the period 1970–2013 (black line). Historical simulations (gray shading) are shown for 1970–2005. Projected changes for 2006–2100 are shown for a higher scenario (RCP8.5; red shading) and a lower scenario (RCP4.5; green shading). The shaded ranges indicate the 10% to 90% confidence intervals of 20-year running averages from the set of climate models. Sources: NCICS and The University of Edinburgh.

3.4.7 Heavy Precipitation

Extreme precipitation is highly variable across the historical record, especially from year to year (Figure 3.47). Days with precipitation of 3 inches or more occur about 1 day per year on average in the Western Mountains. There is no observable trend in the historical record for extreme precipitation, but 3 years since 2010 ranked in the top 10.
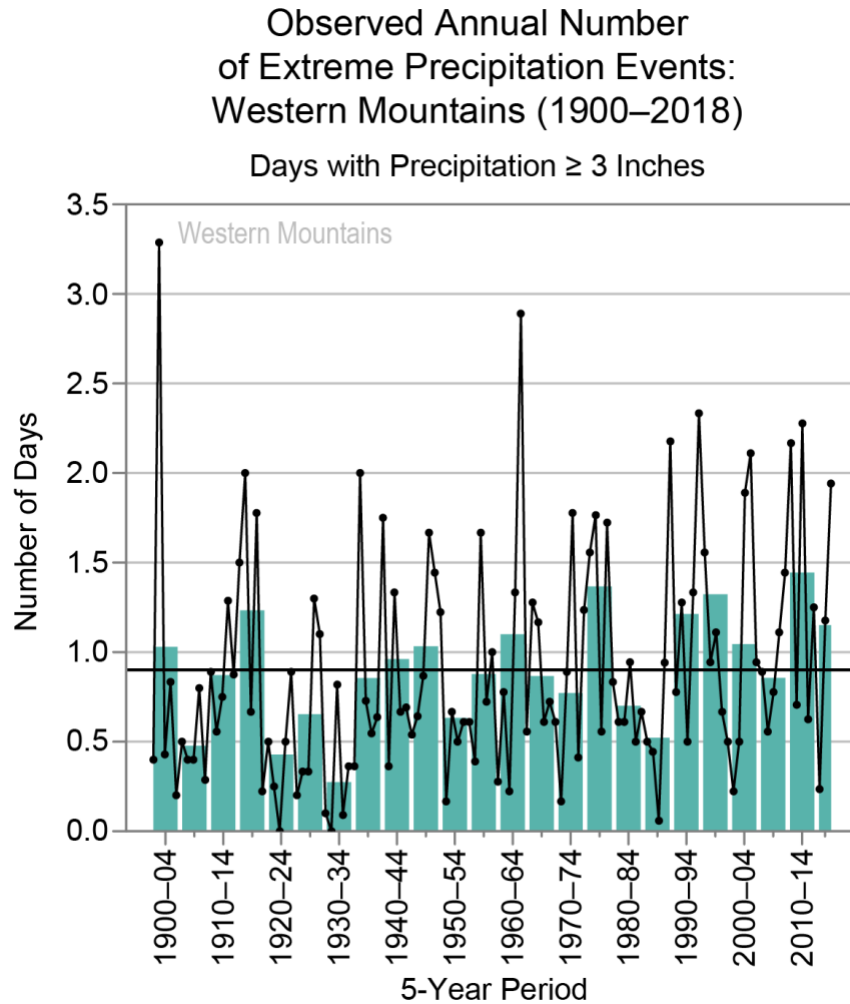
Figure 3.47. The bar graph shows the observed annual number of extreme precipitation events (days with precipitation of 3 inches or more) for the Western Mountains of North Carolina for 1900–2018, as averaged over 5-year periods, with the last bar representing a 4-year period (2015–2018). Dots show annual values. The horizontal black line shows the long-term average of 0.9 extreme precipitation days per year for 1900–2018. Sources: NCICS, NOAA NCEI, and the State Climate Office of North Carolina.

By the end of the century, climate models project a large range of potential changes. This large range is mainly a result of the random nature of extreme rainfall. However, the models show an overall increase in the number of extreme precipitation days in the Western Mountains region. By the end of the century, the annual number of days with precipitation of 3 inches or more is projected to increase by up to 0.3 (115%) under the lower scenario and by up to 0.6 (250%) under the higher scenario, compared to the 1996–2015 average (Figure 3.48). Note that the current value of 0.3 days per year from the Livneh dataset is lower than the station average of 0.9 days per year (Figure 3.47). The Livneh dataset consists of spatially averaged data, which have lower values of extreme rainfall.

Based on the virtual certainty that water vapor in the atmosphere will increase as global warming occurs, it is *very likely* that the risk of extreme precipitation will increase everywhere in the Mountains.
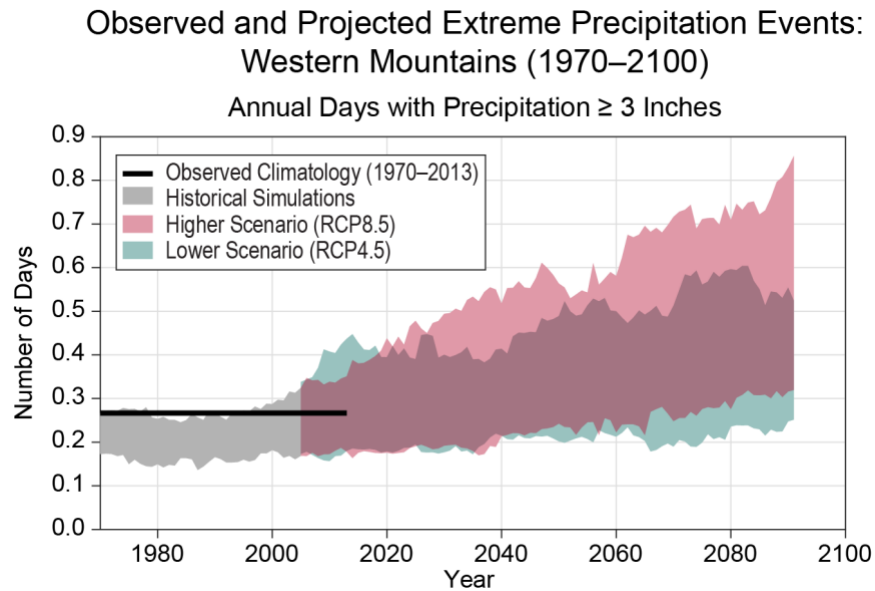

Figure 3.48. These time series show the simulated historical and projected annual number of days with precipitation of 3 inches or more⬚ for the Western Mountains of North Carolina from the LOCA data and the observed climatological value averaged for the period 1970–2013 (black line). Historical simulations (gray shading) are shown for 1970–2005. Projected changes for 2006–2100 are shown for a higher scenario (RCP8.5; red shading) and a lower scenario (RCP4.5; green shading). The shaded ranges indicate the 10% to 90% confidence intervals of 20-year running averages from the set of climate models. Source: NCICS and The University of Edinburgh.

3.4.8 Drought

Drought can be measured using the Palmer Drought Severity Index (PDSI), which uses temperature and precipitation data to calculate the severity of drought at a location by estimating the relative dryness. The values calculated for PDSI range from −10 (dry) to +10 (wet). This metric captures medium- to long-term drought in North Carolina and is used by water managers and climate scientists to quantify and compare droughts across recorded history. Figure 3.49 shows the number of months with PDSI value less than or equal to −2 (moderate, severe, or extreme drought). In the Western Mountains, 1985–1989 was the period with the highest number of months in moderate or more severe drought, with an average of about 6 months per year. The period of 2000–2009 also experienced a high frequency of drought, with an average of 5 months per year.
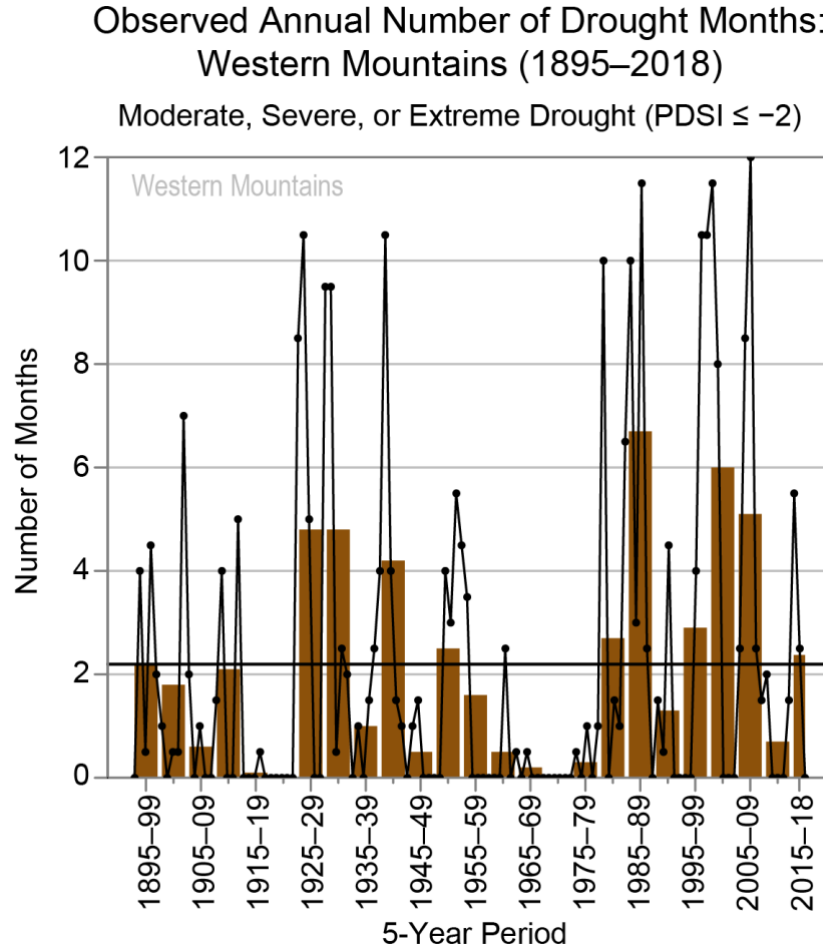
Observed Annual Number of Drought Months: Western Mountains (1895–2018)

Moderate, Severe, or Extreme Drought (PDSI ≤ −2)

Figure 3.49. The bar graph shows the observed annual number of months in drought of moderate or worse severity (PDSI values less than or equal to −2) for the Western Mountains of North Carolina for 1895–2018, as averaged over 5-year periods, with the last bar representing a 4-year period (2015–2018). Dots show annual values. The horizontal black line shows the long-term average of 2.2 drought months per year for 1895–2018. Sources: NCICS, NOAA NCEI, and the State Climate Office of North Carolina.

Droughts are a natural part of the climate of North Carolina. Future droughts are projected to be warmer than historical events with a high level of confidence. The warmer conditions will lead to more rapid drying through increases in potential evapotranspiration. Thus, it is *likely* that future droughts will be more severe in terms of soil moisture deficits and the impacts on rainfed agriculture and natural vegetation.

3.4.9 Winter Storms

Winter storms are large areas of low pressure in the middle and high latitudes that are primarily distinguished by fronts separating warm and cold air masses. They often cause various types of adverse weather conditions, such as strong winds and precipitation of various types, including snow and ice. This section discusses winter storms of all types, while the following two

subsections discuss the specific instances of storms causing snow and ice.

Winter storm tracks have shifted slightly northward (by about 0.4 degrees latitude) in recent decades over the Northern Hemisphere (Bender et al. 2012). More generally, winter storm activity is projected to change in complex ways under future climate scenarios, with increases in some regions and seasons and decreases in others. The Arctic is warming more quickly than lower latitudes (i.e., arctic amplification), due in part to sea ice loss. This reduces the lower-atmosphere temperature difference between the Arctic and the lower latitudes—this difference is an important energy source for winter storms. At the same time, the temperature difference higher up in the atmosphere is projected to increase due to a warming tropical upper troposphere and a cooling high-latitude lower stratosphere.

While these two effects counteract each other with respect to a projected change in midlatitude storm tracks, the simulations indicate that the magnitude of arctic amplification may modulate some aspects (e.g., jet stream position, wave extent, and blocking frequency) of the circulation in the North Atlantic region in some seasons (Barnes and Polvani 2015).

Regional studies of trends in cyclones are challenged to provide definitive results regarding changes in the frequency or intensity of storms, but regardless of these properties, it is ***very likely*** that cyclones of even similar intensity will produce heavier precipitation (e.g., Marciano et al. 2015, Michaelis et al. 2017). Also, with rising sea levels, coastal flooding from cyclones is ***very likely*** to increase (e.g., Colle et al. 2015, Zhang and Colle 2018, Roberts et al. 2017).

Based on the available evidence, our conclusion is that there is ***low confidence*** concerning future changes in the number of winter storms.

3.4.9.1 Snowstorms and Snow Cover
In western North Carolina, winter precipitation often falls as snow at higher elevations but as rain at lower elevations, where temperatures are above freezing near the surface. The foothills and mountain regions have exhibited a long-term decline in winter temperatures from 1910–2017 (Eck et al. 2019). A recent analysis of Western Mountains snowfall found non-significant trends over the period 1910–2017 (Eck et al. 2019). However, an examination of the last 50 years indicates decreasing trends at many stations, particularly those located in the southern portion of the Western Mountains. Snowfall and anomalously low temperatures are favored by large-scale modes of climate variability, particularly the simultaneous occurrence of El Niño and the negative phase of the North Atlantic Oscillation (Eck et al. 2019).

The Fourth National Climate Assessment projects large winter warming under both moderate and higher emissions scenarios. Consistent with the projected warming, a northward shift in the rain–snow transition zone in the central and eastern United States is projected under a higher emissions scenario. By the end of the 21st century, large areas that are currently snow dominated in the cold season are expected to be rain dominated (Krasting et al. 2013, Ning and Bradley 2015). For western North Carolina, the frequency of snowfall is projected to decrease substantially, with snowfall increasingly confined to the higher elevations.

As noted earlier, a definitive understanding of the effects of arctic amplification on midlatitude winter weather remains elusive. Cohen et al. 2020 suggest a linkage between such episodes and enhanced Arctic warming (referred to as arctic amplification), and this adds some uncertainty to future projections of winter climate in North Carolina. Current global climate models (CMIP5) do predict an increase in the frequency of winter storms over the eastern United States, including the most intense storms, under the higher emissions scenario (Colle et al. 2013). However, there are large model-to-model differences in the realism of historical simulations and in the projected changes. Even if there were increases in the frequency or intensity of winter storms, the effects of warmer winters would nevertheless lead to decreases in average annual snowfall.

Another consequence of warming, however, is an expected increase in precipitation intensity. Thus, for events where air is sufficiently cold for precipitation to fall as snow, heavier totals could occur in the coming decades, before more extensive warming leads to only rare snowfall (O'Gorman 2014). However, an increase in heavy snow with warming only occurs with average temperatures colder than what occurs anywhere in North Carolina, including the mountains.

The higher elevations of the North Carolina mountains and even valley locations in counties along the Tennessee border receive substantial snowfall each year during periods of low-level wind flow from the northwest (Keighton et al. 2009). These northwest flow snow (NWFS) events frequently are associated with moisture transport extending downwind from the Great Lakes and are therefore sensitive to ice cover on the lakes (Perry et al. 2007). Ice cover effectively shuts off evaporation from the surfaces of the Great Lakes, resulting in considerably less low-level moisture downwind of the lakes. Model simulations suggest that snowfall may increase downwind of the Great Lakes in the coming decades due to rising temperatures and decreasing seasonal ice cover (Gula and Peltier 2012). Therefore, it is possible that higher-elevation locations along the Tennessee border may see an increase in NWFS, provided temperatures in the lower atmosphere remain sufficiently cold for snow formation.

Although snow generally melts within a few days after a snowstorm in most parts of the state, it is not uncommon for snow to persist for weeks or longer in the higher elevations of the Western Mountains. In fact, at the highest elevations above 5,000 feet, snow may cover the ground nearly continuously some years from late fall through early spring, as was observed during the recent 2009–10 and 2013–14 snow seasons (Martin et al. 2015). The amount of water stored in the snowpack—known as the snow water equivalent (SWE)—increases with snow depth. High values of SWE increase the flood threat during rapid melting, particularly when rain falls on snow-covered ground. Nearly all model simulations suggest that future snow cover duration and SWE will decrease in the middle latitudes as a result of warming and reductions in snowfall (Collins et al. 2013). Therefore, it is *likely* that snow cover lasting more than a few days will increasingly be limited to the highest elevations above 5,000 feet in the coming decades.

Based on the projected increase in temperature, it is ***very likely*** that total snowfall will decrease. It is *likely* that the number of heavy snowstorms will decrease.

3.4.9.2 Ice Storms

Ice storms occur within winter storms, the same as for snowstorms. However, icing requires a specific combination of weather conditions, most importantly precipitating conditions with a below-freezing layer near the surface and an above-freezing layer above the low-level freezing layer. In this situation, snow falling from high levels melts as it falls through the above-freezing layer; it then becomes super-cooled liquid drops while falling through the near-surface freezing layer and freezes on contact with cold surface objects.

The accurate simulation of this weather feature by climate models is challenging because the vertical extent of the below-freezing and above-freezing layers is often quite small and thus non-resolvable by the current generation of climate models. Also, the horizontal resolution in models is insufficient to capture the fine spatial detail of ice-producing conditions. As a result, research on future changes in ice storm frequency and intensity is limited, and the recent Fourth National Climate Assessment did not make any statements on this weather phenomenon.

Freezing rain takes place when a layer of warm air moves over the shallow cold air near the surface, such as during cold-air damming. With warming, it may be easier for these warm layers to develop, and at least one study linked a North Carolina ice storm to warm offshore waters (Ramos de Silva et al. 2006). Thus, it is possible that warming could result in an increase of these warm layers, increasing freezing rain occurrence.

Another important aspect of freezing rain is the soil and ground temperature. Sub-freezing soil temperatures will become less frequent in a warming climate. This factor would serve to decrease the frequency and severity of freezing rain in a warmer climate.

Taken together, the preceding discussion demonstrates that there is considerable uncertainty in projected changes in freezing rain in a warming climate, and more research is needed. Given the evidence currently available, our conclusion is that there is ***low confidence*** concerning future changes in the number of ice storms.

3.4.10 Thunderstorms and Tornadoes

Tornado and severe thunderstorm events cause significant loss of life and property: more than one-third of the $1 billion weather disasters in the United States during the past 25 years were due to such events, and, relative to other extreme weather, the damages from convective weather hazards have undergone the largest increase since 1980 (Smith and Katz 2013).

A particular challenge in quantifying the existence and intensity of these events arises from the data source: rather than measurements, the occurrence of tornadoes and severe thunderstorms is determined by visual sightings by eyewitnesses (such as "storm spotters" and law enforcement officials) or post-storm damage assessments. The reporting has been susceptible to changes in population density, modifications to reporting procedures and training, the introduction of video and social media, and so on. These have led to systematic, non-meteorological biases in the long-term data record.

163

Nonetheless, judicious use of the report database has revealed important information about tornado trends. Since the 1970s, the United States has experienced a decrease in the number of days per year on which tornadoes occur but an increase in the number of tornadoes that form on such days. One important implication is that the frequency of days with large numbers of tornadoes—tornado outbreaks—appears to be increasing (Figure 9.3 in Kossin et al. 2017). The length of the season over which such tornado activity occurs is increasing as well: although tornadoes in the United States are observed in all months of the year, an earlier calendar-day start to the season of high activity is emerging. In general, there is more interannual variability, or volatility, in tornado occurrence (Elsner et al. 2015, Tippett, 2014).

Evaluations of hail and (non-tornadic) thunderstorm wind reports have thus far been less revealing. Although there is evidence of an increase in the number of hail days per year, the inherent uncertainty in reported hail size reduces the confidence in such a conclusion. Thunderstorm wind reports have proven to be even less reliable because, as compared to tornadoes and hail, there is less tangible visual evidence; thus, although the United States has lately experienced several significant thunderstorm wind events (sometimes referred to as derechos), the lack of studies that explore long-term trends in wind events and the uncertainties in the historical data preclude any robust assessment.

It is possible to bypass the use of reports by exploiting the fact that the temperature, humidity, and wind in the larger vicinity—or "environment"—of a developing thunderstorm ultimately control the intensity, structure, and hazardous tendency of the storm. Thus, the premise is that measures of temperature, humidity, and wind at various heights throughout the atmosphere can be used as a proxy for actual severe thunderstorm occurrence. In particular, a measure of the energy available for convection (known as convective available potential energy or CAPE) and vertical wind shear (a change in wind speed or direction with change in altitude) constitutes one widely used means of representing the frequency of severe thunderstorms. This environmental-proxy approach avoids the biases and other issues with eyewitness storm reports and is readily evaluated using the relatively coarse global datasets and global climate models. It has the disadvantage of assuming that a thunderstorm will necessarily form and then realize its environmental potential.

Global climate models consistently project an increase in the frequency of severe thunderstorm environments in the United States over the mid- to late 21st century. The most robust projected increases in frequency are over the U.S. Midwest and Southern Great Plains, during spring (March–May). Based on the increased frequency of very high CAPE, increases in storm intensity are also projected over this same period (Del Genio et al. 2007).

Key limitations of the environmental-proxy approach are being addressed through the applications of high-resolution dynamical downscaling, wherein sufficiently fine model grids are used so that individual thunderstorms are explicitly represented, rather than implicitly represented (as through environmental proxies). The individually modeled thunderstorms can then be quantified and assessed in terms of severity (e.g., Trapp et al. 2011). Prein et al. (2017)

used a convection-permitting model to examine changes in intense hourly precipitation in the central United States, finding an increase in the most intense events and a decrease in lighter events. The dynamical-downscaling results have thus far supported the basic findings of the environmental-proxy studies, particularly in terms of the seasons and geographical regions projected to experience the largest increases in severe thunderstorm occurrence.

Based on these studies, we conclude it is *likely* that severe thunderstorms in the Western Mountains of North Carolina will increase in frequency.

3.5. References

Barnes, E.A., E. Dunn-Sigouin, G. Masato, and T. Woollings, 2014: Exploring recent trends in Northern Hemisphere blocking. *Geophysical Research Letters,* **41** (2), 638–644. http://dx.doi.org/10.1002/2013GL058745

Barnes, E.A. and L.M. Polvani, 2015: CMIP5 projections of Arctic amplification, of the North American/North Atlantic circulation, and of their relationship. *Journal of Climate,* **28** (13), 5254–5271. http://dx.doi.org/10.1175/JCLI-D-14-00589.1

Bender, F.A.-M., V. Ramanathan, and G. Tselioudis, 2012: Changes in extratropical storm track cloudiness 1983–2008: Observational support for a poleward shift. *Climate Dynamics,* **38** (9), 2037–2053. http://dx.doi.org/10.1007/s00382-011-1065-6

Cohen, J., X. Zhang, J. Francis, T. Jung, R. Kwok, J. Overland, T.J. Ballinger, U.S. Bhatt, H.W. Chen, D. Coumou, S. Feldstein, H. Gu, D. Handorf, G. Henderson, M. Ionita, M. Kretschmer, F. Laliberte, S. Lee, H.W. Linderholm, W. Maslowski, Y. Peings, K. Pfeiffer, I. Rigor, T. Semmler, J. Stroeve, P.C. Taylor, S. Vavrus, T. Vihma, S. Wang, M. Wendisch, Y. Wu, and J. Yoon, 2020: Divergent consensuses on Arctic amplification influence on midlatitude severe winter weather. *Nature Climate Change,* **10** (1), 20–29. http://dx.doi.org/10.1038/s41558-019-0662-y

Colle, B.A., Z. Zhang, K.A. Lombardo, E. Chang, P. Liu, and M. Zhang, 2013: Historical evaluation and future prediction of eastern North American and western Atlantic extratropical cyclones in the CMIP5 models during the cool season. *Journal of Climate,* **26** (18), 6882–6903. http://dx.doi.org/10.1175/JCLI-D-12-00498.1

Colle, B.A., J.F. Booth, and E.K.M. Chang, 2015: A review of historical and future changes of extratropical cyclones and associated impacts along the US East Coast. *Current Climate Change Reports,* **1** (3), 125–143. http://dx.doi.org/10.1007/s40641-015-0013-7

Collins, M., R. Knutti, J. Arblaster, J.-L. Dufresne, T. Fichefet, P. Friedlingstein, X. Gao, W.J. Gutowski, T. Johns, G. Krinner, M. Shongwe, C. Tebaldi, A.J. Weaver, and M. Wehner, 2013: Long-term climate change: Projections, commitments and irreversibility. *Climate Change 2013: The Physical Science Basis. Contribution of Working Group I to the Fifth Assessment Report of the Intergovernmental Panel on Climate Change*. Stocker, T.F., D. Qin, G.-K. Plattner, M. Tignor, S.K. Allen, J. Boschung, A. Nauels, Y. Xia, V. Bex, and P.M. Midgley, Eds. Cambridge University Press, Cambridge, United Kingdom and New York, NY, USA, 1029–1136. https://www.ipcc.ch/report/ar5/wg1/

Del Genio, A.D., M.S. Yao, and J. Jonas, 2007: Will moist convection be stronger in a warmer climate? *Geophysical Research Letters,* **34** (16), L16703. http://dx.doi.org/10.1029/2007GL030525

Eck, M.A., L.B. Perry, P.T. Soulé, J.W. Sugg, and D.K. Miller, 2019: Winter climate variability in the southern Appalachian Mountains, 1910–2017. *International Journal of Climatology,* **39** (1), 206–217. http://dx.doi.org/10.1002/joc.5795

Elsner, J.B., S.C. Elsner, and T.H. Jagger, 2015: The increasing efficiency of tornado days in the United States. *Climate Dynamics,* **45** (3), 651–659. http://dx.doi.org/10.1007/s00382-014-2277-3

Gula, J. and W. Peltier, 2012: Dynamical downscaling over the Great Lakes Basin of North America using the WRF regional climate model: The impact of the Great Lakes system on regional greenhouse warming. *Journal of Climate,* **25**, 7723–7742. http://dx.doi.org/10.1175/JCLI-D-11-00388.1

Keighton, S., L. Lee, B. Holloway, D. Hotz, S. Zubrick, J. Hovis, G. Votaw, L.B. Perry, G. Lackmann, S.E. Yuter, C. Konrad, D. Miller, and B. Etherton, 2009: A collaborative approach to study northwest flow snow in the southern Appalachians. *Bulletin of the American Meteorological Society,* **90** (7), 979–992. http://dx.doi.org/10.1175/2009BAMS2591.1

Kossin, J.P., T. Hall, T. Knutson, K.E. Kunkel, R.J. Trapp, D.E. Waliser, and M.F. Wehner, 2017: Extreme storms. *Climate Science Special Report: Fourth National Climate Assessment, Volume I*. Wuebbles, D.J., D.W. Fahey, K.A. Hibbard, D.J. Dokken, B.C. Stewart, and T.K. Maycock, Eds. U.S. Global Change Research Program, Washington, DC, USA, 257–276. http://dx.doi.org/10.7930/J07S7KXX

Krasting, J.P., A.J. Broccoli, K.W. Dixon, and J.R. Lanzante, 2013: Future changes in Northern Hemisphere snowfall. *Journal of Climate,* **26** (20), 7813–7828. http://dx.doi.org/10.1175/JCLI-D-12-00832.1

Kunkel, K.E., M. Palecki, L. Ensor, K.G. Hubbard, D. Robinson, K. Redmond, and D. Easterling, 2009: Trends in twentieth-century U.S. snowfall using a quality-controlled dataset. *Journal of Atmospheric and Oceanic Technology,* **26**, 33–44. http://dx.doi.org/10.1175/2008JTECHA1138.1

Marciano, C.G., G.M. Lackmann, and W.A. Robinson, 2015: Changes in U.S. East Coast Cyclone Dynamics with Climate Change. *Journal of Climate,* **28** (2), 468–484. https://doi.org/10.1175/JCLI-D-14-00418.1

Martin, D.T., L.B. Perry, D.K. Miller, and P.T. Soulé, 2015: Snowfall event characteristics from a high-elevation site in the Southern Appalachian Mountains, USA. *Climate Research,* **63** (3), 171–190. https://www.int-res.com/abstracts/cr/v63/n3/p171-190/

Michaelis, A., J. Willison, G. Lackmann, and W. Robinson, 2017: Changes in winter North Atlantic extratropical cyclones in high-resolution regional pseudo-global warming simulations. **30** (17), 6905–6925. http://dx.doi.org/10.1175/JCLI-D-16-0697.1

Ning, L. and R.S. Bradley, 2015: Snow occurrence changes over the central and eastern United States under future warming scenarios. *Scientific Reports,* **5**, 17073. http://dx.doi.org/10.1038/srep17073

O'Gorman, P.A., 2014: Contrasting responses of mean and extreme snowfall to climate change. *Nature,* **512** (7515), 416–418. http://dx.doi.org/10.1038/nature13625

Perry, L.B., C.E. Konrad, and T.W. Schmidlin, 2007: Antecedent upstream air trajectories associated with northwest flow snowfall in the southern Appalachians. *Weather and Forecasting,* **22** (2), 334–352. http://dx.doi.org/10.1175/waf978.1

Prein, A.F., C. Liu, K. Ikeda, S.B. Trier, R.M. Rasmussen, G.J. Holland, and M.P. Clark, 2017: Increased rainfall volume from future convective storms in the US. **7** (12), 880–884. http://dx.doi.org/10.1038/s41558-017-0007-7

Roberts, K.J., B.A. Colle, and N. Korfe, 2017: Impact of simulated twenty-first-century changes in extratropical cyclones on coastal flooding at the Battery, New York City. *Journal of Applied Meteorology and Climatology,* **56** (2), 415–432. http://dx.doi.org/10.1175/JAMC-D-16-0088.1

Smith, A.B. and R.W. Katz, 2013: U.S. billion-dollar weather and climate disasters: Data sources, trends, accuracy and biases. *Natural Hazards,* **67** (2), 387–410. http://dx.doi.org/10.1007/s11069-013-0566-5

Tippett, M.K., 2014: Changing volatility of U.S. annual tornado reports. *Geophysical Research Letters,* **41** (19), 6956–6961. http://dx.doi.org/10.1002/2014GL061347

Trapp, R.J., E.D. Robinson, M.E. Baldwin, N.S. Diffenbaugh, and B.R.J. Schwedler, 2011: Regional climate of hazardous convective weather through high-resolution dynamical downscaling. *Climate Dynamics,* **37** (3), 677–688. http://dx.doi.org/10.1007/s00382-010-0826-y

Zhang, Z. and B.A. Colle, 2018: Impact of dynamically downscaling two CMIP5 models on the historical and future changes in winter extratropical cyclones along the East Coast of North America. *Journal of Climate,* **31** (20), 8499–8525. http://dx.doi.org/10.1175/JCLI-D-18-0178.1

4. Sea Level Rise and Coastal Water Levels

4.1. Introduction

North Carolina has many square miles of coastal land within a few feet of sea level, making it highly susceptible to inundation from the coastal ocean (Figure 4.1). At any given location and time, water level and, thus, inundation are determined by the area's coastal structure, astronomical (tidal) and meteorological (wind, atmospheric pressure, and precipitation) effects, and oceanic phenomena, primarily the global average sea level. The interaction of climate change with all of these factors will ultimately control coastal water levels in the future, and moderate differences can be expected along North Carolina's coast.

Depending on the rate of greenhouse gas emissions, global average sea level is projected to increase by 1.3–2.4 feet (moderate emissions scenario) to 2.0–3.6 feet (higher emissions scenario) by 2100 (IPCC 2019). Under both scenarios, many areas along the North Carolina coast will be impacted by high tide flooding on a near daily basis by 2100. Studies of storm-driven water levels show substantial changes in the future probability of these events as well. For example, under the higher emissions scenario, storm-driven water levels having a 1% chance of occurring each year in the beginning of the 21st century may have as much as a 30%–100% chance of occurring each year in the latter part of the century. A summary of the physical and geological processes contributing to water levels along the North Carolina coast follows.

4.2. Coastal Structure

North Carolina's Coastal Plain is often described as having two primary provinces: a northern province (Figure 4.1, Zone 2) and a southern province (Figure 4.1, Zone 1). The northern and southern provinces are divided by the Cape Lookout High, or Neuse Arch (Figure 4.1, Zone 3), which functions as a transition between Zones 1 and 2 (Sohl and Owens 1991; Riggs et al. 1995; Riggs 2002).
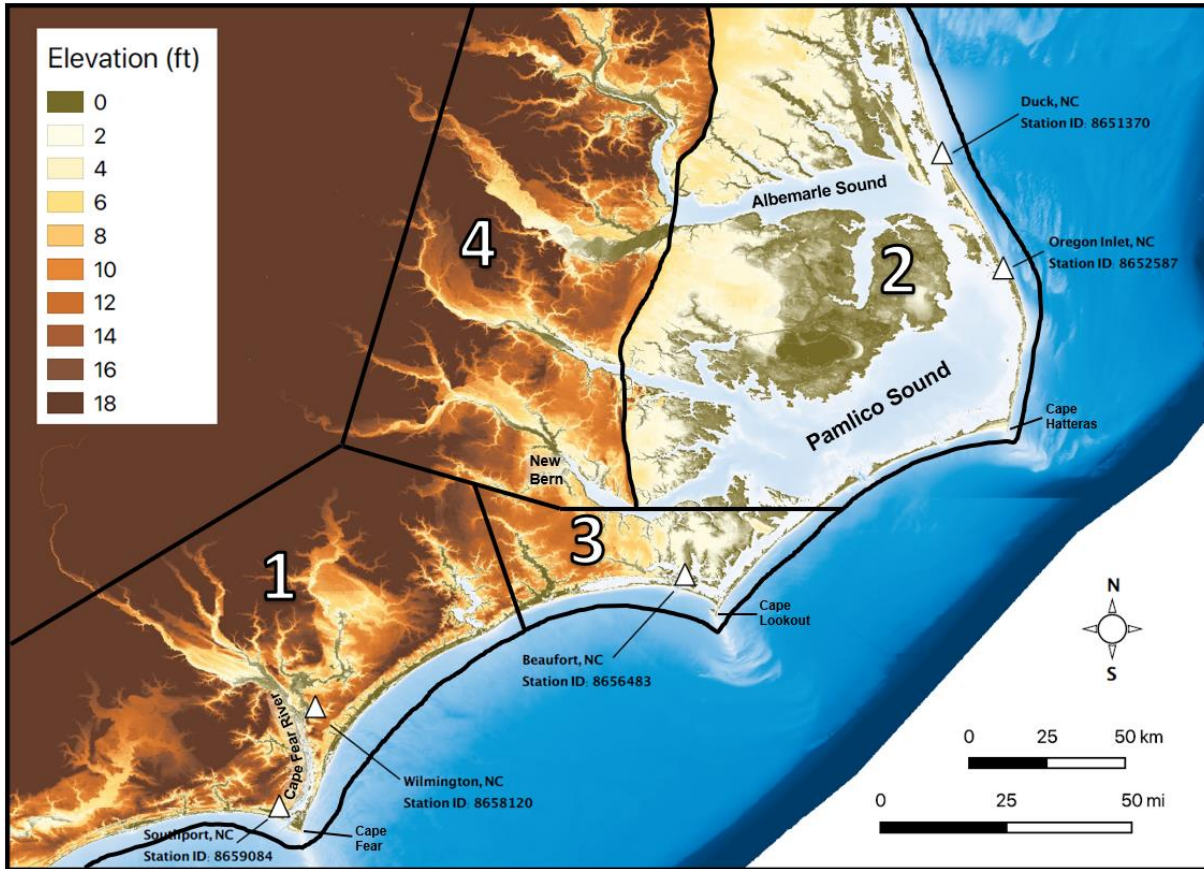
Figure 4.1. The map shows elevation across coastal North Carolina, demonstrating significant differences between the northern (Zone 2) and southern (Zone 1) provinces. Delineation of Zones 1–4 is based on geologic variations of uplift (raising of land) and subsidence (sinking of land) across coastal North Carolina. Source: adapted from N.C. Coastal Resources Commission Science Panel, 2015.

The distinct geology of each province produces quite different coastal zones. The southern province has common exposures of older rock units along the shoreline and steeper land slopes (average 3 feet/mile). This geologic framework produces about 18 short barrier islands with 18 established inlets and narrow back-barrier estuaries (Riggs 2002, Riggs et al. 1995, 2011). The barrier islands are set back from the continental slope, yielding a relatively wide continental shelf. In contrast, the northern province is characterized by a gentle depositional topography with low land slopes (an average of 0.2 feet/mile), a broad coastal plain, and long, narrow islands that are located close to the continental slope and separated by only four established inlets (Riggs et al. 1995, 2011). Between the barrier islands and the mainland lies the very large, shallow, and semi-isolated Albemarle–Pamlico Estuarine System (Figure 4.1, Zone 2). Together with smaller connected sounds and estuaries, this forms the second largest estuarine system in the United States based on surface area.

The northern province, much of which is already very near sea level (Figure 4.1; note gray and white colors indicating an elevation of 0–2 feet), continues to experience relative subsidence (or sinking) of about 4 inches per century (Engelhart et al. 2009, 2011; Kemp et al. 2009, 2011), while the southern province experiences a relative rate of uplift of about 1 inch per century (van de Plassche et al. 2014). Although not directly measured, the central province around Cape Lookout is generally assumed to have subsidence rates between those of the northern and southern provinces.

4.3. Astronomical Tides

Astronomical tides are due to interactions among the gravitational fields of Earth, the sun, and the moon. These interactions vary over time according to the relative position of the three celestial bodies (Pugh 1987). Along North Carolina's outer coast, the associated rise and fall of the water level yields two high and low tides each day. The difference in water level between high and low tide is largely determined by the width of the adjacent continental shelf. The tidal range from Mean Lower Low Water (average height of the lowest tide) to Mean Higher High Water (average height of the highest tide) varies from 5.5 feet at Sunset Beach in the southeast to 3.7 feet at Duck in the northeast (NOAA 2020). A significant tidal signal extends up the Cape Fear Estuary, having a range of 4.7 feet at Wilmington, whereas the small and limited number of inlets substantially damp the tides inside North Carolina's northern sounds, yielding a tidal range of a few inches along the mainland shore (Luettich et al. 2002).

Although less familiar, tidal ranges also vary over longer periods. For example, "king tides" informally refer to the highest astronomical tides of the year and occur when the moon is closest to Earth (North Carolina King Tides Project 2020). In addition, tides vary over semi-annual, annual, 4.4-year, and 18.61-year cycles (Haigh et al. 2011; Ray and Merrifield 2019; Peng et al. 2019). The strongest of the interannual tides along the North Carolina coast has a 4.4-year cycle and will cause high tides to vary by approximately 5% over this period (Haigh et al. 2011, Ray and Merrifield 2019). These long-period tides can contribute to extreme sea level and enhanced coastal flood risk when close to their apex (Eliot 2010).

4.4. Storms, Storm Surge, and Extreme Precipitation

Water level along the North Carolina coast is influenced by extratropical cyclones (midlatitude low-pressure systems occurring most frequently during the cold season; see Chapter 2, Section 2.5.1) as well as tropical cyclones (tropical storms and hurricanes). "Nor'easters" are extratropical cyclones that typically occur within 100 miles of the Mid-Atlantic coast, having strong, sustained winds that blow from the northeast. These storms occur primarily between October and April, are often accompanied by heavy precipitation, and cause significant coastal inundation and erosion due to the prolonged time of impact. Duck, NC, experiences an average of 14.5 extratropical events per year having associated surge exceeding 1 foot (Munroe and Curtis 2017). Although extratropical storms occur more frequently, tropical cyclones are

typically stronger, and a single event can cause loss of life and extensive damage to property. North Carolina's coast experiences a hurricane an average of once every two to three years.

Extratropical and tropical storms cause storm surge, which is primarily driven by onshore winds and secondarily by winds blowing parallel to the coast from the north or east (known as Ekman setup) and by the accompanying low atmospheric pressure. Storm surge can cause large changes in water level and extensive inundation in adjacent coastal areas. Along North Carolina's open coast, storm surge is accompanied by strong wave action and is capable of causing major dune erosion, overtopping, and extensive damage to structures near the ocean front. Along the ocean front, seminal events include Hurricane Hazel (1956) and Hurricane Fran (1996), which generated storm tides (storm surge plus tide) of 18 feet and 12 feet, respectively. In the Albemarle and Pamlico Sounds and many of the lesser sounds, storm surge is enhanced by large over-water fetch lengths, shallow water depths, and a funneling effect as water moves to one end of the sound or up into the river-estuaries. Recent significant surge events along the sounds include surge exceeding 10 feet in New Bern, NC, during Hurricane Florence (2018) and 6 feet in Ocracoke, NC, during Hurricane Dorian (2019). Whereas the ocean front in most populated areas has a constructed dune line that provides protection from storm surge as long as it remains intact, the sounds have no similar protection, and inundation occurs as soon as the water level exceeds the low-lying adjacent topography.

Extreme precipitation can also accompany tropical cyclones, as experienced in the past two decades in eastern North Carolina during Hurricanes Floyd (1999), Matthew (2016), and Florence (2018) (Paerl et al. 2019). Precipitation from events of this magnitude can cause extensive flooding in the Coastal Plain. In many cases, storm surge and precipitation flooding at the coast occur over different time scales. Storm surge happens quickly and is closely synchronized with storm winds, while precipitation flooding occurs later, as precipitation on land traverses watersheds, streams, and rivers before reaching coastal areas. However, Hurricane Florence (2018) provided a counter example, as this slow-moving storm deposited more than 25 inches of precipitation on the central and southeastern North Carolina coastal region, much of which was coincident with the wind-driven storm surge.

4.5. Oceanic Processes

Coastal water levels also respond to multiple oceanic processes. As temperatures increase, water levels increase through a process known as thermal expansion (i.e., as water warms, its volume increases and it physically occupies more space). This is seen most clearly in the annual heating and cooling cycle that results in elevated water levels in the late summer and fall, when the upper ocean heat content reaches a maximum. The increase in the average ocean temperature due to climate change is a major contributor to increasing average sea level (Section 4.6). Water level changes along the U.S. Atlantic Coast have been associated with changes in Gulf Stream strength (coastal water levels increase as the strength of the Gulf Stream decreases; Montgomery 1938, Iselin 1940, Blaha 1984, Park and Sweet 2015, Ezer et al. 2013) and position upon leaving the

coast at Cape Hatteras (Fuglister 1955, Ezer 2019). The Gulf Stream experiences natural 2- to 5-year oscillations about Cape Hatteras that can create changes in coastal sea level that deviate substantially from longer-term trends (Kopp 2013, Ezer 2019). The Gulf Stream is an upper ocean component of a larger oceanic circulation known as the Atlantic meridional overturning circulation, which is believed to have weakened since at least the mid-20th century due to climate change (Caesar et al. 2018, Praetorius 2018) and is projected to continue to weaken in the 21st century (IPCC 2019). Weakening of the Gulf Stream could provide an additional oceanographic link between climate change and increasing average sea level along the North Carolina coast.

Multi-annual to multi-decadal variability in extreme water levels along the U.S. Atlantic Coast has also been related to the state of several patterns of natural variability in sea level pressure and sea surface temperature: the El Niño–Southern Oscillation (Munroe and Curtis 2017, Sweet et al. 2018), the Pacific North American pattern (Munroe and Curtis, 2017), the North Atlantic Oscillation (Talke et al. 2014, Munroe and Curtis 2017, Marcos and Woodworth 2017), and the Atlantic Multidecadal Oscillation (Park et al. 2010). Although in most cases, their relationships to climate change remain unclear, and therefore their impact on future changes in water level is also unclear. However, as is the case with the long-period tides or variations in the Gulf Stream, the variability in extreme water level associated with these processes can have important consequences for flooding over multiyear periods and must be considered when assessing future coastal flood hazards (Wahl and Chambers 2015, 2016; Wdowinski et al. 2016).

4.6. Relative Sea Level

Relative sea level (RSL) is the elevation difference between the sea surface at a specific location and time and the Earth's surface, and therefore changes in RSL are caused by changes to both the Earth's surface and global sea level. The elevation of Earth's surface changes due to ongoing geological processes (Section 4.2), as well as to adjustment due to changes in the ice mass. However, changes in RSL are typically within plus or minus 30% of the global average sea level change (IPCC 2019). RSL is usually averaged over time to minimize the influence of tides, storm surge, and inter-annual oceanic processes (Kopp et al 2015).

Global average sea level changes due to changes in total ocean water mass due to melting of ice sheets and land-based glaciers, as well as thermal expansion (Section 4.5); over recent decades, global average sea level has risen approximately twice as much from increasing ocean water mass as from thermal expansion (Figure 4.2). Global average sea level over the last ~2,500 years has been compiled from multiple techniques, including proxy-based reconstructions via corals and wetlands, tide gauges across the world, and more recently by satellite altimetry. Estimates of global average sea level over the 2,400 years preceding the 20th century show a relatively constant value with variations of ±3.5 inches (Kopp et al. 2016), whereas a consistent upward trend has occurred since about the beginning of the 20th century (Figure 4.3; Hayhoe et al. 2018). Using data from tide gauges and satellite altimetry, a recent report expressed ***high***

confidence that the rate of change of global average sea level has risen from 0.06 inches/year over the period 1901–1990 to 0.08 inches/year over the period 1970–2015, to 0.13 inches/year over the period 1993–2015, and to 0.14 inches/year over the period 2005–2015, indicating a near tripling of the rate of rise in global average sea level during this period (IPCC 2019).
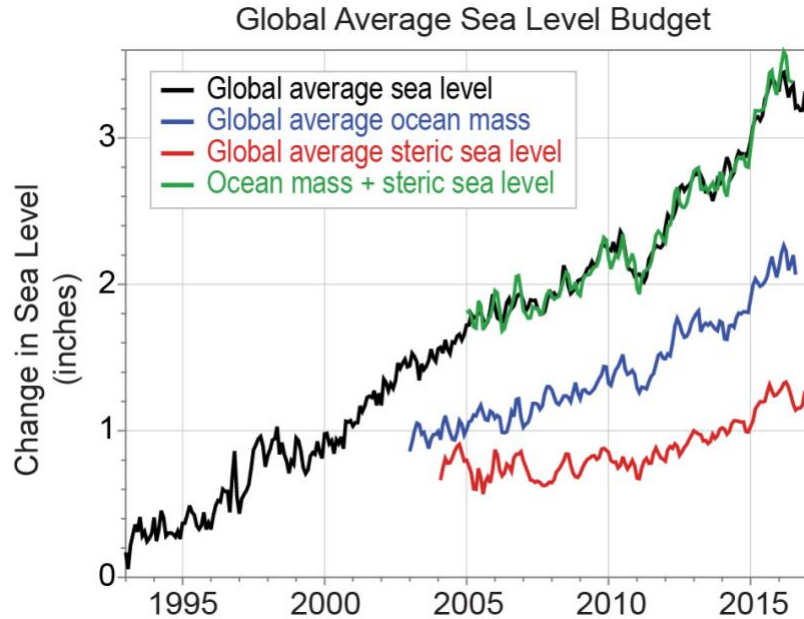

Figure 4.2. The figure shows the relative contributions to changes in global average sea level from changes in ocean mass (from land ice and land water storage; blue line) and changes in ocean volume (or steric changes, due to thermal expansion; red line) since 1993. The combined effect of ocean mass and volume changes is shown by the green line overlying the observed (via satellite) global mean sea level (black line). Minor differences between the two are due to differences in measurement methods. Source: adapted from Leuliette and Nerem 2016.
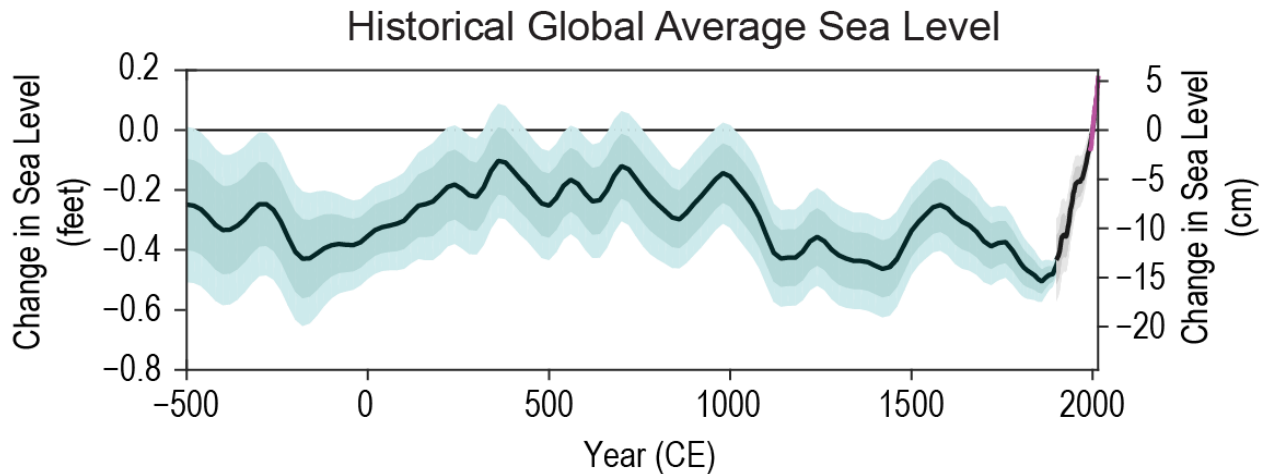
Figure 4.3. The figure shows change in global average sea level from −500 to 1900 CE from geological and tide gauge-based reconstruction (black line with blue error estimates; Kopp et al. 2016), from 1900 to 2010 from tide gauge-based reconstruction (black line with gray error estimates; Hay et al. 2015), and from 1992 to 2015 from satellite-based reconstruction (magenta line; updated from Nerem et al. 2010). Source: adapted from Sweet et al. 2017.

Future projections of global average sea level are based on the response of climate models to plausible trajectories (or scenarios) of atmospheric concentrations of greenhouse gases, aerosols, and chemically active gases, as well as land-use changes. These scenarios are called representative concentration pathways, or RCPs. Three widely quoted RCPs are 1) RCP2.6, a scenario that assumes greenhouse gas emissions peak by 2020 and decline substantially thereafter; 2) RCP4.5, a scenario that assumes greenhouse gas emissions peak by 2040 and then decline; and 3) RCP8.5, a business as usual scenario that assumes greenhouse gas emissions continue to increase through the end of the 21st century.

The most recent report from the U.S. Interagency Sea Level Rise Task Force presents a case for global average sea level rise reaching a rate as high as 1.7 inches/year and median global average sea levels ranging from 12 to 98 inches over year 2000 levels by the year 2100 (Table 4.1). The recent IPCC Special Report on the Ocean and Cryosphere in a Changing Climate (SROCC; IPCC 2019) projects likely global average sea level rise of 0.16–0.35 inches/year under RCP2.6 to about 0.39–0.79 inches/year under RCP8.5, leading to global average sea levels of about 12–43 inches above current levels by the year 2100 (Figure 4.4).

Table 4.1. The table shows the median global average sea level scenarios (referenced to the year 2000) defined by the U.S. Interagency Sea Level Rise Task Force (Sweet et al. 2017).

Global Average Sea Level Scenario	2010 inches	2050 inches	2100 inches
Low	1.2	6.3	12
Intermediate-Low	1.6	9.4	20
Intermediate	2.0	13	39
Intermediate-High	2.0	17	59
High	2.4	21	79
Extreme	2.4	25	98
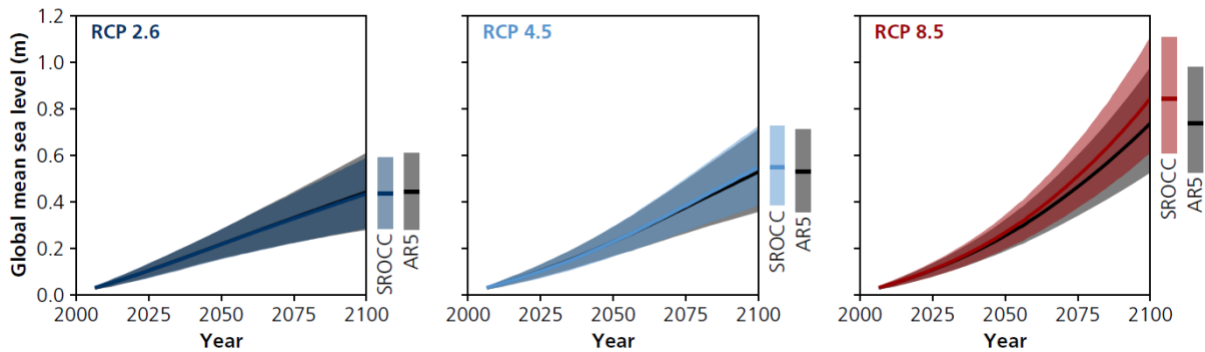
Figure 4.4. The graphs show projected changes in global mean sea level from two different studies (IPCC's Fifth Assessment Report and Special Report on the Ocean and Cryosphere in a Changing Climate [SROCC]) and under three different scenarios (RCP2.6, RCP4.5, and RCP8.5). The shaded region should be considered as the likely range. Source: IPCC 2019.

Long-term coastal water level gauges (or tide gauges) provide a means for determining trends in RSL. North Carolina has five gauges with sufficiently long records to provide stable estimates of trends in RSL (Table 4.1). These values suggest RSL is rising approximately twice as fast along the northeastern coast as the southeastern coast, consistent with the north-to-south trend in subsidence discussed in Section 4.2. Due to the increasing rate of global average sea level rise observed since 1900, the rate of RSL along the North Carolina coast is expected to have increased over this period as well.

Table 4.2. The table shows the trend in relative sea level determined from long-term water level records in North Carolina. (From https://tidesandcurrents.noaa.gov/sltrends/mslUSTrendsTable.html). See Figure 4.1 for locations.

Location	Relative Sea Level Trend (inches/year, 95% confidence interval)	Record Dates
Duck	0.182 ± 0.0268	1978–2018
Oregon Inlet	0.1846 ± 0.0457	1977–2018
Beaufort	0.122 ± 0.0138	1953–2018
Wilmington	0.094 ± 0.0138	1935–2018
Southport	0.079 ± 0.0161	1933–2008

4.7. Impacts of Climate Change on North Carolina Coastal Water Levels

The impacts of climate change on coastal water level will be manifest during both fair weather and severe weather conditions.

During fair weather, the effect of RSL rise can be seen as increasing water levels associated with astronomical tides; at high tide, this has created what is commonly referred to as "sunny day" or "nuisance" flooding. This is already well recognized in areas such as Hampton Roads, VA, and Charleston, SC, where a significant population exists close to sea level. The National Oceanographic and Atmospheric Administration (NOAA) has developed the term "high tide flooding" (HTF), defined as water levels of 1.6–2.1 feet above present Mean Higher High Water (Sweet et al. 2018) and has begun both to track the occurrence of HTF and to predict its future likelihood at locations with known RSL trends along the U.S. coast (Sweet et al. 2019).

Selecting Duck, Beaufort, and Wilmington as representative of the northeastern, central, and southeastern sections of the North Carolina coast, an assessment of HTF since 2000 and predictions of the occurrence frequencies of HTF until 2100 are presented in Figures Figure 4.5, Figure 4.6, and Figure 4.7, assuming global average sea level rise contributions between Intermediate-Low and Intermediate (Table 4.1). (These are roughly equivalent to the SROCC likely global average sea level rise projections under RCP4.5 and RCP8.5, respectively.)

As discussed above and indicated in the top panels of these figures, projections of the rise in RSL decrease from north to south and translate into a similar decrease in the predicted number of HTF days from north to south. However, under this range of RSL rise, at all three locations, HTF could occur as often as one out of every two days during the decade from 2050 to 2060 and daily after about 2080. Under higher RSL rise rates, HTF becomes a daily occurrence at all locations with corresponding increases in water depths.
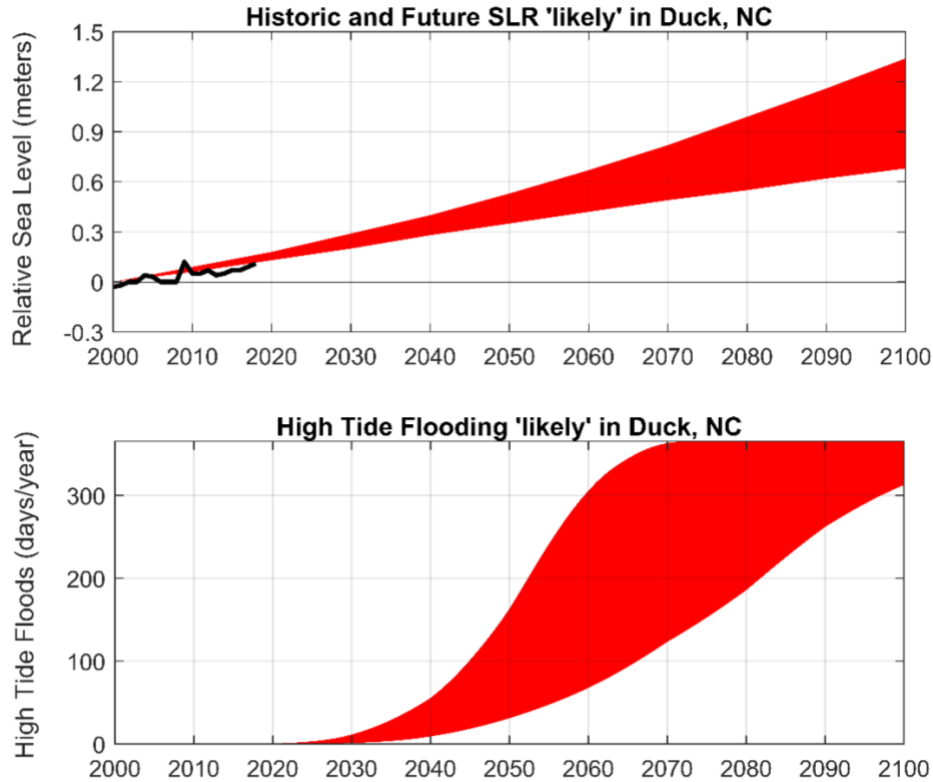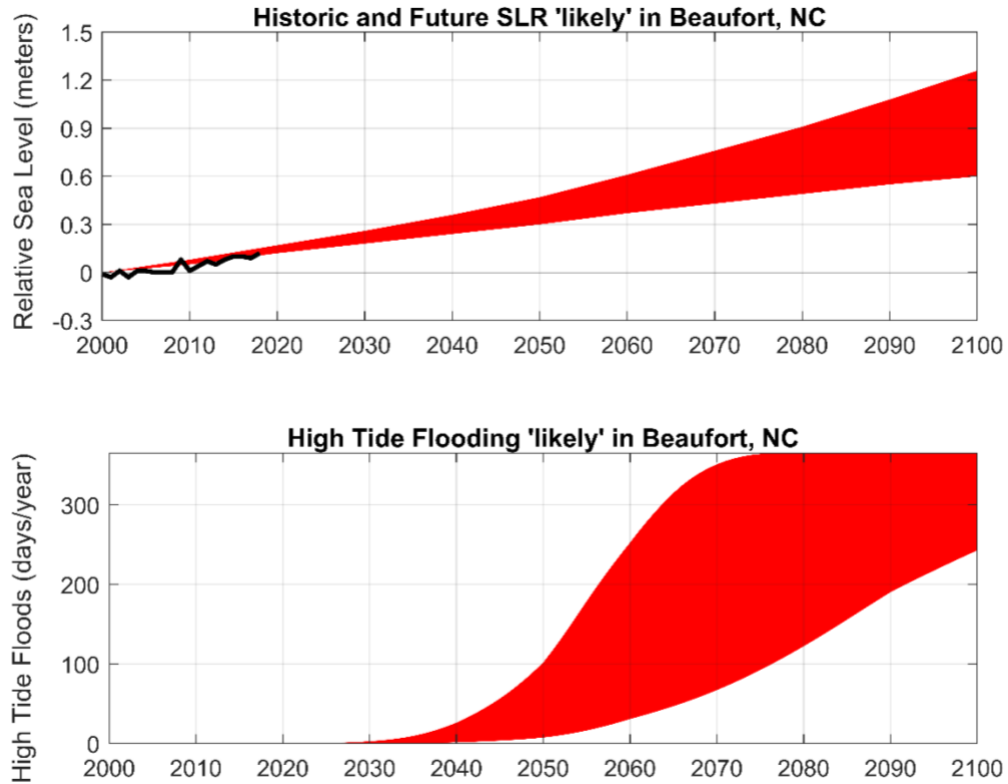
Figure 4.5. The top graph shows observed relative sea level (RSL) for 2000–2018 (black line) and projected RSL through 2100 (red shaded area) at Duck, NC, bounded by Intermediate-Low and Intermediate global average sea level rise scenarios (Table 4.1). These scenarios are roughly equivalent to the likely outcomes under RCP4.5 and RCP8.5 (IPCC 2019). The bottom graph shows the corresponding range in the number of high tide flood days considering only RSL rise and present astronomical tides. High tide flood days for Duck are defined as reaching water levels 1.8 ft above present Mean Higher High Water (Sweet et al. 2018). This figure courtesy of W. Sweet.
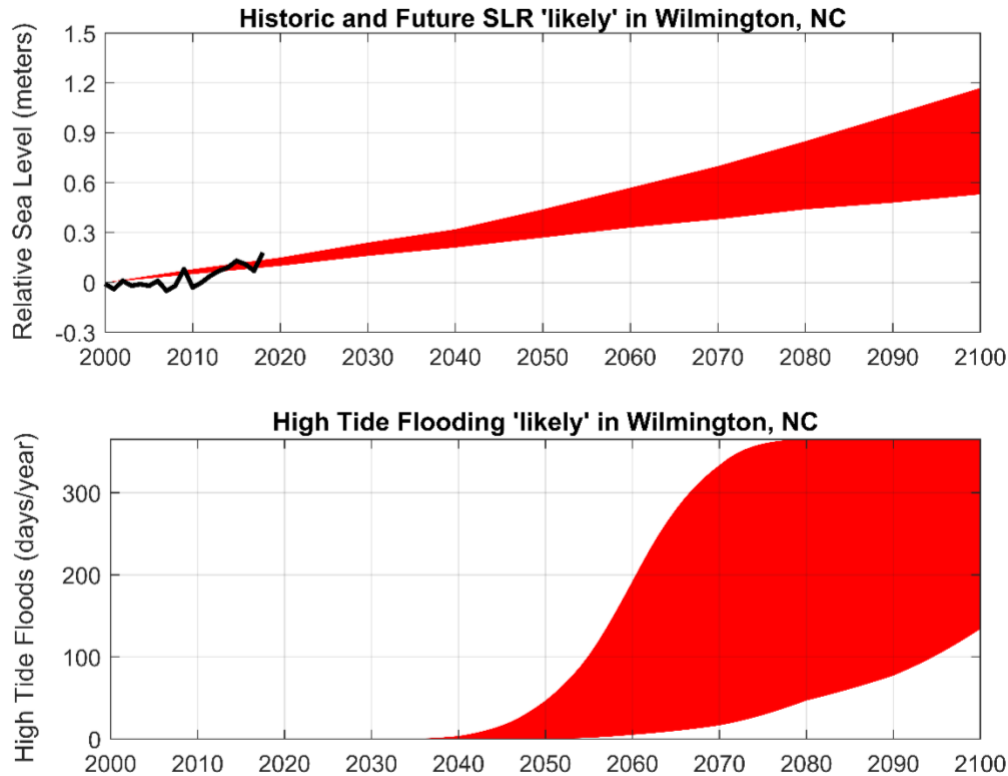
Figure 4.6. The top graph shows observed relative sea level (RSL) for 2000–2018 (black line) and projected RSL through 2100 (red shaded area) at Beaufort, NC, bounded by Intermediate-Low and Intermediate global average sea level rise scenarios (Table 4.1). These scenarios are roughly equivalent to the likely outcomes under RCP4.5 and RCP8.5 (IPCC 2019). The bottom graph shows the corresponding number of high tide flood days considering only RSL rise and present astronomical tides. High tide flood days for Beaufort are defined as reaching water levels 1.8 ft above present Mean Higher High Water (Sweet et al. 2018). This figure courtesy of W. Sweet.

Figure 4.7. The top graph shows observed relative sea level (RSL) for 2000–2018 (black line) and projected RSL through 2100 (red shaded area) at Wilmington, NC, bounded by Intermediate-Low and Intermediate global average sea level rise scenarios (Table 4.1). These scenarios are roughly equivalent to the likely outcomes under RCP4.5 and RCP8.5 (IPCC 2019). The bottom graph shows the corresponding number of high tide flood days considering only RSL rise and present astronomical tides. High tide flood days for Wilmington are defined as reaching water levels 1.8 ft above present Mean Higher High Water (Sweet et al. 2018). This figure courtesy of W. Sweet.

Climate change will also affect coastal water levels associated with severe weather events. As was the case with HTF, rising RSL will increase the water level that results from storm surge associated with the same storm event. However, changes in storm characteristics as the climate warms—particularly projections of increasing storm intensity—offer a second means for increasing water level extremes associated with these storms (see Chapter 2, Section 2.5.3). Finally, the potential for increased precipitation (see Chapter 3, Section 3.2.7) provides another source of water in addition to storm surge.

Using realistic scenarios for both RSL (0, 20 cm [0.7 feet], 40 cm [1.3 feet], 60 cm [2.0 feet], 80 cm [2.6 ft], 100 cm [3.3 ft]) and future hurricane characteristics (see below), storm surge was computed for 2010 and for future conditions along the North Carolina coast (Blanton 2012, NCDPS 2014). The southeastern coast is subject to more intense storms than the northeastern

coast and therefore experiences higher water levels for the same annual probability of occurrence (Figure 4.8). Increases in water level for a given annual probability of occurrence correspond very closely to RSL rise along the open coast (Figure 4.8), although in estuarine areas, the response becomes more nonlinear when RSL exceeds 1.3 feet (NCDPS 2014, Batten et al. 2015). Water levels having a 0.3% and 1.5% probability of occurring each year in 2010 would have a 10% probability of occurring following a 2.6-foot rise in RSL at Duck, NC, and Wrightsville Beach, NC, respectively. In addition, storm statistics were modified to represent reasonable mid-21st century and end-of-21st century scenarios by imposing a 10% reduction in overall hurricane frequency and a 40% increase in the frequency of Category 4 and 5 hurricanes for the mid-century scenario and a 20% reduction in overall hurricane frequency and an 80% increase in the frequency of Category 4 and 5 hurricanes for the end-of-century scenario. Water levels in the northeast showed very little effect of changing the storm statistics, while in the southeast a slightly greater effect was observed (Figure 4.9).
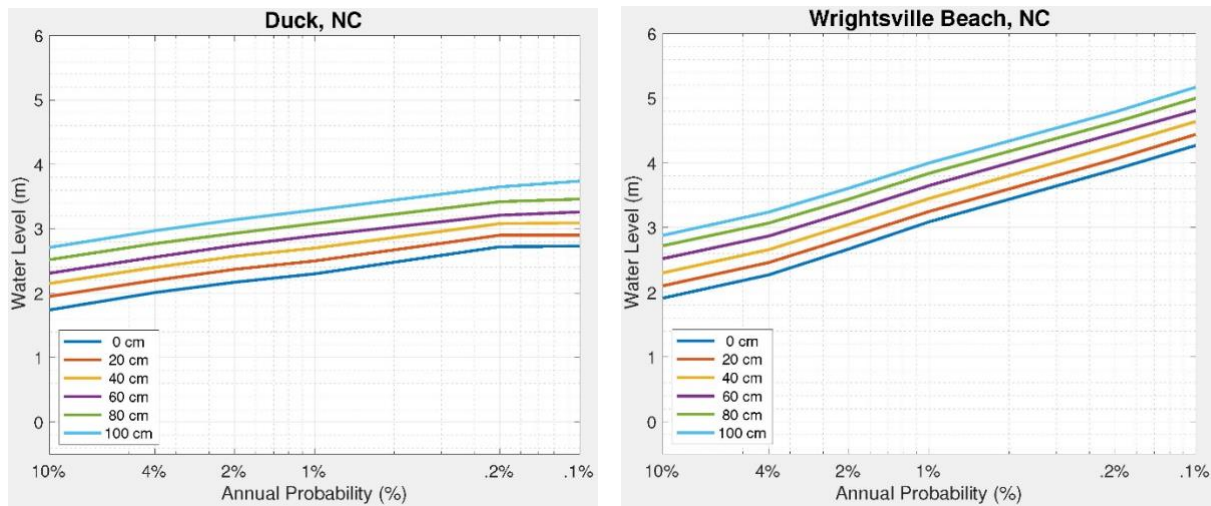

Figure 4.8. Water level expected to occur at different annual probability of occurrence (%) for six different RSL scenarios (0, 20 cm [0.7 feet], 40 cm [1.3 feet], 60 cm [2.0 feet], 80 cm [2.6 feet], 100 cm [3.3 feet]) at Duck (left) and Wrightsville Beach (right), NC. Source: adapted from Blanton 2012.
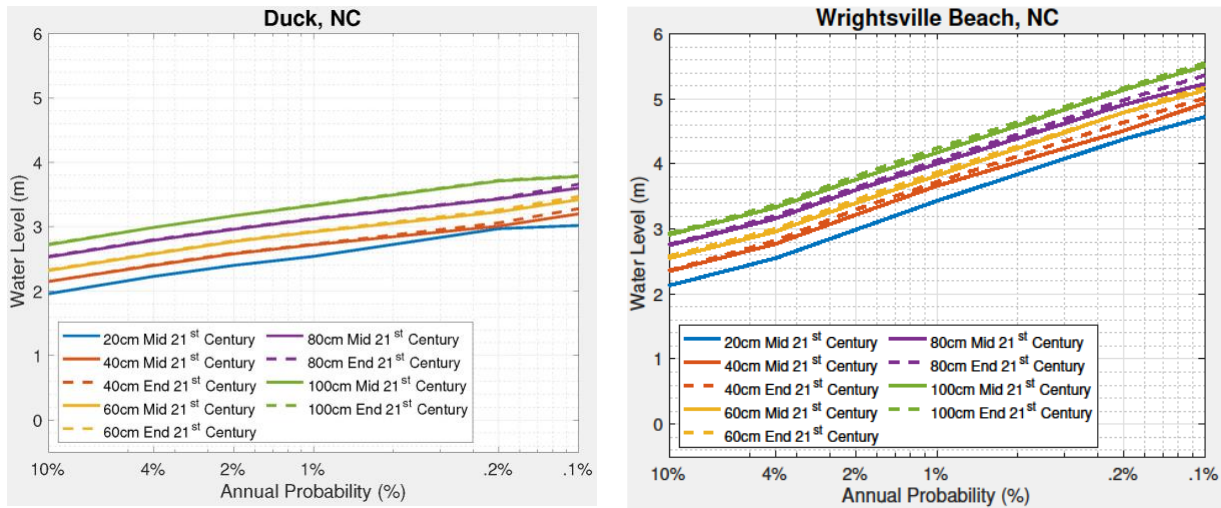
Figure 4.9. Water level expected to occur at different annual probability of occurrence (%) curves for five RSL scenarios (0, 20 cm [0.7 feet], 40 cm [1.3 feet], 60 cm [2.0 feet], 80 cm [2.6 feet], 100 cm [3.3 feet]) at Duck (left) and Wrightsville Beach (right), and including two increases in storm strengths. The mid-21st century period was represented as a 10% reduction in total hurricane frequency and a 40% increase in the frequency of Category 4 and 5 events. The end-21st century period was represented as a 20% reduction in total hurricane frequency and an 80% increase in the frequency of Category 4 and 5 events. Source: adapted from Blanton 2012.

A more recent study considered the effect of RSL on historical water levels observed along the North Carolina coast and found that under the higher scenario (RCP8.5) after 2050, water levels that currently have a 10% probability of occurring each year would have nearly a 100% probability of occurring each year in Wilmington. Furthermore, water levels that currently have a 1% probability of occurring each year would have nearly a 60% probability of occurring each year from 2050 to 2100 (Kopp et al. 2015).

 A third study analyzed the effects of rising sea level and changing tropical cyclone characteristics on water levels in every coastal county along the Atlantic and Gulf of Mexico coasts under the RCP8.5 scenario (Marsooli et al. 2019). These authors found that the historical (1980–2005) 1% annual probability event along the North Carolina coast would have a corresponding probability of 30%–100% in the time period from 2070 to 2095. Further, it was concluded that the change in annual probability was dominated by sea level rise along the northeastern Atlantic Coast but shifted to being dominated by the changing storm characteristics as one moved south to the Gulf of Mexico. Along the North Carolina coast, sea level rise was approximately twice as important as the shift in storm characteristics in affecting changes in storm related water level (Figure 4.10).
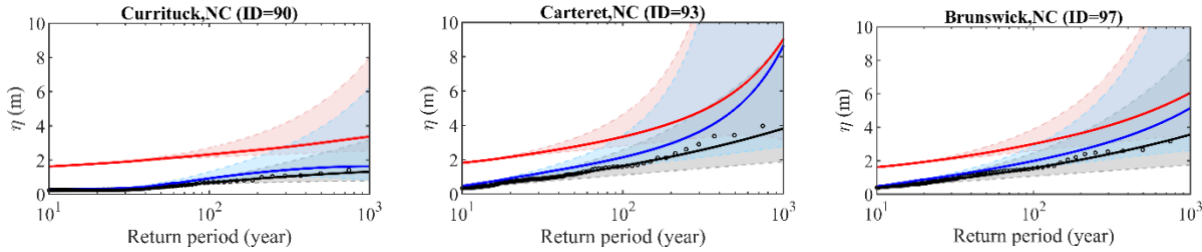
Figure 4.10. Water level versus return period curves for the historical period of 1980–2005 (black) and future period of 2070–2095 (blue: effects of changes in tropical cyclone [TC] characteristics only; red: compound effects of sea level rise and changing TC characteristics) along the northeastern, central, and southeastern North Carolina coast. Observations for the historical period are shown as black circles. Solid lines represent the best estimates of flood return periods. Shaded areas cover the very likely range estimates (i.e., 90% statistical confidence interval). Future projections are a weighted average over six climate models used in the calculations. Water levels are relative to Mean Higher High Water. Annual probability of occurrence (%) equals the reciprocal of the return period in years. Source: courtesy of R. Marsooli.

Collectively, these findings make it clear that climate change is increasing both routine, sunny-day, and extreme storm-related water levels and thereby exacerbating a range of flood hazards in coastal North Carolina. Unfortunately, the HTF analysis is currently limited to only a few North Carolina locations where long-term tide gauge data are available and predictions of future storm surge hazards are also available at only limited locations and under limited assumptions. In particular, additional flood hazard studies are greatly needed for the chronically flood-prone areas surrounding the Albemarle and Pamlico Sounds. Accounting for likely changes to the structure of the North Carolina Outer Banks and the contribution of precipitation and runoff introduces additional levels of complexity to this hazard assessment beyond what has been attempted to date.

4.8. References

Batten, B.K., B. Blanton, S. Taylor, and J. Plummer, 2015: Modeling the influence of sea level rise on future storm surge elevations considering landscape evolution. *Coastal Sediments 2015*. World Scientific. http://dx.doi.org/10.1142/9789814689977_0255

Blaha, J.P., 1984: Fluctuations of monthly sea level as related to the intensity of the Gulf Stream from Key West to Norfolk. *Journal of Geophysical Research: Oceans,* **89** (C5), 8033–8042. http://dx.doi.org/10.1029/JC089iC05p08033

Blanton, B., 2012: Storm Surge Computations for the North Carolina Sea Level Risk Management Study. A RENCI Technical Report TR-12-04. Renaissance Computing Institute, University of North Carolina, 42 pp. https://renci.org/wp-content/uploads/2016/09/StormSurge-White-Paper-2012.pdf

Caesar, L., S. Rahmstorf, A. Robinson, G. Feulner, and V. Saba, 2018: Observed fingerprint of a weakening Atlantic Ocean overturning circulation. *Nature,* **556** (7700), 191–196. http://dx.doi.org/10.1038/s41586-018-0006-5

Eliot, M., 2010: Influence of interannual tidal modulation on coastal flooding along the Western Australian coast. *Journal of Geophysical Research: Oceans,* **115** (C11). http://dx.doi.org/10.1029/2010JC006306

Engelhart, S.E., B.P. Horton, B.C. Douglas, W.R. Peltier, and T.E. Törnqvist, 2009: Spatial variability of late Holocene and 20th century sea-level rise along the Atlantic coast of the United States. *Geology,* **37** (12), 1115–1118. http://dx.doi.org/10.1130/G30360A.1

Engelhart, S.E., W.R. Peltier, and B.P. Horton, 2011: Holocene relative sea-level changes and glacial isostatic adjustment of the U.S. Atlantic coast. *Geology,* **39** (8), 751–754. http://dx.doi.org/10.1130/G31857.1

Ezer, T., L.P. Atkinson, W.B. Corlett, and J.L. Blanco, 2013: Gulf Stream's induced sea level rise and variability along the U.S. mid-Atlantic coast. *Journal of Geophysical Research: Oceans,* **118** (2), 685–697. http://dx.doi.org/10.1002/jgrc.20091

Ezer, T., 2019: Regional differences in sea level rise between the Mid-Atlantic Bight and the South Atlantic Bight: Is the Gulf Stream to blame? *Earth's Future,* **7** (7), 771-783. http://dx.doi.org/10.1029/2019EF001174

Fuglister, F.C., 1955: Alternative analyses of current surveys. *Deep Sea Research (1953),* **2** (3), 213–229. http://dx.doi.org/10.1016/0146-6313(55)90026-5

Haigh, I.D., M. Eliot, and C. Pattiaratchi, 2011: Global influences of the 18.61 year nodal cycle and 8.85 year cycle of lunar perigee on high tidal levels. *Journal of Geophysical Research: Oceans,* **116** (C6). http://dx.doi.org/10.1029/2010JC006645

Hay, C.C., E. Morrow, R.E. Kopp, and J.X. Mitrovica, 2015: Probabilistic reanalysis of twentieth-century sea-level rise. *Nature,* **517** (7535), 481–484. http://dx.doi.org/10.1038/nature14093

Hayhoe, K., D.J. Wuebbles, D.R. Easterling, D.W. Fahey, S. Doherty, J. Kossin, W. Sweet, R. Vose, and M. Wehner, 2018: Our Changing Climate. *Impacts, Risks, and Adaptation in the United States: Fourth National Climate Assessment, Volume II*. Reidmiller, D.R., C.W. Avery, D. Easterling, K. Kunkel, K.L.M. Lewis, T.K. Maycock, and B.C. Stewart, Eds. U.S. Global Change Research Program, Washington, DC, USA, 72–144. http://dx.doi.org/10.7930/NCA4.2018.CH2

IPCC, 2019: *IPCC Special Report on the Ocean and Cryosphere in a Changing Climate*. Pörtner, H.-O., D.C. Roberts, V. Masson-Delmotte, P. Zhai, M. Tignor, E. Poloczanska, K. Mintenbeck, A. Alegría, M. Nicolai, A. Okem, J. Petzold, B. Rama, and N.M. Weyer, Eds. In Press. https://www.ipcc.ch/srocc/

Iselin, C.O., 1940–1947: Preliminary report on long-period variations in the transport of the Gulf Stream system. *Papers in Physical Oceanography and Meteorology,* **8** (1). http://dx.doi.org/10.1575/1912/1048

Kemp, A.C., B.P. Horton, S.J. Culver, D.R. Corbett, O. van de Plassche, W.R. Gehrels, B.C. Douglas, and A.C. Parnell, 2009: Timing and magnitude of recent accelerated sea-level rise (North Carolina, United States). *Geology,* **37** (11), 1035–1038. http://dx.doi.org/10.1130/G30352A.1

Kemp, A.C., B.P. Horton, J.P. Donnelly, M.E. Mann, M. Vermeer, and S. Rahmstorf, 2011: Climate related sea-level variations over the past two millennia. *Proceedings of the National Academy of Sciences of the United States of America,* **108** (27), 11017–11022. http://dx.doi.org/10.1073/pnas.1015619108

Kopp, R.E., 2013: Does the mid-Atlantic United States sea level acceleration hot spot reflect ocean dynamic variability? *Geophysical Research Letters,* **40** (15), 3981–3985. http://dx.doi.org/10.1002/grl.50781

Kopp, R.E., B.P. Horton, A.C. Kemp, and C. Tebaldi, 2015: Past and future sea-level rise along the coast of North Carolina, USA. *Climatic Change,* **132** (4), 693–707. http://dx.doi.org/10.1007/s10584-015-1451-x

Kopp, R.E., A.C. Kemp, K. Bittermann, B.P. Horton, J.P. Donnelly, W.R. Gehrels, C.C. Hay, J.X. Mitrovica, E.D. Morrow, and S. Rahmstorf, 2016: Temperature-driven global sea-level variability in the Common Era. *Proceedings of the National Academy of Sciences of the United States of America,* **113** (11), E1434–E1441. http://dx.doi.org/10.1073/pnas.1517056113

Leuliette, E.W. and R.S. Nerem, 2016: Contributions of Greenland and Antarctica to global and regional sea level change. *Oceanography,* **29** (4), 154–159. http://dx.doi.org/10.5670/oceanog.2016.107

Luettich, J.R., S. Carr, J. Reynolds-Fleming, C. Fulcher, and J. McNinch, 2002: Semidiurnal seiching in a shallow, micro-tidal lagoonal estuary. *Continental Shelf Research,* **22**, 1669–1681. http://dx.doi.org/10.1016/S0278-4343(02)00031-6

Marcos, M. and P.L. Woodworth, 2017: Spatiotemporal changes in extreme sea levels along the coasts of the North Atlantic and the Gulf of Mexico. *Journal of Geophysical Research: Oceans,* **122** (9), 7031–7048. http://dx.doi.org/10.1002/2017JC013065

Marsooli, R., N. Lin, K. Emanuel, and K. Feng, 2019: Climate change exacerbates hurricane flood hazards along US Atlantic and Gulf Coasts in spatially varying patterns. *Nature Communications,* **10** (1), 3785. http://dx.doi.org/10.1038/s41467-019-11755-z

Montgomery, R., 1938: Fluctuations in monthly sea level on eastern U.S. coast as related to dynamics of western North Atlantic Ocean. *Journal of Marine Research,* **1** (2), 165–185. https://images.peabody.yale.edu/publications/jmr/jmr01-02-07.pdf

Munroe, R. and S. Curtis, 2017: Storm surge evolution and its relationship to climate oscillations at Duck, NC. *Theoretical and Applied Climatology,* **129** (1), 185–200. http://dx.doi.org/10.1007/s00704-016-1770-5

N.C. Coastal Resources Commission Science Panel, 2015: North Carolina Sea Level Rise Assessment Report: 2015 Update to the 2010 Report and 2012 Addendum. https://files.nc.gov/ncdeq/Coastal%20Management/documents/PDF/Science%20Panel/2015%20NC%20SLR%20Assessment-FINAL%20REPORT%20Jan%2028%202016.pdf

NCDPS, 2014: North Carolina Sea Level Rise Impact Study: Final Study Report. North Carolina Department of Public Safety, North Carolina Emergency Management Geospatial and Technology Management.

Nerem, R.S., D.P. Chambers, C. Choe, and G.T. Mitchum, 2010: Estimating mean sea level change from the TOPEX and Jason altimeter missions. *Marine Geodesy,* **33** (S1), 435–446. http://dx.doi.org/10.1080/01490419.2010.491031

NOAA, 2020: High and Low Water Conditions (North Carolina). NOAA Tides and Currents. https://tidesandcurrents.noaa.gov/map/index.html?region=North%20Carolina

North Carolina King Tides Project, 2020: [Home page]. http://nckingtides.web.unc.edu/

Paerl, H.W., N.S. Hall, A.G. Hounshell, R.A. Luettich, K.L. Rossignol, C.L. Osburn, and J. Bales, 2019: Recent increase in catastrophic tropical cyclone flooding in coastal North Carolina, USA: Long-term observations suggest a regime shift. *Scientific Reports,* **9** (1), 10620. http://dx.doi.org/10.1038/s41598-019-46928-9

Park, J., J. Obeysekera, and J. Barnes, 2010: Temporal energy partitions of Florida extreme sea level events as a function of Atlantic multidecadal oscillation. *Ocean Science (OS),* **6**, 587–593. http://dx.doi.org/10.5194/os-6-587-2010

Park, J. and W. Sweet, 2015: Accelerated sea level rise and Florida Current transport. *Ocean Science,* **11** (4), 607–615. http://dx.doi.org/10.5194/os-11-607-2015

Peng, D., E.M. Hill, A.J. Meltzner, and A.D. Switzer, 2019: Tide gauge records show that the 18.61-year nodal tidal cycle can change high water levels by up to 30 cm. *Journal of Geophysical Research: Oceans,* **124** (1), 736–749. http://dx.doi.org/10.1029/2018JC014695

Praetorius, S.K., 2018: North Atlantic circulation slows down. *Nature,* **556**, 180–181. http://dx.doi.org/10.1038/d41586-018-04086-4

Pugh, D.T., 1987: *Tides, Surges and Mean Sea-Level—A Handbook for Engineers and Scientists*. John Wiley & Sons, Chichester, U.K.

Ray, R.D. and M.A. Merrifield, 2019: The semiannual and 4.4-year modulations of extreme high tides. *Journal of Geophysical Research: Oceans,* **124** (8), 5907–5922. http://dx.doi.org/10.1029/2019JC015061

Riggs, S.R., W.J. Cleary, and S.W. Snyder, 1995: Influence of inherited geologic framework on barrier shoreface morphology and dynamics. *Marine Geology,* **126** (1), 213–234. http://dx.doi.org/10.1016/0025-3227(95)00079-E

Riggs, S.R., 2002: Life at the edge of North Carolina's coastal system: The geologic controls. *Life at the Edge of the Sea: Essays on North Carolina's Coast and Coastal Culture*. Beal, C. and C. Prioli, Eds. Coastal Carolina Press, Wilmington, NC, 63–96.

Riggs, S.R., D.V. Ames, S.J. Culver, and D. Mallinson, 2011: *The Battle for North Carolina's Coasts: Evolutionary History, Present Crisis, and Vision for the Future*. University of North Carolina, Chapel Hill, NC, 142 pp.

Sohl, N.F. and J.P. Owens, 1991: Cretaceous stratigraphy of the Carolina coastal plain. *The Geology of the Carolinas: Carolina Geological Society, 50th Anniversary Volume*. Horton, J.W., Jr. and V.A. Zullo, Eds. University of Tennessee Press, Knoxville, TN, 191–220.

Sweet, W., G. Dusek, J. Obeysekera, and J.J. Marra, 2018: Patterns and Projections of High Tide Flooding Along the U.S. Coastline Using a Common Impact Threshold. NOAA Technical Report NOS CO-OPS 086. National Oceanic and Atmospheric Administration, National Ocean Service, Silver Spring, MD, 44 pp. https://tidesandcurrents.noaa.gov/publications/techrpt86_PaP_of_HTFlooding.pdf

Sweet, W., G. Dusek, D. Marcy, G. Carbin, and J. Marra, 2019: 2018 State of U.S. High Tide Flooding with a 2019 Outlook. NOAA Technical Report NOS CO-OPS 090. National Oceanic and Atmospheric Administration, National Ocean Service, Silver Spring, MD, 31 pp. https://repository.library.noaa.gov/view/noaa/20691

Sweet, W.V., R.E. Kopp, C.P. Weaver, J. Obeysekera, R.M. Horton, E.R. Thieler, and C. Zervas, 2017: Global and Regional Sea Level Rise Scenarios for the United States. NOAA Tech. Rep. NOS CO-OPS 083. National Oceanic and Atmospheric Administration, National Ocean Service, Silver Spring, MD, 75 pp. https://tidesandcurrents.noaa.gov/publications/techrpt83_Global_and_Regional_SLR_Scenarios_for_the_US_final.pdf

Talke, S.A., P. Orton, and D.A. Jay, 2014: Increasing storm tides in New York Harbor, 1844–2013. *Geophysical Research Letters,* **41** (9), 3149–3155. http://dx.doi.org/10.1002/2014GL059574

Van De Plassche, O., A.J. Wright, B.P. Horton, S.E. Engelhart, A.C. Kemp, D. Mallinson, and R.E. Kopp, 2014: Estimating tectonic uplift of the Cape Fear Arch (southeastern United States) using reconstructions of Holocene relative sea level. *Journal of Quaternary Science,* **29** (8), 749–759. http://dx.doi.org/10.1002/jqs.2746

Wahl, T. and D.P. Chambers, 2015: Evidence for multidecadal variability in US extreme sea level records. *Journal of Geophysical Research: Oceans,* **120** (3), 1527–1544. http://dx.doi.org/10.1002/2014JC010443

Wahl, T. and D.P. Chambers, 2016: Climate controls multidecadal variability in U.S. extreme sea level records. *Journal of Geophysical Research Oceans,* **121** (2), 1274–1290. http://dx.doi.org/10.1002/2015JC011057

Wdowinski, S., R. Bray, B.P. Kirtman, and Z. Wu, 2016: Increasing flooding hazard in coastal communities due to rising sea level: Case study of Miami Beach, Florida. *Ocean & Coastal Management,* **126**, 1–8. http://dx.doi.org/10.1016/j.ocecoaman.2016.03.002

5. Compound Events

5.1. Inland Flooding

Long-term changes in inland flooding occur as a result of changes in climate conditions (e.g., precipitation changes), in water management practices (e.g., dams), or in land use and land cover (e.g., urbanization; Peterson et al. 2013). Additionally, because watersheds store moisture, they effectively have a memory, meaning that periods of extreme dryness or wetness cause soil moisture deficits or excesses that can persist for months or years. This can affect the likelihood and severity of flooding in that watershed over periods (e.g., years) longer than the periods of precipitation deficit or excess. When analyzing long-term changes in inland flooding, all these factors must be considered.

Inland flooding in North Carolina encompasses a range of scales, from local urban flooding to medium-size river basins, and a range of topographies, from flat to mountainous. Most large-scale flooding events in North Carolina result from tropical cyclones or extratropical cyclones (low pressure systems associated with the jet stream; NWS n.d.). Eastern North Carolina experienced three extreme flood-producing hurricanes in the last 20 years, Floyd (1999), Matthew (2016) and Florence (2018). One study found only a 2% probability of three such storms happening in that time frame and suggested that increases in atmospheric water vapor as a result of warming may have played a role (Paerl et al. 2019).

Flooding due to tropical cyclones is not limited to the Coastal Plain. In 1916, 1940, and again in 2004, the remnants of tropical cyclones caused extreme flooding in Western North Carolina, and in 1945 the Piedmont experienced severe flooding due to a tropical cyclone. However, not all major flooding events in North Carolina are caused by tropical cyclones. Winter storms, also known as extratropical cyclones, can also cause severe flooding. For example, in late April 2017, a slow-moving extratropical cyclone produced widespread flooding in central and eastern North Carolina.

For the United States, the Climate Science Special Report stated with ***high confidence*** that the frequency and intensity of heavy precipitation events are projected to continue to increase over the 21st century (Key Finding 3 in Easterling et al. 2017). At the state level, increases in the frequency of heavy rainfall are projected, particularly for the higher scenario (see Figure 2.19 and associated text). In addition, tropical cyclones are expected to produce heavier precipitation, and the strongest storms are projected to be even stronger in the future. Given the connection between extreme precipitation and flooding, and the complexities of other relevant factors, there is ***medium confidence*** that future increases in heavy rainfall will contribute to increases in flooding statewide.

5.2. Wildfires

5.2.1. Introduction

Wildfires are both beneficial and hazardous to the forests, ecosystems, and communities they affect across North Carolina. Fire sustains some forest types while acting as a threat to others. It helps maintain native biodiversity and ecosystem processes while simultaneously threatening human landscapes and interfering with forest management practices (Mitchell et al. 2014; Anderson and Palik 2011). In addition to their potential impacts on forest ecosystems and the built environment, wildfires are also of interest because they can adversely affect human health; wildfire smoke contains a number of harmful constituents, and winds can disperse the smoke over long distances (Naeher et al. 2007, Stefanidou et al. 2008, Holstius et al. 2012, Johnston et al. 2012, Johnston et al. 2011, Elliott et al. 2013, Henderson et al. 2011).

North Carolina lies in the region of the country with the largest annual average number of wildfires in the continental United States and the largest area burned by prescribed fires (Noss 2012, Melvin 2015). With more than half its land area covered by some of the most diverse and productive forests in the country, the state's landscape is rife with potential fuel for wildfires (USDA Forest Service 2019; McNulty et al. 2013; Mitchell et al. 2014; Wear et al. 2007). The mountains of North Carolina encompass the highest elevations and largest range of elevations east of the Mississippi River, some of the wettest and driest locations in the Southeast, and the most diverse forests in North America (Clark et al. 2011).

Climate change has already increased the frequency and severity of wildfires at global and national scales, and in the southeastern United States, the length of the fire season and the average land area burned by wildfire are projected to increase. When considered in combination with increasing development at the wildland–urban interface, an increased risk to property and human life is possible (Vose et al. 2018).

5.2.2. Climate & Wildfire

The likelihood of wildfire outbreaks is affected by several atmospheric variables, most importantly precipitation, temperature, atmospheric water vapor content, incoming solar energy, and wind (e.g. Kunkel 2001). Anomalously dry conditions (drought) can result in the drying of surface litter and in the dormancy or death of vegetation, increasing the combustibility of plant matter. Temperature is also critical because it affects the rate of drying of the surface. Higher temperatures cause more rapid drying of surface litter and faster depletion of soil moisture. Low atmospheric water vapor content leads to lower relative humidity and more rapid drying of the surface. Solar energy absorbed by plant matter will increase drying rates, and thus sunny days increase the likelihood of wildfires. In North Carolina, wind flow from the interior of the North American continent (i.e., from the north and west) is generally characterized by lower values of atmospheric water vapor content compared to wind flow from the Gulf of Mexico and the Atlantic Ocean (i.e., from the south and east). Strong winds increase the rate of surface drying, which can, in turn, increase the risk of wildfire.

In summary, dry surface vegetative matter means high wildfire potential. The conditions most conducive to drying of the surface are deficient precipitation over a period of weeks or months, high temperatures, low atmospheric water vapor content, sunny days, and high winds. In North Carolina, wildfire potential is at its highest in fall after vegetation has become dormant and in the spring before vegetation begins growing.

When wildfire potential is high, other weather factors can influence the occurrence and spread of fires. Lightning from thunderstorms can trigger fires. High winds will enhance the spread of existing fires. Occasional episodes of high winds are a normal part of the North Carolina climate in the spring and late fall because of low pressure storms associated with the jet stream. When combined with other factors favorable for wildfires, major wildfires can occur, as happened in the 2016 Gatlinburg fire (see Box 5.1).

5.2.3. Observed Changes in Wildfire

In North Carolina, there has been a long-term upward trend in the number of wildfires but a downward trend in the acreage burned (Figure 5.1). These long-term changes involve numerous non-climatic factors, and a description of them is beyond the scope of this report. However, the year-to-year changes are influenced by climate factors. For example, the large amounts of acreage burned in 1986, 2008, 2011, and 2016 were coincident with droughts in parts of the state.
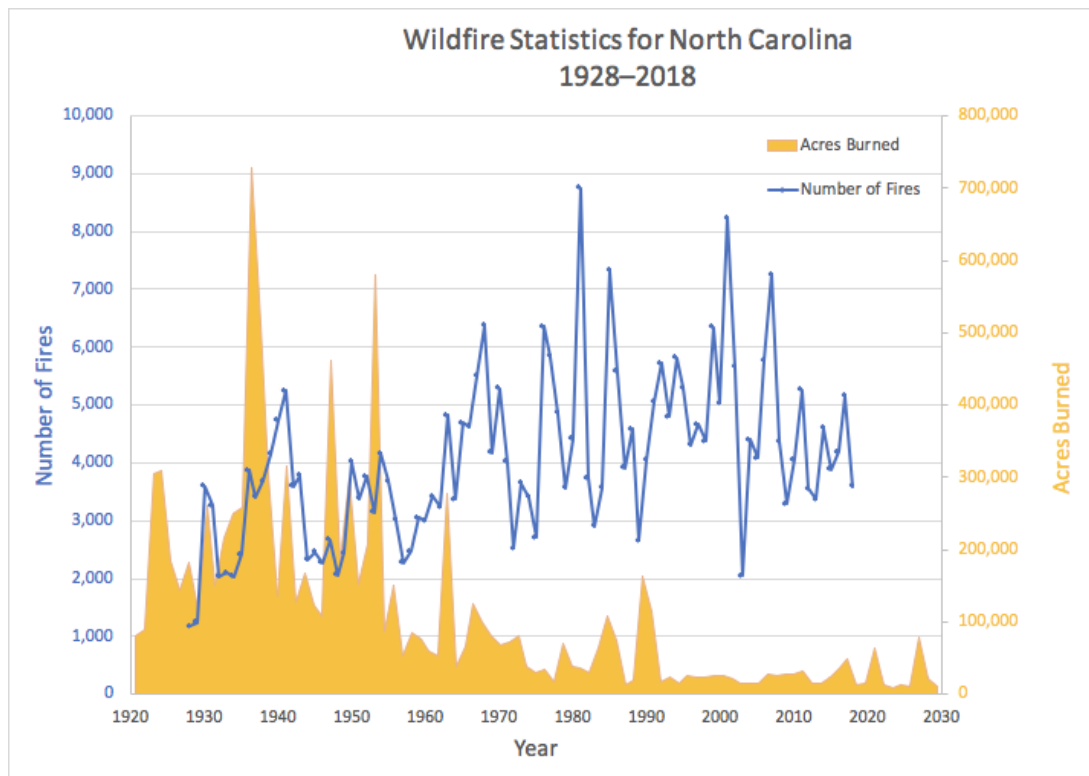
Figure 5.1. This figure shows year-to-year variations in the number of forest fires (blue line, left axis) and acreage burned (orange filled area, right axis) in North Carolina. Long-term trends reflect changes in many non-climatic factors, such as forest management; descriptions of these changes are beyond the scope of this report. Year-to-year fluctuations are often due to climate conditions. For example, high values of acreage burned in 1941, 1955, 1986, and 2016 corresponded to severe drought conditions. Source: NCICS.

5.2.4. Projected Changes in Wildfire

Future changes in precipitation are uncertain in the Southeast. Regardless of changes in precipitation, increasing air temperatures will likely increase regional drying through increased forest water use via evapotranspiration, and this drying will likely increase wildfire occurrence in forests across the region (McNulty 2013).

Recent modeling studies for a range of forests across the contiguous United States found that climate change will increase the frequency of conditions conducive to very large wildfires in all forested areas that were studied (Barbero et al. 2015). In North Carolina, the number of weeks with conditions conducive to very large fires is projected to increase more than 300% for the Coastal Plain by the mid-21st century under the higher scenario (RCP8.5). Increases of 50%–100% are projected for the Western Mountains (Figure 5.2; Barbero et al. 2015).

The Barbero et al. (2015) study does not consider potential mitigating societal factors. For example, as development continues on the margins of forests, forested areas are broken into

smaller units and interrupted by roads and other infrastructure. In addition, the increased exposure of life and property is a motivating factor to implement stronger fire control measures. This societal dimension is considered in Prestemon et al. (2016). Their model projects a relatively small increase in acreage burned by mid-century of 4% in North Carolina, where potential increases from climate change are largely offset by societal factors. However, this conclusion is based only on one study with large uncertainties.

Projected Increase in Number of Weeks with Wildfire Risk
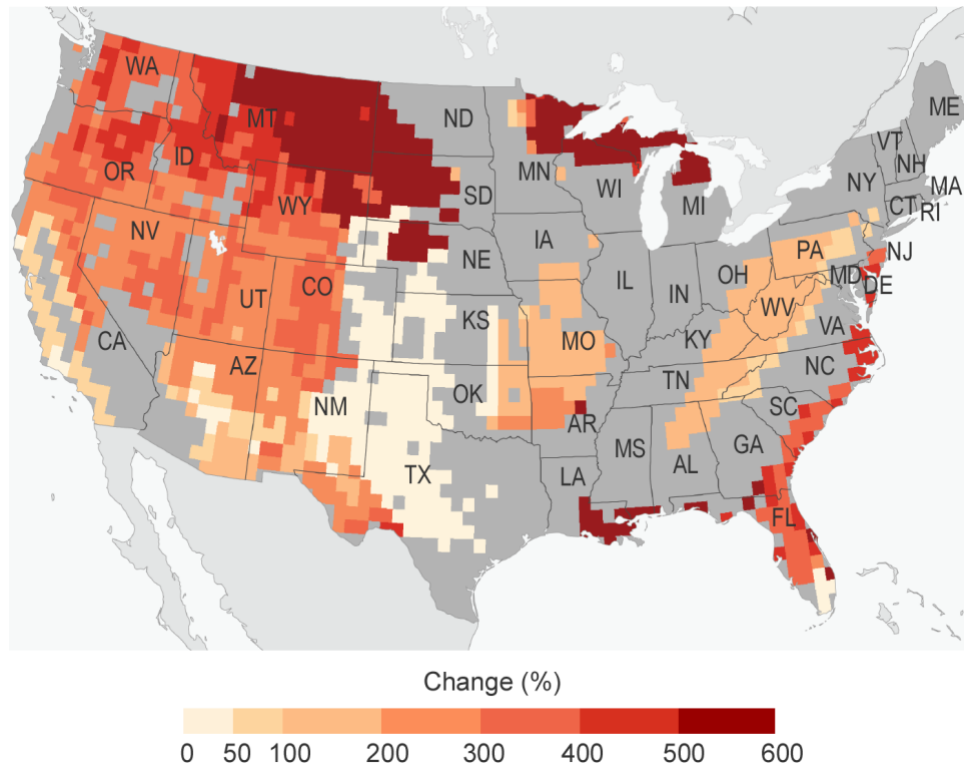
Figure 5.2. The map shows projected percentage increases in weeks with risk of very large fires (VLF; greater than 5,000 hectares) in the contiguous United States by mid-century (2041–2070) compared to the recent past (1971–2000) under a higher scenario (RCP8.5). Large increases of more than 300% are projected for coastal North Carolina, and increases of 50%–100% are projected for the Western Mountains. Gray indicates areas where a VLF model could not be constructed due to a lack of data. Source: Barbero et al. 2015, as adapted in USGCRP 2016. Used with permission from CSIRO Publishing.

Box 5.1: 2016 Wildfire Season

In the fall of 2016, wildfires in North Carolina burned 62,000 acres of land in the mountains alone and more than 77,000 total acres across the state (North Carolina Forest Service 2017). In terms of area burned, it was the worst fire season in North Carolina since the mid-1980s. Unusual climate conditions were responsible for an elevated fire risk. Fall precipitation in

western North Carolina was less than half of normal (Figure 5.3), and the season ranked as the second driest fall (September–November) on record (southern Mountains climate division, NCEI Climate at a Glance). Fall temperatures in western North Carolina averaged 4°F above average, making it the warmest fall on record (Figure 5.4). For the rest of the climate divisions in the state, fall 2016 temperatures ranked from the second warmest in the northern Piedmont to the tenth warmest in the southern Coastal Plain. The unprecedented combination of record high fall temperatures and near-record low fall precipitation led to drought conditions ranging from "extreme" to "exceptional" (the highest category used by the U.S. Drought Monitor) by the end of November 2016 (Figure 5.5) in the far western part of the state.
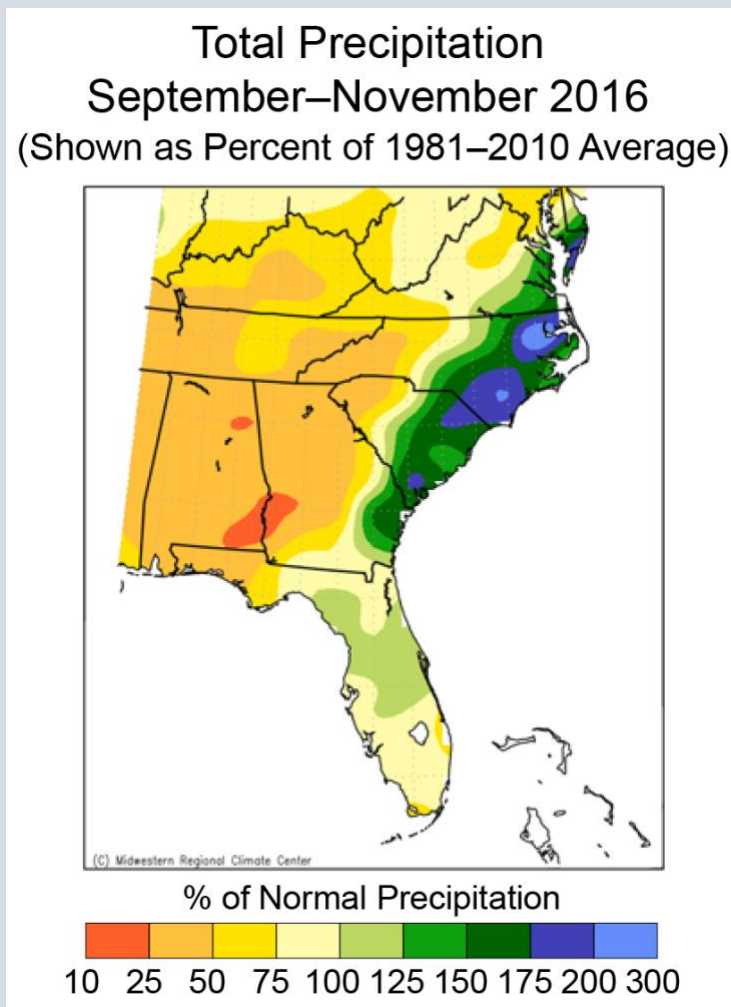
Figure 5.3. The map shows precipitation for fall (September–November) 2016 as a percentage of normal conditions for the southeastern United States. The western half of North Carolina experienced well below average precipitation, less than 50% of normal in the far west. Eastern North Carolina was much wetter, largely due to torrential rain from Hurricane Matthew. Source: Midwestern Regional Climate Center.
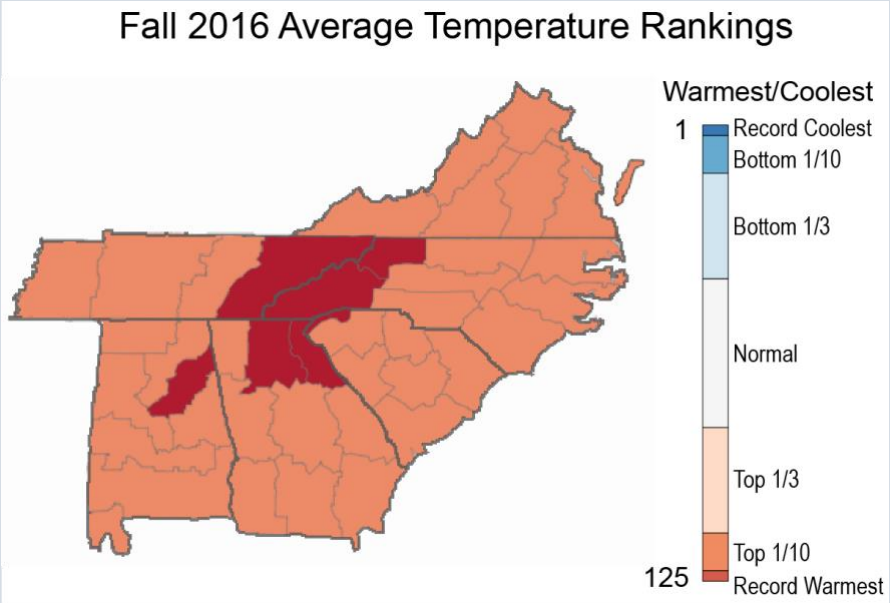
Figure 5.4. The map shows the ranking (out of 124 seasons in the historical record over 1895–2018) of average temperature for fall (September–November) 2016 by climate division for several states in the Southeast. The dark red color indicates a ranking of 124, or the warmest in the historical record. Fall 2016 was the warmest on record for western North Carolina and eastern Tennessee. Source: NCEI Climate at a Glance.
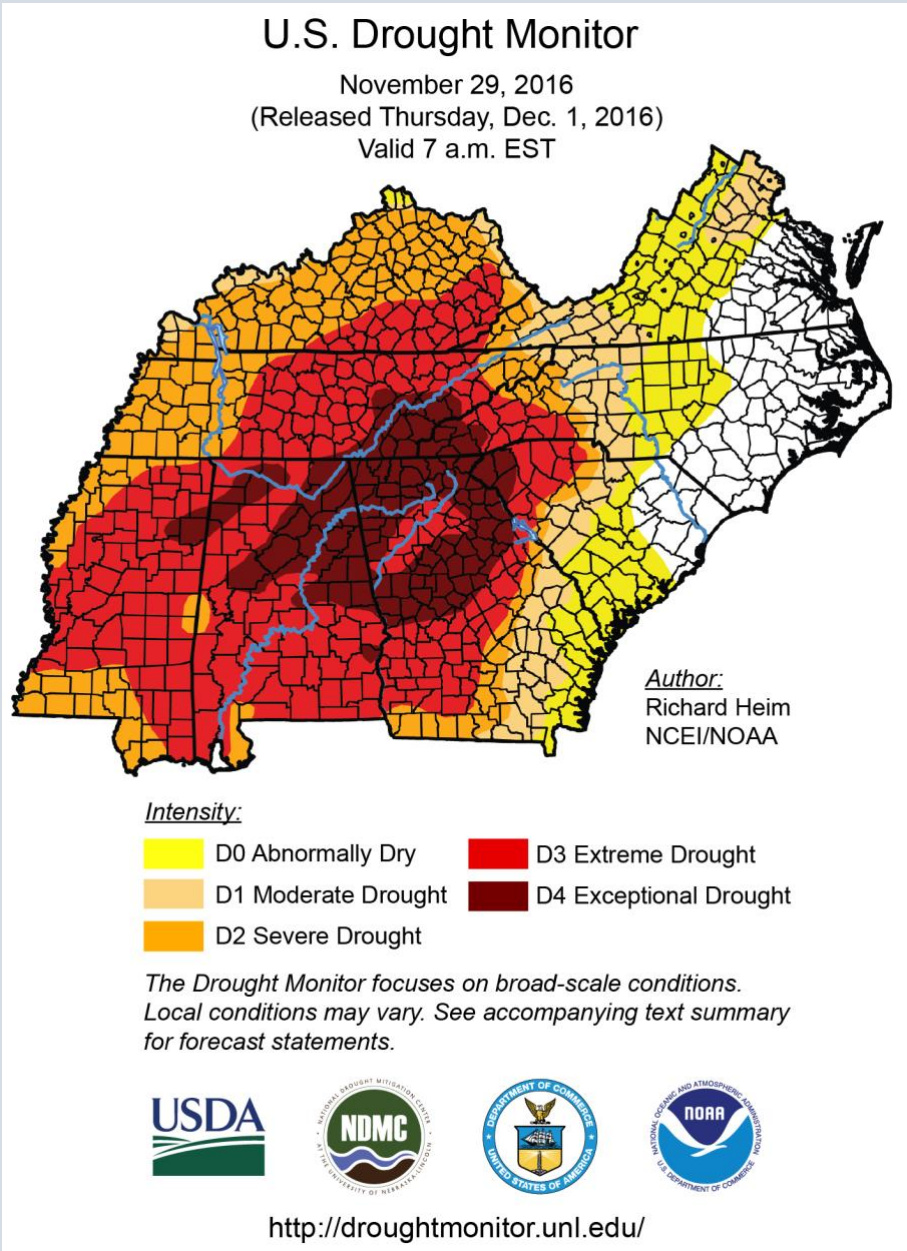
Figure 5.5. This figure shows U.S. Drought Monitor conditions for several states in the Southeast on November 29, 2016. The map shows the western half of North Carolina in a drought status. The far western part of the state was in exceptional drought, the most serious category. The U.S. Drought Monitor is jointly produced by the National Drought Mitigation Center (NDMC) at the University of Nebraska–Lincoln, the United States Department of Agriculture, and the National Oceanic and Atmospheric Administration. Map courtesy of NDMC.

In 2016, strong winds caused an existing fire to grow out of control in Gatlinburg, Tennessee, resulting in the deaths of 14 people, 130 sustained injuries, and damage to 1,684 structures. This area of eastern Tennessee, adjacent to the western North Carolina border, was also in exceptional drought status. The strong winds were not unusual for late November, and it was the combination of those winds and the exceptional drought conditions that provided the favorable wildfire conditions. This fire serves as an example of the significant potential for severe impacts from wildfires, particularly in heavily forested mountainous regions with limited access—environments common in the Western Mountains of North Carolina—when weather and climate conditions are favorable (Gabbert 2016).

5.2.5. Prescribed Fire

Prescribed fire, or "controlled burning," refers to the intentional use of low-intensity fires in a controlled setting under a predetermined set of weather and fuel conditions that are affected by climate (Carter et al. 2018, Mitchell et al. 2014). The use of prescribed fire is a critical tool for maintaining the health of North Carolina's forests and for reducing the risk and impact of wildfires by reducing the hazardous fuels (North Carolina Forest Service n.d.[a]). The frequency of large wildfires is influenced by a complex combination of natural and human factors. Temperature, soil moisture, relative humidity, wind speed, and vegetation (fuel density) are important aspects of the relationship between fire frequency and ecosystems. Forest management and fire suppression practices, such as prescribed burning, can also alter this relationship from what it was in the preindustrial era. Changes in these control parameters can interact with each other in complex ways with the potential for tipping points—in both fire frequency and in ecosystem properties—that may be reached as the climate warms (Wehner et al. 2017).

By mid-century, annual average temperature in North Carolina is projected to increase by 2°–6°F (under both scenarios) and by 3°–11°F by the end of the century, depending on the scenario (see Figure 2.3). In all cases, warmer conditions will lead to more rapid drying, and it is likely that future droughts will be more severe (see Chapter 2 Drought section). Increases in severe drought may increase the occurrence of wildfire while also limiting the ability to use prescribed fires due to a reduction in the number of days that meet the requirements for conducting a controlled burn (Mitchell et al. 2014).

5.2.6. Wildland–Urban Interface

The wildland–urban interface (WUI) describes areas where human development meets and intermingles with undeveloped land, forest, or vegetative fuels (NWCG n.d.). Communities and homes within WUI areas are at an increased risk of damage from wildfire. North Carolina has more acres at the wildland–urban interface than any other state in the country, and that acreage increases every year (North Carolina Forest Service, n.d.[b]). Between 1990 and 2010, the statewide WUI land area increased by more than 28% (USDA Forest Service n.d.[a]), and there was nearly a 62% increase in the number of houses in WUI zones over the same period (USDA

Forest Service n.d.[b]). As urban expansion continues and housing developments extend farther into previously undeveloped areas, the opportunity to use prescribed fire as a means of mitigating wildfire damage may be reduced. This could lead to an increase in the occurrence of wildfire and to other health and economic impacts (Prestemon et al. 2016).

5.2.7. Summary

Future increases in annual and seasonal average temperatures and associated increases in drying rates are *very likely*. Changes in other climate elements that affect wildfire likelihood are uncertain. In particular, there is substantial uncertainty about future changes in precipitation. Nevertheless, it is certain that severe droughts will occur in the future, as they are a natural part of the climate system. Future droughts are *very likely* to be warmer, increasing the drying rate of fuels and leading to higher wildfire likelihood. Thus, it is *likely* that conditions conducive to wildfire occurrence will increase in the future.

5.3. Forest Ecosystem Changes

In addition to the impacts from wildfires, forests in the North Carolina mountains may be affected in other ways by the changing climate. Increased potential evapotranspiration from higher air temperatures likely will lead to decreased forest water yield and increased low flows in streams and rivers during droughts. The environmental conditions in which high-elevation forests have developed may disappear in the future from the projected future warming (McNulty et al. 2013). The Western Mountains encompass the highest elevations, and coolest climates, in the entire Southeast. The cool temperatures to which these forests have adapted may no longer exist in the southern Appalachians, putting the viability of the high-elevation ecosystems at risk.

5.4. Urban Heat Island Effects

The southeastern United States is rapidly changing, with a shift away from rural communities and a trend toward urbanization (Census Bureau 2017). In a rapidly urbanizing landscape, North Carolinians are vulnerable to another climate impact: the urban heat island (UHI) effect, which is the tendency for temperatures to be higher in cities and developed areas than in surrounding rural areas due to the absorption and emission of heat by buildings and other impervious surfaces (Maxwell et al. 2018).

In a warming climate, the UHI effect is projected to be stronger and more significant due to changes in the structure, spatial extent, and population density of urban areas (Hibbard et al. 2017), and in North Carolina, cities are already experiencing longer summer heat waves. For example, Raleigh is one of five U.S. cities (out of 50 large cities analyzed in a recent study) that are seeing increasing trends in all facets of heat waves: frequency, duration, intensity, and timing (Habeeb et al. 2015). These changes will disproportinately affect more vulnerable communities (e.g., lower income, communities of color, elderly populations), who are often located in urban centers and may not have access to sufficient cooling (Carter et al. 2018). The UHI is a climate

stress multiplier, and urban areas are prone to multiple impacts, including elevated emissions of air pollutants and greenhouse gases, compromised human health, and even water quality impairment (Yow 2007).

5.5. Ozone and Particulate Matter

Near-surface ozone and particulate matter are air pollutants that cause significant health impacts (Nolte et al. 2018). North Carolina is affected by both of these pollutants due to natural and human factors both within the state and from out-of-state sources. Climate change could affect the levels of both air pollutants in the state; however, the effect on fine particulate matter (particles that are 2.5 micrometers or less in size, referred to as $PM_{2.5}$) is currently too uncertain to draw firm conclusions about changes in health impacts (EPA 2017). Therefore, this section focuses on the projected climate change impacts on ozone levels. More information about climate change effects on $PM_{2.5}$ can be found in the Fourth National Climate Assessment (Nolte et al. 2018) and the associated EPA report (EPA 2017).

Ozone is a naturally occurring molecule in the atmosphere. In the stratosphere, it serves to protect us from harmful ultraviolet radiation, but ozone near the surface can cause severe health impacts (particularly respiratory issues) in humans. As a pollutant, ozone is formed from reactions involving emissions of oxides of nitrogen (NOx), volatile organic compounds (VOCs), heat, and sunlight. Since ozone levels are influenced by temperature and sunlight, a warming climate can cause increases in this pollutant if hot and sunny days become more frequent (Nolte et al. 2018). But ozone levels are also affected by wind speed, wind direction, precipitation, cloud cover, and the presence of other molecules in the atmosphere (such as methane). Furthermore, the most important determinant of future ozone levels will be the emission rates of precursor elements (mainly NOx and VOCs) that are emitted into the atmosphere.

Nationally, ozone levels have decreased by 21% since 1990, while in North Carolina the five-year average of measured ozone levels has declined by 23% since 1990 (EPA 2019). These reductions help to mitigate the "climate penalty" (Wu et al. 2008) of warming temperatures potentially causing higher ozone levels, particularly if additional reductions continue to occur (Rieder et al. 2018). Climate change is projected to cause an increase in summer ozone levels nationwide under both lower and higher emission scenarios, but there is significant regional variation. In North Carolina, ozone concentrations in the summer could decrease in the future even as temperatures increase if climate-driven meteorological changes result in wetter conditions and increased marine airflows (EPA, 2017; Nolte, 2018). There is also ***high confidence*** that as temperatures increase, the amount of water vapor in the atmosphere will also increase, which could further reduce near-surface ozone concentrations (Fiore et al. 2015, Rieder et al. 2018). However, while there is ***high confidence*** that water vapor will increase, there is ***low confidence*** as to whether summertime precipitation will increase or decrease across the state, which would influence the favorability of background environmental conditions driving ozone concentrations.

In summary, harmful levels of near-surface ozone result from a combination of climate conditions and human-caused emissions of precursor compounds. Near-surface ozone concentrations tend to increase with temperature. However, changes in other climate conditions, such as increased precipitation, can counteract the temperature effect. Overall, it is uncertain what the net effect will be. Thus, it is *as likely as not* that future ozone concentrations will increase.

5.6. References

Anderson, P. and B. Palik, 2011: Silviculture for Climate Change. (October 2011). U.S. Department of Agriculture Forest Service, Climate Change Resource Center. https://www.fs.usda.gov/ccrc/topics/silviculture

Barbero, R., J.T. Abatzoglou, N.K. Larkin, C.A. Kolden, and B. Stocks, 2015: Climate change presents increased potential for very large fires in the contiguous United States. *International Journal of Wildland Fire*. http://dx.doi.org/10.1071/WF15083

Carter, L., A. Terando, K. Dow, K. Hiers, K.E. Kunkel, A. Lascurain, D. Marcy, M. Osland, and P. Schramm, 2018: Southeast. *Impacts, Risks, and Adaptation in the United States: Fourth National Climate Assessment, Volume II*. Reidmiller, D.R., C.W. Avery, D. Easterling, K. Kunkel, K.L.M. Lewis, T.K. Maycock, and B.C. Stewart, Eds. U.S. Global Change Research Program, Washington, DC, USA, 743–808. http://dx.doi.org/10.7930/NCA4.2018.CH19

Census Bureau, 2017: Press kit: County and Metro Area Population. U.S. Census Bureau. https://www.census.gov/newsroom/press-kits/2017/20170323_popestimates.html

Clark, J.S., D.M. Bell, M.H. Hersh, and L. Nichols, 2011: Climate change vulnerability of forest biodiversity: Climate and competition tracking of demographic rates. *Global Change Biology,* **17** (5), 1834–1849. http://dx.doi.org/10.1111/j.1365-2486.2010.02380.x

Easterling, D.R., K.E. Kunkel, J.R. Arnold, T. Knutson, A.N. LeGrande, L.R. Leung, R.S. Vose, D.E. Waliser, and M.F. Wehner, 2017: Precipitation change in the United States. *Climate Science Special Report: Fourth National Climate Assessment, Volume I*. Wuebbles, D.J., D.W. Fahey, K.A. Hibbard, D.J. Dokken, B.C. Stewart, and T.K. Maycock, Eds. U.S. Global Change Research Program, Washington, DC, USA, 207–230. http://dx.doi.org/10.7930/J0H993CC

Elliott, C., S. Henderson, and V. Wan, 2013: Time series analysis of fine particulate matter and asthma reliever dispensations in populations affected by forest fires. *Environmental Health,* **12** (1), 11. http://dx.doi.org/10.1186/1476-069X-12-11

EPA, 2017: Multi-Model Framework for Quantitative Sectoral Impacts Analysis: A Technical Report for the Fourth National Climate Assessment. EPA 430-R-17-001. U.S. Environmental Protection Agency (EPA), Washington, DC, 271 pp. https://cfpub.epa.gov/si/si_public_record_Report.cfm?dirEntryId=335095

EPA, 2019: National Air Quality and Emissions Trends Report, 2018. U.S. Environmental Protection Agency, Office of Air Quality Planning and Standards, Research Triangle Park, NC. https://gispub.epa.gov/air/trendsreport/2018/

Fiore, A.M., V. Naik, and E.M. Leibensperger, 2015: Air quality and climate connections. *Journal of the Air & Waste Management Association,* **65** (6), 645–685. http://dx.doi.org/10.1080/10962247.2015.1040526

Gabbert, B., 2016: "Analyzing the fire that burned into Gatlinburg." *Wildfire Today*. https://wildfiretoday.com/2016/12/05/analyzing-the-fire-that-burned-into-gatlinburg/

Habeeb, D., J. Vargo, and B. Stone, 2015: Rising heat wave trends in large US cities. *Natural Hazards,* **76** (3), 1651–1665. http://dx.doi.org/10.1007/s11069-014-1563-z

Henderson, S.B., M. Brauer, Y.C. MacNab, and S.M. Kennedy, 2011: Three measures of forest fire smoke exposure and their associations with respiratory and cardiovascular health outcomes in a population-based cohort. *Environmental Health Perspectives,* **119** (9), 1266–1271. http://dx.doi.org/10.1289/ehp.1002288

Hibbard, K.A., F.M. Hoffman, D. Huntzinger, and T.O. West, 2017: Changes in land cover and terrestrial biogeochemistry. *Climate Science Special Report: Fourth National Climate Assessment, Volume I*. Wuebbles, D.J., D.W. Fahey, K.A. Hibbard, D.J. Dokken, B.C. Stewart, and T.K. Maycock, Eds. U.S. Global Change Research Program, Washington, DC, USA, 277–302. http://dx.doi.org/10.7930/J0416V6X

Holstius, D.M., C.E. Reid, B.M. Jesdale, and R. Morello-Frosch, 2012: Birth weight following pregnancy during the 2003 Southern California wildfires. *Environmental Health Perspectives,* **120** (9), 1340–1345. http://dx.doi.org/10.1289/ehp.1104515

Johnston, F., I. Hanigan, S. Henderson, G. Morgan, and D. Bowman, 2011: Extreme air pollution events from bushfires and dust storms and their association with mortality in Sydney, Australia 1994–2007. *Environmental Research,* **111** (6), 811–816. http://dx.doi.org/10.1016/j.envres.2011.05.007

Johnston, F.H., S.B. Henderson, Y. Chen, J.T. Randerson, M. Marlier, R.S. DeFries, P. Kinney, D.M.J.S. Bowman, and M. Brauer, 2012: Estimated global mortality attributable to smoke from landscape fires. *Environmental Health Perspectives,* **120** (5), 695–701. http://dx.doi.org/10.1289/ehp.1104422

Kunkel, K.E., 2001: Chapter 9: Surface Energy Budget and Fuel Moisture. *Forest Fires*. Johnson, E.A. and K. Miyanishi, Eds. Academic Press, San Diego, 303–350. http://dx.doi.org/https://doi.org/10.1016/B978-012386660-8/50011-8

Maxwell, K., S. Julius, A. Grambsch, A. Kosmal, L. Larson, and N. Sonti, 2018: Built Environment, Urban Systems, and Cities. *Impacts, Risks, and Adaptation in the United States: Fourth National Climate Assessment, Volume II*. Reidmiller, D.R., C.W. Avery, D. Easterling, K. Kunkel, K.L.M. Lewis, T.K. Maycock, and B.C. Stewart, Eds. U.S. Global Change Research Program, Washington, DC, USA, 438–478. http://dx.doi.org/10.7930/NCA4.2018.CH11

McNulty, S., P. Caldwell, T.W. Doyle, K. Johnsen, Y. Liu, J. Mohan, J. Prestemon, and G. Sun, 2013: Forests and climate change in the Southeast USA. *Climate of the Southeast United States: Variability, Change, Impacts, and Vulnerability*. Ingram, K.D., K.; Carter, L.; Anderson, J., Ed. Island Press, Washington DC, 165–189.

Melvin, M.A., 2015: 2015 National Prescribed Fire Use Survey Report. Technical Report 02-15. Coalition of Prescribed Fire Councils, 17 pp. https://stateforesters.org/sites/default/files/publication-documents/2015%20Prescribed%20Fire%20Use%20Survey%20Report.pdf

Mitchell, R.J., Y. Liu, J.J. O'Brien, K.J. Elliott, G. Starr, C.F. Miniat, and J.K. Hiers, 2014: Future climate and fire interactions in the southeastern region of the United States. *Forest Ecology and Management,* **327**, 316–326. http://dx.doi.org/10.1016/j.foreco.2013.12.003

Naeher, L.P., M. Brauer, M. Lipsett, J.T. Zelikoff, C.D. Simpson, J.Q. Koenig, and K.R. Smith, 2007: Woodsmoke health effects: A review. *Inhalation Toxicology,* **19** (1), 67–106. http://dx.doi.org/10.1080/08958370600985875

Nolte, C.G., P.D. Dolwick, N. Fann, L.W. Horowitz, V. Naik, R.W. Pinder, T.L. Spero, D.A. Winner, and L.H. Ziska, 2018: Air Quality. *Impacts, Risks, and Adaptation in the United States: Fourth National Climate Assessment, Volume II*. Reidmiller, D.R., C.W. Avery, D. Easterling, K. Kunkel, K.L.M. Lewis, T.K. Maycock, and B.C. Stewart, Eds. U.S. Global Change Research Program, Washington, DC, USA, 512–538. http://dx.doi.org/10.7930/NCA4.2018.CH13

North Carolina Forest Service, 2017: 2017—Biennial Report.
https://ncforestservice.gov/publications/2017BiennialReport.pdf

North Carolina Forest Service, n.d.(a): Prescribed Fire Overview, accessed November 14, 2019.
https://ncforestservice.gov/fire_control/fc_prescribedfire.htm

North Carolina Forest Service, n.d.(b): The Wildland/Urban Interface, accessed November 14, 2019.
https://www.ncforestservice.gov/fire_control/fc_wui.htm

Noss, R.F., 2012: *Forgotten Grasslands of the South: Natural History and Conservation*. Island Press, Washington, DC, 320 pp.

NWCG, n.d.: NWCG Glossary of Wildland Fire, PMS 205. National Wildfire Coordinating Group, accessed November 14, 2019. https://www.nwcg.gov/glossary/a-z#letter_w

NWS, n.d.: Flooding in North Carolina. NOAA National Weather Service, accessed November 5, 2019. https://www.weather.gov/safety/flood-states-nc

Paerl, H.W., N.S. Hall, A.G. Hounshell, R.A. Luettich, K.L. Rossignol, C.L. Osburn, and J. Bales, 2019: Recent increase in catastrophic tropical cyclone flooding in coastal North Carolina, USA: Long-term observations suggest a regime shift. *Scientific Reports,* **9** (1), 10620. http://dx.doi.org/10.1038/s41598-019-46928-9

Peterson, T.C., R.R. Heim, R. Hirsch, D.P. Kaiser, H. Brooks, N.S. Diffenbaugh, R.M. Dole, J.P. Giovannettone, K. Guirguis, T.R. Karl, R.W. Katz, K. Kunkel, D. Lettenmaier, G.J. McCabe, C.J. Paciorek, K.R. Ryberg, S. Schubert, V.B.S. Silva, B.C. Stewart, A.V. Vecchia, G. Villarini, R.S. Vose, J. Walsh, M. Wehner, D. Wolock, K. Wolter, C.A. Woodhouse, and D. Wuebbles, 2013: Monitoring and understanding changes in heat waves, cold waves, floods and droughts in the United States: State of knowledge. *Bulletin of the American Meteorological Society,* **94** (6), 821–834. http://dx.doi.org/10.1175/BAMS-D-12-00066.1

Prestemon, J.P., U. Shankar, A. Xiu, K. Talgo, D. Yang, E. Dixon, D. McKenzie, and K.L. Abt, 2016: Projecting wildfire area burned in the southeastern United States, 2011–60. *International Journal of Wildland Fire,* **25** (7), 715–729. http://dx.doi.org/10.1071/WF15124

Rieder, H.E., A.M. Fiore, O.E. Clifton, G. Correa, L.W. Horowitz, and V. Naik, 2018: Combining model projections with site-level observations to estimate changes in distributions and seasonality of ozone in surface air over the U.S.A. **193**, 302–315. http://dx.doi.org/10.1016/j.atmosenv.2018.07.042

Stefanidou, M., S. Athanaselis, and C. Spiliopoulou, 2008: Health impacts of fire smoke inhalation. *Inhalation Toxicology,* **20** (8), 761–766. http://dx.doi.org/10.1080/08958370801975311

USDA Forest Service, 2019: Forests of North Carolina, 2018. Resource Update FS-225. U.S. Department of Agriculture, Forest Service, Asheville, NC, 2 pp. http://dx.doi.org/10.2737/FS-RU-225

USDA Forest Service, n.d.(a): Area of Wildland–Urban Interface (WUI) by State, accessed November 14, 2019. https://www.nrs.fs.fed.us/data/wui/state_summary/#wui-area

USDA Forest Service, n.d.(b): Houses in the Wildland–Urban Interface (WUI) by State, accessed November 14, 2019. https://www.nrs.fs.fed.us/data/wui/state_summary/#wui-houses

USGCRP, 2016: *The Impacts of Climate Change on Human Health in the United States: A Scientific Assessment*. U.S. Global Change Research Program, Washington, DC, 312 pp. http://dx.doi.org/10.7930/J0R49NQX

Vose, J.M., D.L. Peterson, G.M. Domke, C.J. Fettig, L.A. Joyce, R.E. Keane, C.H. Luce, J.P. Prestemon, L.E. Band, J.S. Clark, N.E. Cooley, A. D'Amato, and J.E. Halofsky, 2018: Forests. *Impacts, Risks, and Adaptation in the United*

States: Fourth National Climate Assessment, Volume II. Reidmiller, D.R., C.W. Avery, D. Easterling, K. Kunkel, K.L.M. Lewis, T.K. Maycock, and B.C. Stewart, Eds. U.S. Global Change Research Program, Washington, DC, USA, 232–267. http://dx.doi.org/10.7930/NCA4.2018.CH6

Wear, D.N., D.R. Carter, and J. Prestemon, 2007: The U.S. South's Timber Sector in 2005: A Prospective Analysis of Recent Change. Gen. Tech. Rep. SRS-99. U.S. Department of Agriculture, Forest Service, Southern Research Station, Asheville, NC, 44 pp. https://www.srs.fs.usda.gov/pubs/gtr/gtr_srs099.pdf

Wehner, M.F., J.R. Arnold, T. Knutson, K.E. Kunkel, and A.N. LeGrande, 2017: Droughts, floods, and wildfires. *Climate Science Special Report: Fourth National Climate Assessment, Volume I*. Wuebbles, D.J., D.W. Fahey, K.A. Hibbard, D.J. Dokken, B.C. Stewart, and T.K. Maycock, Eds. U.S. Global Change Research Program, Washington, DC, USA, 231–256. http://dx.doi.org/10.7930/J0CJ8BNN

Wu, S., L.J. Mickley, E.M. Leibensperger, D.J. Jacob, D. Rind, and D.G. Streets, 2008: Effects of 2000–2050 global change on ozone air quality in the United States. *Journal of Geophysical Research: Atmospheres,* **113** (D6). http://dx.doi.org/10.1029/2007JD008917

Yow, D.M., 2007: Urban Heat Islands: Observations, Impacts, and Adaptation. *Geography Compass,* **1** (6), 1227–1251. http://dx.doi.org/10.1111/j.1749-8198.2007.00063.x

6. Engineering Design Standards

6.1. Building Design

Physical infrastructure (buildings, roads, utility systems, etc.) is generally constructed to last for several decades. Such infrastructure will experience the effects of global warming over its lifetime. Design of infrastructure incorporates the effects of climate. For example, the capacity of heating and air-conditioning equipment is based on the average and extreme temperature and humidity conditions at the location of the building. Specifically, percentile measures of the temperature and humidity climate called "design" values are calculated from observed weather data. Traditionally, the design calculation uses the historical climate of a location to determine the capacity. However, as the climate warms, these design considerations will change and the capacity may no longer be optimum for the new climate conditions.

There have been no systematic quantitative studies of the impacts of warming and associated climate conditions on infrastructure design standards for North Carolina. The development of a set of design standards for North Carolina that incorporate potential effects of global warming is a large undertaking and beyond the scope of this report. However, the results of a recent study for Langley Air Force Base (Kunkel et al. 2017), located in Hampton, Virginia, are presented to provide qualitative insights into potential future changes for North Carolina, particularly for the eastern half of the state, where the general climate conditions are similar to those at Langley.

Climate model simulations project large changes, relative to historical variability, in global temperature and atmospheric water vapor content. It is not surprising, then, that all of the temperature- and humidity-related design values increase substantially by 2065 under both higher (RCP8.5) and lower (RCP4.5) future scenarios. Temperature design values are thresholds that are exceeded only a small percentage of all hours and are expressed as percentiles of the ranked distribution of all temperature observations at a location. Percentiles commonly used by design professionals are 1.0% and 0.4%, which translate to an average of 87 hours and 35 hours, respectively, that the design temperature is exceeded in an average year. The design value percentage chosen for any given application reflects a tradeoff between the costs of building and the tolerance for uncomfortable conditions inside the building. Two types of temperature metrics are used in design: 1) the dry-bulb temperature, which is the actual air temperature, and (2) the wet-bulb temperature, which combines temperature and humidity and reflects the total load on air conditioning systems to both cool and dehumidify air. For Langley, the 0.4% dry-bulb temperature increases from 93°F to 97°F under the lower scenario and from 93°F to 100°F under the higher scenario (Figure 6.1). The 0.4% wet-bulb temperature increases from 80°F to 83°F under the lower scenario and from 80°F to 84°F under the higher scenario.
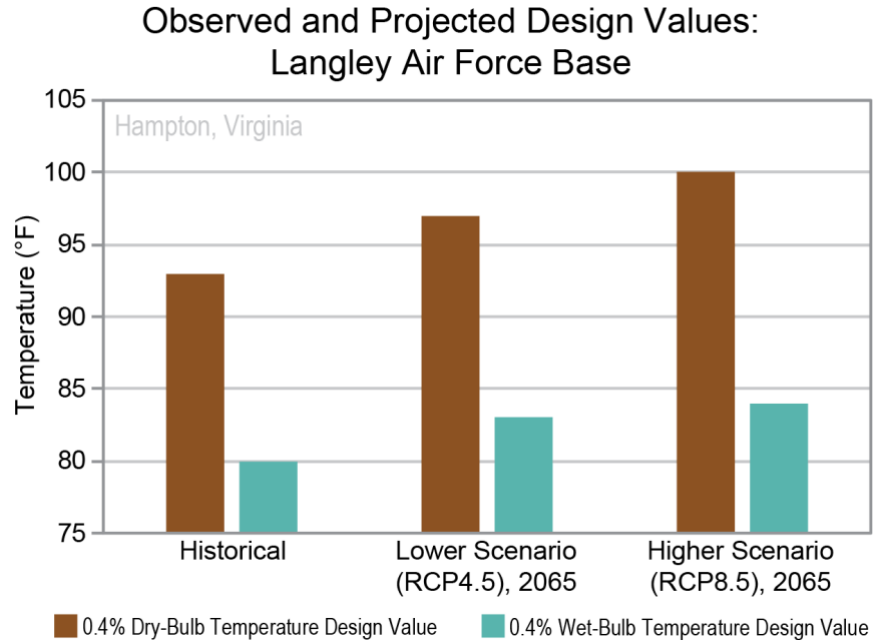
Figure 6.1. This figure shows historical (1976–2005) and projected (2065) values of the 0.4% dry-bulb (brown) and wet-bulb (green) design temperatures for Langley Air Force Base. Source: Kunkel et al. 2017.

The energy required for cooling in an air conditioning system consists of two components. The first, referred to as the sensible component, is the cooling of dry air. The second, referred to as the latent component, is the energy used in dehumidification of the air. In humid climates such as North Carolina, the latent component of energy required for cooling is a substantial component of air conditioning load. The ventilation cooling load index (VCLI) is a metric representing these two components. VCLI values for Langley AFB also increase significantly under the future scenarios (Figure 6.2), indicating a higher energy demand for cooling. The latent component increases from the current value of 4.6 to future values of 6.6 (under the lower scenario) and 7.9 (under the higher scenario). The sensible component increases from the current value of 1.0 to future values of 2.2 and 2.8, under the lower and higher scenarios, respectively.
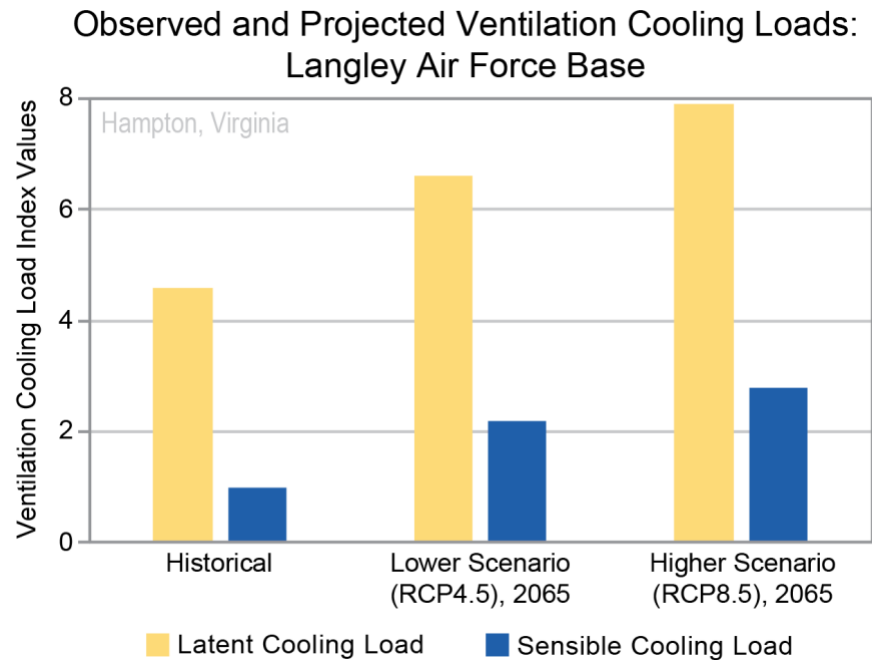
Figure 6.2. This figure shows historical (1976–2005) and projected (2065) values of the ventilation cooling load index for Langley Air Force Base. Source: Kunkel et al. 2017.

To summarize, both cold and hot design temperatures are projected to warm. In addition, all design metrics associated with absolute atmospheric water vapor content are projected to increase. This means that the peak energy demand associated with air conditioning is projected to increase while the peak energy demand for heating is projected to decrease.

6.2. Extreme Precipitation

Basic physics dictates that increases in greenhouse gas concentrations will gradually warm the ocean surface waters, as well as the land surface. The increase in ocean surface temperatures will cause an increase in near-surface absolute humidity over the oceans because the saturation value of absolute humidity is an exponential function of temperature, increasing about 3.5% per °F. This increase is projected to have an important consequence: the amount of water vapor available to precipitation-producing weather systems will increase. An analysis of extreme precipitation events has shown that the magnitude of such events scales closely with the water vapor amount. Thus, it is *very likely* that rainfall design values will increase in the future as the globe warms. Runoff control infrastructure designed according to current design values will fail more frequently in the future, leading to increased frequency of flooding in those areas protected by that infrastructure.

For North Carolina, projected increases in water vapor from climate models are in the range of 10%–15% for the lower scenario and 15%–20% for the higher scenario by the middle of the 21st century (Figures S.1 and S.2 in Kunkel et al. 2013). These changes in water vapor suggest increases of 10%–20% in rainfall design values by the middle of the 21st century.

6.3. The Future

Current design values are based on historical data and do not incorporate recent trends; thus, some standards may already be out of date. Several professional societies, however, are actively working on methods to incorporate climate change into national standards, and updated standards appropriate for use in a changing climate may be available in the near future. For example, the American Society of Civil Engineers (ASCE), and specifically the Committee on Adaptation to a Changing Climate (https://www.asce.org/climate-change/committee-on-adaptation-to-a-changing-climate), is being proactive in its ongoing efforts to update design codes and standards (e.g., ASCE Manual of Practice 140). In addition, the Federal Highway Administration has published its own manual to deal with transportation-related flooding that already includes climate considerations (FHWA 2015). The American Society of Heating, Refrigerating and Air-Conditioning Engineers is preparing a climate change chapter for its 2020 Handbook of Fundamentals. It is very likely that most design standards and codes will be updated to incorporate climate change, but they will need to be continuously updated in the future as we learn more.

6.4. References

FHWA, 2015: Climate Change Adaptation Guide for Transportation Systems Management, Operations, and Maintenance, FHWA-HOP-15-026. Department of Transportation, Federal Highway Administration, Washington, DC. https://ops.fhwa.dot.gov/publications/fhwahop15026/

Kunkel, K.E., T.R. Karl, D.R. Easterling, K. Redmond, J. Young, X. Yin, and P. Hennon, 2013: Probable maximum precipitation and climate change. *Geophysical Research Letters,* **40** (7), 1402–1408. http://dx.doi.org/10.1002/grl.50334

Kunkel, K.E., S.M. Champion, L. Sun, and J. Rennie, 2017: Climate Model Data Support to the Assistant Secretary of Air Force (ASAF) Climate Projection Engineering Weather Data (EWD) Project. Final Report, Contract N61340-14-C-6103 P00013. 53 pp.

Appendix A: Datasets and Scenarios

A.1. Observational Datasets Used in Climate Studies

Historical seasonal and annual temperature and precipitation conditions for North Carolina were analyzed using data from NOAA's National Centers for Environmental Information (NCEI) Climate Divisional Dataset (nClimDiv), version 2. This dataset is of monthly time resolution and has incorporated several modern techniques to correct for non-climatic shifts in the raw data resulting from changes in location and instrumentation of observation stations as well as other changes in observation methodologies. It is now the standard dataset used by NCEI to assess the state of the climate in the continental United States.

Graphics illustrating daily extreme metrics of temperature and precipitation were based on NOAA NCEI's Global Historical Climatology Network-Daily (GHCN-D), version 3. This dataset is a comprehensive compilation of available data from climate observing stations. It includes the complete records of digital data from stations in the U.S. Cooperative Observer Program (COOP), which is the core climate network of the United States. Some stations in the COOP have observations extending back to the late 19th century. The core observations of COOP stations include daily precipitation, daily maximum temperature, daily minimum temperature, daily snowfall, and daily snow depth. The stations are sited with the intent to provide a representative sampling of all areas of the state. The great value of this network is its longevity and spatial sampling. For this reason, it is the best observational resource to establish long-term variations and trends in the surface climate of North Carolina.

Hurricane statistics (Figure 2.28) were derived from the International Best Track Archive for Climate Stewardship (IBTrACS; Knapp et al. 2010). This dataset has global coverage and extends back to the 19th Century. Wet-bulb data (Figure 2.27) were obtained from meteorological reanalysis data, specifically the Modern-Era Retrospective Analysis for Research and Applications, Version 2 (MERRA-2; Gelaro et al. 2017). A reanalysis dataset is an assimilation of meteorological observations that produces an estimate of the 4-dimensional state of the atmosphere. The MERRA-2 reanalysis has global coverage and extends back to 1980.

A.2. Projections and Scenarios

Projections of future climate use analyses of data from the Coupled Model Intercomparison Project Phase 5 (CMIP5, Taylor et al. 2012). Specifically, CMIP5 data were used as the foundation for a new statistically downscaled dataset derived from the CMIP5 simulations, named the Localized Constructed Analogs (LOCA, Pierce et al. 2014). The LOCA data include 32 CMIP5 models covering the period 1950–2100, including the historical period of 1950–2005, and a high emissions scenario and a low emissions scenario for 2006–2100. The LOCA data include maximum temperature, minimum temperature, and precipitation at a daily resolution and at 1/16th degree spatial resolution.

The projected time series figures also include observations, but these observations are derived from the Livneh dataset (Livneh et al. 2013) rather than nClimDiv (Vose et al. 2014) or GHCN-D (Menne et al. 2012). The LOCA projections use the Livneh data as the basis for the statistical downscaling, so the Livneh observational data provide a more consistent basis for comparing projections to observations. The Livneh dataset ends in 2013, so these plots do not include observations for the most recent years, and there are sometimes other small differences between the two sets of observations.

Projections from computer models in this report are based on a set of hypothetical future scenarios called Representative Concentration Pathways, or RCPs. There are four RCPs, and they encompass a range of potential greenhouse gas concentrations based on emissions of greenhouse gases and aerosols as well as the effects of land-use change (e.g., see Jay et al. 2018). Most of the projections referenced in this report are based on two of the RCPs: a higher scenario (RCP8.5), in which greenhouse gas emissions continue to increase through the end of the century, and a lower scenario (RCP4.5), in which emissions increase at a slower rate, peak around the middle of the century, and then begin to decrease (Figure A.1). The RCP4.5 scenario assumes the adoption of climate policies aimed at reducing emissions and total temperature change. The numbers 8.5 and 4.5 indicate the resulting radiative forcing (see Chapter 1) in Watts per square meter as of 2100.
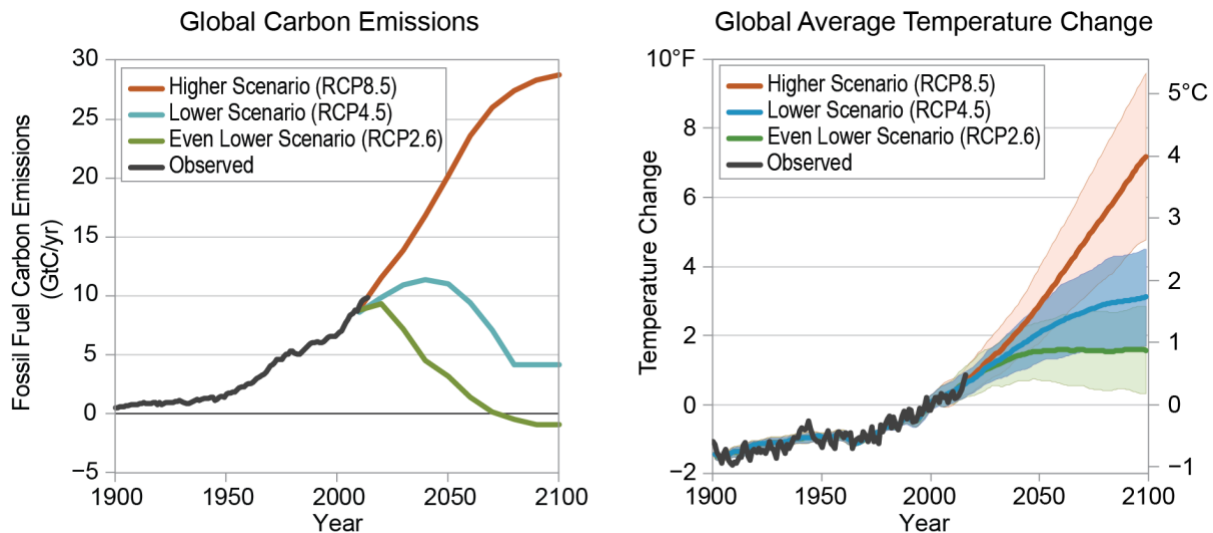
Figure A.1. (left) Observed and projected global carbon emissions. The black line shows observed carbon emissions (1900–2016) resulting from human activities. Under the higher scenario used in this report (RCP8.5, burnt orange line), emissions continue to increase through the end of the century. Under the lower scenario used in this report (RCP4.5, blue line), emissions increase at a slower rate, peak around midcentury, and then decline in response to climate change mitigation policies. Also shown is an even lower scenario (RCP2.6, green line), which assumes rapid emissions reductions and eventually net negative emissions. (right) Observed temperatures and the projected future temperature changes associated with the

three RCP scenarios shown in the left panel. Temperature changes are shown relative to the 1986–2015 global average. Source: Hayhoe et al. 2018.

A.3. References

Gelaro, R., W. McCarty, M.J. Suárez, R. Todling, A. Molod, L. Takacs, C.A. Randles, A. Darmenov, M.G. Bosilovich, R. Reichle, K. Wargan, L. Coy, R. Cullather, C. Draper, S. Akella, V. Buchard, A. Conaty, A.M. da Silva, W. Gu, G.-K. Kim, R. Koster, R. Lucchesi, D. Merkova, J.E. Nielsen, G. Partyka, S. Pawson, W. Putman, M. Rienecker, S.D. Schubert, M. Sienkiewicz, and B. Zhao, 2017: The Modern-Era Retrospective Analysis for Research and Applications, Version 2 (MERRA-2). *Journal of Climate,* **30** (14), 5419–5454. http://dx.doi.org/10.1175/JCLI-D-16-0758.1

Hayhoe, K., D.J. Wuebbles, D.R. Easterling, D.W. Fahey, S. Doherty, J. Kossin, W. Sweet, R. Vose, and M. Wehner, 2018: Our Changing Climate. *Impacts, Risks, and Adaptation in the United States: Fourth National Climate Assessment, Volume II*. Reidmiller, D.R., C.W. Avery, D. Easterling, K. Kunkel, K.L.M. Lewis, T.K. Maycock, and B.C. Stewart, Eds. U.S. Global Change Research Program, Washington, DC, USA, 72–144. http://dx.doi.org/10.7930/NCA4.2018.CH2

Jay, A., D.R. Reidmiller, C.W. Avery, D. Barrie, B.J. DeAngelo, A. Dave, M. Dzaugis, M. Kolian, K.L.M. Lewis, K. Reeves, T. West, and D. Winner, 2018: Overview. *Impacts, Risks, and Adaptation in the United States: Fourth National Climate Assessment, Volume II*. Reidmiller, D.R., C.W. Avery, D. Easterling, K. Kunkel, K.L.M. Lewis, T.K. Maycock, and B.C. Stewart, Eds. U.S. Global Change Research Program, Washington, DC, USA, 33–71. http://dx.doi.org/10.7930/NCA4.2018.CH1

Knapp, K.R., M.C. Kruk, D.H. Levinson, H.J. Diamond, and C.J. Neumann, 2010: The International Best Track Archive for Climate Stewardship (IBTrACS). *Bulletin of the American Meteorological Society,* **91** (3), 363–376. http://dx.doi.org/10.1175/2009BAMS2755.1

Livneh, B., E.A. Rosenberg, C. Lin, B. Nijssen, V. Mishra, K.M. Andreadis, E.P. Maurer, and D.P. Lettenmaier, 2013: A long-term hydrologically based dataset of land surface fluxes and states for the conterminous United States: Update and extensions. *Journal of Climate,* **26** (23), 9384–9392. http://dx.doi.org/10.1175/JCLI-D-12-00508.1

Menne, M.J., I. Durre, B. Korzeniewski, S. McNeal, K. Thomas, X. Yin, S. Anthony, R. Ray, R.S. Vose, B.E. Gleason, and T.G. Houston. 2012: *Global Historical Climatology Network-Daily (GHCN-Daily), Version 3*. NOAA National Climatic Data Center. http://dx.doi.org/doi:10.7289/V5D21VHZ

Pierce, D.W., D.R. Cayan, and B.L. Thrasher, 2014: Statistical downscaling using Localized Constructed Analogs (LOCA). *Journal of Hydrometeorology,* **15** (6), 2558-2585. http://dx.doi.org/10.1175/jhm-d-14-0082.1

Taylor, K.E., R.J. Stouffer, and G.A. Meehl, 2012: An overview of CMIP5 and the experiment design. *Bulletin of the American Meteorological Society,* **93** (4), 485–498. http://dx.doi.org/10.1175/BAMS-D-11-00094.1

Vose, R.S., S. Applequist, M. Squires, I. Durre, M.J. Menne, C.N. Williams, Jr., C. Fenimore, K. Gleason, and D. Arndt. 2014: *NOAA's Gridded Cimate Divisional Dataset (CLIMDIV)*. NOAA National Climatic Data Center. http://dx.doi.org/doi:10.7289/V5M32STR
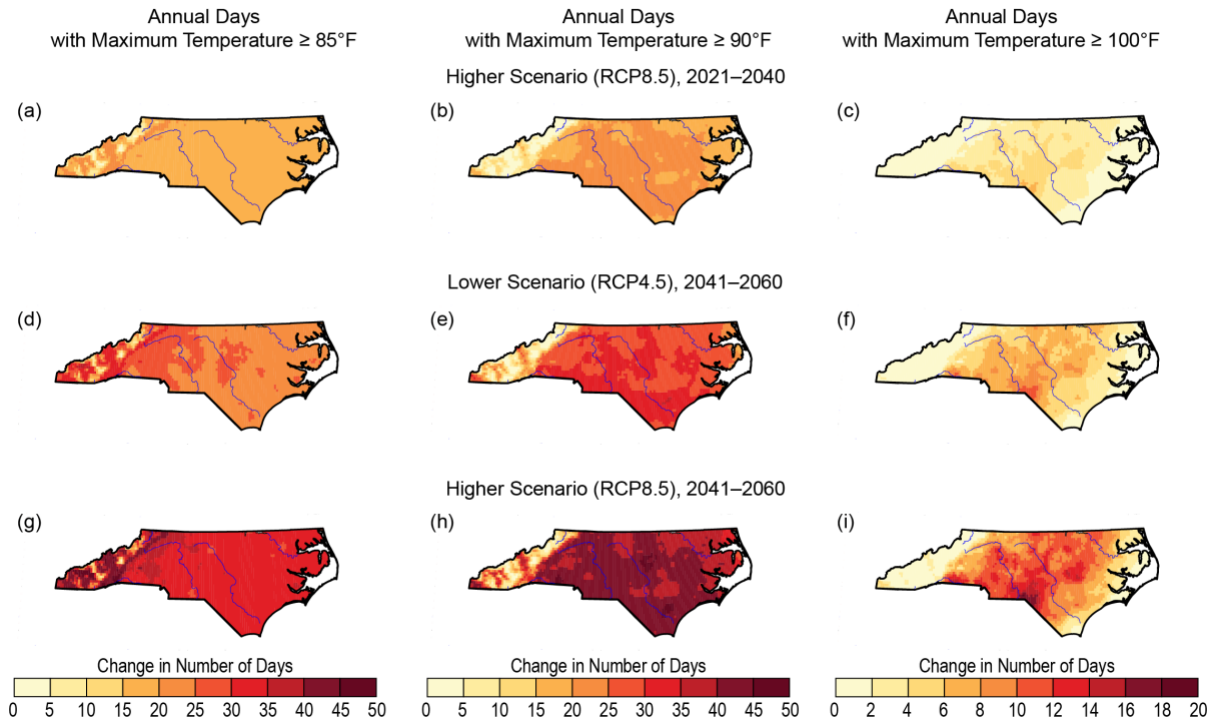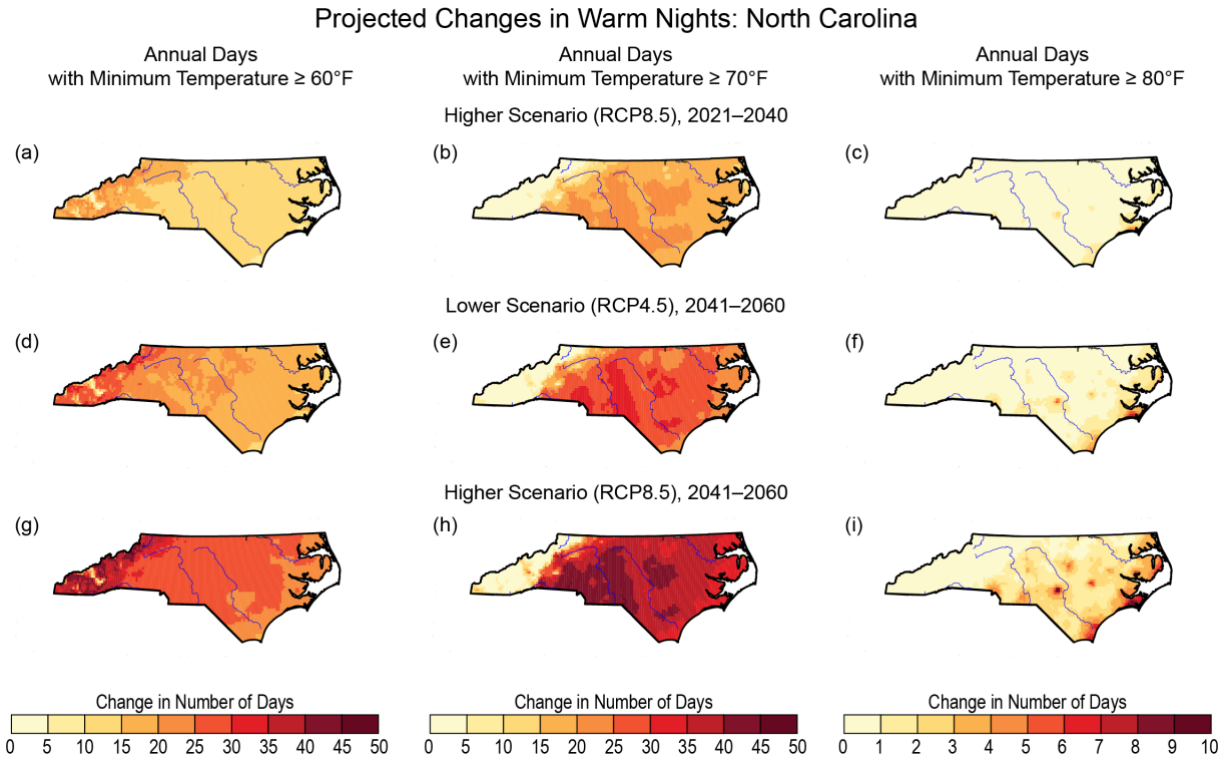
Appendix B: Supplemental Graphics

Figure B.1. The maps show projected changes in the number of days per year on which the maximum temperature is at or above 85°F (left column), 90°F (center column), and 100°F (right column) for North Carolina for two mid-century time periods and two climate futures. All projected values are shown as changes compared to 1996–2015 averages. Panels (a)–(c) show projected changes for 2021–2040 under a higher scenario (RCP8.5). Panels (d)–(f) depict projected changes for 2041–2060 under a lower scenario (RCP4.5), and panels (g)–(i) show projected changes under the higher scenario for the same period. Temperatures above these thresholds are far more common in the Piedmont and Coastal Plain regions. Days on which the maximum temperature exceeds both 85°F and 90°F are projected to increase across most of the state, with the greatest increases seen later in the century and under the higher scenario. By mid-century, the number of days on which the maximum temperature exceeds 100°F remains rare in the Western Mountains and along the North Carolina coast, but such hot days are projected to increase across the rest of the state. Source: The University of Edinburgh and NCICS.

Observed and Projected Hot Days:
North Carolina (1970–2100)

(a) Annual Days with Maximum Temperature ≥ 100°F

(b) Annual Days with Maximum Temperature ≥ 90°F

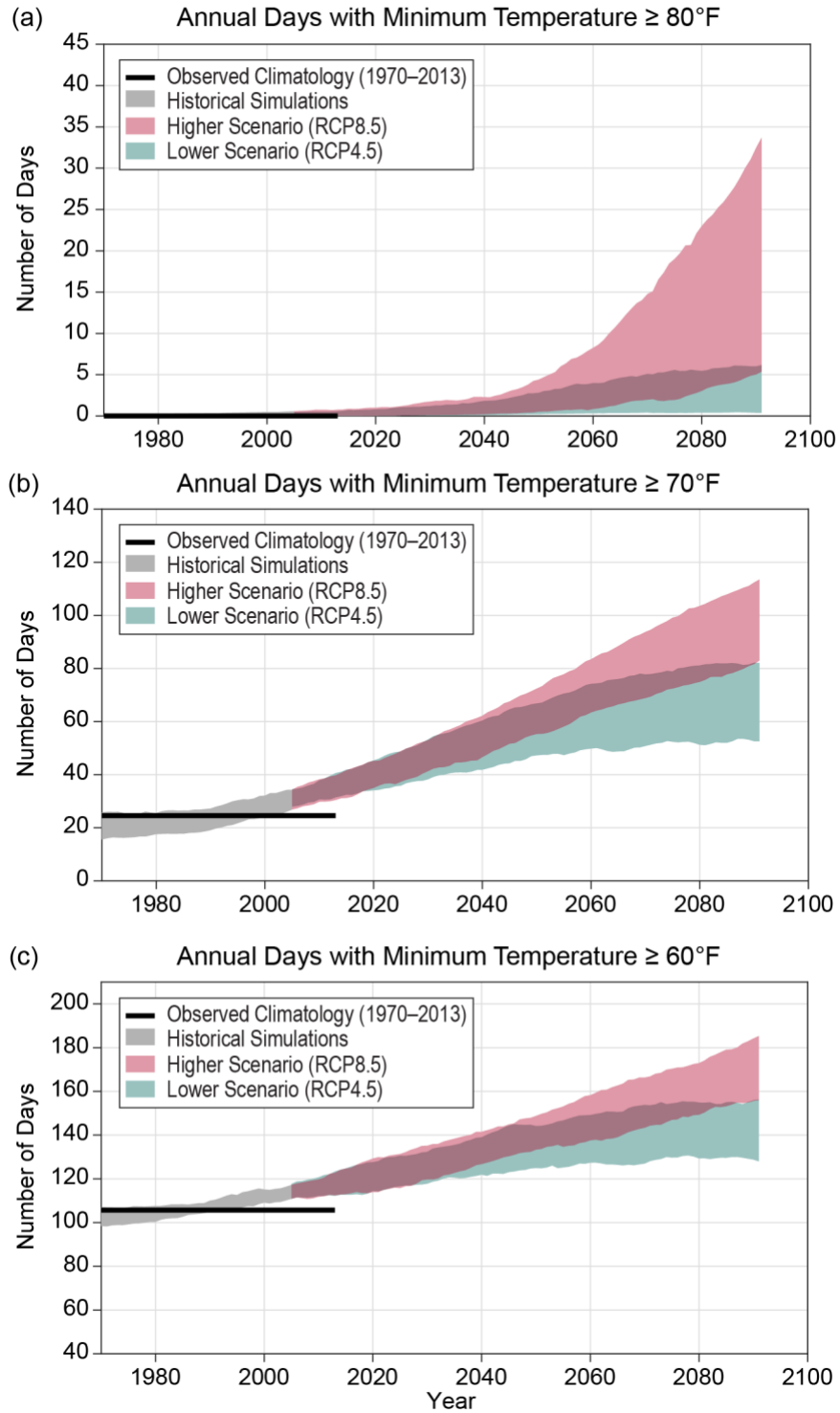(c) Annual Days with Maximum Temperature ≥ 85°F
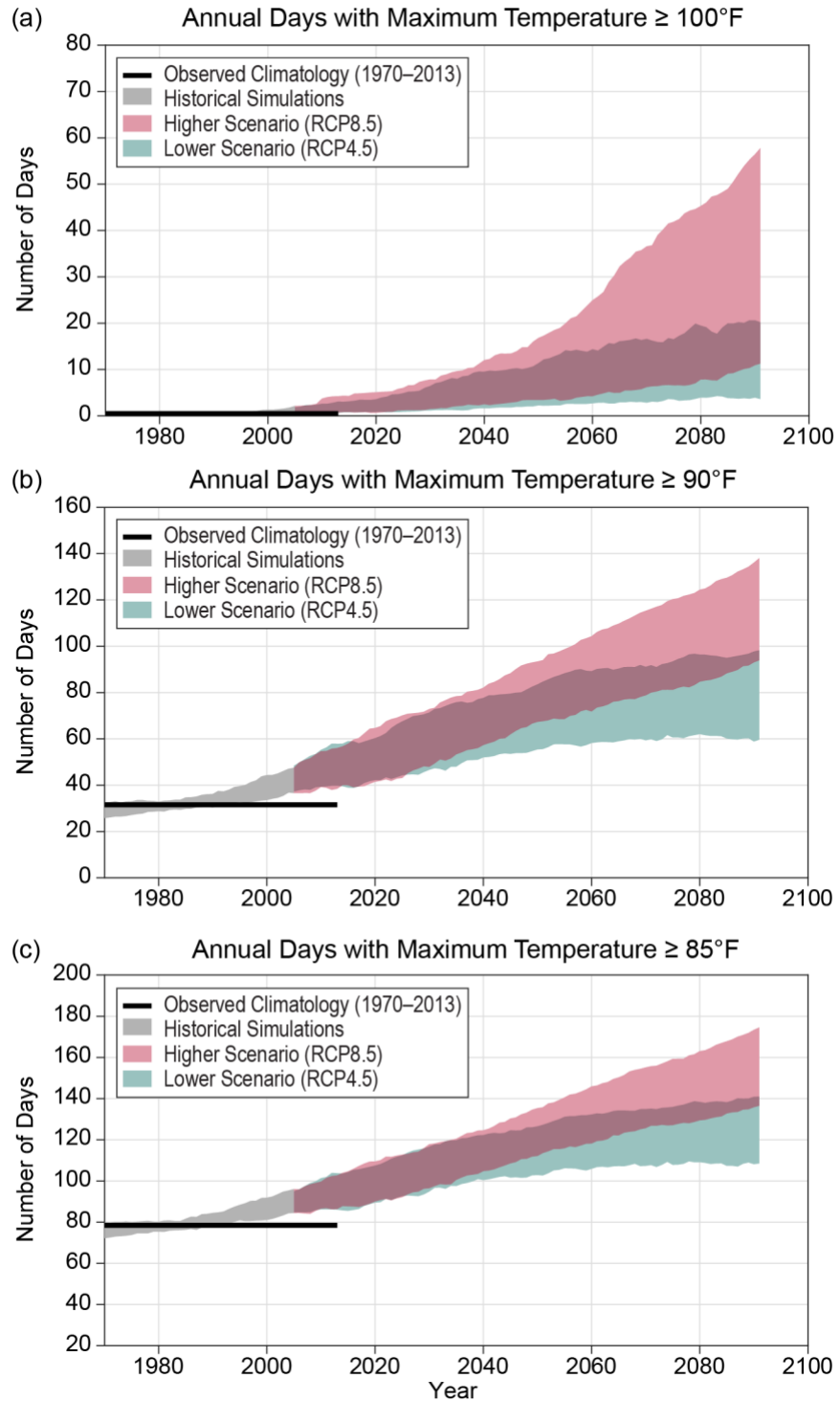
Figure B.2. These time series show the simulated historical and projected number of days per year on which the maximum temperature is at or above 100°F (a), 90°F (b), and 85°F (c) for North Carolina from the LOCA data and the observed climatological values averaged for the

period 1970–2013 (black line). Historical simulations (gray shading) are shown for 1970–2005. Projected changes for 2006–2100 are shown for a higher scenario (RCP8.5; red shading) and a lower scenario (RCP4.5; green shading). The shaded ranges indicate the 10% to 90% confidence intervals of 20-year running averages from the set of climate models. Days above 85°F are a common occurrence across the state, while days above 90°F occur about half as often. Days above 100°F are very rare and occur mostly in the Piedmont and Coastal Plain regions. Climate models project increases in the number of days above each threshold temperature, with all increases being largest later in the century and under the higher scenario (RCP8.5). Source: The University of Edinburgh and NCICS.

Figure B.3. The maps show projected changes in the number of days per year on which the minimum temperature is at or above 60°F (left column), 70°F (center column), and 80°F (right column) for North Carolina for two mid-century time periods and two climate futures. All projected values are shown as changes compared to 1996–2015 averages. Panels (a)–(c) show projected changes for 2021–2040 under a higher scenario (RCP8.5). Panels (d)–(f) depict projected changes for 2041–2060 under a lower scenario (RCP4.5), and panels (g)–(i) show projected changes under the higher scenario for the same period. Temperatures above these thresholds are far more common in the Piedmont and Coastal Plain regions. The number of days on which the minimum temperature exceeds 60°F are projected to increase across most of the state, with the greatest increases seen later in the century and under the higher scenario. Days on which the minimum temperature exceeds 70°F are rare in the Western Mountains, even by mid-century, but are projected to increase across the Piedmont and Coastal Plain. Days on which the minimum temperature exceeds 80°F will remain rare across most of North Carolina. Source: The University of Edinburgh and NCICS.

Figure B.4. These time series show the simulated historical and projected number of days per year on which the minimum temperature is at or above 80°F (a), 70°F (b), and 60°F (c) for North Carolina from the LOCA data and the observed climatological values averaged for the period

1970–2013 (black line). Historical simulations (gray shading) are shown for 1970–2005. Projected changes for 2006–2100 are shown for a higher scenario (RCP8.5; red shading) and a lower scenario (RCP4.5; green shading). The shaded ranges indicate the 10% to 90% confidence intervals of 20-year running averages from the set of climate models. Historically, nights exceeding 80°F have not occurred. However, climate models project that North Carolina may start to experience such hot nights towards the end of the century under both the higher and lower emissions scenarios. The number of days on which the minimum temperature exceeds both 60°F and 70°F has increased since 1970, with increases projected to continue under both scenarios. Source: The University of Edinburgh and NCICS.

Projected Changes in 5-Day Maximum and Minimum Temperatures: North Carolina

Annual Hottest 5-Day Maximum Temperature

Annual Coldest 5-Day Minimum Temperature
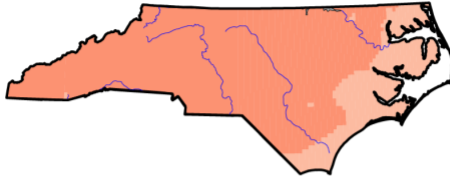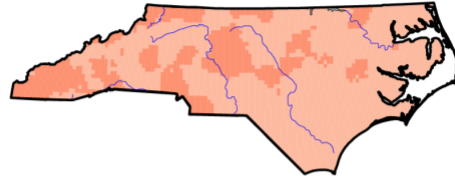
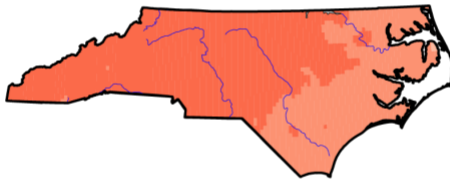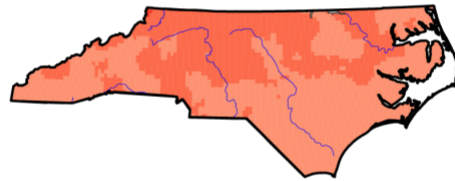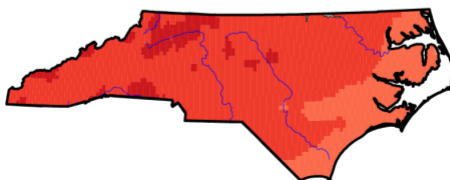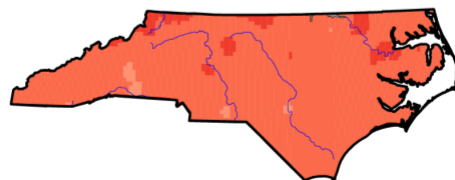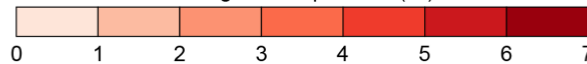Figure B.5. The maps show the projected change in temperatures for the hottest (left column) and coldest (right column) 5-day period each year, averaged over North Carolina for two mid-century time periods and two climate futures. All projected values are shown as changes compared to 1996–2015 averages. Panels (a) and (b) show projected changes for 2021–2040 under a higher scenario (RCP8.5). Panels (c) and (d) depict projected changes for 2041–2060 under a lower scenario (RCP4.5), and panels (e) and (f) show projected changes under the higher scenario for the same period. The largest increases in temperature are seen across the Western Mountains and Piedmont regions during the later time period and under the higher scenario. Source: The University of Edinburgh and NCICS.
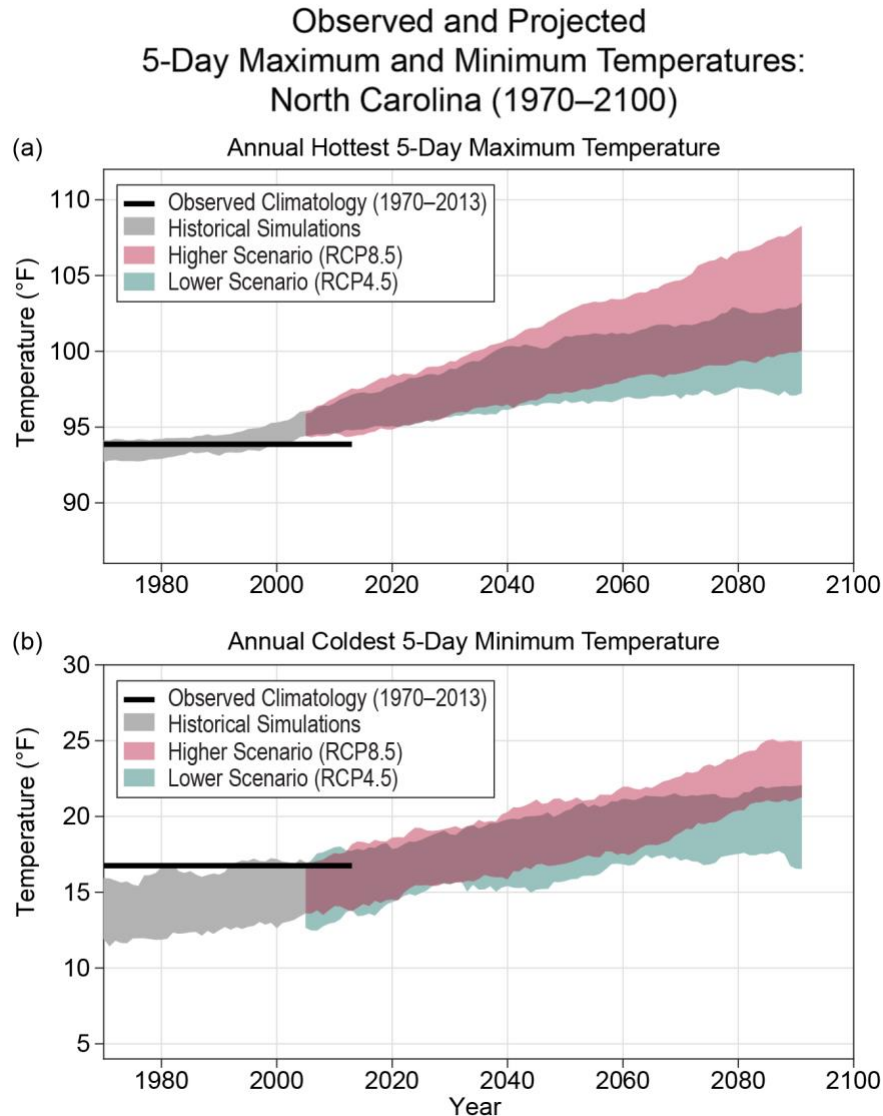
Figure B.6. These time series show the simulated historical and projected temperatures for the hottest (a) and coldest (b) 5-day period each year, averaged over North Carolina from the LOCA data and the observed climatological values averaged for the period 1970–2013 (black line). Historical simulations (gray shading) are shown for 1970–2005. Projected changes for 2006–2100 are shown for a higher scenario (RCP8.5; red shading) and a lower scenario (RCP4.5; green shading). The shaded ranges indicate the 10% to 90% confidence intervals of 20-year running averages from the set of climate models. Since 1970, there has been a general increase in temperature for both the annual hottest and coldest 5-day periods. Climate models project that by the end of the century, the hottest annual 5-day temperature will increase by a greater amount than the coldest 5-day temperature. Source: The University of Edinburgh and NCICS.
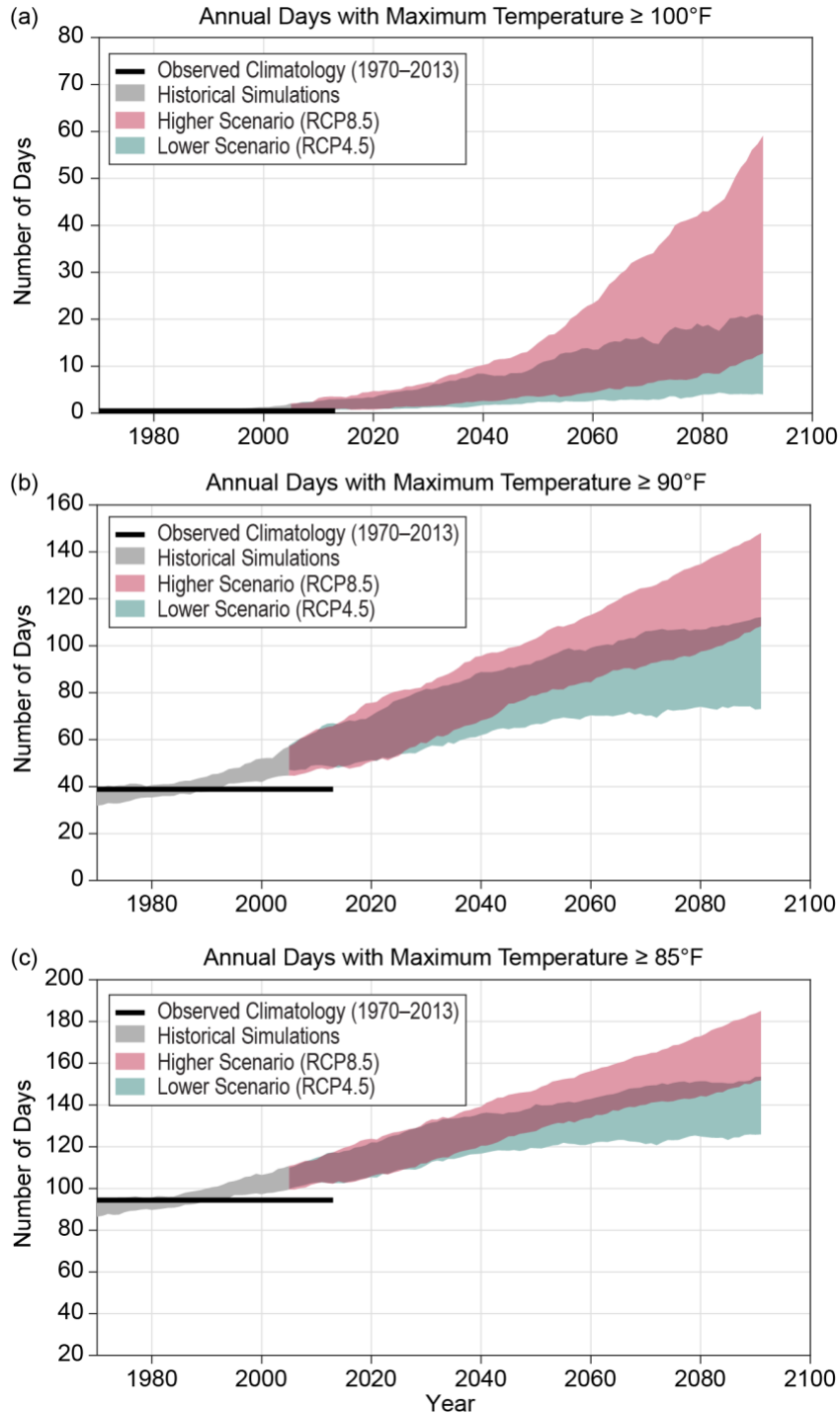
Figure B.7. These time series show the simulated historical and projected number of days per year on which the maximum temperature is at or above 100°F (a), 90°F (b), and 85°F (c) for the Coastal Plain region of North Carolina from the LOCA data and the observed climatological values averaged for the period 1970–2013 (black line). Historical simulations (gray shading) are

shown for 1970–2005. Projected changes for 2006–2100 are shown for a higher scenario (RCP8.5; red shading) and a lower scenario (RCP4.5; green shading). The shaded ranges indicate the 10% to 90% confidence intervals of 20-year running averages from the set of climate models. Temperatures above 85°F are common in the coastal region in summer, while days above 90°F occur about half as often, and days above 100°F are rare but have occurred. Climate models project increases in the number of days exceeding 85°F and 90°F by the end of the century, especially under the higher scenario. Models also show that days above 100°F could become more common. Source: The University of Edinburgh and NCICS.
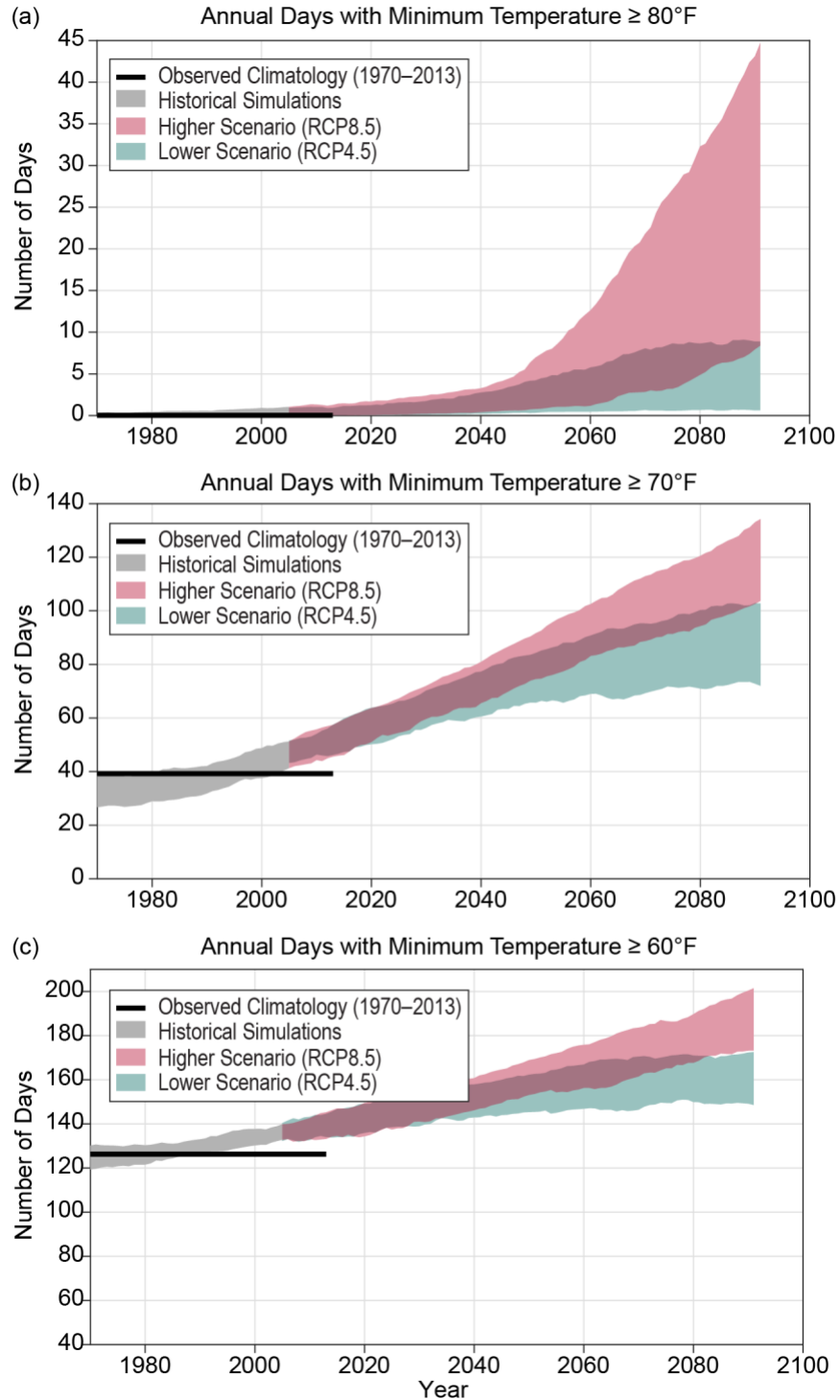
Figure B.8. These time series show the simulated historical and projected number of days per year on which the minimum temperature is at or above 80°F (a), 70°F (b), and 60°F (c) for the Coastal Plain region of North Carolina from the LOCA data and the observed climatological values averaged for the period 1970–2013 (black line). Historical simulations (gray shading) are

shown for 1970–2005. Projected changes for 2006–2100 are shown for a higher scenario (RCP8.5; red shading) and a lower scenario (RCP4.5; green shading). The shaded ranges indicate the 10% to 90% confidence intervals of 20-year running averages from the set of climate models. Historically, nights exceeding 80°F have not occurred in the Coastal Plain. However, climate models project that the region may experience such hot nights by the end of the century, under both the higher and lower emissions scenarios. The number of days per year on which the minimum temperature exceeds both 60°F and 70°F has increased since 1970, with increases projected to continue under both scenarios. Source: The University of Edinburgh and NCICS.
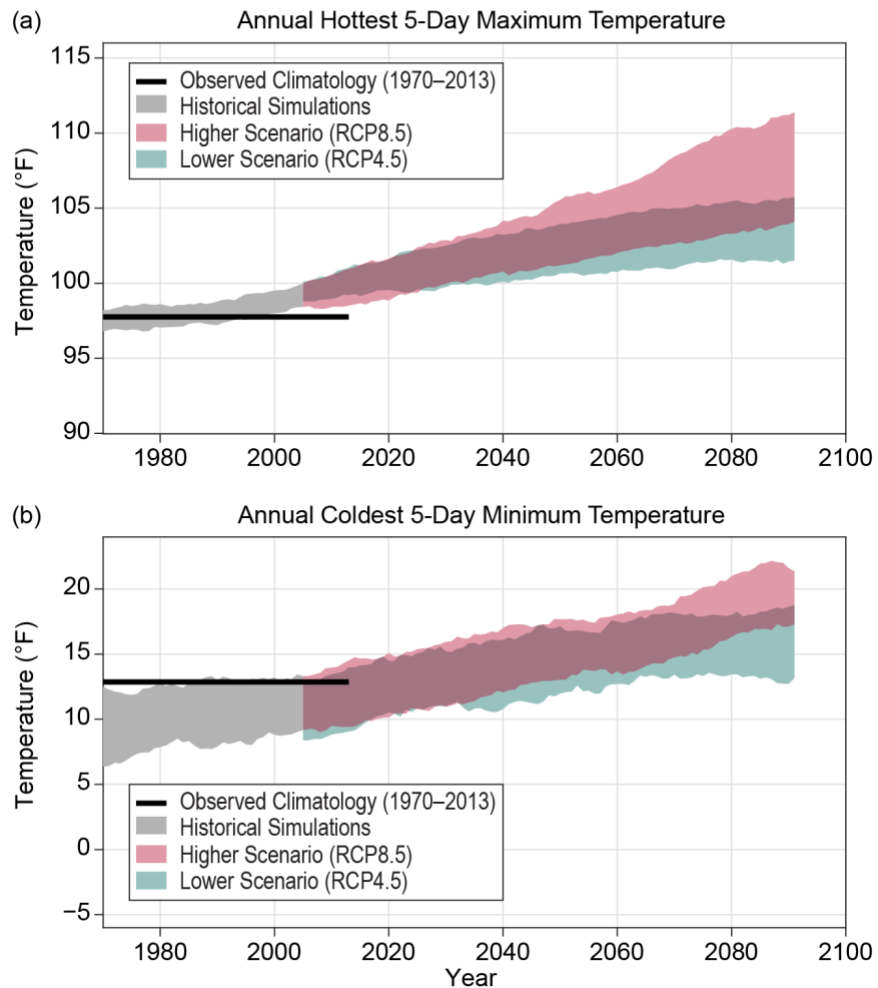
Figure B.9. These time series show the observed and projected temperatures for the hottest (a) and coldest (b) 5-day period each year, averaged over the Coastal Plain region of North Carolina. Observed values for the period 1970–2013 (black line) are generally within the envelope of model simulations shown for the historical period 1970–2005 (gray shading). Projected changes for 2006–2100 are shown for a higher scenario (RCP8.5; red shading) and a lower scenario (RCP4.5; green shading). Shaded ranges indicate the 10% to 90% confidence intervals from the set of climate models. Since 1970, there has been a general increase in temperature for both the annual hottest and coldest 5-day periods. Climate models project similar increases in the hottest and coldest 5-day average temperature each year, by the end of the century. Source: The University of Edinburgh and NCICS.

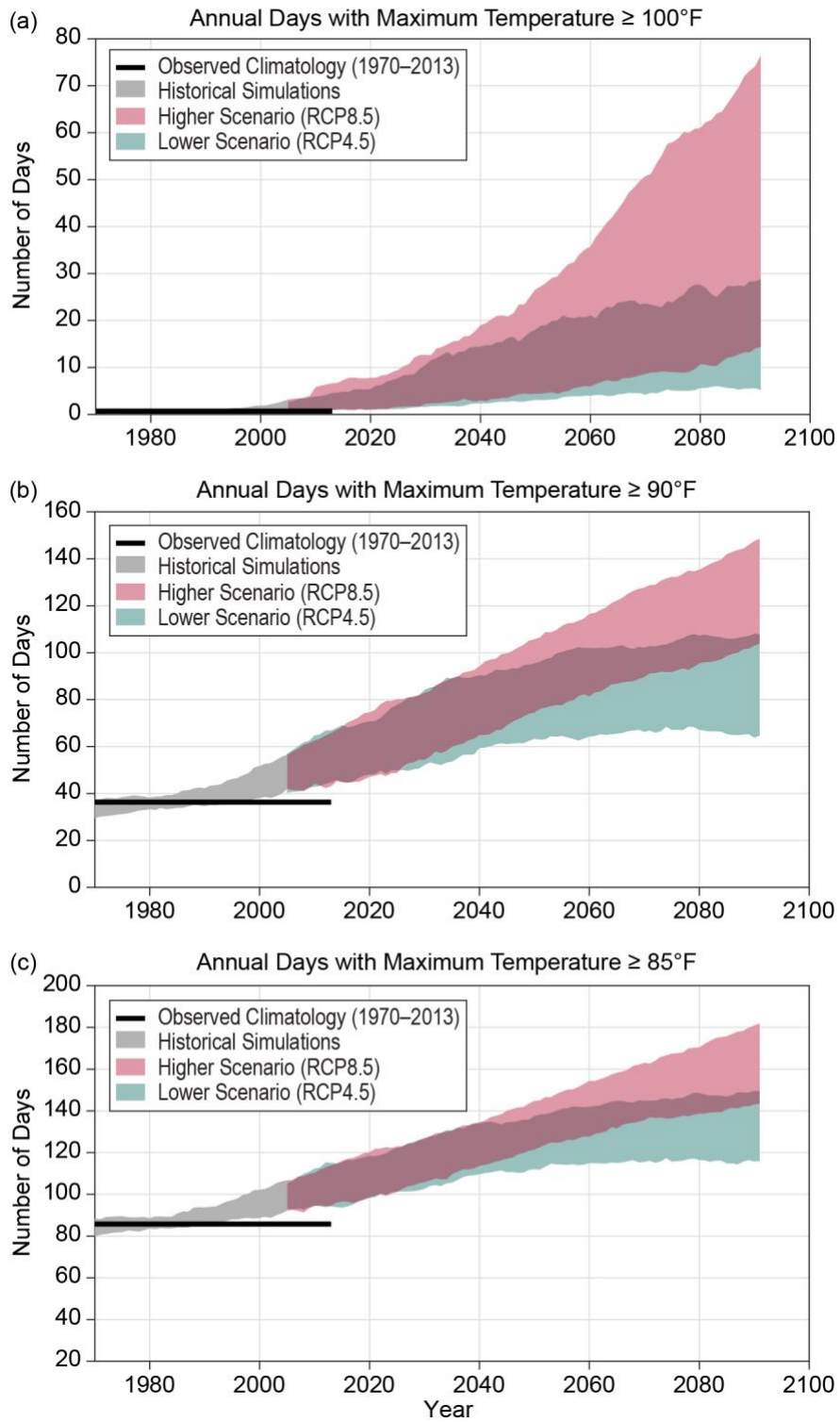## Observed and Projected Hot Days: Piedmont (1970–2100)

Figure B.10. These time series show the simulated historical and projected number of days per year on which the maximum temperature is at or above 100°F (a), 90°F (b), and 85°F (c) for the

Piedmont region of North Carolina from the LOCA data and the observed climatological values averaged for the period 1970–2013 (black line). Historical simulations (gray shading) are shown for 1970–2005. Projected changes for 2006–2100 are shown for a higher scenario (RCP8.5; red shading) and a lower scenario (RCP4.5; green shading). The shaded ranges indicate the 10% to 90% confidence intervals of 20-year running averages from the set of climate models. Temperatures above 85°F are a common occurrence in the Piedmont in summer, while days above 90°F occur about half as often. Temperatures above 100°F are rare but have occurred. Climate models project increases in the number of days exceeding 85°F and 90°F by the end of the century, especially under the higher scenario. Models also show that days above 100°F could become more common. Source: The University of Edinburgh and NCICS.

Observed and Projected Warm Nights: Piedmont (1970–2100)
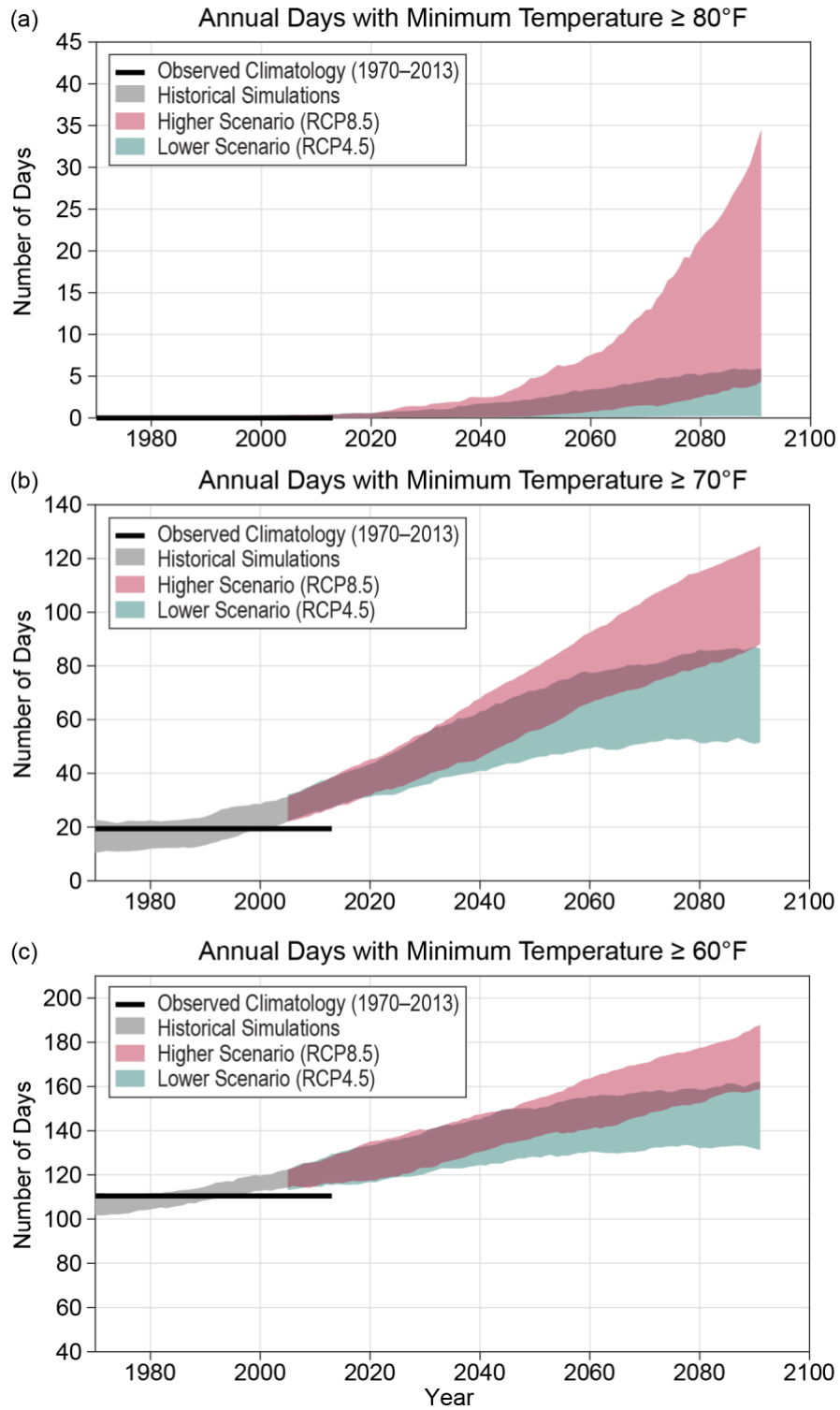

Figure B.11. These time series show the simulated historical and projected number of days per year on which the minimum temperature is at or above 80°F (a), 70°F (b), and 60°F (c) for the

Piedmont region of North Carolina from the LOCA data and the observed climatological values averaged for the period 1970–2013 (black line). Historical simulations (gray shading) are shown for 1970–2005. Projected changes for 2006–2100 are shown for a higher scenario (RCP8.5; red shading) and a lower scenario (RCP4.5; green shading). The shaded ranges indicate the 10% to 90% confidence intervals of 20-year running averages from the set of climate models. Historically, nights exceeding 80°F have not occurred in the Piedmont. However, climate models project that the region may experience such hot nights by the end of the century under both the higher and lower emissions scenarios. The number of days per year on which the minimum temperature exceeds both 60°F and 70°F has increased since 1970, with increases projected to continue under both scenarios. Source: The University of Edinburgh and NCICS.

Observed and Projected
5-Day Maximum and Minimum Temperatures:
Piedmont (1970–2100)

(a)

Annual Hottest 5-Day Maximum Temperature

Legend:
- Observed Climatology (1970–2013)
- Historical Simulations
- Higher Scenario (RCP8.5)
- Lower Scenario (RCP4.5)

Temperature (°F)

(b)

Annual Coldest 5-Day Minimum Temperature

Legend:
- Observed Climatology (1970–2013)
- Historical Simulations
- Higher Scenario (RCP8.5)
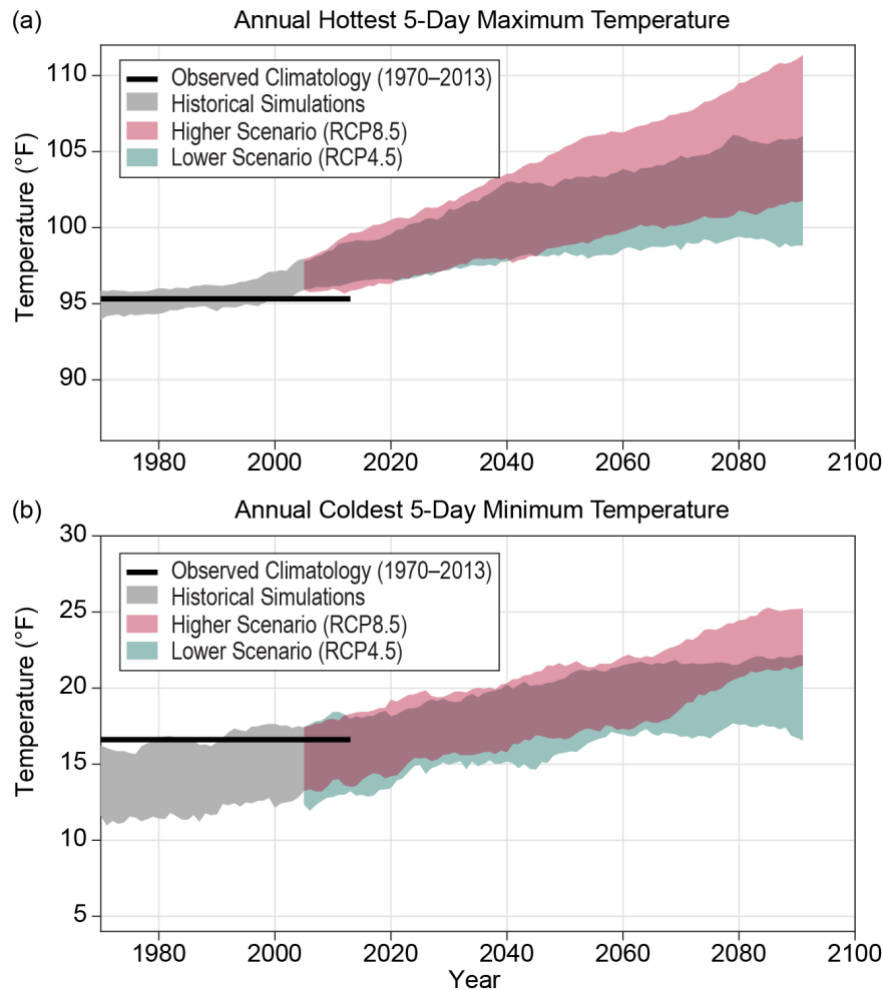- Lower Scenario (RCP4.5)

Temperature (°F)

Year

Figure B.12. These time series show the simulated historical and projected temperatures for the hottest (a) and coldest (b) 5-day period each year averaged over the Piedmont region of North Carolina from the LOCA data and the observed climatological values averaged for the period 1970–2013 (black line). Historical simulations (gray shading) are shown for 1970–2005. Projected changes for 2006–2100 are shown for a higher scenario (RCP8.5; red shading) and a lower scenario (RCP4.5; green shading). The shaded ranges indicate the 10% to 90% confidence intervals of 20-year running averages from the set of climate models. Since 1970, there has been a general increase in temperature for both the annual hottest and coldest 5-day periods. Climate models project that by the end of the century, the hottest annual 5-day temperature will increase by a greater amount than the coldest 5-day temperature. Source: The University of Edinburgh and NCICS.

Observed and Projected Hot Days: Western Mountains (1970–2100)

(a)

Annual Days with Maximum Temperature ≥ 100°F

Legend:
- Observed Climatology (1970–2013)
- Historical Simulations
- Higher Scenario (RCP8.5)
- Lower Scenario (RCP4.5)

(b)

Annual Days with Maximum Temperature ≥ 95°F

Legend:
- Observed Climatology (1970–2013)
- Historical Simulations
- Higher Scenario (RCP8.5)
- Lower Scenario (RCP4.5)

(c)

Annual Days with Maximum Temperature ≥ 85°F

Legend:
- Observed Climatology (1970–2013)
- Historical Simulations
- Higher Scenario (RCP8.5)
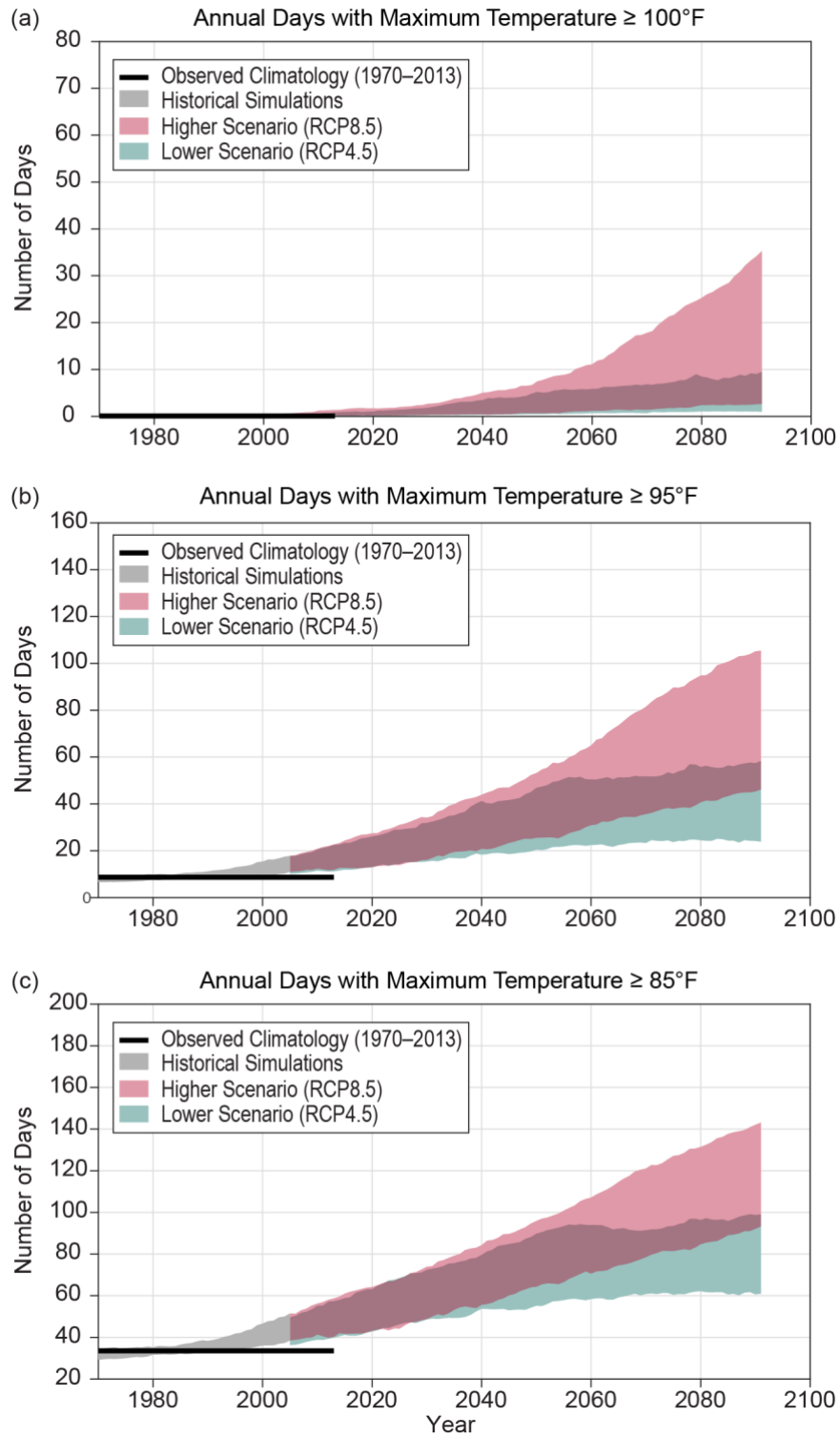- Lower Scenario (RCP4.5)

Figure B.13. These time series show the simulated historical and projected number of days per year on which the maximum temperature is at or above 100°F (a), 95°F (b), and 85°F (c) for the

227

Western Mountains region of North Carolina from the LOCA data and the observed climatological values averaged for the period 1970–2013 (black line). Historical simulations (gray shading) are shown for 1970–2005. Projected changes for 2006–2100 are shown for a higher scenario (RCP8.5; red shading) and a lower scenario (RCP4.5; green shading). The shaded ranges indicate the 10% to 90% confidence intervals of 20-year running averages from the set of climate models. Temperatures above 85°F are a somewhat common occurrence in the mountains in summer, while days above 95°F rarely occur. Temperatures above 100°F are an extremely rare occurrence in the mountains and have only been seen a few times since 1970. Climate models project large increases in the number of days exceeding each temperature threshold by the end of the century, especially under the higher scenario. Source: The University of Edinburgh and NCICS.

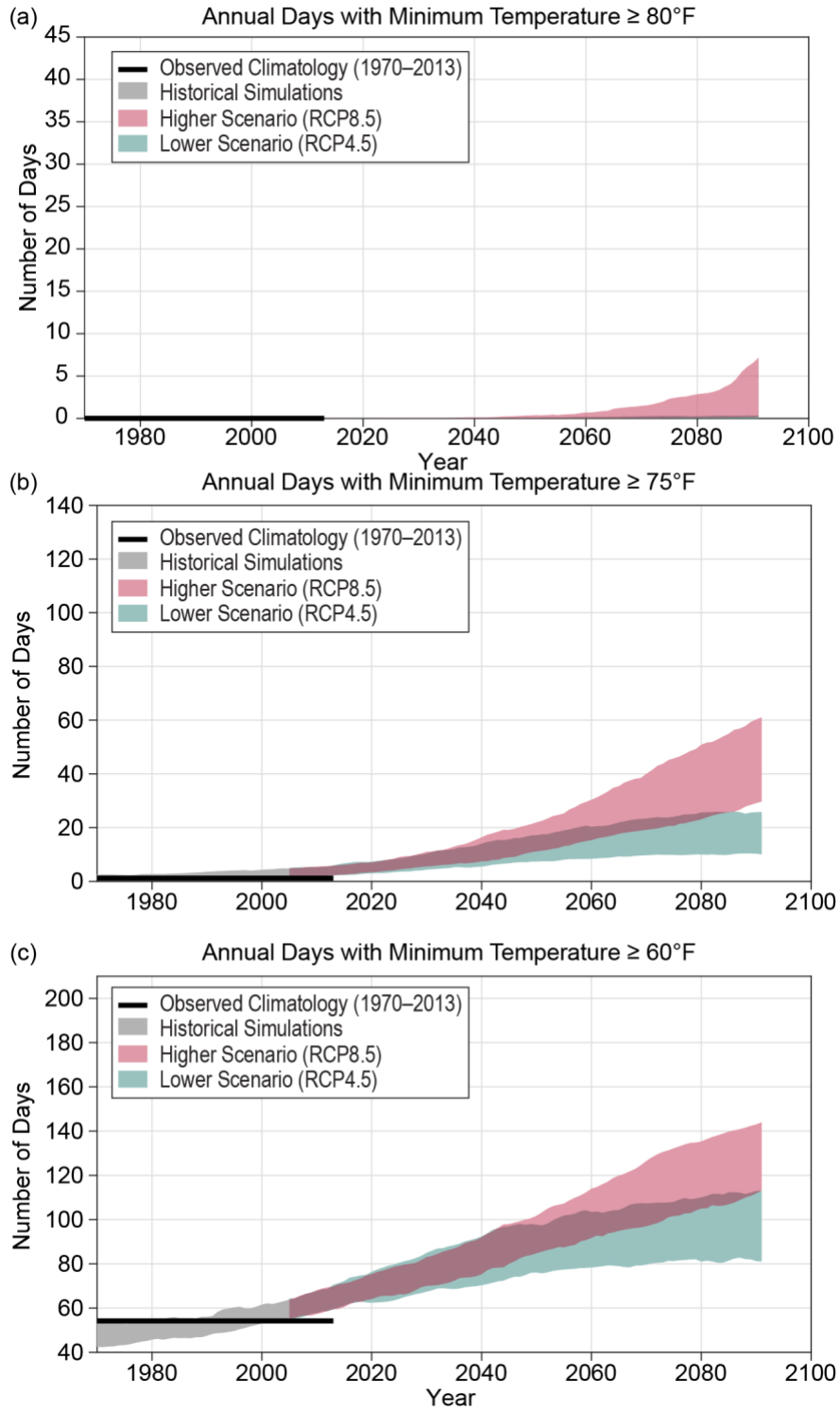## Observed and Projected Warm Nights: Western Mountains (1970–2100)

Figure B.14. These time series show the simulated historical and projected number of days per year on which the minimum temperature is at or above 80°F (a), 75°F (b), and 60°F (c) for the

Western Mountains region of North Carolina from the LOCA data and the observed climatological values averaged for the period 1970–2013 (black line). Historical simulations (gray shading) are shown for 1970–2005. Projected changes for 2006–2100 are shown for a higher scenario (RCP8.5; red shading) and a lower scenario (RCP4.5; green shading). The shaded ranges indicate the 10% to 90% confidence intervals of 20-year running averages from the set of climate models. Historically, nights with temperatures exceeding 75°F or 80°F have not occurred in the mountains. However, under both the higher and lower scenarios, climate models project an increase in the number of days on which the minimum temperature exceeds 75°F by mid- to late century. Under a higher scenario, the region may also experience nights exceeding 80°F towards the end of the century. Days on which the minimum temperature exceeds 60°F have increased since 1970, with increases projected to continue under both scenarios. Source: The University of Edinburgh and NCICS.

Observed and Projected
5-Day Maximum and Minimum Temperatures:
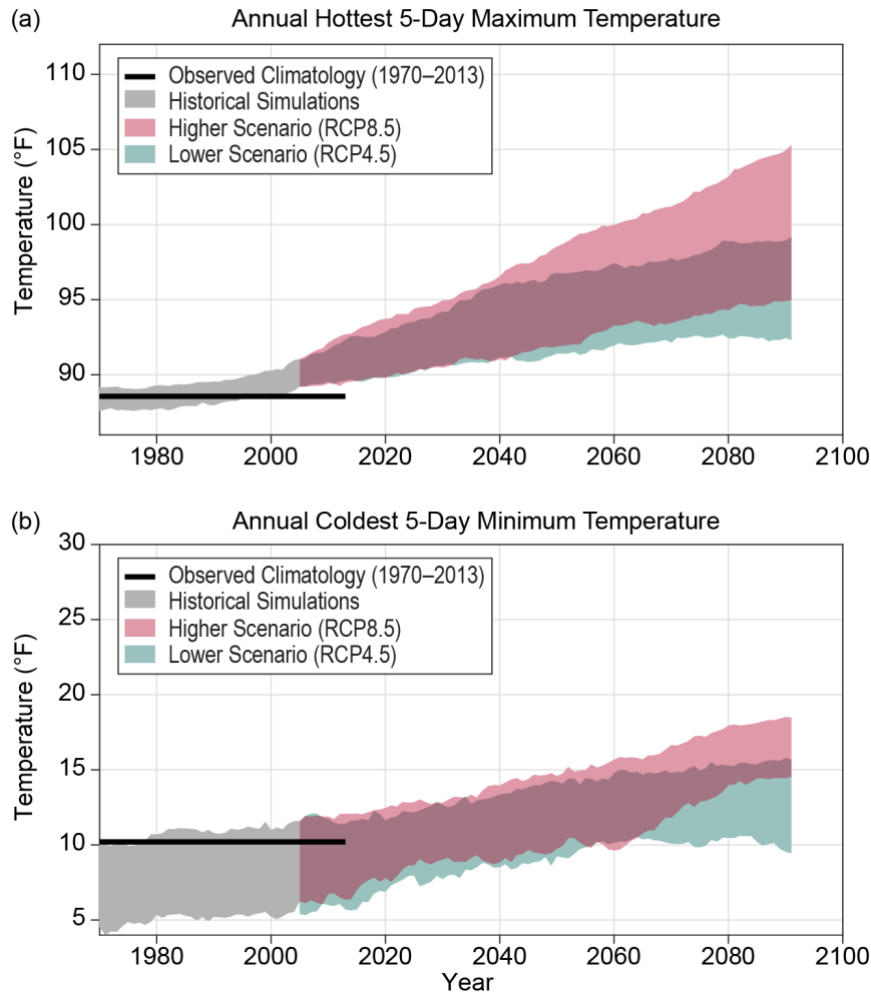## Western Mountains (1970–2100)

Figure B.15. These time series show the simulated historical and projected temperatures for the hottest (a) and coldest (b) 5-day period each year averaged over the Western Mountains region of North Carolina from the LOCA data and the observed climatological values averaged for the period 1970–2013 (black line). Historical simulations (gray shading) are shown for 1970–2005. Projected changes for 2006–2100 are shown for a higher scenario (RCP8.5; red shading) and a lower scenario (RCP4.5; green shading). The shaded ranges indicate the 10% to 90% confidence intervals of 20-year running averages from the set of climate models. Since 1970, there has been a general increase in temperature for both the annual hottest and coldest 5-day periods. Climate models project that by the end of the century, the hottest annual 5-day temperature will increase by a greater amount than the coldest 5-day temperature. Source: The University of Edinburgh and NCICS.

Appendix C: Acronyms and Abbreviations

AFB	Air Force Base
AMO	Atlantic Multidecadal Oscillation
C	Celsius
CAPE	convective available potential energy
CDD	cooling degree day
cm	centimeter
CMIP5	Climate Model Intercomparison Project Phase 5
CO$_2$	carbon dioxide
COOP	Cooperative Observer Program
CSAP	Climate Science Advisory Panel
CSSR	Climate Science Special Report
DEQ	Department of Environmental Quality
ECOnet	Environment and Climate Observing Network
ENSO	El Niño–Southern Oscillation
EPA	Environmental Protection Agency
ESRL	Earth System Research Laboratory
ETC	extratropical cyclone
F	Fahrenheit
GHCN-D	Global Historical Climatology Network-Daily
GIA	glacial isostatic adjustment
GISTEMP	Goddard Institute for Space Studies Surface Temperature Analysis
GMSL	global mean sea level
GS	Gulf stream
GtC	gigatons of carbon
GWP	global warming potential
HadCRUT4	Hadley Centre Climatic Research Unit Gridded Surface Temperature Dataset 4.5
HDD	heating degree day
H$_2$O	water
HTF	high tide flooding
IPCC	Intergovernmental Panel on Climate Change
K	kelvin
LOCA	Localized Constructed Analogs
m	meter
MHHW	mean higher high water
mm	millimeter
MRCC	Midwestern Regional Climate Center

NAO	North Atlantic Oscillation
NAVD88	North American Vertical Datum of 1988
NCA4	Fourth National Climate Assessment
NCAR	National Center for Atmospheric Research
NCCSR	North Carolina Climate Science Report
NCEI	National Centers for Environmental Information
NCEP	National Centers for Environmental Prediction
NCICS	North Carolina Institute for Climate Studies
nClimDiv	NOAA's Climate Divisional Dataset
NCSU	North Carolina State University
NDMC	National Drought Mitigation Center
NO$_x$	oxides of nitrogen
NOAA	National Oceanic and Atmospheric Administration
NWFS	northwest flow snow
PDO	Pacific Decadal Oscillation
PDSI	Palmer Drought Severity Index
PET	potential evapotranspiration
PM$_{2.5}$	particulate matter that are 2.5 micrometers or less in size
ppm	parts per million
RCP	Representative Concentration Pathway
RSL	relative sea level
SLR	sea level rise
SST	sea surface temperature
SWE	snow water equivalent
TC	tropical cyclone
TSU	Technical Support Unit
UHI	urban heat island
USCRN	U.S. Climate Reference Network
USGCRP	U.S. Global Change Research Program
VCLI	ventilation cooling load index
VLF	very large fire
VOC	volatile organic compound
WUI	wildland–urban interface
yr	year